Investigating the role of the RNA binding protein HuR in skeletal development and disease.

Thesis submitted in accordance with the requirements of the University of Liverpool for the degree of Doctor in Philosophy

By

Kirsty Anne Johnson

July 2018

For my boy, Alfie.

ACKNOWLEDGEMENTS

Firstly, I would like to thank my supervisor Dr Simon Tew for being a remarkably understanding and supportive mentor throughout some of the most academically and personally challenging times over the past 4 years - without your advice, guidance and support this thesis would not have been possible. Thank you to Professor George Bou-Gharios for your words of wisdom and guidance during my transition into the world of transgenics and for your enthusiasm and encouragement at every meeting. Thanks to Dr Peter Milner for your help with surgery and scoring, and extended thanks to Dr Ke Lu and the technical staff at BSU for your help, training and support.

A huge thanks to all past and present members of MSBI for the laughs and encouragement - you have all made the past 4 years a memorable experience and kept me going when things inevitably went wrong. And to my new group 'Lab B', particularly Sarah and Fi - thank you for the many chats and *nearly there's* during the writing up of this thesis, and to Dada for being understanding and supportive while writing!

These acknowledgements would not be complete without thanking my friends and family. Thank you to my friends for the games nights, BBQs and laughs that provided a welcomed distraction. To Emma, Clare and Ryan - thank you for being the best siblings to your 'big little sister', even if you only phone me to speak to Alfie! My mum and dad, thank you for everything. Thank you for your support, for the endless baby sitting and for trying to understand the 'mouse stuff'. Without you both I would not be who or where I am today (and I'd probably be trying to pay off nursery fees!). A special thanks to the Nan who gave up work to spend more time with her grandchildren - you are so missed Jen. To Dave, thank you for always supporting me, encouraging me and being the rock I needed. Even in the middle of one of my many meltdowns you kept me sane. And finally, this thesis is dedicated to my boy Alfie. You have been the biggest pick-me-up and you always know how to put a smile on my face. I hope I inspire you to always follow your dreams.

And will you succeed? Yes! You will, indeed! (98 and ¾ percent guaranteed)
Kid, you'll move mountains!

ABSTRACT

Osteoarthritis is a complex multifactorial degenerative disease that is characterised by progressive loss of articular cartilage and inflammation of the synovium resulting pain and loss of mobility. HuR is a ubiquitously expressed RNA binding protein involved in the post-transcriptional regulation of target mRNAs and can reduce their rate of turnover. Previously published data suggests that HuR is spatially regulated within developing cartilage and is involved in the regulation of chondrocyte genes and osteoarthritis. Furthermore, knockout of HuR in mice at pre-implantation stage leads a skeletal dysplasia, among other phenotypes. This project aimed to determine whether HuR activity is important for maintaining cartilage and skeletal phenotype appropriately.

An inducible, cartilage-specific HuR knockout mouse model and a non-inducible limb bud and mesenchyme-specific HuR knockout mouse model were generated utilising the Cre/LoxP system, were Cre expression is driven by an aggrecan promotor and a Prx1 enhancer, respectively. Using these novel transgenic mouse models of HuR knockout, the role of HuR in embryonic development, during osteoarthritis and in chondrocytes was characterised.

Induced aggrecan-driven knockout of HuR leads to severe dysregulation of skeletal development during embryogenesis, resulting in a lack of mineralisation of axial components including the ribs and spine, and craniofacial structures. Similarly, Prx1-driven knockout of HuR during embryonic development leads to altered mineralisation of the skeleton, most strikingly in the developing limbs. This is similar in many respects to the phenotype observed following a broader knockout of HuR at an earlier developmental stage and suggests a role for HuR during endochondral ossification. *In vitro* assays using murine primary chondrocytes suggest that HuR may be required for the appropriate regulation of a number of known chondrocyte marker genes including Sox9, Runx2 and Mmp13, of which the latter two are known to be critically involved in the regulation of chondrocyte hypertrophy and endochondral ossification.

The roles of RNA binding protein-mediated post transcriptional gene control is still not well understood in orthopaedic tissues. This study indicates that spatial and temporal mis-control of the protein HuR can lead to impaired skeletal mineralisation, suggesting that it performs an important function in chondrogenesis and /or osteogenesis.

Table of Contents

List of Figures

List of Tables

Abbreviations

AC	Articular cartilage
ACAN	Aggrecan
Acan	Aggrecan gene
AdamTS	A disintegrin and metalloproteinase with thrombospondin motifs
AGO	Argonaute
AP	Anterior-posterior
AP1+2	Activator protein 1+2
ARE	Adenylate-uridylate-rich elements
AUF1	AU-rich binding factor 1
Bapx1	Bagpipe homeobox protein homolog 1
BMP	Bone morphogenetic protein
BMSC	Bone marrow-derived stem cells
BSU	Biomedical Service Unit
C2H302NH4	Ammonium acetate
CMV	Cytomegalovirus
CNCCs	Cranial neural crest cells
Col10a1	Collagen Type II alpha I
Col2a1	Collagen Type X alpha I
Cox2	Cyclooxygenase 2
Cre	Causes recombination
CS	Chondroitin sulfate
DGCR8	DiGeorge syndrome critical region in gene 8
DMM	Destabilisation of the medial meniscus
DMSO	Dimethyl sulfoxide

dsRBM	Double-stranded RNA binding motifs
dsRNA	Double-stranded RNA
E	Embryonic day
ECM	Extracellular matrix
EDTA	Ethlenediaminettraacetic acid
EGF	Epidermal growth factor
eGFP	Enhanced green fluorescent protein
ELAVL1	ELAV-like protein 1 gene
Fabp2	Fatty acid-burning protein 2
FBS	Fetal bovine serum
FGF	Fibroblast growth factor
GAGs	Glycosaminoglycans
GAPDH	Glyceraldehyde 3-phosphate dehydrogenase
HAC	Human articular chondrocytes
HNS	HuR nucleocytoplasmic shuttling domain
Hsf1	Heat shock transcription factor 1
HuR	Human antigen R
IGD	Inner-globular domain
IGF	Insulin-like growth factor
Ihh	Indian hedgehog
IL-1	Interleukin -1
iMACs	Immature murine articular chondrocytes
IP	Intraperitoneal
IVD	Intervertebral disc
kb	Kilobase
KCl	Potassium Chloride
KH	K homology domain
KOH	Potassium hydroxide

KS	Keratin sulfate
KSRP	KH-type splicing regulatory protein
Lef1	Lymphoid enhancer binding factor 1
Mdm2	Murine double minute 2
MEF	Murine embryonic fibroblast
MIA	Monoiodoacetate
miRNA	Micro RNA
MMP	Matrix metalloproteinase
MMP13	Matrix metalloproteinase 13
MOI	Multiplicity of infection
mRNA	Messenger RNA
MSX1+2	Msh homeobox 1
MT-MMPs	membrane type MMPs
NBF	Neutral buffered formalin
NFAT1	Nuclear factor of activated T-cells
NF-κb	Nuclear factor kappa-light-chain-enhancer of activated B cells
NMD	Nonsense mediated decay
nt	Nucleotide
OA	Osteoarthritis
PCM	Pericellular matrix
POC	Primary ossification center
Pol	Polymerase
Ppr1	PTH/PTHrP receptor 1
pre-miRNA	Precursor micro RNA
pri-miRNA	Primary micro RNA
PRX1	Paired related homeobox 1
PTBP2	Polypyrimidine tract-binding protein 2

PTHrP	Parathyroid hormone-related protein
RBD	RNA binding domain
RBP	RNA binding protein
RIP-seq	RNA immunoprecipitation sequencing
RISC	RNA-induced silencing complex
RNA	Ribonucleic acid
ROI	Region of interest
RRM	RNA recognition motif
RUNX2	Runt-related transcription factor 2
SNP	Single nucleotide polymorphism
SOX9	SRY-box 9
Stau1	Staufen 1
TAE	Tris-acetate-EDTA
TGFβ	Transforming growth factor beta
TIMP	Tissue inhibitor of metalloproteinase
TJR	Total joint replacement
TNF-α	Tumor necrosis factor alpha
TTP	Tristetraprolin
UTR	Untranslated region
UV	Ultraviolet
VEGF	Vascular endothelial growth factor
VOI	Volume of interest
WT	Wild type

1 General Introduction

1.1 Background

Osteoarthritis is the most common and chronic form of joint disease associated with age and mechanical wear (Sulzbacher, 2013). Osteoarthritis affects weight-bearing joints, predominately the knees, hips and hands, and leads to joint pain, stiffness and loss of function. Other risk factors for osteoarthritis include obesity, joint trauma and co-morbidities such as diabetes and metabolic and endocrine diseases (Mobasheri *et al*., 2014).

Our laboratory is interested in the post-transcriptional regulation of messenger RNAs (mRNAs) in cartilage biology and during osteoarthritis progression. Previous work has identified RNA binding proteins as regulators of anabolic and catabolic gene expression in chondrocytes (McDermott *et al.* 2016). In particular, siRNA-mediated knockdown of the RNA binding protein HuR in SW1353 chondrosarcoma cells and human articular chondrocytes led to a significant increase in the expression of matrix metalloproteinase 13 (MMP13), a collagenase implicated in the destruction of the articular surface and known to be elevated in osteoarthritic cartilage (Karsdal and Madsen, 2008).

This thesis expands upon these observations, examining how HuR influences chondrocyte function *in vivo* during development and disease as well as determining its importance in regulating chondrocytic molecular markers *in vitro*.

1.2 Structure and function of synovial joints

1.2.1 Cartilage structure and function

Articular hyaline cartilage is an aneural, avascular and alymphatic specialised form of connective tissue that covers the articular ends of subchondral bone in diarthroidial joints and acts to reduces joint stress by providing a low-friction gliding surface and distributing load (Yu and Urban, 2010). Articular cartilage is composed of the extracellular matrix (ECM) with a sparse distribution of highly specialised cells called chondrocytes (Dijkgraaf *et al*., 1995). The ECM is mainly

composed of water, collagen and proteoglycans and lesser amounts of other non-collagenous proteins and glycoproteins. This chemical composition allows the ECM to retain water and allows the articular cartilage to withstand the pressures of repetitive loading (Clouet *et al*., 2009, Fox *et al*., 2009).

Articular cartilage is split into four zones: the superficial zone, the middle zone, the deep zone and the calcified zone (Figure 1.1) (Clouet *et al*., 2009). These zones differ according to the type and orientation of the collagen fibres, the shape and activity of the chondrocytes, the amount of proteoglycans present and, consequently, the water content (García-Carvajal, 2013).

The superficial zone contains an outer surface that is in contact with the synovial fluid to provide a low friction surface and contains low levels of proteoglycans and collagen fibres types I, II and III that are tightly packed parallel to the articular surface. This zone contains a relatively high number of chondrocytes that have a flattened morphology. Surface zone chondrocytes contribute to low friction articulation of the joint by secreting lubricating molecules such as hyaluronic acid and lubricin (Rhee *et al*., 2005). This contributes to the unique tribological properties of articular cartilage and enables low friction articulation of synovial joints (Greene *et al*., 2011).

The middle zone contains a less dense and less organised structure of types II, VI, IX and XI collagen fibres. This zone makes up 40-60% of total cartilage volume and deforms the most during compressive loading (Grogan *et al.* 2013). Chondrocytes in the middle zone have a rounded morphology and synthesise large amounts of the proteoglycan aggrecan. They differ in their synthesis of other small proteoglycans compared to chondrocytes in other parts of the tissue (Goldring *et al*., 2006).

The deep zone represents approximately 30% of articular cartilage volume and contains collagen fibres types II, IX and XI that are organised perpendicular to the articular surface; this provides the greatest resistance to compressive force. Chondrocytes of this zone are rounded and form columns that align parallel to the collagen fibres, perpendicular to the joint surface (Fox *et al.* 2009).

The calcified zone contains a sparse population of hypertrophic chondrocytes and acts as an interface between tissues by anchoring collagen fibrils of the deep zone to the subchondral bone (Fox *et al*., 2009, Clouet *et al*., 2009).

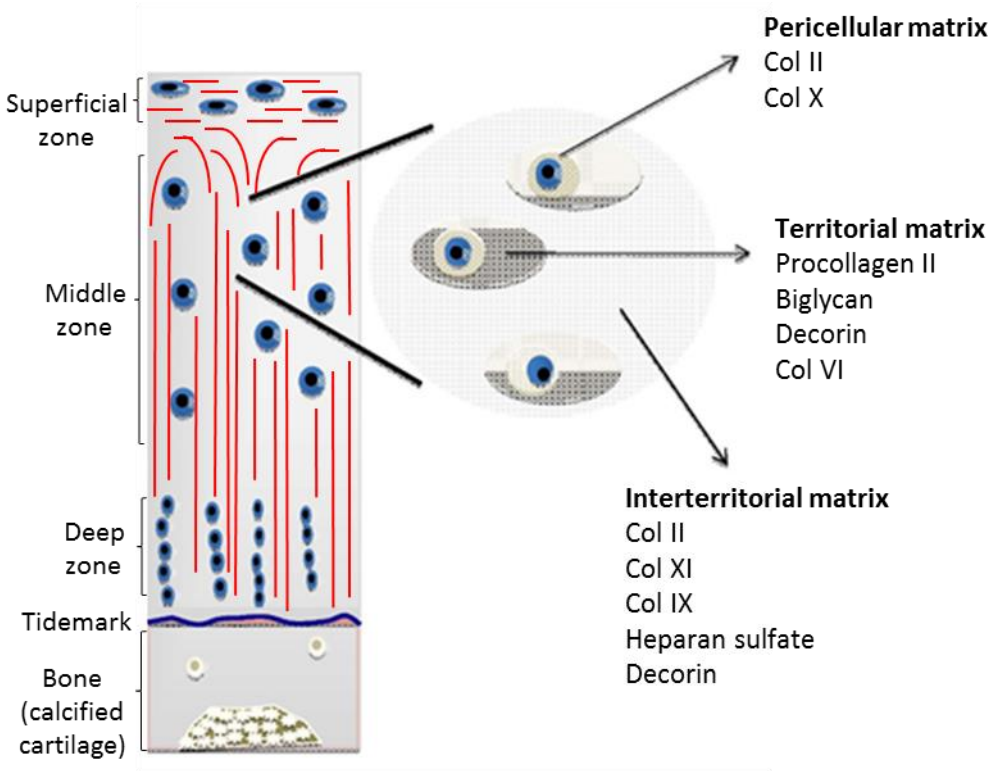

Figure 1.1. Organisation of healthy articular cartilage and the zones of the ECM. Each zone is characterised by different morphology and function of chondrocytes and the orientation of collagen fibres (red). In the superficial zone the fibres are horizontal and chondrocytes secrete lubricant. The fibres of the middle zone run obliquely and chondrocytes are rounded. Fibres run perpendicular to the articular cartilage in the deep zone and chondrocytes align parallel to the collagen fibres. The ECM is divided into zones based on the distance from chondrocytes. The pericellular zone immediately surrounds the chondrocyte, the territorial zone is next to the pericellular zone and the interterritorial zone is the furthest. The expression of different molecules differ between each zone of the ECM (Adapted from García-Carvajal, 2013).

1.2.2 Extracellular matrix

The biomechanical properties of cartilage and the physical function of joints are critically dependent on the integrity of the ECM. In normal articular cartilage, water constitutes up to 60% to 80% of the total weight, this water is drawn in by the high concentration of negatively charged glycosaminoglycans and gives cartilage its ability to withstand loading. The remaining dry weight is made up of type II collagens and the proteoglycan aggrecan (Fox *et al*., 2009; van der Kraan *et al*., 2002).

The ECM can be divided into the pericellular matrix, the territorial matrix and the interterritorial matrix based on distance to the chondrocytes (Figure 1.1) (van der Kraan *et al*., 2002). The pericellular matrix (PCM) immediately surrounds the chondrocytes and contains type VI collagen fibrils in a cross-linked network around the cells. Combined, the chondrocyte and its surrounding pericellular microenvironment have been termed the 'chondron' (Poole, 1997). The territorial matrix surrounds the pericellular matrix and contains high concentrations of proteoglycans including aggrecan, hyaluronan and decorin. The territorial matrix also contains large amounts of collagen type VI which help the chondrocytes to attach to the macromolecular framework of the matrix. (Fox *et al*.,2009). The interterritorial matrix is the most distant from the chondrocytes and the largest of the 3 regions. Type II, XI and IX collagen fibrils are arranged perpendicular to the joint surface in the middle zone, which allows the retention of proteoglycans in the interterritorial matrix (Guilak *et al*., 1999).

1.2.2.1 Collagens

Collagens are a family of glycoproteins that are present in the ECM with different suprastructural organisations and account for up to 60% of the dry weight of cartilage (Table 1.1) (Eyre, 2002; Birk and Bruckner, 2005). All collagens are trimers and contain three polypeptide α chains folded into triple helices and subsequently collagen fibrils, forming the structural framework of the articular cartilage ECM. In developing cartilage, the fibril network is a copolymer of collagens type II, IX and XI, with type II being the most abundant. Collagens type III, VI, XII and XIV are also found in small amounts in cartilage

(Eyre, 2002). Collagen fibrils are organised in a unique cross-linked network with anchoring proteins including chondronectin and fibronectin (Dijkgraaf *et al*., 1995). This fibrillar architecture, which changes between the zones of articular cartilage, is critical to the integrity of the articular cartilage (Eyre, 2004).

Table 1.1. The functions of different collagen types and their relative abundance within the extracellular matrix (Adapted from Eyre, 2004 and Luo, 2017).

Collagen	**Function**	**% of total collagen**	**Distribution in cartilage**
Type II	Major fibrillar collagen Forms the main scaffold by cross-linking with collagen type XI to provide integrity and strength to the tissue	90% (75% foetal)	Broadly distributed in articular cartilage
Type III	Fibrillar collagen Involved in matrix repair and remodelling	10%	Broadly distributed in articular cartilage
Type VI	Microfibrillar collagen Forms a network that aids in the attachment and integrity of chondrocytes to the PCM by interacting with ECM proteins including collagen II and XIV and decorin	<1%	Found in the pericellular matrix of articular cartilage
Type IX	Fibril-forming collagen Crucial for maintenance of cartilage matrix and aids in tensile properties by forming a stable collagen network Found at the surface of chondrocytes and interacts with	1% (10% foetal)	Mainly found in type II collagen-containing tissues including the growth plate and adult articular cartilage

	cartilage proteoglycans to aid in the organisation of the pericellular matrix		
Type X	Network-forming collagen Homotrimeric collagen and plays a key role in modifying the cartilage matrix during endochondral ossification for calcification	1%	Found exclusively in the hypertrophic zone of growth plate
Type XI	Fibril-forming collagen Found in the centre of collagen fibrils and regulates collagen fibril formation	3% (10% foetal)	Broadly distributed in articular cartilage
Type XII	Interacts with microfibrils and contributes to mechanical stability	<1%	Expressed at the junction between synovial fluid and articular cartilage surface
Type XIII	Fibril associated collagen Transmembrane protein involved in cell-matrix and cell-cell adherence junctions; also contributes to the differentiation of osteoblasts	<1%	Localised to the plasma membrane
Type XIV	Large non-fibrillar ECM protein Maintains the integrity and mechanical properties of the tissue	<1%	Found uniformly throughout the articular cartilage Absent from growth plate

1.2.2.2 Proteoglycans

Proteoglycans are a family of complex glycoproteins that consist of a central core protein with one or more covalently linked glycosaminoglycan (GAG) side chains such as keratin sulphate, chondroitin sulphate, dermatan sulphate or heparin sulphate (Iozzo and Schaefer, 2015). Proteoglycans make up 20 to 30% of the dry weight of cartilage and, together with the collagen network, provide the cartilage with the abilities to withstand compressive load (Kiani *et al*., 2002; Hunziker *et al*., 2002). Prominent proteoglycans found within articular cartilage include aggrecan, decorin, biglycan and fibromodulin (Roughley and Lee, 1994).

1.2.2.2.1 Aggrecan

Aggrecan, a member of the lectican family (also known as hyalectins due to their interaction with hyaluronic acid (HA)), is the most abundant proteoglycan in the ECM and the most crucial for the proper function of articular cartilage (Kiani *et al*., 2002). The aggrecan core protein consists of three globular domains (G1, G2 and G3) and an inter-globular domain (IGD) that connects G1 and G2. Between G2 and G3 is a large sequence modified with ~100 chondroitin sulfate (CS) and ~30 keratin sulfate (KS) GAG side chains (Figure 1.2A) (Kiani *et al*., 2002). Aggrecan within the extracellular matrix occurs in the form of proteoglycan aggregates (Muir, 1978). Each aggregate contains a central filament of HA with multiple aggrecan molecules non-covalently attached to its N-terminal G1 domain. Link proteins (LP) stabilise the interaction between the aggrecan core proteins and HA (Figure 1.2A) (Wight *et al*., 1992).

GAG attachment regions are highly polyanionic and hydrophilic so when packed at high density, proteoglycans are able to draw water into the tissue by generating a large osmotic swelling potential (Figure 1.2B). This causes the aggrecan-matrix network to swell and expand, while being resisted by the collagen fibril network (Kiani *et al*., 2002). When force is loaded upon the articular cartilage, the equilibrium is disrupted and the water is displaced. Aggrecan molecules are therefore brought into closer proximity which increases the swelling potential of the aggrecan. Aggrecan will rehydrate upon removal of the force and restore normal equilibrium (Roughley and Mort, 2014).

Aside from its structural role in the ECM, aggrecan is involved in the control and modification of normal bone growth by regulating the expression of key growth factors and signalling molecules (Lauing *et al*., 2014). Postnatal morphogen gradient formation in the growth plate is also reliant on the proper sulfation patterns of the GAG chains attached to aggrecan (Cortes *et al*., 2009).

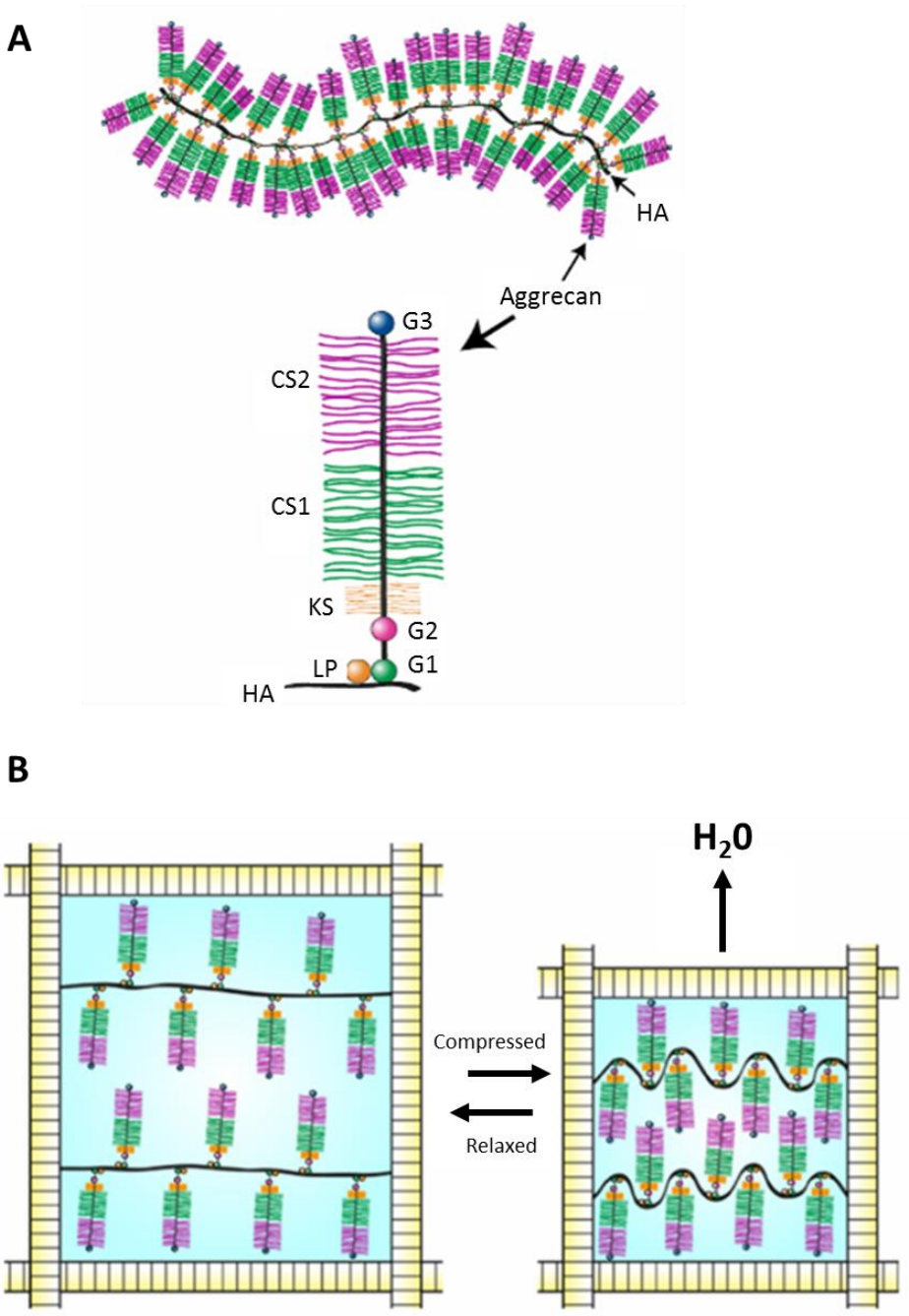

Figure 1.2. Aggrecan structure and function. **A) The structure of proteoglycan aggregates.** A central hyaluronan (HA) filament with aggrecan and link proteins (LP) attached. G1, G2 and G3 domains are indicated, keratin sulfate (KS) and chondroitin sulfate-rich domains (CS1, CS2). **B) The function of aggrecan in articular cartilage**. Aggregates are surrounded by collagen fibrils. Aggregates swell as CS and KS chains draw in water in a relaxed state. During compression, the water is displaced and CS and KS chains are brought closer. (Taken from Roughley and Mort, 2014).

1.2.2.3 Articular chondrocytes

Articular chondrocytes are the only cellular component of articular cartilage and, when joint development is complete, maintain a stable phenotype throughout adulthood (Goldring, 2012). Chondrocytes arise during development from the differentiation of condensed mesenchymal progenitor cells and are critically involved in the growth and patterning of the embryonic skeleton, while in adult articular cartilage they proliferate and secrete extracellular matrix in order to maintain the cartilage (Goldring, 2012; Akkiraju and Nohe, 2015). The main role of chondrocytes in the superficial and middle zone is the synthesis and turnover of ECM components including collagen, proteoglycans and glycoproteins. Chondrocytes function in a low oxygen environment and rely on diffusion of nutrients and metabolites from the articular surface due to the avascular nature of articular cartilage (Archer and Francis-West, 2003).

1.2.3 Cartilage and skeletal development

The multiple types of cartilage that contribute to the primary skeleton are formed from the differentiation or chondrogenesis of cells from three mesenchymal lineages (sclerotome, somatopleure and neural crest ectomesenchyme) (Bobick and Kulyk, 2008). Bones of the axial and appendicular skeletons develop through endochondral ossification. This begins with mesenchymal condensation of osteo- chondroprogenitors which is necessary for the subsequent formation of cartilage templates by chondrocyte differentiation (Tsang *et al*., 2015; Long and Ornitz, 2013). These osteo-chondroprogenitors undergo lineage restriction toward either chondrocytes or osteoblasts (Tsang *et al*., 2014).

There are defined stages of cartilage and bone formation which include the commitment to a specialist cell lineage, mesenchymal condensation, proliferation, disposition of the extracellular matrix (ECM), mineralisation and maintenance (de Crombrugghe *et al.* 2001).

1.2.3.1 Mesenchymal condensation/chondrogenesis

Bone growth is mediated and controlled by the vertebrate growth plate. The growth plate is formed via defined stages of a differentiation process were chondrocytes differentiate, proliferate and undergo hypertrophy resulting in an increase in cell size (Figure 1.3) (Tsang *et al*., 2015).

Chondrogenesis starts at embryonic day 9 (E9) in murine embryonic development (Cheah *et al*., 1991). Hox genes, in particular Hoxa13 and Hoxd13, have been shown to control mesenchymal condensation, while bone morphogenetic proteins (BMPs) are essential for the formation of chondrogenic mesenchymal condensations (Long and Ornitz, 2013). Other extracellular signals involved in mesenchymal condensation include TGFβ (transforming growth factor-β), FGFs (fibroblast growth factors), IGF (insulin-like growth factor) and EGF (epidermal growth factor) (Bobick and Kulyk, 2008).

More mesenchymal progenitors are recruited to the primordial cartilage and once committed to the chondrocyte lineage, chondroprogenitors differentiate into chondrocytes. The transcription factor Sox9, from the SRY-related high mobility family, is essential for the onset and regulation of the chondrocyte lineage (Bi *et al*., 1999). Sox9 recruits Sox5 and Sox6 and forms a trio that are required for the regulation of subsequent chondrocyte differentiation by binding and activating genes for cartilage-specific extracellular matrix components such as collagen type II and XI and aggrecan, and specifying cell fate (Han and Lefebvre, 2008).

1.2.3.2 Endochondral ossification

Fibroblast-like chondrocytes proliferate and organise into columns, at which point proliferation ceases and chondrocytes differentiate into rounded prehypertrophic chondrocytes, synthesising molecules such as collagens type II, IX and XI and aggrecan. A cartilage template is then formed surrounded by the perichondrium (Bobick and Kulyk, 2008). Msx1 and 2 (Msh homeobox 1 and 2), β-catenin, Lef1 (Lymphoid enhancer binding factor 1), AP1 and 2 (Activator protein 1 and 2) and Runx2 are also implicated in chondrogenic differentiation

and skeletal patterning (Bobick and Kulyk, 2008). Cartilage calcification is mediated by the secretion of matrix vesicles by mature hypertrophic chondrocytes (Tsang *et al*., 2015). A bone collar is formed around the hypertrophic zone by the secretion of bone matrix from perichondrial cells that have differentiated into osteoblasts. Osteoblasts and bone matrix organise into a periosteum which later forms the diaphysis of the bone (Figure 1.3) (Tsang *et al*., 2014).

Vascularisation of the calcified cartilage occurs at E14.5 in mice with the development of the primary ossification centre (POC). This brings osteoblasts and chondroclasts which produce proteolytic enzymes that degrade the mineralised cartilage ECM and replace it with bone matrix to form trabecular bone (Tsang *et al*., 2015, Akkiraju and Nohe, 2015). The chondro-osseous junction forms and divides the cartilage template into two epiphyses encompassing the growth plate (Tsang *et al*., 2015). The epiphyseal growth plate is therefore divided into four different anatomical zones based on the morphological and biochemical properties of the cells each zone inhabits (Ballock and O'Keefe, 2003).

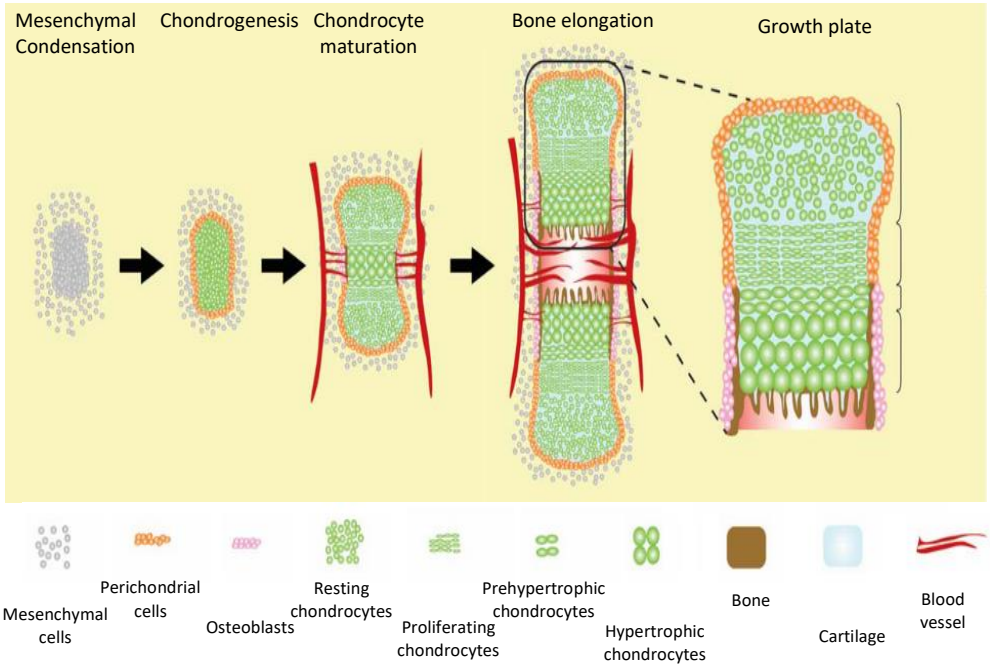

Figure 1.3. The process of endochondral ossification. Endochondral bone formation begins with mesenchymal cells aggregating at the site of future bone. Mesenchymal cells at the centre of the condensation differentiate into chondrocytes and synthesis cartilage matrix. Chondrocytes then undergo proliferation and hypertrophy, while adjacent perichondrial cells differentiate into osteoblasts and deposit bone matrix. Vascularisation of the calcified cartilage occurs which brings osteoclasts/chondroclasts and degrade the cartilage matrix, which is replaced with bone. (Adapted from Tsang *et al.* 2014).

1.2.3.3 ATDC5 cells

Our understanding of the underlying mechanisms of chondrogenesis and endochondral ossification has been facilitated by utilising chondrocytic cell lines (Newton *et al.,* 2012). ATDC5 cells are a commonly used model for *in vitro* research of chondrocyte development as Atsumi (1990) reported they undergo a well-characterised cellular condensation stage, sequential chondrogenic differentiation and mineralisation when treated with insulin (Figure 1.4) (Shukunami *et al.,* 1997).

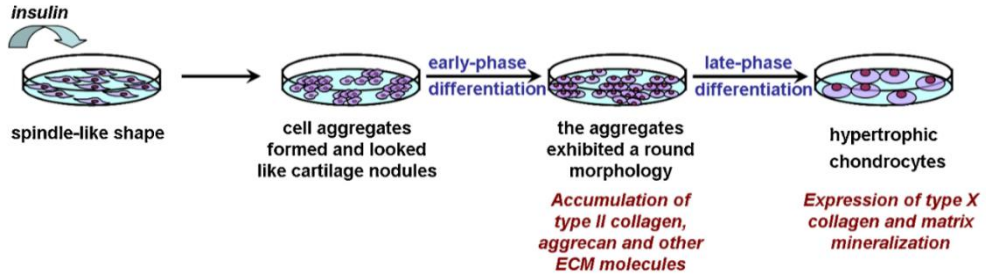

Figure 1.4. Schematic diagram depicting ATDC5 differentiation during chondrogenesis. ATDC5 cells treated with insulin undergo condensation and express collagen type II and aggrecan. As cells become hypertrophic during differentiation collagen type X is expressed, followed by matrix mineralisation (Taken from Yoa and Wang, 2013).

ATDC5 cells rapidly proliferate meaning large amounts of cells can be obtained for *in vitro* culture systems and during expansion are maintained in an undifferentiated state. Upon treatment of ATDC5 cells with insulin, cells undergo condensation and then exhibit a chondrocyte phenotype with the expression of collagen type II and aggrecan. Collagen type X is then expressed as the chondrocytes become hypertrophic, followed by mineralisation (Yao and Wang, 2013). This cell line is therefore an ideal model to study the molecular mechanisms occurring during chondrogenesis.

1.2.3.4 Transcription Factors

Endochondral ossification and skeletal development is regulated by several transcription factors including Sox9 and Runx2 (Amano *et al.,* 2009; Yoshida *et al., 2004*). Transcription factors control the transcriptional rate of target genes from DNA to mRNA by binding to specific DNA sequences. Abnormal expression of these transcription factors has also been implicated in the development of cartilage pathology such as osteoarthritis (Zhang and Wang, 2015).

1.2.3.4.1 Sox9

SRY-box 9 (Sox9) is a HMG-box-containing transcription factor that is critical for the differentiation of mesenchymal progenitor cells into chondrocytes during cartilage morphogenesis (Bi *et al*., 1999). Sox9 is a master transcription factor during chondrogenesis and acts on cis-elements within many genes encoding cartilage matrix proteins promoting their transcription (Lefebvre and Dvir-Ginzberg 2017). Genes regulated by Sox9 include aggrecan, collagen XI and Col2a1, often via cartilage specific enhancer elements such as that located within the first intron of the mouse Col2a1 gene (de Crombrugghe *et al*., 2000, Lefebvre *et al*., 1997, Sekiya *et al*., 2000). Haploinsufficiency of Sox9 results in an autosomal dominant human disease called campomelic dysplasia, were inadequate chondrocyte differentiation causes severe skeletal malformations such as shortening and bowing of the long bones and scoliosis (Wagner *et al*., 1994, Foster *et al*., 1994). It has also been demonstrated that Sox9 is required for cartilage formation in mouse embryonic stem cell chimeras in which Sox9-deficient cells were unable to express chondrocyte-specific extracellular matrix genes and therefore were unable to differentiate down the chondrogenic lineage (Bi *et al*., 1999). Furthermore, mouse embryos containing a conditional homozygous deletion of Sox9 present with defective joint formation and severe generalised chondrodysplasia (Akiyama *et al*., 2002). Sox9 overexpression also resulted in skeletal disorder as a result of a suppression of chondrocyte hypertrophy, a delay in terminal differentiation and subsequently a delay in ossification (Kim *et al.* 2011). Together these studies indicate that dosage of Sox9 is important for normal chondrocyte function. A previous study also demonstrated that retroviral transduction of Sox9 could improve the

phenotype of dedifferentiated human articular chondrocytes from osteoarthritis patients (Tew *et al.* 2005).

Decreased Sox9 expression is a hallmark of human osteoarthritis (Lee and Im, 2011). Interestingly, an inducible cartilage-specific deletion of Sox9 in postnatal mice did not result in the onset of osteoarthritis by 18 months of age. These mice did, however, present with disruptions to cartilage homeostasis of the growth plate, the articular cartilage and the intervertebral discs of the spine (Henry *et al*., 2012). Sox9 is also subject to post-transcriptional regulation and its mRNA has been reported to be unstable with a short half-life in chondrocytic cells (Tew and Hardingham 2006). The micro RNA, mi-145, has been shown to directly target Sox9 and inhibit its expression in human chondrocytes (Martinez-Sanchez *et al*., 2012). Inhibiting Sox9 via mi-145 results in reduced expression of Col2a1 and aggrecan, and an increase in the expression levels of MMP13 - a known marker of osteoarthritis (Martinez-Sanchez *et al*., 2012). These studies highlight the importance of Sox9 as an essential transcription factor during the sequential steps of the chondrocyte differentiation pathway.

1.2.3.4.2 Runx2

Runx2 is an essential transcription factor that regulates hypertrophic chondrocyte differentiation in late stage endochondral ossification and bone formation, and has been shown to regulate markers of endochondral ossification including Indian hedgehog (Ihh), Col10a1 and MMP13 (Komori, 2010). Total Runx2 deficiency in mice results in neonatal lethality due to a complete lack of bone formation as a result of an absence of osteoblast differentiation and a delay in chondrocyte maturation (Komori *et al.* 1997). Runx2 expression levels are increased in human osteoarthritis cartilage (Zhong *et al.* 2016), and an overexpression of Runx2 in chondrocytes has been shown to increase expression levels of the matrix-degrading enzymes including MMP13 and ADAMTS5 via a direct interaction with their promoters (Tetsunaga *et al.* 2011).

1.2.3.4.3 Nfat1

Recent studies suggest that NFAT1, a member of the Nuclear Factor of Activated T-cells (NFAT) transcription factor family, regulates chondrocyte functions through its age-dependant expression in articular cartilage and plays an important role in maintaining the permanent cartilage phenotype in mice (Zhang and Wang, 2015). Epigenetic studies have also suggested that dynamic histone methylation regulates the age-dependant NFAT1 expression in articular chondrocytes (Rodova *et al*., 2011). *Nfat*-deficient mice present with a phenotype that is comparable to osteoarthritis with phenotypes including articular cartilage degradation and chondrocyte clustering, chondro-osteophyte formation and thickening of the subchondral bone (Wang *et al*., 2009).

1.2.3.4.4 Prx1

The paired-related homeobox genes *Prx1* and *Prx2* are expressed in the early limb bud mesenchyme and function as transcriptional coactivators (Martin *et al*., 1995). Prx1 plays a major role in chondrogenesis and patterning of the developing skeleton in mice and chick embryos, with expression studies revealing that Prx1 is primarily expressed in undifferentiated mesenchyme and regulates skeletal development of the limb via bone morphogenetic protein (BMP) signalling pathways (Kuratani *et al*., 1994, Nohno *et al*., 1993, Cserjesi *et al*., 1992). Prx1-null mice display severe defects in the developing skeleton including deformities in the craniofacial, appendicular and axial structures, supporting the idea that Prx1 plays a role in the regulation of skeletal primordia growth (Martin *et al*., 1995).

1.2.3.5 Hox genes in axial skeleton development

Transcription factors are vital to the process of pattern formation throughout the axial and appendicular skeleton. During embryonic development, members of the homeobox (Hox) transcription family are expressed in distinct spatial and temporal patterns prior to mesenchymal differentiation. Hox genes are a family of 39 highly conserved transcription factors that control axial patterning and integration of the musculoskeletal tissues and one of the major functions of these genes is to provide a specific identity to segmental units of the embryo.

(Mallo *et al.* 2010). The genes in each cluster are further subdivided into 13 paralogous groups based on sequence similarity and the similarity in expression domains The co-linear arrangement of these genes along the chromosome, arranged on four chromosomal clusters HoxA-D, reflect their spatial and temporal expression along the anterior-posterior (AP) axis of the body, with genes located in the 5' region of the cluster being expressed posteriorly while genes in the 3' region are expressed in the anterior regions (Graham *et al.* 1989, Pineault and Wellik 2014). Transcriptional and post-transcriptional mechanisms can also regulate Hox gene expression at multiple levels (Mallo and Alonso, 2013).

1.2.3.5.1 Craniofacial development

The vertebrate craniofacial skeleton and the pharyngeal skeleton are derived from cranial neural crest cells (CNCCs) (Creuzet *et al.* 2005). Hox genes encode the major inhibitors of the craniofacial program carried by CNCCs, with their inhibition essential for proper jaw formation (Couly *et al.* 2002).

Mice that are homozygous for a targeted mutation of Hoxa2 are born with cleft palates and display severe craniofacial abnormalities including a duplication of the ossification centres of the bones of the mid-ear and a mirror-image duplication of the lower jaw (Gendron-Maguire *et al.* 1993). Single mutants in Hox5 and Hox6 paralogous groups resulted in abnormal phenotypes at the cervicothoracic transition (McIntyre *et al.* 2007).

1.2.3.5.2 Lumbar column and rib development

Previously, it has been suggested that *Hox* paralogous groups play a dominant role in controlling the specification of characteristic morphologies of specific anatomical regions of the vertebral column. Compound mutants of the *Hox10* paralogous group first described *Hox* genes in their regional patterning along the AP axis (Wellik and Capecchi, 2003). Mice with combination deletions of the three Hox10 genes resulted in the development of extra ribs along the thoracic-lumbar region suggesting Hox10 genes are involved in supressing rib development in normal skeletal development. In contrast, ectopic expression of Hoxa10 in the paraxial mesoderm of mice resulted in no rib formation

(Carapuço *et al.* 2005). Phenotypic defects have been noted in mutants for Hox genes from *Hox5-9* with sternal versus floating rib production being controlled by *Hox9* genes (McIntyre *et al.* 2007). Inactivation of *Hox6* in mice resulted in smaller rib cages with an abnormal phenotype, including the loss of the first rib and distal fusions of ribs associated to thoracic vertebrae 2 to 4 (Figure 1.5) (McIntyre *et al.* 2007).

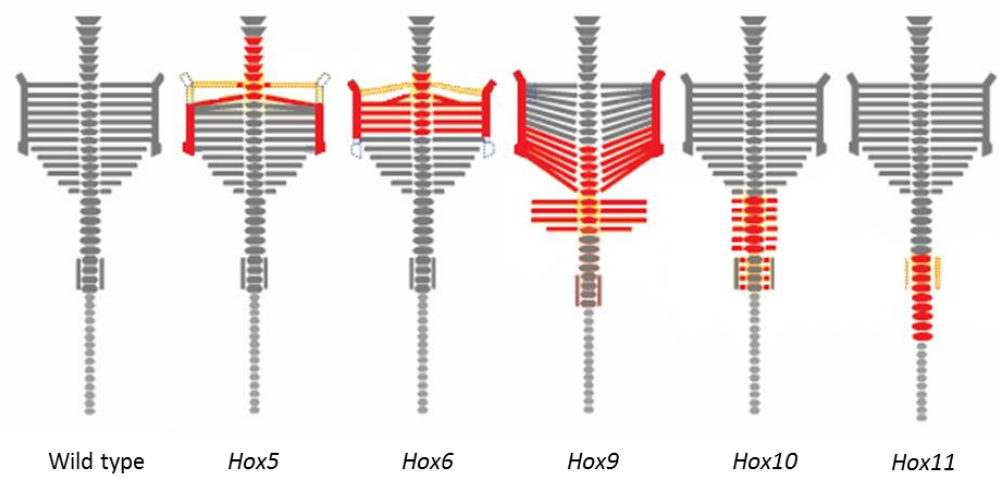

Figure 1.5. Schematic diagram comparing phenotypes and affected regions of Hox paralogous deficient mice (red). Each *Hox* paralogous group mutant has a unique morphological characteristic in the vertebrae despite overlapping of affected regions between mutants. Adapted from (McIntyre *et al.,* 2007).

1.2.3.6 Hox genes in limb bud development

The vertebrate limb is divided into three segments: 1) the proximal stylopod, which includes the humorous and femur, 2) the medial zeugopod that includes the radius/ulna in the forelimb and tibia/fibula in the hindlimb, and 3) the distal autopod including the paw bones and digits (Pineault and Wellik, 2014). The HoxA and HoxD clusters have major roles during limb development and contribute to the specification of these regions in both the forelimb and hindlimb. During limb bud development from the lateral plate mesoderm, HoxD

genes are activated by remote enhancers that are located within two gene deserts flanking the cluster.

The initiation of Hox gene expression occurs very early in limb bud development with the posterior Hox genes expressing in overlapping patterns. Hox paralogs, Hox9-13 pattern the limb skeleton along the proximal-distal axis. As limb bud development progresses Hox paralogous groups become restricted to their appropriate functional domains. In this instance Hox9 and Hox 10 are restricted to the stylopod, Hox11 in the zeugopod and Hox13 in the autopod (Figure 1.6) (Davis *et al.* 1995, Fromental-Ramain *et al.* 1996).

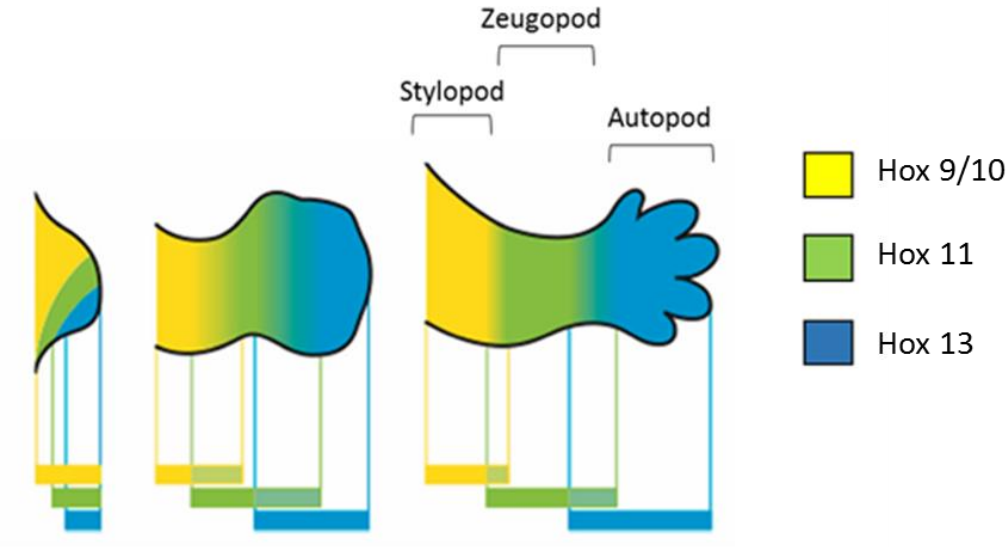

Figure 1.6. Schematic representation of the limb bud development. Hox paralogous are progressively restricted to specific limb regions during development. *Hox9-13* are expressed in an overlapping fashion early in the developing limb bud. *Hox9/10* are restricted to the developing stylopod, *Hox11* to the zeugopod and *Hox13* in the autopod. (Adapted from Pineault and Wellik, 2014).

Skeletal development is disrupted in the absence of Hox genes (Newman and Wallis, 2003). E15 double mutants deficient for both HoxA and HoxD result in a severely truncated single cartilage model in the forelimbs with a lack of autopod development, while in mutant new-borns ossification resulted in a single bone rod with no zeugopod development (Kmita *et al.* 2005).

1.3 Osteoarthritis

Osteoarthritis is the most common and chronic form of degenerative joint disease and a major cause of severe pain and disability for those affected (Martel-Pelletier *et al.,* 2016). Pathological changes that occur in osteoarthritic joints include the progressive destruction and loss of articular cartilage, a thickening of the subchondral bone, osteophyte formation, inflammation of the synovium, hypertrophy of the joint capsule and the degeneration of the ligaments and menisci of the knee (Chen *et al.,* 2017; Rahmati *et al*., 2017). The main clinical symptoms for patients presenting with osteoarthritis include chronic pain, joint instability, stiffness and a radiographic joint space narrowing (Chen *et al.,* 2017). There are several risks associated with the onset and progression of osteoarthritis including genetic predisposition, obesity, prior joint injury and, most commonly, aging (Yucesoy *et al.,* 2015).

Family based studies, linkage analysis and association studies have extensively investigated the genetic contribution to osteoarthritis, with an estimate of heritability of 40% being reported for the knee (Yucesoy *et al.,* 2015). Over 80 gene mutations or single-nucleotide polymorphisms (SNPs) have recently been confirmed as being associated with osteoarthritis pathogenesis via genome-wide association studies performed on large number of osteoarthritis and control populations throughout the world (Chen *et al.,* 2017). These include mutations or SNPs in genes important for structural factors including collagen type II and those involved in the TGF-β signalling pathway including Smad3 (Chen *et al.,* 2017). Genetic association studies have also helped identify the effects of specific gene variants on osteoarthritis pathogenesis, however they have also identified the need for more genetic linkage studies to be carried out

in order to identify the chromosomal regions involved in the disease process (Yucesoy *et al.,* 2015).

Obesity is currently a worldwide epidemic and it has long been recognised that there is an association between obesity and osteoarthritis (Felson *et al.,* 1988). Patients with obesity develop osteoarthritis earlier and have more severe symptoms and a higher risk for infection. Additionally, obesity contributes to low-grade systemic inflammation through the secretion of adipokines as a result of an increase in biomechanical loading on the knee joint. For example, in high-fat diet-inducted mouse obesity models and in obese patients, levels a pro-inflammatory cytokines, including IL-1β, IL-6 and TNF-α were elevated (Chen *et al.,* 2017).

Knee injury increases the risk for osteoarthritis more than four times and is the major cause of knee osteoarthritis in young adults, with a reported 41-51% of patients with prior knee injury presenting with radiographic signs of knee osteoarthritis in later years (Roos, 2005). The most common injuries that may lead to osteoarthritis are cartilage tissue tear, joint dislocation and ligament strains, all of which can negatively affect joint stability (Blalock *et al.,* 2015). In both mouse injury models and patients with traumatic knee osteoarthritis there are signs of inflammation of the joint, including an increase in cytokine and chemokine production, inflammatory cell infiltration, synovial tissue expansion and NF-κβ pathway activation (Lieberthal *et al.,* 2015).

Chronic low-grade inflammation contributes to the development and progression of osteoarthritis (Scanzello *et al.,* 2017). During the progression of osteoarthritis, the entire synovium joint, including the cartilage, subchondral bone and the synovium, are involved in the inflammation process, with inflammatory factors such as IL-1β and TNF-α, as well as chemokines, contributing to the systemic inflammation that leads to the activation of the NF-κB signalling pathway in both synovial cells and chondrocytes. Evidence that inflammation signals contribute to osteoarthritis pathogenesis comes from the recent Kyoto Encyclopaedia of Genes and Genomes (KEGG) pathway analysis, which found that inflammation occurs through cytokine-induced mitogen-

activation protein (MAP) kinases, NF-κB activation and oxidative phosphorylation (Li et al., 2014).

Aging, however, is the most prominent risk factor associated with osteoarthritis. Half of all people aged over 65 years develop osteoarthritis, with incidence rates being substantially higher in females than males (Sulzbacher, 2013, Kopec *et al*., 2010). Patients usually present with an increase in the prevalence of pain, joint dysfunction and stiffness (Buckwalter *et al*., 2004). In addition to cartilage, aging affects other joint tissues, including synovium, subchondral bone and muscle, which is thought to contribute to changes in joint loading (Chen *et al*., 2017). Aging causes chondrocytes to increase production of inflammatory cytokines, alongside a reduction in repair response (Kuyinu *et al*., 2016).

Osteoarthritis is now considered a disease of the whole joint as an organ and changes in gene expression and signalling pathways aid in the pathogenesis and progression of osteoarthritis (Loeser *et al*., 2012, Tew *et al*., 2014). Potential therapies for osteoarthritis may affect the different stages of disease differently and so it is important to determine these stages (Figure 1.7) (Poulet, 2017).

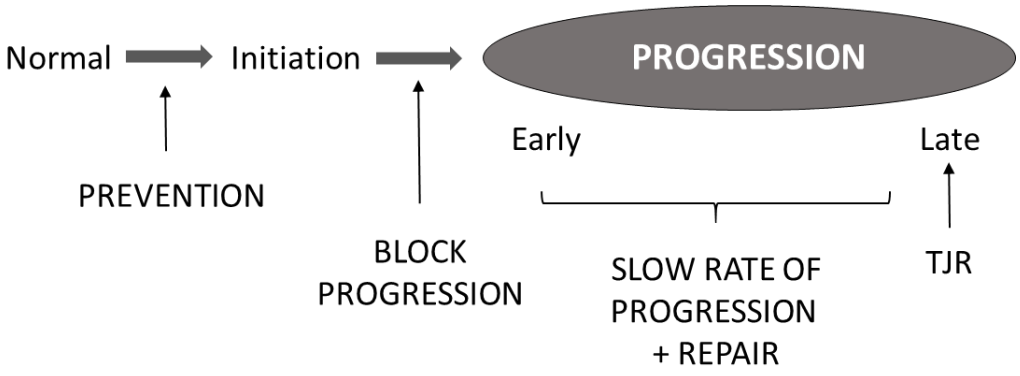

Figure 1.7. The stages of osteoarthritis progression and potential therapy target points. Prevention therapy can be targeted to events that would usually increase stress on the joint over time. Targeted approaches to early stage of progression would be more successful than targeting late stage disease, were the only treatment maybe total joint replacement (TJR). (Adapted from Poulet, 2017).

1.3.1 Osteoarthritis pathogenesis

The initial stage of osteoarthritis is characterised by a repair response mediated by growth factors acting upon the chondrocytes. This stage marks the beginning of osteoarthritis but may not manifest clinically for many years (Sulzbacher, 2013). One of the earliest pathological changes after the onset of osteoarthritis occurs under mechanical stress when chondrocytes become activated and start to synthesise IL-1α and IL-1β, TNF-α and prostaglandins, which promote catabolic activity and can lead to differences in the appearance of the articular cartilage of the joint (Loeser *et al*., 2012, Sulzbacher, 2013).

The production of collagen type X by hypertrophic chondrocytes in the early stages of osteoarthritis, marks the terminal differentiation of chondrocytes that regulates the expression of proteolytic enzymes such as MMPs and ADATMTS' which degrade the proteoglycan and collagen network (Akkriaju *et al.,* 2015). The major drivers in the onset of osteoarthritis are therefore the degradation of both aggrecan and collagen by these proteases (Troeberg and Nagase, 2012)

Abnormal remodelling and a thickening of the subchondral bone occurs at later stages of disease progression which subsequently leads to the formation of osteophytes that serve to correct instability in the joint caused by osteoarthritis (Figure 1.8) (Kuyinu *et al*., 2016). Other pathological changes include inflammation of the synovium and the degradation of ligaments and the menisci (Figure 1.8) (Loeser *et al*., 2012). Prolonged mechanical stress on the articular cartilage can also cause chondrocytes to release vascular endothelial growth factor (VEGF) which can lead to vascularisation of the synovium and vascular invasion of the calcified cartilage (Sulzbacher, 2013).

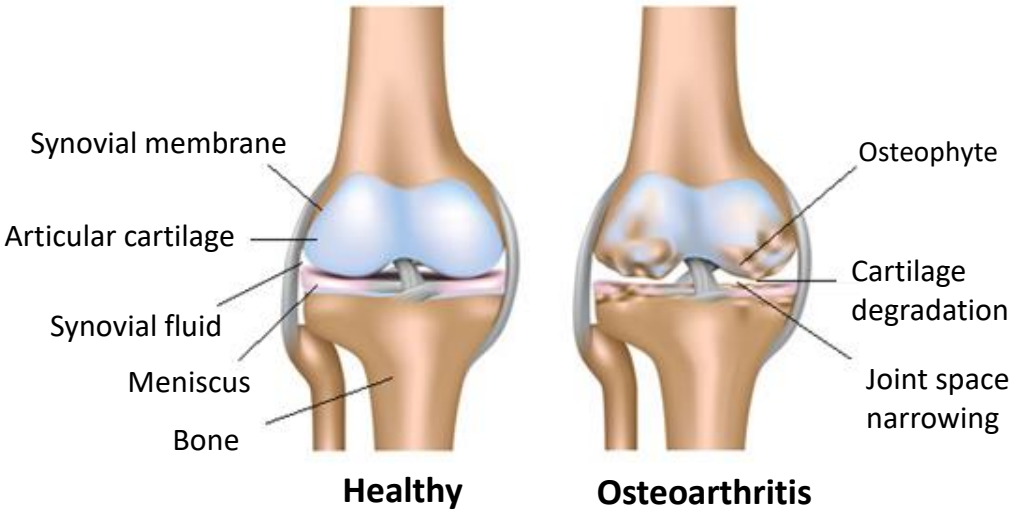

Figure 1.8. Healthy knee joint vs osteoarthritic knee joint. Characteristic features of osteoarthritis are shown including cartilage degradation, osteophyte formation and joint space narrowing.

In healthy tissue chondrocytes remain in a quiescent state, with limited turnover of cartilage matrix. At the onset of disease, chondrocytes are activated and undergo cellular proliferation and increase their production of matrix proteins and matrix-degrading enzymes. Matrix-degrading enzymes are members of the matrix metalloproteinase (MMP) family and include aggrecanases, collagenases, serine and cysteine proteinases (Troeberg and Nagase, 2012).

1.3.1.1 Aggrecanases

Loss of aggrecan forms part of the initial changes in the cartilage extracellular matrix as osteoarthritis develops. Although this is a reversible process, loss of aggrecan leads to a reduction in tissue hydration and produces an environment were irreversible breakdown of the collagen network can occur (Verma and Dalal, 2011). The ADAMTS enzymes (A Disintegrin And Metalloproteinase with ThromboSpondin motifs) are a family of metalloproteinases that are involved in developmental and homeostatic processes (Kelwick *et al.* 2015). Several members of the ADAMTS family, including ADAMTS-1, ADAMTS-4, ADAMTS-5,

ADAMTS-8 and ADAMTS-9 have been shown to degrade aggrecan at a specific Glu-Ala site in the integlobular domain between the N-terminal G1 and G2 globular regions (Fosang *et al.* 2008, Stanton *et al.* 2011), forming a sub family of enzymes known as aggrecanases.

ADAMTS-5 has been established as the major aggrecanase in healthy and osteoarthritic mouse cartilage. ADAMTS-5 deficient mice are protected from aggrecan loss and cartilage erosion in both inflammatory and non-inflammatory models of arthritis (Glasson *et al.* 2005, Stanton *et al.* 2005). In normal cartilage, a tight regulation of ADAMTS-5 is crucial for maintaining a fine balance between aggrecan anabolism and catabolism. In this case, ADAMTS-5 is regulated by tissue inhibitor of matrix metalloproteinases (TIMPs) but during osteoarthritis the ADAMTS-5/TIMP balance is shifted in favour of catabolism (Malfait *et al.* 2002).

TIMPs are important regulators of ECM turnover, tissue remodelling and cellular behaviour due to their function as endogenous inhibitors of MMPs, and in some instances, of ADAM and ADAMTS (Brew *et al.,* 2010). TIMPs are also involved in various biological processes, many of which are independent of MMP inhibition, including cell proliferation, anti-angiogenic, pro-and anti-apoptotic and synaptic plasticity activities (Brew *et al.,* 2010). There are four paralogous genes encoding TIMPs-1 to -4. While all four TIMPs inhibit MMPs, they each have varying affinities for different inhibitor-protease pairs (Murphy *et al.,* 2011). TIMP-3 inhibits several members of the ADAM and ADAMTS families, giving it the broadest inhibition spectrum, and also differs from the others in being tightly bound to the ECM. In mice, global deletion of TIMP3 causes lung emphysema-like alveolar damage and faster apoptosis of mammary epithelial cells after weaning, suggesting that TIMP3 is a major regulator of MMP activity *in vivo* (Leco *et al.,* 2001). TIMP3 also regulates the processing of TNF-α by ADAM17, therefore playing a key role in innate immunity (Murphy *et al.,* 2011).

1.3.1.2 Matrix metalloproteinases

MMPs participate in the onset of osteoarthritis via the degradation of collagen (Troeberg and Nagase 2012). MMPs are zinc-dependant enzymes that play a

critical role in the degradation of all types of ECM proteins including proteoglycans and collagen, a process central to the pathology of osteoarthritis (Troeberg and Nagase, 2012). In normal articular cartilage, chondrocytes maintain an equilibrium in which the rate of matrix synthesis equals the rate of degradation, which is maintained by TIMPs (Cawston and Young 2010). Among other matrix-degrading enzymes, including ADAMTSs, MMPs are synthesised at low levels as inactive proenzymes that require enzymatic cleavage to become activated, thus contributing to the maintenance of homeostasis (Cawston and Young, 2010). In osteoarthritis however, there is a change to this steady state which can cause inflammatory cytokines such as interleukin-1 beta (IL-1β) and tumor necrosis factor-alpha (TNF-α) to stimulate the activation and production of proteolytic enzymes and can disrupt the MMP (or ADAMTS)/TIMP balance and lead to breakdown of the cartilage matrix (Burrage *et al*., 2006).

MMPs are classified into four major groups, based upon the ECM substrates that they cleave: collagenases, gelatinases, stromelysins and membrane type MMPs (MT-MMPs) (Cawston and Young, 2010). MMP-2 and MMP-9 are gelatinases whose protein levels are increased in the synovial fluid and tissues of patients suffering from rheumatoid arthritis (Yoshihara *et al*., 2000). MMP-3 (or Stromelysin-1) is a stromelysin that is expressed in cartilage and upregulated during osteoarthritis (Chen *et al.* 2014). Other stromelysins include MMP-7, -10 and -11, which act upon proteoglycans, fibronectin and laminin (Knäuper *et al*., 1993). MT-MMPs include MMP -14 to -17 and MMP-24 and contain a transmembrane and intracellular domain that anchors them to the cell surface (Verma and Hansch, 2007). The collagenases consist of MMP-1, -8 and -13 which cleave native fibrillary collagens, but differ in their specificity for different collagens. MMP-1 and MMP-8 cleaves collagen type III and I respectively, while MMP-13 cleaves collagen type II (Poole *et al*., 2002, Burrage *et al*., 2006)

1.3.1.2.1 MMP13

MMP13 is thought to be the collagenase that plays the greatest role in the pathology of osteoarthritis with an increase in its expression in the cartilage of patients suffering from the disease (Wang *et al.* 2013). While MMP13 is highly efficient at degrading collagen type II, it also degrades proteoglycans, collagens

type IV and IX, osteonectin and perlecan (Wang *et al*., 2013, Goldring, 2012). Global knockout of MMP13 in mice demonstrated marked defects in the growth plate cartilage with an increase in the hypertrophic zone and delayed ossification (Takaishi *et al*., 2008). Transgenic mice that overexpress MMP13 specifically in the cartilage develop a phenotype of cartilage degradation that strongly resembles that found in osteoarthritis, while cartilage degradation in MMP13 deficient mice is inhibited even in the presence of aggrecan depletion (Little *et al*., 2009, Neuhold *et al*., 2001). MMP-13 activity has therefore been implicated as the main collagenolytic activity in osteoarthritis progression.

1.4 Animal models of osteoarthritis

Large-scale gene expression studies have showed changes in gene expression in late stage osteoarthritis using human cartilage from end stage disease (Geyer *et al*., 2009; Loughlin, 2015). For example, the arcOGEN consortium has been the most powerful osteoarthritis genome-wide association study to date, with the analysis of over 7400 cases of osteoarthritis (arcOGEN, 2012). This study highlighted a number of biological pathways conferring genetic susceptibility to osteoarthritis. However, it remains very difficult to obtain human tissue from various stages of osteoarthritis and pair it with age-matched control tissue. Animal models therefore provide a powerful research tool to allow the study of osteoarthritis pathogenesis and progression under controlled conditions were the onset of disease and stages can be better defined and evaluated (Little and Zaki, 2012; Loeser *et al*., 2013).

In vivo animal models are used to study the pathogenesis of osteoarthritis and the therapeutic potential of treatment modalities (Lampropoulou-Adamidou and Lelovas, 2014). Animal models provide genetically controlled tissue samples that are age-matched to study the pathogenesis of osteoarthritis. Osteoarthritis models have been developed in both small and large animals; however the most commonly utilised animal model remains the mouse for several reasons. These include the similarities to human osteoarthritis in the natural progression of the disease, the scope for genetic modification, as well as the short timescale over which mice develop osteoarthritis and/or age and the low cost compared

to larger animals (McCoy, 2015). Osteoarthritis is variable in both etiology and treatment and outcomes for patients (Blalock *et al*., 2015). There are a variety of routes to end stage osteoarthritis and they may represent a spectrum of diseases with the same endpoint. It is therefore important that osteoarthritis is classified into various clinical phenotypes and as such, classify the animal models of osteoarthritis into groups and sub-groups that share a relationship with the human osteoarthritis phenotypes (Figure 1.9) (Kuyinu *et al*., 2016).

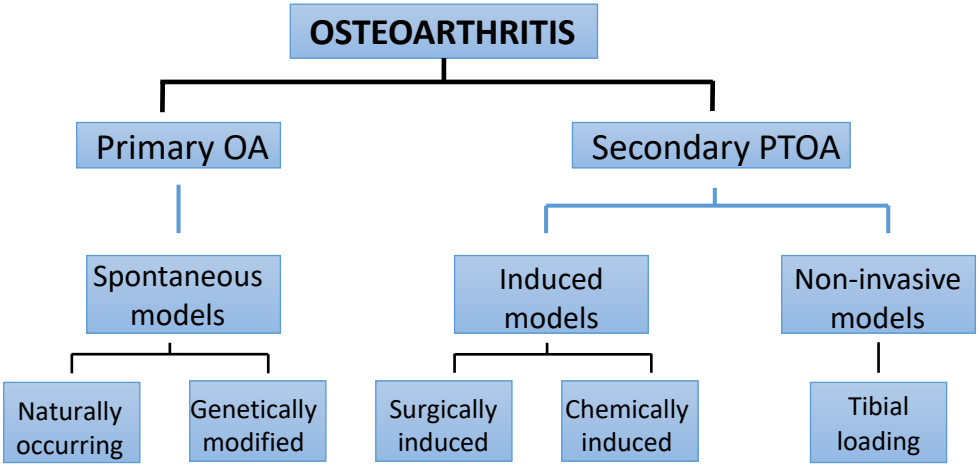

Figure 1.9. Animal models that replicate human primary osteoarthritis and secondary post-traumatic osteoarthritis in vivo. Typically, osteoarthritis is classified into primary and secondary osteoarthritis based on disease etiology. Primary osteoarthritis is naturally occurring while secondary post-traumatic osteoarthritis is usually associated with risk factors and causes leading to osteoarthritis, for example trauma. (OA: Osteoarthritis, PTOA: Post-traumatic osteoarthritis). Adapted from (Kuyinu *et al*., 2016).

1.4.1 Spontaneous models of osteoarthritis

The natural slow progression in human primary osteoarthritis is closely mimicked by the progression of osteoarthritis in certain animal models including the mouse, guinea pig and rabbit (Kuyinu *et al*., 2016). Osteoarthritis

is a degenerative disease and as such occurs predominantly in the elderly population, this aging is the major risk factor for spontaneous osteoarthritis; the most common form in humans (Chen *et al*., 2017). Several laboratory animals develop osteoarthritis spontaneously including the most common C57/BL6 strain, which develops osteoarthritic changes in the knee at 17 months of age with an incidence rate of 39-61% (Wilhelmi and Faust, 1976). These animal models are therefore valuable tools for studying natural OA pathogenesis (Chen *et al.,* 2017).

The STR/ort mouse is a well described model of spontaneous and naturally occurring osteoarthritis (Mason *et al*., 2001). In 1951, Strong isolated the STR/1N mouse strain during an extensive selective-breeding programme that was designed to identify traits for resistance to tumour induction at the site of injected carcinogens (Strong, 1944). Subsequent strains were treated with the carcinogen 20-methylcolanthrene for multiple generations creating the NHO strain. This was further treated with the carcinogen 4-methylcholantrene, which ended with the generation of the STR/1N strain, later renamed STR/ort, who exhibit obesity and spontaneous osteoarthritis at a young age (Staines *et al.,* 2017). STR/ort mice develop osteoarthritis in knee, ankle, elbow and temporomandibular joints and show progressive molecular changes in osteoarthritis that are comparable to human disease, including loss of hyaline cartilage, osteophyte formation and subchondral bone sclerosis. The severity of articular cartilage lesions in STR/ort mice increases with age, with early osteoarthritis histologically visible at 18 weeks of age and late stage visible at 40 weeks. Additionally, mild osteophytes had developed by 18 weeks compared to an increase in osteophyte maturation score by 40 weeks (Poulet *et al*., 2012). These mice, however, have a 50% greater body weight compared to other strains of mice, which may explain why osteoarthritis occurs at a much earlier stage (Mason *et al.,* 2001). A correlation between osteoarthritis and chondrocyte metabolism was discovered utilising the STR/ort mouse model. This study found an upregulation of Wnt signalling, which renders adult articular chondrocytes susceptible to premature aging and cell death and contributes to osteoarthritis pathogenesis (Pasold *et al*., 2013)

Spontaneous models serve as a useful tool for osteoarthritis research as they simulate the slow progression of osteoarthritis in humans. However, there are major drawbacks to these models, such as the cost and length of time required for osteoarthritis to develop. These models do not manifest osteoarthritis until maturity and therefore short-term studies are difficult. The variability of disease incidence and progression between individual animals is also a major drawback (Kuyinu *et al*., 2016; Fang and Beier, 2014).

1.4.2 Genetically modified models of osteoarthritis

The ability to develop transgenic (or genetically modified) mice has become a powerful and extensively utilised tool in osteoarthritis research and has allowed researchers to understand specific genetic contributions to the pathogenesis of the disease (McCoy, 2015). For example, mice deficient in the glycoprotein ADAM15 develop osteoarthritis more rapidly compared to wild type mice (Böhm *et al*., 2005). MMP13-knockout mice that had undergone DMM surgery (destabilisation of the medial meniscus) are resistant to articular cartilage degeneration, indicating that MMP13 is required for the structural cartilage damage present in osteoarthritis (Little *et al*., 2009).

1.4.2.1.1 Cre-LoxP recombination

Global and conditional gene deletions often result in embryonic lethality (Mak *et al*., 2011; Ghosh *et al*., 2009). To overcome these problems the Cre/loxP system was developed. Cre recombinase is a 38 kDa protein from the bacteriophage P1 that catalyses the recombination between two loxP recognition sites (Hamilton and Abremski, 1984). Opposite orientation of the two loxP sites mediate the inversion of the intervening DNA by Cre recombinase, while loxP sites in the same orientation mediate the excision of the intervening DNA leaving only one loxP sequence at the post-recombination site (Figure 1.10) (Nagy, 2000). LoxP sites located on different chromosomes can mediate a chromosomal translocation (Bouabe *et al.,* 2013). The first mouse *in vivo* experiments demonstrated that the Cre recombinase worked to recombine loxP sites in a mouse when expressed from a transgene (Lakso *et al*., 1992).

Some conventional knockout mutations lead to embryonic lethality which hinders the ability to see effect of such a knockout later in development. In order to circumvent this problem, conditional deletion or overexpression of genes has been utilised using the Cre/loxP system to target the function of genes in an inducible manner that controls temporal and tissue-specific expression of the gene (Cascio *et al*., 2014). A requirement for temporal control of Cre-mediated recombination is that the inducible Cre recombinase be activated only by an exogenous ligand, not endogenous ligands. The inducible Cre recombinases are fusion proteins that are fused to specific mutated estrogen hormone ligand binding domains (Cre-ER^{T2}), this allows the Cre recombinase to be kept in an inactive form in the cytoplasm. Upon binding to the exogenous estrogen ligand 4-hydroxytamoxifen, Cre recombinase translocates to the nucleus allowing for external temporal control of Cre activity, all without being activated by endogenous estrogen (Figure 1.10) (Feil *et al*., 1997; Indra., 1999; Jaisser, 2000).

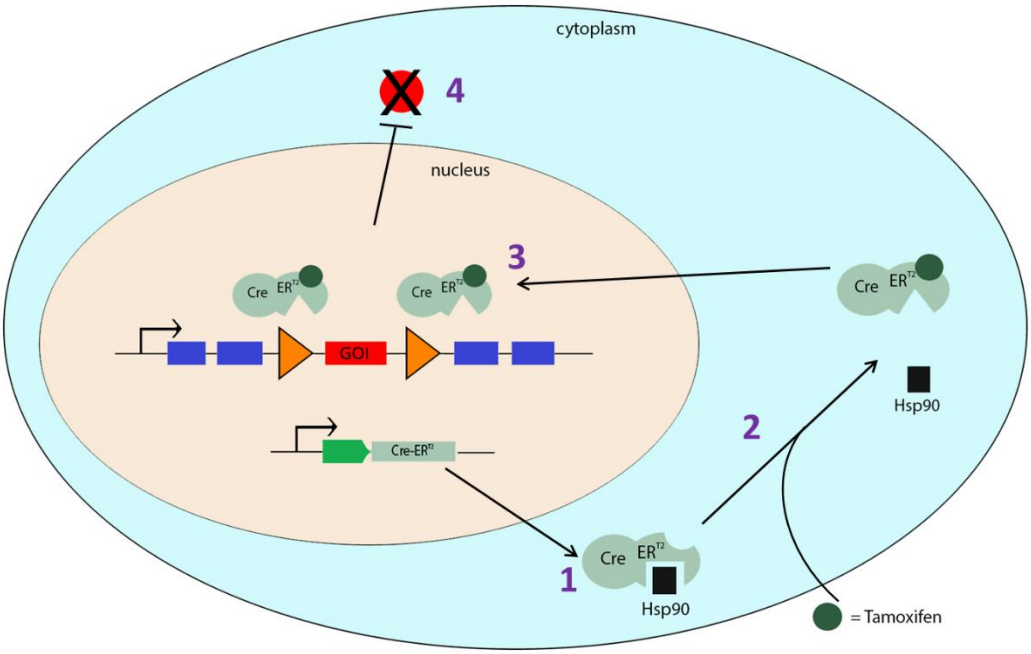

Figure 1.10. Schematic diagram of CreERT2-mediated loxP-deletion system in mice. The excision site for the gene of interest (GOI) is flanked by two loxP sites (orange arrows). The CreER^{T2} transgene is introduced into mice by crossbreeding. **(1)** The Cre is fused to mutated hormone-binding domains of the estrogen receptor with a G400V/M543A/L544A triple mutation. The CreER recombinases are inactive via binding to Hsp90, but can be activated by the synthetic estrogen receptor ligand 4-hydroxytamoxifen (OHT). **(2)** Upon treating the mice with tamoxifen, which is metabolised to OHT, the Cre recombinases become activated and move into the nucleus **(3)**. This allows for the excision of floxed chromosomal DNA in both a spatially and temporally manner **(4)**.

The key to utilising this system to look into the effects of a particular gene in a tissue-specific manner is to identify a regulatory element that can direct the expression of the Cre recombinase in the tissue of interest. The excision of floxed chromosomal DNA can be controlled both spatially and temporally by combining tissue-specific expression of the CreER^{T2} genes with tamoxifen-dependent activity in double transgenic mice and treating the mice with tamoxifen (Zhang *et al.*, 2012). Cre recombinase has been placed under several gene promotors to target chondrocytes. Collagen type II is an early marker of chondrogenesis and is expressed from E9.5 in mouse cranial mesenchyme; however the expression of *Col2a1* promoters do not become restricted to

cartilage until E12.5 (Davidson *et al.,* 2014). Transgenic mice were generated were Cre recombinase was driven by the *Col2a1* promoter, resulting in *Col2a1*-driven Cre-ER^{T2} mice (Zhu *et al*., 2008). These mice demonstrated deletion of the target gene in a cartilage-specific and tamoxifen-inducible manner with high efficiency (Chen *et al*., 2007). The aggrecan promoter, *A1*, is expressed in embryonic and adult cartilage, being mainly restricted to differentiated chondrocytes (Han and Lefebvre, 2008). This enhancer was a direct target of the SOX trio, were Sox9 was unable to bind without L-Sox5/Sox6 (Han and Lefebvre, 2008). This enhancer has since been used to generate a murine line that expresses both luciferase and Cre-ER^{T2} recombinase specifically in chondrocytes, allowing the expression of the transgene to be monitored in real time using luciferase as a visual aid (Cascio *et al*., 2014). Prx1-Cre mice were also developed were the Cre recombinase expression was placed under the control of a 2.4kb regulatory element from the Prx1 promoter that was sufficient to drive expression in undifferentiated mesenchyme in the developing limb bud and in craniofacial structures during embryonic development from as early as E10.5 (Martin and Olson, 2000; Logan *et al.,* 2002). A study utilising the Prx1 enhancer in Prx1CreER-GFP mice showed that transgene expression occurs in a subpopulation of periosteal cells and that these cells exhibit chondrogenic and osteogenic differentiation in culture, indicating that the transgene is expressed in osteochondro progenitor cells in the periosteum (Kawanami *et al.,* 2009). The development of mice harbouring a transgene under the influence of the Cre/loxP system allows researchers to carry out inducible gene knockout studies in cartilage tissues in a time-specific manner.

While genetically modified animals serve as a useful tool for studying osteoarthritis more rapidly than spontaneous models, many risk factors for human osteoarthritis may occur later in life. Similarly, genetic variations contributing to the risk of human osteoarthritis generally occur via mechanisms more subtle than complete gene inactivation, for example single nucleotide polymorphisms and epigenetic changes (SNPs) (Fang and Beier, 2014). Despite these limitations, mouse models have already contributed extensively to the understanding of cartilage biology, including the biology of normal joints and the mechanisms underlying osteoarthritis pathogenesis. In parallel to

technological advantages, the continued use of mouse models will continue to contribute to the underlying mechanisms of osteoarthritis and perhaps aid in the development of therapeutic interventions in the future.

1.4.2.2 Non-invasive model of post-traumatic osteoarthritis

Non-invasive models of osteoarthritis can initiate post-traumatic osteoarthritis and negate the need of any chemical or surgical intervention, which can cause inflammatory changes as a result of infection and relies on the ability of the researcher to consistently reproduce the surgery on all animals (Kuyinu *et al.,* 2016). These models cause injury to the joint through mechanical loading in a precise and reproducible manner, but without breaking the skin or disrupting the joint capsule. Advantages to using non-invasive models are that early adaptive processes, which occur immediately after injury, can also be investigated using non-invasive models, and these models more accurately mimic the mechanically-induced mechanisms involved in human osteoarthritis caused by injury (Christiansen *et al*., 2015)

Tibial compression involves subjecting mice to mechanical trauma via cyclic axial compressive loads that is applied to the lower leg through the ankle and knee joint, with loads transmitted through natural points of articulation and the contralateral joint remaining untreated as an internal control (de Souza *et al*., 2005). Tibial compression has been used to demonstrate the induction of focal cartilage lesions and to determine differences in the short and long-term effects on the integrity of articular cartilage after single or multiple loading sessions (Poulet *et al*., 2011). Results showed that cartilage injury can be induced after only one loading episode and that multiple loading episodes induces an osteoarthritis phenotype which includes proteoglycan loss and the formation of osteophytes that increase in severity and are restricted to the lateral femur (Poulet *et al*., 2011).

1.4.3 Induced models of post traumatic osteoarthritis

1.4.3.1 Destabilisation of the medial meniscus (DMM)

Tears to medial meniscus represent a major predisposing factor of joint instability and cartilage degradation in humans, and therefore the development

of osteoarthritis (Blalock *et al.,* 2015). The murine surgical model of destabilisation of the medial meniscus (DMM) is the most widely used model of post-traumatic osteoarthritis as it mimics clinical meniscal injury and has become a gold standard for studying the onset and progression of the disease (Culley *et al.,* 2015). DMM is performed by transection of the medial meniscotibial ligament (MMTL). Following the initial incision, the joint capsule on the medial side is incised using scissors to expose either the intercondylar region or the MMLT, which anchors the medial meniscus to the tibial plateau. The MMLT is cut, releasing the ligament from the tibial plateau thus destabilising the medial meniscus resulting in joint instability, resulting severity can vary between performing surgeons depending on the technique used (Culley *et al.,* 2015). This instability leads to cartilage degradation, osteophyte formation and subchondral bone sclerosis (Glasson *et al*., 2004). Changes at the histological level can be seen from 6 hours post-surgery and include changes in the expression levels of cartilage matrix proteases. This rapid induction of osteoarthritis allows studies to be performed in a relatively short time frame (Burleigh *et al*., 2012). When used simultaneously with genetically modified or engineered mouse models, DMM surgery allows the study of a given gene in osteoarthritis initiation and/or progression. In mice, it has been reported that sex hormones play a critical role in the progression of osteoarthritis in the DMM surgical model, with males presenting with more severe osteoarthritis than females (Ma *et al.,* 2007).

Examination of the roles of AdamTS4 and AdamTS5 were performed using the murine DMM model. These studies identified AdamTS5 as the primary aggrecanase in mice after AdamTS5-deficient mice were protected from cartilage degradation following DMM surgery, but AdamTS4-deficient mice were not (Glasson *et al*., 2005; Glasson *et al*., 2004). Syndecan-4, a transmembrane heparin sulfate proteoglycan that regulates mesenchymal cell function during tissue repair, has also been shown to be functionally involved in cartilage remodelling. It was reported that Syndecan-4 knockout in transgenic mice prevented osteoarthritic damage to cartilage after DMM-induced osteoarthritis (Echtermeyer *et al.,* 2009).

The mouse DMM model has also been used to examine gene expression profiles shortly after joint destabilisation, replicating what might happen after a medial meniscal tear in humans (Burleigh *et al*., 2012). Transcriptional analysis revealed changes in the regulation of extracellular matrix genes in late stage osteoarthritis (8 weeks post DMM surgery) induced by DMM (Gardiner *et al*., 2015). It has also been shown that male mice who had undergone DMM surgery presented with more severe osteoarthritis than their female counterparts, revealing a role for hormones and sex in the progression of osteoarthritis (Ma *et al*., 2007). The DMM model is therefore ideal for studying osteoarthritis pathophysiology and its underlying mechanisms due to its reliability and reproducibility (Kuyinu *et al*., 2016).

1.4.3.2 Chemically induced models of osteoarthritis

Rapid osteoarthritis progression can also be induced using intra-articular injection of chemicals. Among the most commonly used approaches is the injection of monoiodoacetate (MIA), an inhibitor of glycolysis that causes chondrocyte death, neovascularisation, necrosis of the subchondral bone and inflammation (Guzman *et al*., 2003). The initiating event and pathological changes, however, are not typical of human osteoarthritis and differences in the transcriptome of cartilage from MIA-induced arthritis and human osteoarthritis have been reported (Barve *et al.* 2007). Other approaches include injection of carrageenan, collagenase and sodium urate; however the resulting pathology from these alternative approaches are also not generally accepted as being representative of human osteoarthritis (van Osch *et al*., 1993). While chemically induced models of osteoarthritis result in a rapid induction of disease, these models are less clinically relevant than other osteoarthritis models due to vast differences in the cartilage transcriptome when compared to human osteoarthritis (Barve *et al*., 2007).

1.5 Post transcriptional regulation

While it is known that osteoarthritis is a multi-factoral disease of the joint, genetic factors contribute to the development and progression of the disease

(Vincent and Watt, 2018; Chen *et al*., 2015). Recent evidence suggests that epigenetic and post-transcriptional regulation of critical genes in articular chondrocytes and in patients with osteoarthritis may contribute to the development and progression of disease (Fernández-Tajes *et al*., 2014).

The post-transcriptional regulation of mRNA in articular chondrocytes is an efficient way to control the speed at which gene expression changes and appears to be important for sustaining cellular metabolism, coordinating chondrocyte maturation, stability and the degradation of RNAs, as well as maintaining the homeostasis of extracellular matrix synthesis (Bushati and Cohen, 2007; Tew and Clegg, 2010). To achieve correct spatial and temporal distribution of proteins, mRNAs are subjected to a complex array of regulatory controls during their transcription and translation. This can occur at a variety of levels including alternative splicing, transport, alternative polyadenylation and altered mRNA stability (Glisovic *et al*., 2008).

In the vast majority of genes, UTRs are important regulatory elements that play major roles in the post-transcriptional regulation of gene expression (Matoulkova *et al.,* 2012). In cooperation with various RNA-interacting factors, UTRs regulate mRNA stability, sub-cellular localisation, mRNA export to the cytoplasm and influence the total amount of synthesised protein during translation (García-Mauriño *et al.,* 2017). Primary mRNA transcripts are endonucleolytically cleaved and most acquire a poly(A) tail in a nuclear process known as mRNA 3’ end formation, a crucial step that is essential for the development of mature mRNA (Millevoi and Vagner, 2010). The 3’ end is cleaved at polyadenylation site (pA site) and the poly(A) tail is then attached to the primary transcript by poly(A) polymerase (PAP). Poly(A) binding protein (PABP) then recognises and binds to the poly(A) sequence, which requires a minimum of 27 adenines for stable 3’ end protection (Millevoi and Vagner, 2010). Polyadenylation is an important process that protects the 3’ end from degrading exonucleases and for the export of mRNA to the cytoplasm (Millevoi and Vagner, 2010).

UTRs possess a variety of cis-acting regulatory elements that are recognised by binding trans-acting elements. Their interplay is crucial for the post-

transcriptional regulation of gene expression (Matoulkova *et al.,* 2012). Adenylate uridylate (AU-rich) elements (AREs) are the most common regulation elements within the 3' UTR and are the major elements responsible for translational repression and mRNA destabilisation (Barreau *et al.,* 2005). Their presence is typical for short-lived mRNAs involved in early or transient regulatory responses (Matoulkova *et al*., 2012).

While the rate of transcription and translation controls mRNA and protein levels, the stability and rate of decay is also involved in its expression levels in a highly controlled manner and can be perturbed during osteoarthritis (Tew *et al*., 2014)

Many aspects of mRNA stability and translatability are controlled by regulatory molecules that interact with the transcript itself. These most commonly include RNA binding proteins (RBPs) and small non-coding RNAs such as microRNAs (miRNAs). Interactions with RNA binding proteins or miRNAs leads to transcripts existing as ribonucleoprotein complexes within the cytoplasm (Gerstberger *et al*., 2014; Wahl *et al*., 2009). RBPs and miRNAs interact specifically with the target transcript via nucleotide sequence and/or secondary structure. (Jiang and Coller, 2012). Both RBPs and miRNAs have been implicated in the pathogenesis of osteoarthritis in recent studies. A recent study by our group demonstrated for the first time how RNA binding proteins are able to post-transcriptionally regulate gene expression in human chondrocytes (McDermott *et al.* 2016). Human articular chondrocytes were isolated from osteoarthritic knees and, alongside the SW1353 chondrosarcoma cell line, were treated with siRNA to mediate the knockdown of RNA binding proteins. siRNA are dsRNA with 2nt 3' end overhangs that activate RNA interference (RNAi), leading to the degradation of mRNAs in a sequence-specific manner dependent upon complimentary binding of the target mRNA (Ambesajir *et al.,* 2012). qRT-PCR analysis revealed significant increases in SOX9 mRNA, mRNA half-life and protein expression when the RNA binding protein tristetraprolin (TTP) was knocked down, indicating that TTP contributes to SOX9 mRNA instability. This also resulted in a stimulation of aggrecan mRNA expression. MMP13 expression was also significantly increased upon HuR knockdown and a number of known

transcriptional repressors of MMP13 were found to be regulated by HuR. HuR therefore appears to act as an overall negative regulator of MMP13, particularly due to its influence on supressing the expression of RUNX2, SP1 and USF1, all transcriptional repressors of MMP13 (McDermott *et al.* 2016).

Recent studies have also identified miRNAs that are involved in many pathological conditions, including osteoarthritis, and are also involved in the post-transcriptional regulation of catabolic and anabolic mRNAs. MMP13 was also identified as a direct target of miR-411 in chondrocytes and an overexpression of miR-411 led to an inhibition of MMP-13 expression (Wang *et al.* 2015).

1.5.1 Micro RNAs

Micro RNAs (miRNAs) are endogenous non-coding RNAs that have been implicated in the negative regulation of protein expression and RNA stability (Chen *et al*., 2015). miRNAs are first processed in the nucleus and RNA polymerase II (Pol II) is mainly responsible for the transcription of miRNA genes (Lee *et al.,* 2004). Pol II-dependent miRNA gene expression enables temporal control, so that a specific set of miRNAs can be synthesised according to specific conditions and cell types. The product of Pol II-mediated expression is known as the pri-miRNA, which are usually several kilobases long and contain local hairpin structures. The pri-miRNA produced by Pol II is cleaved at the stem of the hairpin, which releases approximately 60-70 nucleotides called the precursor miRNA (pre-miRNA) (Zeng and Cullen, 2003). This processing step is performed by Drosha, which requires the DiGeorge syndrome critical region in gene 8 (DGCR8) in humans (Drosha-DGCR8 complex). Drosha, in conjunction with DGCR8, forms a large complex known as the microprocessor complex (Han *et al.,* 2004). DGCR8 guides Drosha to slice pri-miRNA. Drosha cleaves RNA duplexes and thus processes the pri-miRNA to the pre-miRNA (Han *et al.,* 2006). Pre-miRNAs are transported into the cytoplasm for further processing to become mature miRNAs. The nuclear cleavage process by Drosha defines one end of the mature miRNA. The pre-miRNA is released in the cytoplasm and is

subsequently processed by the endonuclease cytoplasmic Rnase III enzyme, Dicer, to create a mature miRNA (Hutvágner *et al.,* 2001). Dicer is a highly specific enzyme that measures ~22nt from the pre-existing terminus of the pre-miRNA and cleaves the miRNA strand (Figure 1.11). In order to degrade target mRNAs, miRNAs are bound by argonaute (AGO) subfamily proteins, forming a ribonucleoprotein complex called the RISC (RNA-induced silencing complex) (Nakanishi, 2016). The miRNA-RISC complex induces gene silencing via translational repression or mRNA cleavage through sequence-specific interactions with the 3' untranslated regions (UTRs) of specific target mRNAs (Figure 1.11) (Miyaki *et al*., 2009; Bushati and Cohen, 2007).

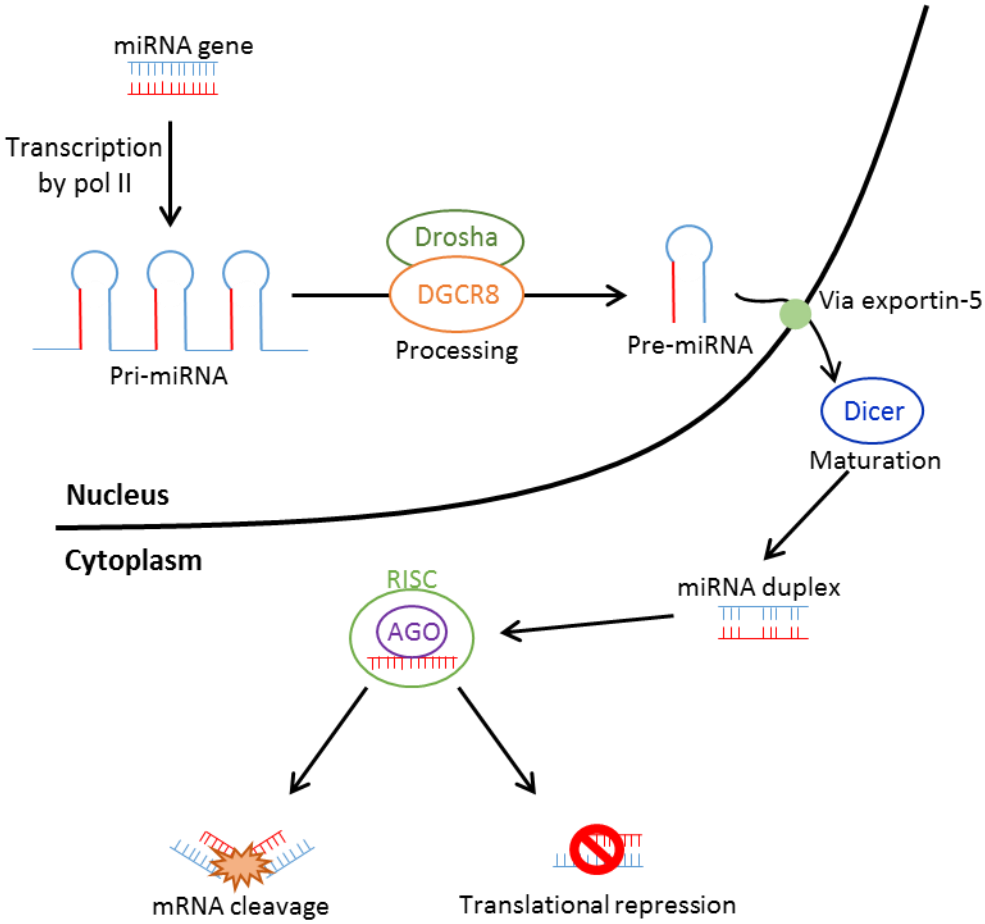

Figure 1.11. Schematic of how miRNAs are processed and their actions on mRNAs. miRNAs are processed in the nucleus and transcribed to pri-miRNA by polymerase II. Pri-miRNA is processed by DGCR8/Drosha complex to pre-miRNA, exported to the cytoplasm via exportin-5, where it is processed by Dicer to create mature miRNA. Argonaute binds mature miRNA, forming a complex called RISC, which induces gene silencing via mRNA cleavage or translational repression (Adapted from Lin and Gregory, 2015)

The first miRNA to be specifically implicated in cartilage regulation was miR-140, the expression of which was found to be restricted to the cartilage of the jaw, head and fins in a zebrafish model (Wienholds *et al*., 2005). Cartilage-specific expression of miR-140 has also been reported in murine embryos, were histone deacetylase 4 (HDAC4) was also identified as a target of miR-140 (Tuddenham *et al*., 2006). HDAC4-null mice display premature ossification due to early onset of chondrocyte hypertrophy, while mice overexpressing HDAC4 results in an inhibition of chondrocyte hypertrophy and differentiation (Vega *et al*., 2004). These studies establish HDAC4 as a central regulator of chondrocyte

hypertrophy. Interestingly, expression levels of miR-140 are reduced in human osteoarthritis cartilage and is shown to correlate with MMP13 and IGFBP-5 expression, both chondrocyte markers (Glasson *et al.,* 2005). It has also been reported that miR-140 expression is suppressed by IL-1β, an inflammatory cytokine, which results in the chondrocyte-specific upregulation of the miR-140 target ADAMTS5 (Glasson *et al*., 2005, Stanton *et al*., 2005). Combined, these findings indicate that miR-140 contributes a key role in cartilage development, matrix homeostasis and osteoarthritis (Miyaki *et al.,* 2009).

miRNAs and RBPs have generally been considered separate transcript degradation pathways, however it has recently been suggested that RBPs can be implicated in the regulation of miRNA activity through synergistic activity at the level of transcript decay, and by directly affecting the miRNAs (Jiang and Coller, 2012).

1.5.2 RNA binding proteins

RNA binding proteins are regulators of post-transcriptional gene regulation and are involved in the regulation of all steps of RNA biogenesis (Wurth, 2012). RNA binding proteins are classified based on their specific RNA binding domain and are able to regulate the fate of their target mRNA in a time- and space-dependant manner (Gerstberger *et al*., 2014). There are 4 main classifications of RNA binding domain families: RNA recognition motifs (RRM), zinc-finger domains, K homology (KH) domains and double-stranded RNA binding motifs (dsRBMs) (Cléry, 2013). The RRM is the most abundant RNA-binding domain and subsequently the most studied (Maris *et al.,* 2005). HuR is a ubiquitously expressed RNA binding protein that contains 3 RRMs that bind to AU rich elements of mRNAs and works by stabilising target mRNAs to post-transcriptionally regulate many biological processes including cellular proliferation, growth and survival pathways (Dai *et al.,* 2011). Zinc fingers are classical DNA-binding proteins that also bind RNA (Lunde *et al.,* 2007). TTP is a well characterised member of a protein family that contain tandem CCCH zinc fingers and is crucial in preventing chronic inflammation as a feedback inhibitor by shutting down the pro-inflammatory response (Sanduja *et al.,* 2012). The KH domain is found in proteins that have different functions including

transcriptional and translational regulation and splicing (Cléry, 2013). KH-type splicing regulatory protein (KSRP) binds to AU-rich element-containing mRNAs and is involved in the regulation of mRNA stability, with KH domains 3 and 4 of KSRP being required to promote ARE (adenosine and uridine-rich sequence element)-containing mRNA decay. KSRP is also an integral part of the Dicer and Drosha complexes and regulates the biogenesis of a subset of mRNAs (Trabucchi *et al.,* 2009). dsRBMs are essential for the preferential binding of dsRNA-binding proteins to double stranded RNA (dsRNA). dsRNA-binding proteins contain one or more dsRBMs and primarily interact with the A-form double helix, which has a shallow and broad minor groove and a narrow and deep major group in contrast to the typical dsDNA B-form helix, with no binding to ssRNA, ssDNA or dsDNA (Coolidge and Patton, 2000). Staufen1 (Stau1) is a dsRNA-binding protein involved in many post-transcriptional regulatory processes including its direct interaction with the ribosome to regulate translation, Staufen-mediated mRNA decay and alternative splicing (Ricci *et al.,* 2014). While Stau1 is not essential for development, Stau1-deficient mice have defects in locomotor activity (Vessey *et al.,* 2008). Together with miRNAs RNA binding proteins can also form micro ribonucleoprotein (miRNPs) and bind to complementary sequences in target mRNAs to regulate translation and RNA stability (Wurth, 2012).

AREs are a major class of *cis*-elements located in the 3' UTR that target mRNAs for degradation thereby regulating transcript stability and its translational efficiency and localisation (Fan and Steitz, 1998b; Wurth, 2012). RNA binding proteins bind to specific sequences in the 3' UTRs of target mRNAs via RNA binding domains thereby regulating mRNA decay (Wurth, 2012). RNA binding proteins have not yet been extensively studied in musculoskeletal diseases, but evidence exists that a number of them have key roles to play in ensuring homeostasis of these tissues. Recently, transgenic mouse models have been generated which target the proteins involved in the regulation and stability of ARE-containing mRNAs and examine the role of factors affecting mRNA decay rates. TTP is a signal-induced anti-inflammatory RNA-binding protein that binds ARE-elements to promote mRNA decay by guiding unstable mRNAs or pro-inflammatory proteins for degradation and preventing translation in order to

shut-down the pro-inflammatory response and prevent chronic inflammation (Sanduja *et al.,* 2012). Mice deficient in TTP develop a severe inflammatory phenotype 1-8 weeks after birth, including the development of erosive arthritis, alopecia, dermatitis, left-sided cardiac valvulitis, myeloid hyperplasia and autoimmunity (Taylor *et al.,* 1996). The arthritis observed in TTP-null mice resembles inflammatory synovitis in humans, while cartilage and bone erosion coupled with synovial lining cell proliferation and altered patterns of joint involvement are similar to those seen in rheumatoid arthritis in humans (Taylor *et al.* 1996). These effects are caused largely, but not exclusively, by an increase in the stability of TNF mRNA leading to the overproduction of this cytokine in the myeloid compartment. Many of the observed phenotypes can be prevented with an injection of monoclonal antibodies that neutralise TNFα (Taylor *et al.,* 1996), or by creating dual knockouts of TTP and TNFα receptor (Carballo and Blackshear, 2001). TTP is also able to auto-regulate its own expression by binding to an ARE within its 3'UTR (Brooks *et al.* 2004). Interestingly, in human articular chondrocytes, previous work from our group has shown that TTP can regulate SOX9 mRNA stability and that TTP can bind to SOX9 mRNA 3'UTR elements (McDermott, 2016).

1.5.2.1 HuR

1.5.2.1.1 Structure and general function of HuR

Human antigen R (HuR; also known as ELAVL1) is a member of the ELAV (embryonic lethal abnormal vision) RNA-binding protein family. HuR is a ubiquitously expressed RNA binding protein that contains two N-terminal RNA recognition motifs (RRMs) with high affinity to AU-rich elements, one C-terminal RRM and the HuR nucleocytoplasmic shuttling domain between (HNS) RRM 2 and 3 (Güttinger *et al.,* 2004; Uren *et al.,* 2011) (Figure 1.12). HuR is predominantly nuclear were it is involved in the regulation of transcript splicing (Fan and Steitz, 1998). Alternative splicing of pre-mRNAs is a mechanism that produces multiple transcripts from a single gene, thereby contributing to transcriptome diversity. This process is the deviation from the normal process

were introns are removed and exons are ligated in a sequential order, instead certain exons are skipped resulting in various forms of mature mRNA (Wang *et al.,* 2015). HuR activity and function is associated with its subcellular distribution, translational and post-translational modifications and transcriptional regulation (Wang *et al.,* 2013). RNA-binding proteins are key to the regulation of splicing and can interact with intronic and/or exonic sequences (Akaike *et al.,* 2014). It has been reported that polypyrimidine tract-binding protein 2 (PTBP2), itself an alternative splicing regulator expressed primarily in the brain, is alternatively spliced by HuR, were HuR knockdown increases the expression of exon 10 by 65% compared to exon 9 and 11 (Lebedeva *et al.,* 2011). Exon 10 is flanked by HuR binding sites and the skipping of this exon leads to nonsense mediated decay (NMD) (Spellman *et al.,* 2007). The nucleocytoplasmic shuttling domain allows HuR to shuttle to the cytoplasm were it binds to AU-rich elements (ARE) located in the 3' untranslated region (UTR) of target mRNAs to modulate transcript stability and/or translation (Fan and Steitz, 1998c; Brennan and Steitz, 2001).

Figure 1.12. Schematic diagram of the domain organisation of HuR. HuR contains 3 RNA recognition motifs (RRMs) and a hinge region (HNS) between RRM2 and RRM3.

Previous work has led to the identification of the low-molecular-weight chemical inhibitor of HuR, MS-444 (Meisner *et al.,* 2007). MS-444 is produced by a gram-positive bacteria *Micromonospora* and was originally characterised as a myosin light chain (MLC) kinase inhibitor (Blanco *et al*., 2016). As well as its role as a MLC kinase inhibitor, it was later found that MS-444 also inhibits HuR

homodimerisation and HuRs cytoplasmic translocation thereby preventing its function as a stabiliser of target mRNAs, and resulting in growth inhibition and loss of cytokine expression in inflammatory cell models (Meisner *et al.* 2007). This was the first time HuR had been identified as a drugable protein and also highlighted MS-444 as a potentially valuable tool for studying HuR function.

Previously, it was identified that there was an enhanced expression of HuR during colon tumorigenesis, which correlated with poor clinical prognosis (Young *et al.,* 2009). More recently, treatment with MS-444 was able to attenuate colorectal cancer tumour growth both *in vitro* and *in vivo* through enhanced apoptosis and decreased angiogenesis, supporting the notion that HuR may potentially be a valuable therapeutic target in a variety of cancers and that pharmacological inhibitors of HuR such as MS-444 may be useful tools in this process (Blanco *et al.,* 2016).

It has been suggested that HuR may bind to its target mRNAs in the nucleus and escort them to the cytoplasm while competing with mRNA decay inducing RBPs. This is due to HuR's apparent reliance on stress signals when binding to target mRNAs that result in HuR becoming phosphorylated or methylated (Kim *et al*., 2008; Li *et al*., 2002). For example, ultra-violet light stress has been associated with the mobilisation of prothymosin α (ProTα), an oncoprotein that promotes cell proliferation and prevents cell death, from the nucleus to the cytoplasm in a HuR-mediated fashion (Lal *et al*., 2005).

Cross-linking immunoprecipitation analysis has identified over 4700 transcripts in the human genome that are known to associate with HuR (Uren *et al*., 2011; Lebedeva *et al*., 2011). *In vitro* studies have also shown that HuR is implicated in many pathophysiological processes, including tumorigenesis, cell-cycle control and inflammation, by targeting several mRNAs associated with development including growth factors, cyclins and cyclin inhibitors, proto-oncogenes and cytokines (Abdelmohsen *et al*., 2007; Brennan *et al.,* 2001; Katsanou *et al.,* 2005).

The HuR protein is extensively expressed in many cell types, including adipose, intestine, spleen and testis. As such, HuR has been implicated in a variety of

biological processes and has been linked to a number of diseases, particularly cancer and inflammation (Srikantan *et al.,* 2012). A number of cancer-related transcripts containing ARE's, including mRNAs for proto-oncogenes, cytokines, growth factors, and invasive factors, have been characterised as HuR targets. Increasing evidence supports HuR as the first RBP that is shown to play a critical role in carcinogenesis and caner progression by functioning as either an oncogene or a tumor suppressor regulating the expression of various target genes. Clinical data suggest that HuR overexpression is significantly related to specific clinical and pathological features, advanced stage, positive lymph nodes and poor survival in cancer patients (Wang *et al.,* 2013).

HuR has also been implicated in promoting inflammation and inflammatory diseases. The pro-inflammatory influence of HuR is linked to its interaction with mRNAs encoding pro-inflammatory proteins, most prominently TNF-a and IL-6, leading to their increased production in a variety of cell types, including fibroblasts and macrophages (Katsanou *et al.,* 2005). Some anti-inflammatory cytokines also repress HuR function, for example IL-10 inhibits inflammation, in part by repressing the HuR-mediated stabilisation of mRNAs encoding pro-inflammatory cytokines in monocytes and inflammatory cells in the myocardium (Krishnamurthy *et al.,* 2009). The involvement of HuR in rheumatoid arthritis was suggested based on its promotion of TNF-a expression, while HuR-regulated COX-2 was associated with the development of rheumatoid and osteoarthritic cartilage (Srikantan *et al.,* 2012). Interestingly, there is evidence for functional antagonism between HuR and TTP. In normal cells, COX-2 is regulated by AREs present in the mRNA, with HuR having been demonstrated in promoting the stability of COX-2 (Dixon *et al.,* 2000; Dixon *et al.,* 2001). In cancer cells however, a dysregulation in COX-2 mRNA stability promotes tumor growth and contributes the immune evasion and resistance to cancer immunotherapy (Liu *et al.,* 2015). Previously, it has been demonstrated that during colon carcinogenesis increased HuR expression occurs alongside the reduction of TTP expression, correlated with an increase in COX-2 expression and substantially increasing its half-life (Young *et al.,* 2009). This suggested that TTP antagonises HuR-mediated COX-2 mRNA stability and implied that TTP reduction and HuR gain of function are both required for COX-2 overexpression

(Young *et al.,* 2009). In inflammation, it has been reported that HuR does not alter the levels of target cytokine mRNAs in the absence of TTPs destabilising functions, but synergises with a translational silencer called TIA-1 to reduced mRNA translation of the target cytokines (Katsanou *et al.,* 2005).

Many studies implicating HuR in additional diseases are rapidly emerging. In most of these, HuR elicits phenotypic trails previously described, including the promotion of inflammation, proliferation, angiogenesis and resistance to apoptosis. HuR has been implicated in cardiovascular disease, neurological pathologies, muscular disorders and lymphoproliferative disease (Srikantan *et al.,* 2012).

1.5.2.1.2 Regulation of HuR

There are many molecules that regulate the transcriptional and post-transcriptional regulation of HuR. For example, in gastric tumorigenesis the activation of AKT signalling increases the binding of the transcription factor p65/RelA (Rel-like domain-containing proteins) to a putative NF-κB (nuclear factor kappa-light-chain-enhancer of activated B cells) binding site in the HuR promoter (Kang *et al*., 2008). This study revealed HuR to be a direct transcription target of NF-κB (Kang *et al*., 2008). In addition, HuR is regulated by many miRNAs and RNA-binding proteins at the post-transcriptional level including TTP, RNPC1 (ribonucleoprotein C1), Mdm2 (murine double minute 2) and Hsf1 (heat shock transcription factor 1) (Figure 1.13) (Embade *et al*., 2012; Gabai *et al*., 2012; Al-Ahmadi *et al*., 2009). Interestingly, in normal cells, TTP binds and controls HuR mRNA through competition for the binding of HuR itself (auto-regulation) to its 3'UTR. An imbalance in HuR-TTP levels results in an increase in the invasiveness of cells during cancer progression (Astakhova *et al.,* 2009; Talwar *et al*., 2011).

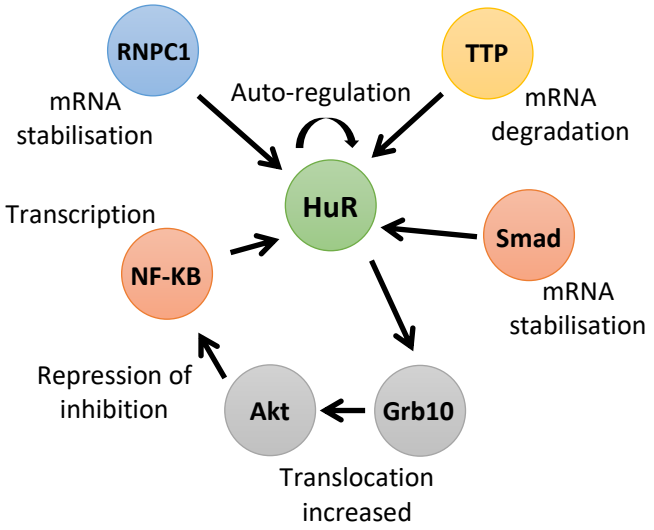

Figure 1.13. Translational and post-translational regulators of HuR
(Adapted from Govindaraju and Lee, 2013).

As HuR is predominantly nuclear, the export of HuR to the cytoplasm is needed for HuR to function as an mRNA stabiliser. There are many stimuli that can alter HuR-dependant mRNA stability including cytokines, inflammatory mediators and oxidative stress and can result in alterations in HuR trafficking and changes in HuRs affinity for its target mRNAs (Abdelmohsen *et al.,* 2008). This process is regulated by post translational modifications of HuR (Shen and Malter, 2015). Post-translational modifications give rise to acetylation, methylation and phosphorylation upon the chemical addition of different functional groups (acety-, methyl- and phosphor-, respectively). It has previously been reported that HuR is phosphorylated at many sites during nuclear export under various stress stimuli and this process results in an increase in the mRNA decay of target transcripts (Winzen *et al*., 1999; Doller *et al.,* 2008). For example, oxidative stress, via cell-cycle checkpoint kinase 2 (Chk2) phosphorylation of HuR in human diploid fibroblasts, leads to an increase in SIRT1 mRNA due to dissociation of HuR-bound SIRT1 mRNA (Abdelmohsen *et al.,* 2007). HuR is also subject to methylation. This was observed in cells overexpressing CARM1 and in macrophages stimulated with lipopolysaccharide, in both instances TNFα was stabilised (Li *et al.,* 2002). Interestingly, this methylation also involves

competition of HuR with TTP for binding the ARE-containing TNFα mRNA (Dean *et al.,* 2001; Carballo *et al.,* 1998).

Primary sequence specificity is often crucial for binding-site recognition by RNA binding proteins (Li *et al.,* 2014). Experimental computational analysis have been utilised to identify consensus binding sequences for RNA binding proteins and has led to the identification of a 17-20 base long RNA general consensus sequence (NNUUNUUU) that is rich in uracil and was found in almost all mRNAs that have previously been reported as HuR targets (de Silanes *et al.,* 2004; Li *et al.,* 2014).

SELEX (systematic evolution of ligands by exponential enrichment) is a low-throughput method for detection of RNA binding protein sequence-binding preferences *in vitro* (Tuerk and Gold, 1990). This method involves the selection of high-affinity binding sequences from a randomised RNA oligonucleotide pool through purified protein, each then followed by PCR amplification. Resulting products are subsequently cloned and sequenced, which identifies a set of short sequences that are preferred by the particular protein (Li *et al.,* 2014). Using the SELEX method, previous studies have reported that HuR has a ~10 fold higher affinity to the U-rich sequence than for the AU-rich sequence, suggesting this may be the preferred binding sequence of HuR (Sokolowski *et al.,* 1999). RIP-seq is a method used to investigate direct and indirect targets of a protein. Using a novel conditional knock-out model of HuR during CD4+ T activation, Techasintana *et al* performed RIP-seq then combined the data with data from RNA-seq to determine the direct and indirect target transcripts of HuR (Techasintana *et al.,* 2014). This study showed that HuR may regulate genes in multiple canonical pathways involved in T cell activation as it identified known, and new, putative HuR-associated targets that are crucial for cytokine production, particularly the CD28 family signalling pathway (Techasintana *et al.,* 2014).

1.5.2.1.3 In vivo models of HuR

A transgenic mouse model was used to overexpress HuR in the myeloid lineage which led to translational silencing of the ARE-containing transcripts, including TNF-α (tumor necrosis factor alpha) and Cox2 (cyclooxygenase 2), despite normal turnover (Katsanou *et al*., 2005). A role for HuR in germ cell function has also been suggested as a result of impaired gametogenesis in transgenic mice that overexpress HuR globally (Levadoux-Martin *et al*., 2003). Cre/loxP-mediated postnatal global deletion of HuR in 8 week old mice resulted in cachexia and leathality within 10 days of tamoxifen administration, suggesting that HuR is essential for postnatal life. These HuR-null mice also presented with atrophy of organs involved in the immune and hematopoietic systems including bone marrow, thymus, spleen and lymph nodes (Ghosh *et al*., 2009). At the cellular level, HuR function was essential for cell survival as ablation of HuR led to a rapid induction of apoptosis in progenitor cells, whereas quiescent stem cells and differentiated cells were unaffected. As HuR levels declined, expression of the oncogene P53 that is critical for cell death was induced in progenitor cells. It was also reported that HuR binds and stabilises Mdm2 mRNA, a critical regulator of p53, suggesting that HuR acts to regulate p53 levels in progenitor cells and promote cell survival. This was the first time HuR had been reported as an essential post-transcriptional regulator in the survival of progenitor cell populations in hematopoietic and intestinal systems *in vivo.* This study, however, did not examine the functions of HuR in differentiated cells and quiescent stem cells, which do not require HuR for survival.

Previous work generated a conditional allele of HuR by flanking its ATG-containing second exon with two loxP sites, these mice were then crossed with transgenic mice that expressed Cre in the germ line in order to generate HuR null mice in the F2 progeny (Katsanou *et al*, 2009). Germline knockout of HuR in mice led to embryonic lethality after E14.5 (embryonic day 14.5) due to defects in labryrinth branching morphogenesis and syncytiotrophoblast differentiation during placental development (Katsanou *et al*., 2009). To overcome this embryonic lethality, HuR was knocked out using the Cre/loxP system where Cre was under the control of the *Sox2* promotor. This allowed efficient loss of HuR

function in epiblasts that give rise to the embryo but not in the trophectoderm-derived trophoblast cell types of the placenta. The epiblast-specific deletion of HuR in *Sox2 Cre*$^{+}$ *Elavl1*$^{-/-}$ embryos led to smaller embryos past E14.5 that had lung dysmorphia and were devoid of spleens, and embryonic lethality between E17.5 and E19.5. Interestingly, HuR-null embryos displayed severe defects in skeletal development with a reduction in limb size with minimal ossification zones in scapulae, femurs and tibia, a fusion of the digits and a delay in endochondral ossification and osteogenic ossification of the craniofacial structures, with the exception of the mandibles (Figure 1.14). Another interesting observation was an incomplete fusion of the thoracic cage due to an open and bifid xyphiod process and a complete absence of ossified neural spines and zygapophyses in HuR null embryos. A less penetrant phenotype also occurred in less than 15% of embryos were HuR null embryos developed severe nasal clefting (Katsanou *et al*., 2009).

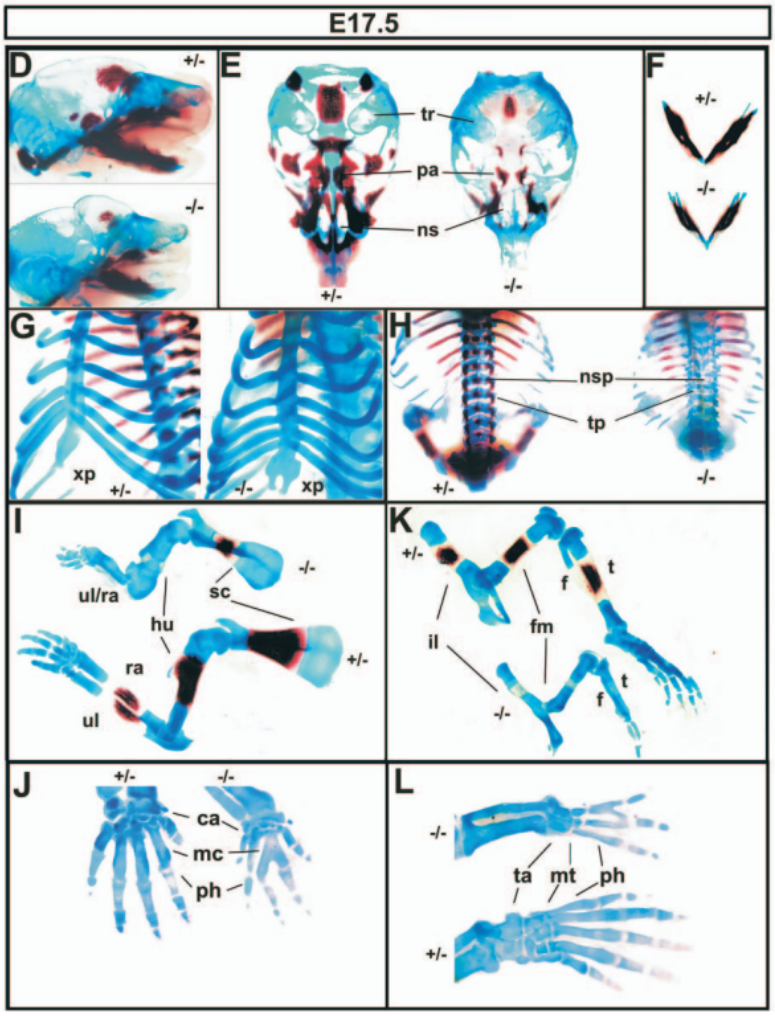

Figure 1.14. Comparison of alcian blue (cartilage) and alizarin red (bone) stained Sox2 Cre^{+} Elavl1$^{+/-}$ and Sox2 Cre^{+} Elavl1$^{-/-}$ E17.5 embryos. Craniofacial structures (D-F), ribs (G-H) and long bones (I, K) all show deformities in the development of the skeleton with a lack of mineralisation in HuR-deficient embryos. There is also a fusion of the digits in the forepaw (J) and hind paw (L) (Taken from Katsanou *et al*., 2009).

Cytoplasmic HuR has the ability to interfere with the binding or activity of multiple other ARE binding proteins that function to promote mRNA turnover, and contribute to the stabilisation of different target mRNAs (Brennan and Steitz, 2001). It has therefore been suggested that HuR may regulate gene

expression by modulating the activity of miRNAs, which would result in the enhanced translation or stability of mRNA (Bhattacharyya *et al*., 2006).

Recently, our laboratory has reported that siRNA-mediated knockdown of HuR mRNA *in vitro* resulted in a reproducible and significant increase in the expression levels of MMP13 in human articular chondrocytes (McDermott *et al*., 2016). In the same study, immunohistochemical analysis of developing mouse cartilage found that HuR protein is ubiquitously expressed throughout the developing embryo. Interestingly however, the condensing mesenchyme in the digits revealed a "checkerboard" pattern of HuR protein expression were cells that were strongly positive for HuR were positioned alongside cells with a weakened stain for HuR. HuR protein expression was also found to be reduced in hypertrophic chondrocytes of the costal cartilage, in the long bones of the fore and hind limb and in cells adjacent to the perichondrium in E16.5 embryos, these areas are implicated in the regulation of long bone growth and mineralisation (Vortkamp *et al*., 1996). In relation to MMP13, protein levels of HuR were reduced in hypertrophic chondrocytes and those in the earlier stages of differentiation were MMP13 expression levels were increased. Curiously, HuR levels do not affect the rate of MMP13 mRNA decay, which suggests that the regulation of MMP13 by HuR may occur in an indirect manner (McDermott *et al*., 2016). This data suggests a complex role of HuR in skeletal and embryonic development or that HuR indirectly regulates chondrocyte function through the post-transcriptional control of one or more regulatory genes.

1.6 Research Aims and Hypothesis

There is evidence from the literature that HuR influences skeletal development as well as the expression of markers of joint disease. Based upon this, the hypothesis of this thesis was that HuR regulates cartilage differentiation during development and degradation during disease progression. To test this hypothesis, the overall aims of this project were to:

1. Determine the role of HuR in embryonic development using murine cartilage-specific and skeletal-specific knockout models of HuR.

2. Investigate the role of HuR in joint disease using skeletally mature, tamoxifen inducible, aggrecan-promoter driven Cre recombinase knockout mice and their response to osteoarthritis induced using the DMM model.

3. Identify molecular mechanisms affected by HuR *in vitro* utilising both primary murine chondrocyte cultures and the ATDC5 chondrogenic cell line.

2 Materials and Methods

2.1 Animals

2.1.1 Animal Husbandry

Mixed background C57BL/6 X CBA B6BAF1 were used for all murine transgenic studies and all animal procedures were licensed by the UK Home Office under the Animal (Scientific Procedures) Act 1986; project licence numbers (PPL) 70/7288 and 70/9047. Mice were housed at a specific pathogen free (SPF) mouse facility in the Biomedical Services Unit (BSU) at the University of Liverpool. Mice received 12 hours of light and dark and 45 ± 10% humidity at a temperature of 22 ± 2°c. Access to water and food was *ad libitum*.

2.1.2 Transgenic Mice

2.1.2.1 Generation of HuR floxed Acan -11kb Cre mice

Cryopreserved HuR^{fl} embryos were gifted from Dimitris Kontoyiannis at the Alexander Fleming Biomedical Sciences Research Center, Greece. Embryos were re-derived in the BSU facility at the University of Liverpool. Mixed background females were housed with vasectomised males and pseudopregnant females identified by the presence of a copulation plug. Embryos were transferred into pseudopregnant females. Resulting pups were genotyped for HuR and mated with Acan-A1-$CreER^{T2}$*luc* mice to generate $HuR^{fl/WT}$AcanA1-$CreER^{T2}$*luc*$^{+/-}$ F1 progeny mice. F1 mice were backcrossed to $HuR^{fl/fl}$ mice to produce F2 $HuR^{fl/fl}$AcanA1-$CreER^{T2}$*luc* $^{+/-}$ progeny.

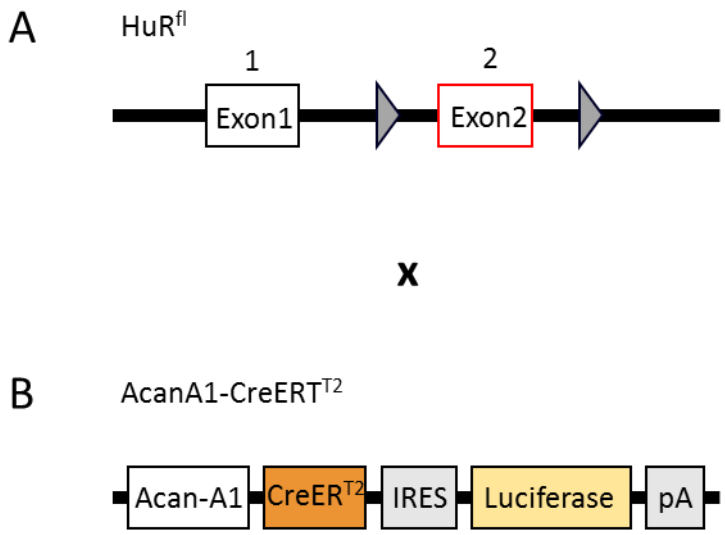

Figure 2.1. Schematic diagram showing the crossing of HuR$^{fl/fl}$ and AcanA1-CreER^{T2}luc mouse lines. HuR$^{fl/WT}$AcanA1-CreER^{T2}*luc*$^{+}$ mice were inter-crossed to yield a double transgenic line with the genotype HuR$^{fl/fl}$ AcanA1-CreER^{T2}*luc*$^{+}$.

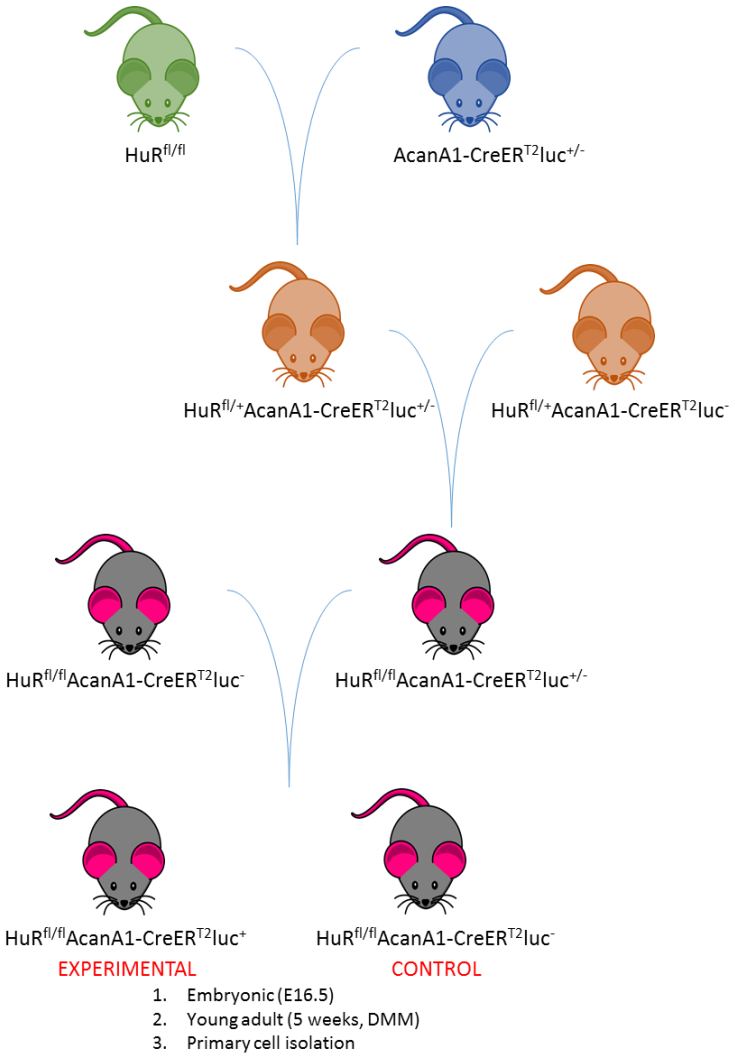

Figure 2.2. Schematic of breeding programme to generate experimental mice and their control counterparts in HuR$^{fl/fl}$AcanA1-CreER^{T2}luc mice. Experimental and control mice genotypes are shown.

2.1.2.2 Generation of HuR floxed PRX1-Cre embryos

6 week old, male PRX1-Cre mice were purchased from The Jackson Laboratory (005584). After acclimatisation the mice were bred with HuR$^{fl/fl}$ females to generate HuR$^{fl/WT}$PRX1-Cre$^{+/WT}$ F1 mice. In order to induce HuR flox recombination, the HuR$^{fl/WT}$PRX1-Cre$^{+/WT}$ F1 progeny were backcrossed to HuR$^{fl/fl}$ mice to produce a 25% occurrence of HuR$^{fl/fl}$PRX1-Cre^{+} F2 embryos that would have recombination at the HuR flox sites.

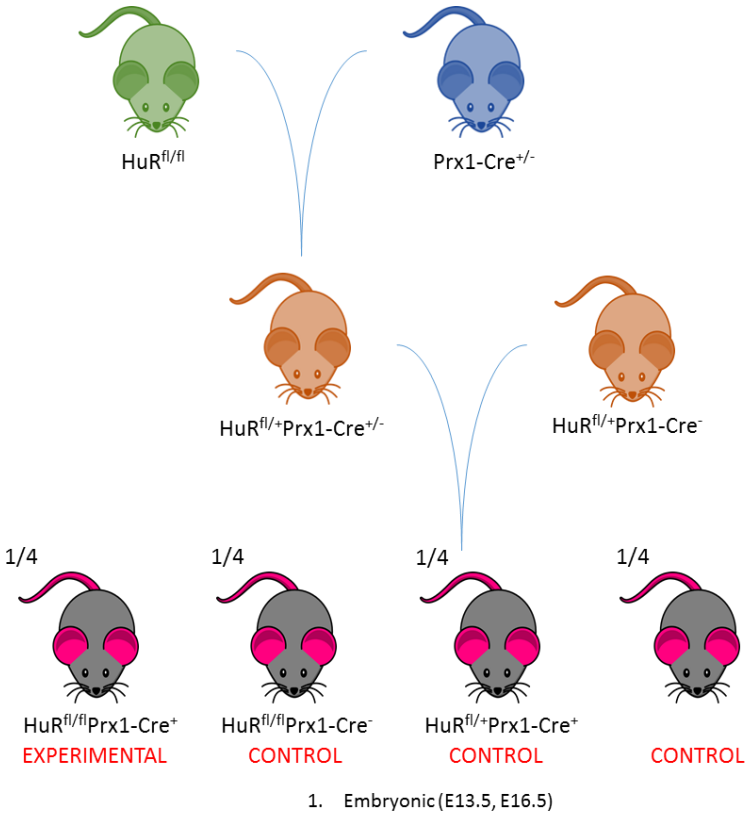

Figure 2.3. Schematic of breeding programme to generate experimental mice and their control counterparts in HuR$^{fl/fl}$Prx1-Cre mice. Experimental and control mice genotypes are shown.

2.1.3 Genotyping of transgenic mice

2.1.3.1 Reagents

Table 2.1. Reagent list and volumes for genotyping lysis buffer

Reagent	**Volume**
50mM Tris-HCL (pH8)	4.5mL 2M stock
0.1M NaCl	5mL 3M stock
1% SDS	10% 18mL
20mM EDTA	7.2mL 500mM stock
dH_20	144.3mL

Autoclaved and stored at room temperature

2.1.3.2 Proteinase K based extraction of genomic DNA

Ear notches of adult mice and tail and rib samples from mice embryos were used for genotyping. Samples were digested in 100µl lysis buffer and 10mg/µl proteinase K solution (Thermo Fisher; AM2548) at 55°C overnight. Samples were cooled, vortexed and 100µl of 3M ammonium acetate pH5.2 was added to precipitate the proteins out of solution. Samples were vortexed briefly, incubated on ice for 5mins and centrifuged at 12,000g for 10mins at 4°C. 100µl chloroform was added and samples centrifuged at 12,000g for 10mins at 4°C. The upper aqueous phase was moved into a new Eppendorf containing 500µl of cold 100% molecular grade EtOH and 10µg GlycoBlue™ (Thermo Fisher; AM9516). Samples were inverted twice to mix and centrifuged at 12,000g for 10mins at 4°c. EtOH was removed and 500µl of 70% EtOH was added to wash the pellet. Samples were briefly centrifuged at 12,000g for 1min. EtOH was removed and the pell*et al*lowed to air dry for no longer than 10mins. The pellet was re-suspended in TE buffer (50µl for ear notches, 100µl for tail and ribs) and placed at -20°c for long term storage.

2.1.3.3 Genotyping of transgenic mice by PCR

2.1.3.3.1 Primers

Table 2.2. List of primer sequences and their respective product size used for genotyping of transgenic mice

Primer Name	**Species**	**5'-3' sequence**	**Annealing Tm**	**Target**	**Product size**
HELp00_8 *Forward*	Mouse	TGGACAGGACT GGACCTCTGCT TTCCTAGA	68	*Fabp2 (internal)*	194bp
HELp00_9 *Reverse*	Mouse	TAGAGCTTTGC CACATCACAGG TCATTCAG	68	*Fabp2 (internal)*	
HELp01_0 *Forward*	Mouse	GCATTACCGGT CGATGCAACGA GTGATGAG	68	*Cre*	389bp
HELp01_1 *Reverse*	Mouse	GAGTGAACGA ACCTGGTCGAA ATCAGTGCG	68	*Cre*	
HuR_geno Forward	Mouse	GTTCCATGGCT CCCCATATC	60	*HuR*	442bp WT 549bp Recombinant
HuR_geno Reverse	Mouse	AGCTTTGCAGA TTCAACCTC	60	*HuR*	

100ng of purified genomic DNA was gently mixed with 10µl REDExtract-N-Amp™ PCR ReadyMix™ (Sigma-Aldrich; R4775), 100nM forward and reverse primer to a total volume of 20µl. An internal control primer set was used to observe the presence of DNA.

2.1.3.3.2 PCR cycling parameters

Samples were run on a ThermoCycler 2720 (Applied Biosystems) using the following parameters:

Cre/Internal

Activation of polymerase	93°C	1min	
Denaturation	93°C	1min	30 cycles
Annealing	68°C	2min	
Final step	72°C	5min	
Hold	4°C	-	

HuR

Activation of polymerase	94°C	2min	
Denaturation	94°C	1min	30 cycles
Annealing	60°C	1min	
Extension	72°C	1min	
Final step	72°C	10min	
Hold	4°C	-	

2.1.3.4 Analysis of genotype PCR reactions by gel electrophoresis

1.5% (*w/v*) gels were made using agarose (Sigma; A9539) added to 1X Tris-acetate-EDTA (TAE) buffer and microwaved for 1min 15sec per 100mL. 8µl of PeqGREEN (VWR; 732-2960) was added per 100mL of agarose/TAE buffer when temperature had lowered to 55°C, to enable visualisation of DNA bands under ultraviolet (UV) light. Gels were run at 10V/cm for 40mins and visualised using a UV transilluminator (BioRad ChemiDoc XRS) at 254nm.

2.1.4 Timed matings

Mice were paired for two nights and vaginal plug checks carried out daily. The first day of a vaginal plug equated to embryonic day 0.5 (E0.5).

2.1.4.1 Tamoxifen and progesterone preparation and administration

An aliquot of 50mg of tamoxifen (Sigma; T5648) was dissolved in 500µl of absolute ethanol and vortexed vigorously. The solution was then mixed with

4500µl corn oil (Sigma; C8267) and sonicated for 4x 30secs at lower pulse set to 2, Amp 20% to a final concentration of 10mg/µl. An aliquot of 50mg progesterone (Sigma; P0130) was prepared in the same way.

Tamoxifen was administered via intraperitoneal injection (IP) at a dose of 1mg/10g body weight in mice aged 6 weeks. Pregnant mice were dosed with 3mg tamoxifen and 1.5mg progesterone. Fresh batches of tamoxifen and progesterone were made prior to each injection.

2.1.5 DMM surgery

All mice received 3 separate doses of 1mg/10g body weight tamoxifen via IP injection at 6 weeks of age. Mice were anesthetised with isoflurane and micro-surgical techniques were used to destabilise the medial meniscus of the right knee joints from 10 week old male $HuR^{fl/fl}$Agg-$CreER^{T2}$*luc*$^{-}$ (control) and HuR^{fl}Agg-$CreER^{T2}$*luc*$^{+}$ mice, while left knees were not operated upon. An incision was made into SHAM control mice and the wound closed without destabilisation of the medial meniscus. All surgery was performed by veterinary surgeon Dr Peter Milner according to previous protocol (Glasson *et al*., 2007).

2.2 Murine Tissue

2.2.1 Collection

Mice were culled via a raising concentration of CO_2 followed by cervical dislocation and tissues were collected immediately. Embryos from pregnant females were collected, the yolk sac and placenta removed, and then immediately immersed into ice cold 95% ethanol to ensure embryo mortality. All surgical tools were autoclave sterilised.

2.2.1.1 Embryo

2.2.1.1.1 Whole mount alizarin red/alcian blue staining (McLeod, 1980)

For embryos E15 and above

Embryos were fixed in 95% ethanol for 5 days or longer (up to 3 months). Skin, viscera and adipose tissue was removed and embryos placed in 100% acetone for 2 days to remove fat and keep embryo firm. Acetone was removed and embryos stained for 3 days at 37°C in at least 10mL of freshly prepared staining solution as follows:

Table 2.3. Reagent list and volumes for alizarin red and alcian blue staining solution

Reagent	**Volume**
0.3% alcian blue 8GX (Sigma-Aldrich; A9186) in 70% EtOH	1 volume
0.1% alizarin red S (Sigma-Aldrich; A5533) in 95% EtOH	1 volume
Glacial acetic acid	1 volume
70% EtOH	17 volumes

Embryos were washed with distilled water and cleared in a 1% aqueous solution of potassium hydroxide (KOH) for 12-48hours until skeleton was clearly visible through the surrounding tissue. Embryos were then cleared through 20%, 50% and 80% glycerol / 1% aqueous KOH solution for ~4 days each and stored in 100% glycerol.

2.2.1.2 Tissue processing

2.2.1.2.1 For histological processing (Schmitz et al., 2010)

Murine knee joints collected for histological analysis was fixed in 10% neutral buffered formalin (NBF) for 48hours followed by decalcification in 10% EDTA for 3 weeks, changing for fresh solution frequently. Samples were finally embedded in paraffin wax.

2.2.1.2.2 For RNA processing

Articular cartilage was isolated from the femoral head and tibial plateau using a curved micro rongeur surgical tool (Figure 2.4). Tissue taken for RNA analysis was frozen in liquid nitrogen (LN_2) and ground to powder in a 35mm agate

mortar and pestle (Sigma-Aldrich; Z112496). 1mL TRIzol® reagent (Invitrogen; 15596026) was added to each sample, incubated at room temperature for 30 minutes and then these extracts were stored at -80°C until RNA purification was performed (as described in 1.7).

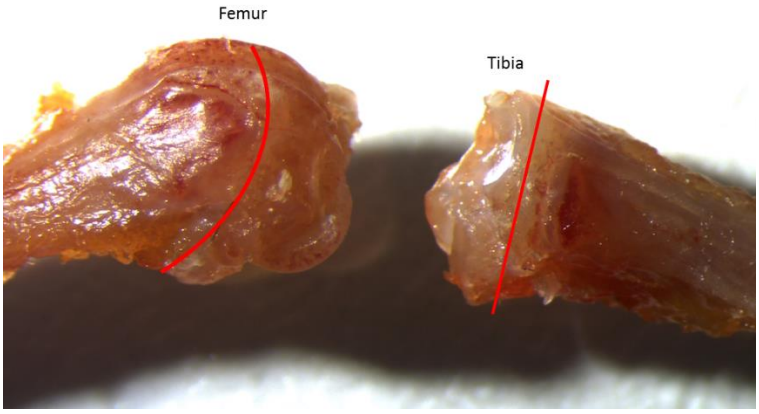

Figure 2.4. Photograph of dissected murine femur and tibia depicting the site of articular cartilage removal. The micro rongeur allows the articular cartilage of the femur to be removed in a curved manner.

2.2.2 Recombination genotyping assay

2.2.2.1 Primers

Table 2.4. List of primer sequences used for recombination genotyping.

Primer Name	Species	5'-3' sequence	Tm	Target	Product size
HuR_recomb *Forward*	Mouse	GATGCCAGCAAG CTCTTTAC	60	*HuR*	964bp Non-recombined
HuR_recomb *Reverse*	Mouse	TAGCAGGTACCG TCTCCACA	60	*HuR*	193bp Recombined

To assess recombination at the HuR flox sites, a PCR assay was designed with primers flanking the potentially recombined region (Table 2.4). Tissue from tamoxifen injected mice or embryos from tamoxifen injected females were digested using the proteinase K method previously described (section 1.1.3.2). 100ng/µl of purified genomic DNA was again used for multiplex PCR using 10µl REDExtract-N-Amp™ PCR ReadyMix™ and the following primer pair. Previous positively recombined DNA was used as a control.

2.2.2.2 Recombination assay PCR cycling parameters

Samples were run on a ThermoCycler 2720 using the following parameters:

Activation of polymerase	94°C	2min	
Denaturation	94°C	2min	35 cycles
Annealing	60°C	2min	
Extension	72°C	2min	
Final step	72°C	10min	
Hold	4°C	-	

PCR products were run on a 1.5% (*w/v*) agarose gel at 10v/cm for 45mins and DNA bands visualised under UV light.

2.3 Microcomputed Tomography (µCT)

Knee joints were scanned in 75% EtOH in a SkyScan 1272 high resolution µCT scanner (Skyscan Aartselaar, Belgium) at 4.5µm voxel size. Scans were obtained at 50kV and 200µA with a 0.5mm aluminium filter and a rotation set of 0.3° (180° rotation) and reconstructed using NRecon (version 1.6.10.4; Skyscan). Embryos were also scanned at 20µm voxel size with a rotation set of 0.5°.

2.3.1 Data viewer

Dataviewer (SkyScan; Version 1.5.0) allows visualisation of the reconstructed datasets and was used to re-orientate scans so that the cross-section within the transverse plane was perpendicular to the long axis of the bone. Each dataset was resaved in the correct orientation for detailed analysis.

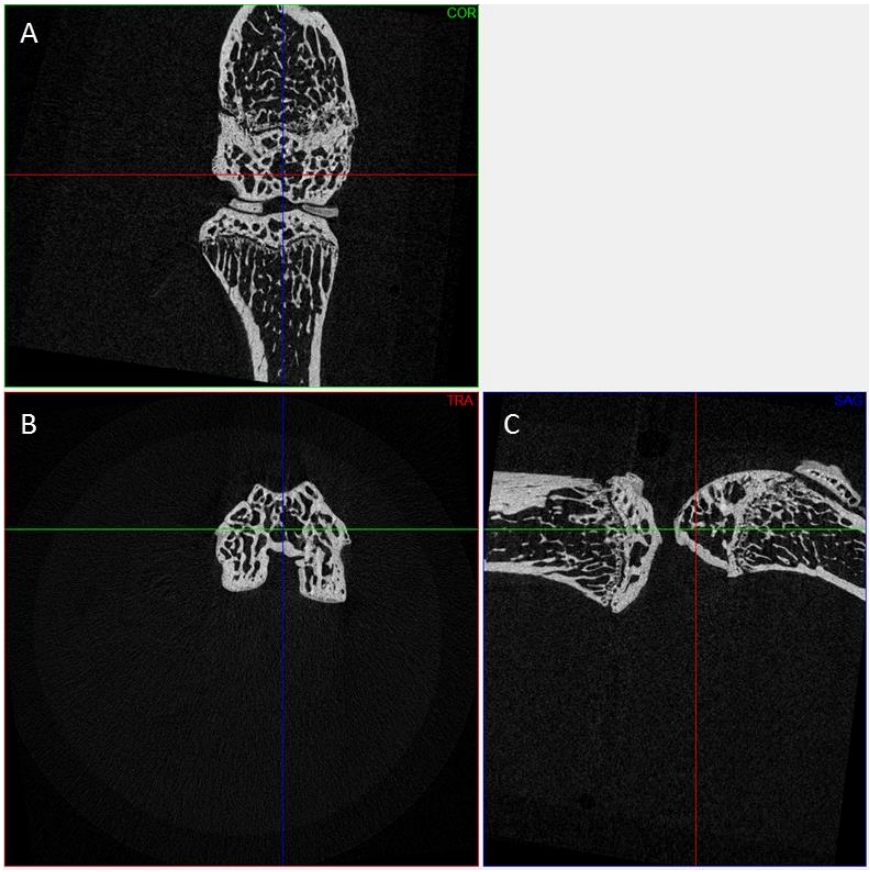

Figure 2.5. Orientation of knee joints in DataViewer. (A) Coronal, (B) transverse and (C) sagittal planes of mouse knee joints were orientated in all samples prior to volume of interest selection.

2.3.2 CT-Analyser (*CTan*)

CT-An (SkyScan; Version 1.15.4.0+) is an application used to measure the quantitative parameters and construct visual models from scanned 3D datasets obtained from the µCT SkyScan 1272. Re-orientated datasets were loaded and the region of interest (ROI) was free-hand selected from across the whole knee joint. ROIs included the tibial epiphysis, meniscus and the femoral lateral and medial condyles. Each selected ROI was saved as a new dataset and analysed using CT-An BATch MANager (BatMan) software (SkyScan) and morphometric parameters were recorded.

2.3.3 CTvox

Embryo datasets were loaded in CTvox and transfer function parameters changed to enable visualisation of the embryonic skeleton. Lighting effects and shadows were added to increase the realism of the resulting image. Finally, the Flight Recorder option within CTvox was used to produce fly-through animations of the 3D datasets from scanned embryo datasets.

2.4 Histology

2.4.1 Tissue processing

(Schmitz et al., 2010)

For histological analysis, embryos and knee joints were processed in a tissue processor (Leica TP1020) as described in Table 2.5.

Table 2.5. Tissue processing protocols for whole mount stained embryos and decalcified bones

Reagent	**Immersion period under vacuum (minutes)**	
	Whole mount stained embryos and embryos limbs E14.5 to E18.5	*Decalcified bone*
70% Ethanol	30	15
95% Ethanol	30	60
100% Ethanol	10	60
100% Ethanol	10	60
100% Ethanol	10	60
100% Ethanol	10	60
Xylene	30	60
Xylene	30	60
Wax	120	120
Wax	120	120

Knee joints were embedded in wax with the patella oriented downwards and 6µm coronal sections were taken across the whole of the knee joint with every slide containing 4 sections. Embryos were oriented with the left side downwards and 5µm sagittal sections were taken across the limbs and whole embryo. Sections were cut using the Micron HM355S microtome with cool-cut and tissue transfer system (Thermo Scientific).

2.4.2 Staining

(Carson, 1996).

Every 4th slide of adult limbs, representing approximately every 72µm across the whole joint, and every 3rd slide from embryo limbs were stained with toluidine blue (0.04% in 0.1*M* sodium acetate buffer [pH 4]) and counter-stained with 0.2% fast green on an automatic slide stainer (Leica; ST5020) using the protocol in Table 2.6.

Table 2.6. Toluidine blue staining protocol

Reagent	**Immersion period**
Xylene	10 minutes
Xylene	10 minutes
100% EtOH	2 minutes
90% EtOH	2 minutes
70% EtOH	2 minutes
Buffer A*	1 minutes
0.04% Toluidine Blue	15 minutes
H_20	10 seconds
H_20	10 seconds
0.2% Fast Green	5 seconds
H_20	20 seconds
Acetone	10 seconds
Acetone	10 seconds
Xylene	3 minutes
Xylene	3 minutes

(*Buffer A: 847ml acetic acid [2.85ml glacial acetic acid in 500ml dH_20] and 153ml sodium acetate [6.8g sodium acetate in 500ml dH_20])

Cleared embryo limbs that had previously been whole mount stained with alizarin red and alcian blue were dewaxed in 100% xylene twice for 20mins before being mounted.

2.4.3 Digital slide scanning

Sections were scanned on a TissueFaxs200 digital slide scanner (TissueGnostics) at x20 magnification in brightfield and visualised using Histoquest Software (Version 4.0.4.148, TissueGnostics).

2.4.4 Scoring

One section from every slide of toluidine blue stained coronal mice knee joints were scored by two independent researchers using the OARSI histopathology initiative scoring system that was previously adapted (Glasson *et al.* 2010, Poulet *et al.* 2011) as described in Table 2.7.

Table 2.7. Detailed list of murine knee joint osteoarthritis scoring system

Grade	**Osteoarthritic damage**
0	Normal articular cartilage surface
0.5	Loss of toluidine blue staining but no lesions
1	Lesions in the superficial zone of articular cartilage
2	Lesions down to the intermediate zone
3	Lesions down to the tidemark with or without possible loss of articular cartilage up to 20% of the surface of the condyle
4	Loss of articular cartilage tissue from 20-50% of the condyle surface
5	Loss of articular cartilage tissue from 50-80% of the condyle surface
6	More than 80% loss of surface and/or exposed subchondral bone

2.5 Western blot

2.5.1 Reagents

Table 2.8. 2X SDS sample buffer preparation

Reagent	**Volume**
1M Tris-HCl, pH 6.8	625µL
Glycerol	2.5mL
10% SDS	2mL
0.5% Bromophenol blue	200µL
ddH_20	Up to 9.5mL

Table 2.9. 10X TBS preparation

Reagent	**Volume**
Tris base	24.2g
NaCl	80g
ddH_20	up to 1l
PH	7.4

2.5.2 Protein extraction

2.5.2.1 Guanidine protein extraction

100mg wet weight pulverised cartilage and xiphoid from three $HuR^{fl/fl}CreER^{T2}luc^{+}$ and three $HuR^{fl}CreER^{T2}luc^{-}$ mice were independently added to guanidine extraction buffer (4M guanidine hydrochloride, 65mM dithiothreitol, 50mM sodium acetate and 1x complete mini protease inhibitor cocktail [Roche; 04693124001]) at a concentration of 100mg/ml. Samples were agitated for 20 hours at 4°C.

2.5.2.2 Ethanol precipitation

Samples were centrifuged at 12,000g for 10mins at 4°C. Supernatant was removed to a new vial. One volume of protein solution was added to nine volumes of ice cold 100% ethanol, mixed and then incubated overnight at -20°C. Samples were centrifuged at 12,000g for 15mins at 4°C, the supernatant was discarded and the pellet was washed by resuspension in 90% ethanol before centrifuging again at 12,000g for 5mins at 4°C. This wash step was repeated once more to remove traces of Guanidine. Samples were air dried until all ethanol had evaporated and pellets were re-suspended in 40µl 2x reducing sodium dodcyl sulfate (SDS) sample buffer (Table 2.8).

2.5.3 Pierce™ Bicinchoninic acid protein assay (BCA) kit

One Albumin standard was diluted in dH_20 into several concentrations ranging from 0-2000µg/mL (0=blank). 25µl of each standard and 25µl of each sample were pipetted into a microplate well (655180; Greiner) in triplicate and 200µl of BCA Working Reagent (50:1, Reagent A:B) was added to each well. The plate

was mixed on a plate shaker for 30 secs and the plate covered and incubated for 30mins at 37°C. The plate was cooled to room temperature and the absorbance at 562nm measured using a BMG LABTECH SPECTROstar Nano microplate reader.

2.5.4 Measurement of protein

The average 562nm absorbance measurement of the blank standard replicates was subtracted from the 562nm measurements of all other individual standards and unknown sample replicates. A standard curve was produced by plotting the average Blank-corrected 562nm measurement for each BSA standard vs its concentration in µg/mL. The standard curve was used to determine the protein concentration of each unknown sample.

2.5.5 Western Blot

1µl of β-mercaptoethanol was added to 20mg of protein sample and boiled for 10 minutes at 100°C. Samples were loaded onto a 4-12% NuPAGE gel (ThermoScientific; NP0322BOX) alongside a Novex pre-stained protein standard (Life Technologies; LC5800) and run in 1X NuPage SDS running buffer (Novex; NP002) at 100V for 15 minutes then 150V for 45 minutes. Separated proteins were transferred to a 0.2µm nitrocellulose transfer membrane (Perkin Elmer; NBA083G001EA) in 1x NuPage transfer buffer (Novex; NP00061-1) at 35V for 90 minutes. Following transfer, membrane was shaken with 10ml of blocking buffer (5% skimmed milk powder in 1x Tris-buffered saline (TBS) (Table 2.9) for 60 minutes at room temperature. The membrane was then incubated with primary antibodies raised against HuR (HuR 32A2 Monoclonal Antibody HRP; Insight Biotechnology; sd-5261) and GAPDH (Anti-GAPDH antibody produced in rabbit; Sigma Aldrich; G9545), diluted 1:1000 in 10ml blocking buffer, on a shaker at -20°C overnight. It was then washed in once in 1x TBS, twice in 1x TBS/0.1% Tween and once again in TBS for 5 minutes each. Fluorescently conjugated goat anti-Mouse (IRDye 800CW; Li-Cor; 925-32210) and Goat anti-Rabbit (IRDye 680RD; Li-Cor; 925-68071) secondary antibodies were added to 10ml blocking buffer and incubated with the membrane for 60 minutes at room

temperature. The membrane was then washed as before allowed to dry before imaging.

2.5.6 Li-Cor analysis

Using secondary antibodies labelled with IRDye near-infrared (NIR) fluorescent dyes, IRDye 800cw multiplexed with IRDye 680RD, on the same membrane allows for 2-colour detection when imaging fluorescence. Protein expression was measured on the Odyssey® CLx Imaging System (Li-Cor Biosciences) at both 800nm and 680nm. Bands were quantified and normalised using Image Studio™ (Version 5.2).

2.6 Cell culture

2.6.1 Primary murine chondrocytes

2.6.1.1 Isolation of murine cartilage

Protocol adapted from (Gosset et al. 2008).

One litter (8-11 animals) of 3-5 day old mice were culled via cervical dislocation. Mice were placed in a sterile flow hood in the back-down position and the skin cut from the navel to the sternum, then along the ribs. For costal cartilage, the diaphragm and soft tissue were removed from the rib cage. The isolated rib cages were placed in 1x PBS. Skin and soft tissue was removed using a scalpel and was cartilage removed from calcified bone. For articular cartilage, skin and soft tissue was also removed from the hind legs and the femoral condyles and tibial plateau from each mouse was isolated using scalpels and placed in 1x PBS. Ribs and articular cartilage were rinsed independently with 1x PBS.

2.6.1.2 Isolation of immature murine chondrocytes

Culture medium:

Table 2.10. List of reagents and volumes for the preparation of culture medium

Reagent	**Volume**
DMEM (Life Technologies; 31885-049)	500mL
Penicillin	100 U
Streptomycin	100µg/mL

Table 2.11. List of reagents and volumes for the preparation of 3mg/ml^{-1} digestion solution

Reagent	**Volume**
Culture medium	25mL
Collagenase D (Sigma Aldrich; 11088866001)	75mg

2.6.1.2.1 Immature murine costal chondrocytes

Cartilage pieces were incubated in 15ml digestion solution for 45min at 37°c, 5% CO2. A 0.5mg ml^{-1} collagenase D solution was prepared by diluting 2.5ml digestion solution with 12.5ml culture medium. Tissue fragments were agitated using a 25ml pipette to detach soft tissue and cartilage pieces placed in a new Petri dish with 15ml collagenase D solution at 0.5mg ml-1 overnight at 37°c, 5% CO2.

2.6.1.2.2 Immature murine articular chondrocytes (iMACs)

Cartilage pieces were incubated in 10ml digestion solution for 45min at 37°c, 5% CO2. Using a 25ml pipette, cartilage pieces were placed in a new Petri dish with 10ml fresh digestion solution for 45min at 37°c, 5% CO2. Cartilage pieces were agitated using a 25ml pipette to detach soft tissue and cartilage pieces

were placed in a new Petri dish with 10ml collagenase D solution at 0.5mg ml-1 overnight at 37°c, 5% CO2.

2.6.1.3 Primary chondrocyte seeding

2.6.1.3.1 Immature murine costal chondrocytes

The 15ml collagenase D solution with cartilage pieces was placed in a 50ml tube and successively passed through 25ml, 10ml and 5ml Pasteur pipettes to disperse cell aggregates and yield a suspension of cells. The cell suspension was filtered through a 50µM cell strainer over a 50ml tube and centrifuged at 400g for 10mins. The pellet was washed with 10ml 1x PBS and re-suspended with 40ml culture medium plus 10% FBS (Sigma; F7524-500). Cells were seeded on a 10cm culture dish at a density of 25 x 10^3 cells cm^{-2}.

2.6.1.3.2 Immature murine articular chondrocytes

The 10ml collagenase D solution with cartilage pieces were placed in a 15ml tube and successively passed through 25ml, 10ml and 5ml Pasteur pipettes to disperse cell aggregates and yield a suspension of cells. The cell suspension was filters through a 50µM cell strainer over a 15ml tube and centrifuged at 400g for 10mins. The pellet was washed with 5ml 1x PBS and re-suspended with 15ml culture medium plus 10% FBS (Sigma; F7524-500). Cells were seeded on a 10cm culture dish at a density of 8 x 10^3 cells cm^{-2}.

2.6.1.4 Culture of immature murine chondrocytes

Cultures were maintained under sterile conditions in a 37°c incubator with 5% CO_2. Immature murine costal chondrocytes and iMACs reached confluence 6-7 days after seeding. Culture media was changed 2 days after seeding. Once confluent, cells were trypsinised and transferred to T75 flasks and allowed to reach confluence before experiment.

2.6.1.5 Optimisation of optimum MOI for iMACs

In order to assess the multiplicity of infection (MOI) that would yield optimum uptake of Cre adenovirus, and therefore HuR flox site recombination, in immature murine chondrocytes without causing cell death, a green fluorescent protein (GFP) tagged adenovirus (Vector Biolabs; 1060) was used to transduce

cells. Immature murine chondrocytes were seeded at 260 x 10^3 per well in 6-well plates and the following day treated with GFP adenovirus at MOIs between 100 and 200 in 2mL of media per well. Cells were incubated for 24hours at 37°C, 5% CO_2. The virus-transduced media was removed and 2mL fresh media was added and cells incubated for a further 24 hours. The expression of GFP was viewed with an ultraviolet (UV) microscope (Nikon Eclipse Ti). Cells were re-suspended in 200µl FACs reagent (1g BSA, 100mg NaN_3, 100mL PBS) and detected with a FACScan flow cytometer (BD Biosciences, Accuri FloCytometer) with CellQuest software (BD Biosciences; Version 5.1).

2.6.1.6 Adenoviral mediated excision of HuR

Immature murine articular chondrocytes were seeded at 30 x 10^3 cells per well in a 12-well plate. After 24hours cells were transduced with a Cre recombinase adenovirus (Vector Biolabs; 1045) or the GFP adenovirus at MOI's of 200. Cells were incubated for 24hours then media removed and 500µl TRIzol® reagent added and incubated for 10mins and stored at -80°C for RNA isolation.

2.6.1.7 Tamoxifen induced excision of HuR

2.6.1.7.1 Preparation of 4-OH Tamoxifen

5mg 4-Hydroxytamoxifen (4-OH-T) (COMPANY) was dissolved in 1.25mL 100% EtOH to produce 10mM stock solution. 5µl of 10mM 4-OH-T was diluted in 495µl of DMEM to make 100µM solution. 10µl of the 100µM solution was diluted in 990µl of DMEM to make a 1µM solution. 100µl of the 1µM solution was added to 900µl DMEM (supplemented with 10% FBS and P/S) and added to cells at a final concentration of 100nM per well in a 12 well dish. Fresh 4-OH-T was made per experiment.

2.6.1.7.2 Treatment of iMAC's with tamoxifen

Immature murine articular chondrocytes were seeded at 30 x 10^3 cells per well in a 12-well plate. The following day, 1000µl of fresh culture medium containing 100nM 4-OH-T was added to cells and incubated for 24hours at 37°C, 5% CO_2. Media containing 4-OH-T was replaced with fresh culture media and RNA extracted from cells in 500µl TRIzol® reagent at 0, 24, 48 and 72 hours for qRT-PCR analysis.

2.6.1.8 MS-444 mediated knockdown of HuR

MS-444 was dissolved in DMSO to a final concentration of 10mM. Immature murine articular chondrocytes were seeded at 30 x 10^3 cells per well in a 12-well plate. The following day cells were treated with 10mM MS-444 per 1mL media and cells incubated for 24hours at 37°C, 5% CO_2. Media was then replaced with fresh culture media and RNA extracted from cells in 500µl TRIzol® reagent at 0, 24, 48 and 72 hours for qRT-PCR analysis.

2.6.2 ATDC5 cells

ATDC5 cells (RIKEN Cell Bank, Japan) were cultured in proliferation media consisting of DMEM/F-12, GlutaMAX, 5% FBS and 1% P/S at 37°c, 5% CO_2. Cells were seeded at 6400 cells/cm^2 unless otherwise stated.

2.6.2.1 Foetal Bovine Serum Batch test

ATDC5 cells are sensitive to changes in FBS batches. For this reason an FBS batch test was performed prior to carrying out experimental work on these cells. Cells were seeded in 6 well plates and DMEM/F-12, GlutaMAX (Life Technologies; 31331-093) supplemented with P/S and 5% FBS from various companies were independently added to cells. Media was changed every other day and RNA was extracted from cells on days 0, 2, 4, 6, 10 and 12 in 500µl TRIzol® reagent for qRT-PCR.

2.6.2.2 Insulin-mediated differentiation

To initiate ATDC5 differentiation in the chondrogenic lineage, differentiation media consisting of proliferation media supplemented with 10µg/ml human recombinant insulin (Sigma Aldrich; I2643), 10µg/mL human transferrin (Sigma Aldrich; 10652202001) and 30nM sodium selenite (Sigma Aldrich; S9133) was added to cells 24hours after seeding. Cells were cultured for 14 days and differentiation media was carefully changed every 2 days and then daily from day 10 onwards.

2.7 Real time reverse transcription polymerase chain reaction (qRT-PCR)

2.7.1 TRIzol based RNA extraction

Samples previously stored in TRIzol® reagent at -80°C were thawed on ice. 100µl of chloroform was added for every 500µl TRIzol® reagent and shaken vigorously for 15secs and incubated for 2mins at room temperature. Samples were centrifuged at 12,000g for 15mins at 4°c. The RNA-rich upper aqueous phase was pipetted into a fresh 1.5mL centrifuge tube with 250µl isopropanol and 50µg/ml GlycoBlue™ (Invitrogen; AM9516) for precipitation. Samples were inverted to mix, incubated at -20°C for 10mins and centrifuged at 12,000g for 10mins at 4°c. Supernatant was discarded and pellet washed in cold 75% EtOH was added to each tube before centrifuging at 12,000g for 5mins at 4°c. The supernatant was discarded and the pell*et al*lowed to air dry for 10mins. The pellet was gently re-suspended in 25µl or RNase-free water. The concentration and quality of RNA was quantified using a Nanodrop spectrophotometer (Thermo Scientific; Nanodrop 2000).

2.7.2 cDNA synthesis

1µl Random Primer (Promega; C1181) was added to 1µg RNA and incubated for 5mins at 70°C. Samples were immediately placed on ice and the following was added to each sample:

Table 2.12. cDNA synthesis reagents per sample

Reagent	**Volume**
Reverse Transcriptase Buffer (Promega; M1701)	5µl
dNTP mix, 10mM (Promega; C1145)	5µl
RNAsin Plus (Promega; N2611)	0.6µl
Molony-murine leukemia virus (M-MLV) Reverse Transcriptase (Promega; M1701)	1µl

Samples were incubated for 60mins at 37°C followed by 5mins at 95°C and stored at -20°C.

2.7.3 Quantitative Real-Time PCR (qRT-PCR)

10ng of template cDNA was amplified in an AB 7300 Real Time PCR System (Applied Biosystems). The following reagents were prepared in a mastermix and added to the cDNA to a total volume of 20µl as described in Table 2.13.

Table 2.13. qRT-PCR mastermix preparation per sample

Reagent	**Volume**
Takyon Rox SYBR MasterMix dTTP Blue (Eurogentec; UF-RSMT-B0701)	10µl
Forward Primer (100nM)	2µl
Reverse Primer (100nM)	2µl
dH_20	to 20µl total

2.7.3.1 qRT-PCR cycling parameters

Samples were ran in three technical or biological replicates using the following PCR parameters:

Activation of Takyon™	94°C	2min	
Denaturation	94°C	10sec	40 cycles
Annealing/Extension	60°C	60sec	
Hold	4°C	-	

2.7.3.2 Calculation of relative gene expression step using the comparative Ct Method

Murine specific primers were used (Table 2.14). Average sample CT values were normalised to the housekeeping gene β-Actin and the ΔCT calculated for each gene using the following equation

$= 2^{-(average\ CT\ of\ gene\ of\ interest\ -\ average\ CT\ of\ housekeeping\ gene)}$ (Livak and Schmittgen, 2001)

2.7.3.3 Primers

Table 2.14. List of primer sequences for qRT-PCR analysis

Primer Name	**5'-3' Forward Primer Sequence**	**5'-3' Reverse Primer Sequence**
HuR	TGCAAAGCTTATTCGGGATAAAG	GTGCTGATTGCTCTCTCTGCAT
MMP13	CGATGAAGACCCCAACCCTAA	ACTGGTAATGGCATCAAGGGATA
Sox9	AGTACCCGCACCTGCACAAC	TACTTGTAGTCCGGGTGGTCTTTC
Col2a1	TGGGTGTTCTATTTATTTATTGTCTTCCT	GCGTTGGACTCACACCAGTTAGT
Col10a1	CATGCCTGATGGCTTCATAAA	AAGCAGACACGGGCATACCT
Acan	CATGAGAGAGGCGAATGGAA	TGATCTCGTAGCGATCTTTCTTCT
RunX2	GACGAGGCAAGAGTTTCACC	GGACCGTCCACTGTCACTTT
Hoxa5	TCTCGTTGCCCTAATTCATCTTT	CATTCAGGACAAAGAGATGAACAGAA
Hoxb9	CAGGGAGGCTGTCCTGTCTAATC	CTTCTCTAGCTCCAGCGTCTGG
Hoxc6	CCTTCCTTATCCTGCCACCT	GCTGGAACTGAACACGACAT
Hoxc8	CGAAGGACAAGGCCACTTAAAT	AGGTCTGATACCGGCTGTAAGTTT
Hoxd4	TTCGGTGAACCCCAACTACAC	AAATTCCTTTTCCAGTTCTAGGACTTG
Hoxd13	GGTTTCCCGGTGGAGAAGTAC	TGGACACCATGTCGATGTAGC
Ihh	CCCCAACTACAATCCCGACA	TCATGAGGCGGTCGGC
Pthrp	AGTTAGAGGCGCTGATTCCTACA	GGACACTCCACTGCTGAACCA
β-Actin	GACAGGATGCAGAAGGAGATTACTG	CCACCGATCCACACAGAGTACTT

Primers were designed using Primer-BLAST (NCBI) and the efficiency of primers was tested using the following equation:

$$Efficiency = \left(10^{\frac{1}{slope}} - 1\right) x\ 100$$

The best housekeeping gene was determined using the geNorm algorithm (Appendices Supplementary Figure 1) (Vandesompele *et al.,* 2002).

2.8 Statistics

GraphPad Prism (Version 6) was used to perform statistical analysis. Individual statistics including normalisation is detailed for each experiment.

3 HuR in embryonic skeletal development

3.1 Introduction

HuR-deficient embryos display severe skeletal defects in the ossification of the ribs, limbs and craniofacial structures (Katsanou *et al.* 2009). In our laboratory, we have previously shown that HuR expression levels are reduced in various areas of embryos, including hypertrophic chondrocytes and the perichondrium, regions that are known to regulate cartilage development, long bone growth and mineralisation (McDermott *et al.* 2016). Interestingly, siRNA-mediated knockdown of HuR *in vitro* increased levels of MMP13 significantly (McDermott *et al*. 2016). It was also shown that HuR protein levels are also reduced in areas were MMP13 levels are increased in developing mouse embryos. Taken together, these findings suggest a role for HuR in embryonic development (McDermott *et al.* 2016).

Enhancers are able to drive the tissue specific expression of a target gene. A highly conserved non-exonic 359bp enhancer sequence, A1, has previously been identified 10kb upstream of the aggrecan transcription start site. Activated by its binding to the Sox trio, A1 was found to drive gene expression in differentiated articular and growth plate chondrocytes in both transgenic embryos and adult mice (Han and Lefebvre 2008). This aggrecan enhancer was subsequently used to create a murine line expressing both luciferase and the ligand-dependant chimeric Cre recombinase, Cre-ER^{T2} (Cascio *et al.* 2014). This allowed the expression of the transgene to be controlled in a temporal and cartilage-specific manner, while luciferase activity allowed expression to be monitored in real time.

A proximally located 2.4kb Prx1 limb enhancer was also identified in the 5' region of the Prx1 gene that is sufficient to drive the expression of a transgene in mesenchymal cells during limb bud development, in the lateral plate mesoderm and the cranial mesenchyme (Martin and Olson 2000). Cre activity was first observed at E9.5 in the limb buds and by E16.5 in the entire limb bud and inter-limb flank, and in the craniofacial mesenchyme. Cre-recombinase was later placed under the regulation of the Prx1 enhancer and lead to Cre

expression throughout the early limb bud mesenchyme and in a subset of craniofacial mesenchyme from E9.5 onwards (Logan *et al.* 2002)

Previous studies have described the effect of general HuR knockout in developing embryos (Katsanou *et al.* 2009, Herjan *et al.* 2013). Importantly however, HuR ablation has not been more closely examined in a cartilage-specific and skeletal-specific manner. We have therefore generated both a cartilage-specific, inducible knockout mouse model of HuR using the Cre/LoxP system were CreER^{T2}*luc* is under the control of the aggrecan enhancer A1; and a non-inducible skeletal-specific knockout mouse model of HuR were Cre is under the control of a PRX1 enhancer element controlling limb bud and craniofacial development. By utilising Cre recombinases that enable the knockout of HuR in temporal and spatial manner, we are able to specifically examine the role of HuR during cartilage and bone development.

3.2 Results

3.2.1 Aggrecan-enhancer driven knockout of HuR results in reduced and altered cartilage mineralisation during embryonic development

Previously, a 0.77kb genomic DNA fragment containing the second exon of the HuR gene was flanked with *loxP* sequences to generate HuR$^{fl/fl}$ mice (Figure 3.1A) (Katsanou *et al.* 2009). To investigate the *in vivo* functions of HuR in a cartilage-specific and inducible manner, cryopreserved embryos containing the HuR floxed site were re-derived in surrogate mothers and at sexual maturity were subsequently crossed with transgenic mice expressing CreER^{T2} under the control of the aggrecan enhancer A1 (Figure 3.1B) (Han and Lefebvre 2008). The resulting HuR$^{fl/WT}$AcanA1-CreER^{T2}*luc*$^{+}$ F1 progeny were subsequently backcrossed to yield an F2 progeny of HuR$^{fl/fl}$AcanA1-CreER^{T2}*luc*$^{+}$ mice.

To knockout HuR during embryonic development, HuR$^{fl/fl}$AcanA1-CreER^{T2}*luc*$^{+/-}$ mice were inter-crossed via timed matings and vaginal plugs checked for embryonic day E0.5. Pregnant females were dosed with 3mg tamoxifen and 1.5mg progesterone via intraperitoneal injection at E9.5, the start of aggrecan

expression. Progesterone was given in order to counteract any potential for miscarriage due to the toxicity of tamoxifen. 4-hydroxy-tamoxifen is an estrogen ligand which allows Cre ER^{T2} to recombine the *loxP* sites that flank HuR and thereby excising HuR (Figure 3.2). Embryos were collected at E16.5. In order to test the efficiency of *loxP* recombination a DNA-based PCR assay needed to be developed.

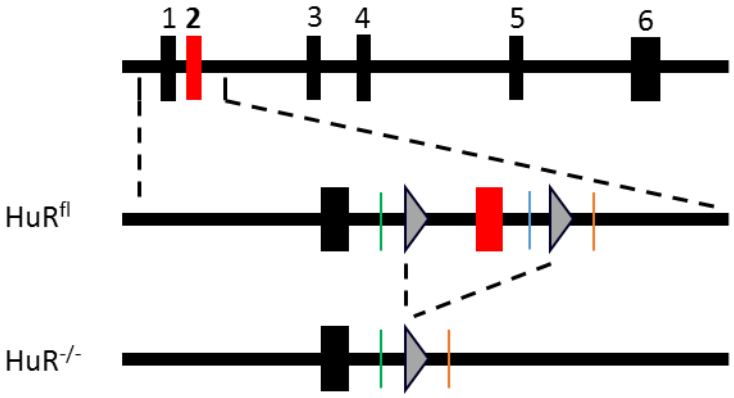

Figure 3.1. Schematic diagram of the complete Elavl1 locus on mouse chromosome 8. Magnifications of the region containing the second exon (red) in the floxed (HuR^{fl}) and Cre-recombined locus ($HuR^{fl/fl}$). LoxP genes are indicated as arrowheads). Forward primer remained the same (green) while the reverse primers are indicated in blue for genotyping and orange for the recombination assay.

3.2.1.1 Genotyping and development of recombination assay

Frequent genotyping of transgenic mice populations is required during conditional gene targeting and monitoring of tissue-specific Cre recombination efficiency. The first step in the identification of embryo genotypes was to perform a PCR for both HuR and Cre recombinase, as well as the internal control fatty acid-binding protein 2 (Fabp2). $HuR^{fl/fl}$AcanA1-$CreER^{T2}luc^{-}$ mice were used as control for subsequent experiments. Gel electrophoresis revealed double transgenic embryos that contained both the floxed HuR alleles and Cre recombinase (Figure 3.2A).

We needed to confirm that Cre-mediated recombination of the *loxP* sites had occurred in the tamoxifen dosed double-mutant embryos. We first designed a recombination assay by designing primers that flanked the *loxP* sites and optimised PCR conditions on DNA extracted from the tails of both HuR$^{fl/fl}$ AcanA1-CreER^{T2}luc^{+} and HuR$^{fl/fl}$AcanA1-CreER^{T2}luc^{-} embryos. AcanA1-Cre is expressed in the tail of mice (Cascio *et al.* 2014) and so recombination of *loxP* sites should have been detectable in this tissue. However, we did not see any detectable levels of recombination in the tail DNA. Previous Sox-9 mediated knockout of HuR resulted in changes in the ossification of the ribs; we therefore decided to check whether recombination had occurred at detectable levels in the DNA of the ribs of HuR$^{fl/fl}$AcanA1-CreER^{T2}*luc*$^{+}$ embryos. The recombination assay followed by gel electrophoresis revealed recombination in the ribs when compared to the ribs of HuR$^{fl/fl}$AcanA1-CreER^{T2}*luc*$^{-}$ embryos. Fabp2 as an internal control ensured DNA was present in all samples (Figure 3.2B).

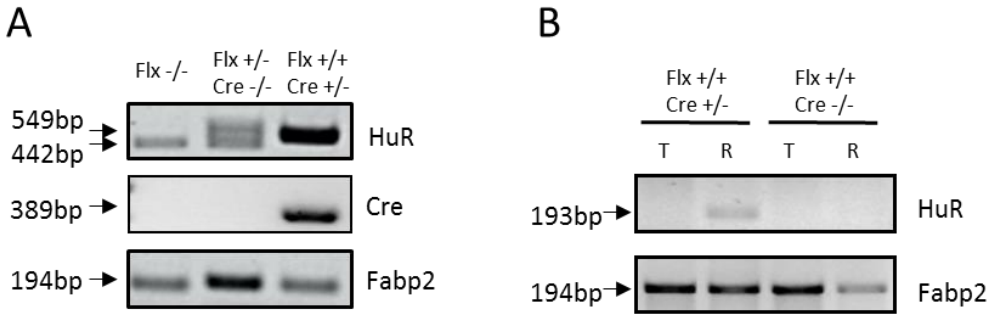

Figure 3.2. Genotyping of transgenic HuR^{fl}AcanA1-CreER^{T2}luc embryos. A) A representative sample of wild-type, heterozygous and homozygous floxed embryos were PCR genotyped and samples ran on a 1.5% agarose gel for DNA separation. (B) Recombination assay detailing successful knockout of the loxP flanked HuR fragment in the ribs of transgenic HuR$^{fl/fl}$AcanA1-CreER^{T2}l*uc*$^{+}$ embryos as depicted by the 193bp fragment. HuR$^{fl/fl}$AcanA1-CreER^{T2}luc^{+} and HuR$^{fl/fl}$AcanA1-CreER^{T2}luc^{-} mice were injected with tamoxifen and Cre negative mice used as controls for recombination assay.

3.2.1.2 Alizarin red and alcian blue whole-mount staining of Aggrecan A1-driven HuR knockout E16.5 embryos

After confirming the genotype, selected HuR$^{fl/fl}$AcanA1-CreER^{T2}*luc*$^{+}$ and HuR$^{fl/fl}$AcanA1-CreER^{T2}*luc*$^{-}$ littermate embryos were stained with alizarin red and alcian blue to more closely examine any abnormalities in skeletal development. Embryos were stained with alcian blue for 1-4h followed by alizarin red for 3-4h using the whole mount stain protocol described by (Rigueur and Lyons 2014). In this protocol embryos are cleared into 1% KOH for 12h then transferred to 50% glycerol: 50% KOH. Staining showed a reduction in ossification particularly in the craniofacial regions and ribs of HuR deficient embryos (Figure 3.3D-F) when compared to Cre^{-} littermates (Figure 3.3A-C). A lack of alcian blue staining was also observed in HuR deficient embryos in the areas surrounding the nasal cavity including the lateral, septal and in particular the alar cartilages (Figure 3.3F). Interestingly, there were no immediate differences in the staining of the long bones of the forelimbs. Using this protocol however, embryos lacked a penetration of alcian blue and alizarin red stain in underlying tissues, while a higher concentration of glycerol : KOH during clearing meant embryos did not clear well. In order to get optimal alcian blue / alizarin red staining a new protocol was adopted.

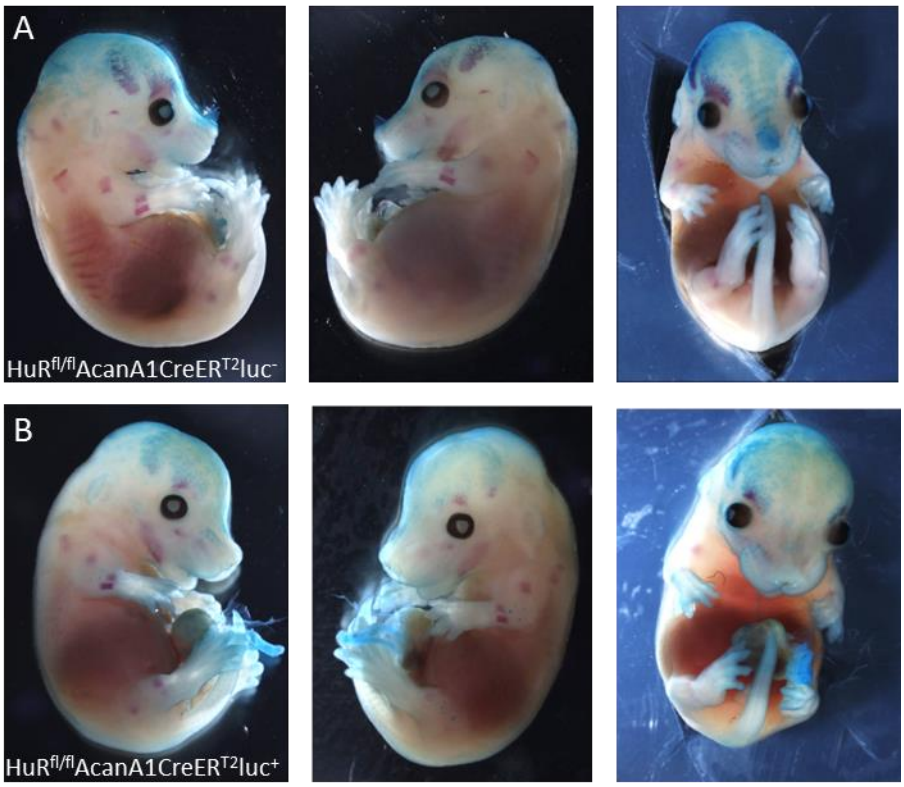

Figure 3.3. Protocol one alizarin red and alcian blue whole mount staining of representative of HuR$^{fl/fl}$AcanA1-CreER^{T2}luc^{+} and HuR$^{fl/fl}$AcanA1-CreER^{T2}luc^{-} embryos at E16.5. Initial whole mount staining using the Rigueur and Lyons (2014) protocol allowed visualisation of mineralised structures including the long bones of the fore- and hind-limbs and the ribs of Cre^{-} (A) and HuR knockout (B) embryos. Altered ossification can be seen in the ribs and craniofacial structures of the HuR knockout embryos (B) and in the lack of alcian blue staining of the craniofacial structures when compared to Cre^{-} (A). (HuR$^{fl/fl}$AcanA1-CreER^{T2}luc^{+} *n=4*, HuR$^{fl/fl}$AcanA1-CreER^{T2}luc^{-} *n=3*).

New litters of E16.5 HuR$^{fl/fl}$AcanA1-CreER^{T2}*luc*$^{+}$ and HuR$^{fl/fl}$AcanA1-CreER^{T2}*luc*$^{-}$ embryos were whole mount stained with alizarin red and alcian blue using a protocol adapted from McLeod (1980). This protocol allowed for complete visualisation of the skeleton and a distinction between alizarin red stained bone and alcian blue stained cartilage. This staining approach demonstrated a similar altered ossification pattern in HuR knockout embryos to that observed in previous whole-mount stained embryos with the older method, however the new method improved visualisation of the skeletal structures (Figure 3.4A & B). Microscopic examination of HuR$^{fl/fl}$AcanA1-CreER^{T2}*luc*$^{+}$ embryos revealed severe defects in skeletal development. HuR knockout embryos exhibited deficient

mineralisation in the craniofacial structures of the frontal and dentary bones. Similar to the previous observations in Figure 3.3D-F, structures surrounding the nasal cavity in knockout embryos were less defined and remain mostly cartilaginous (Figure 3.4C). Whole mount staining also revealed that skeletal structures including the ribs and intervertebral discs remained predominantly cartilaginous, highlighting a potential disruption to the endochondral ossification process in these tissues (Figure 3.4C). There was, however, no visual differences observed in the long-bones of HuR knockout embryos compared to their Cre^- littermates.

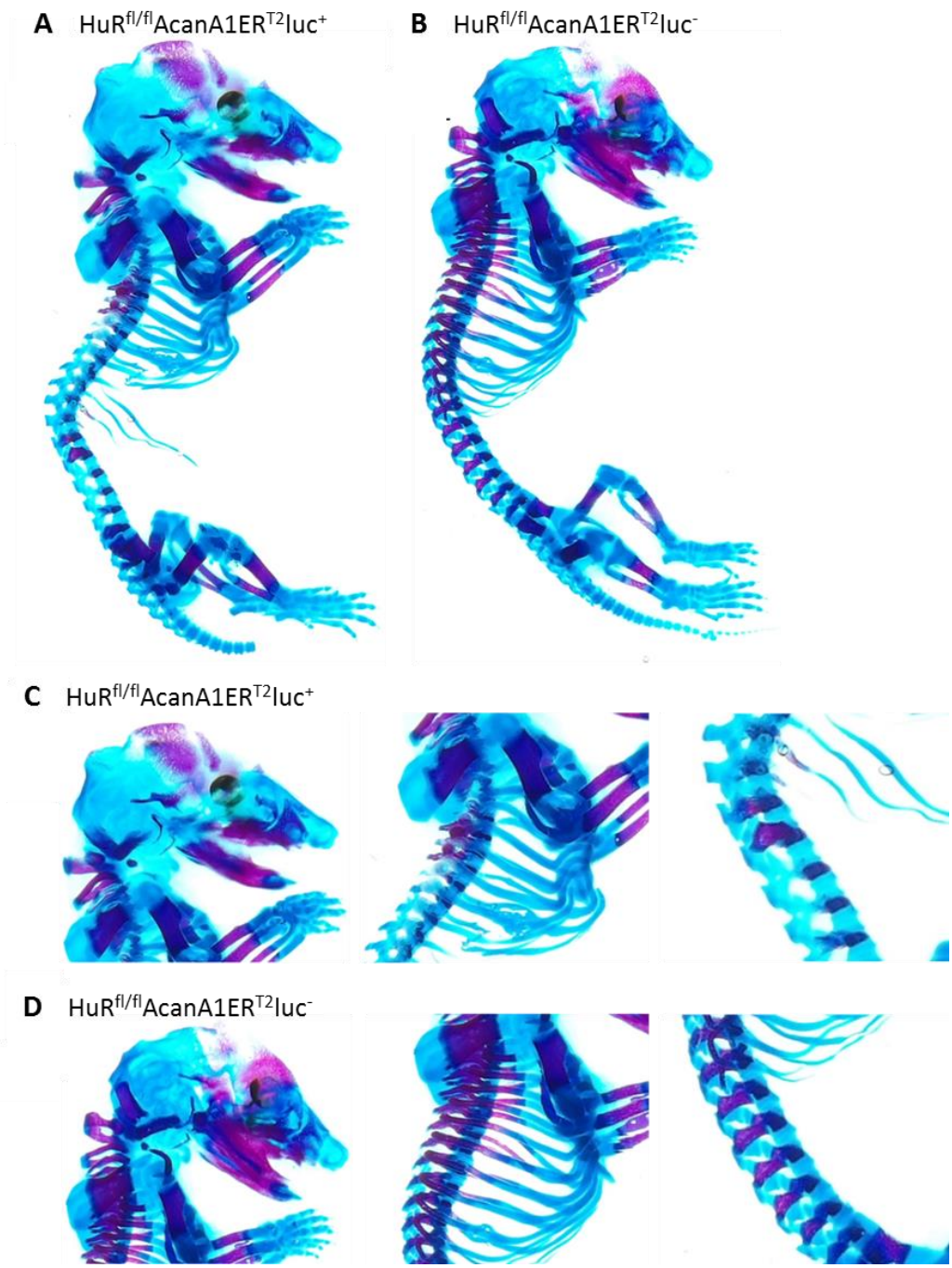

Figure 3.4 . Representative skeletal staining of HuR$^{fl/fl}$AcanA1-CreER^{T2}luc^{+} embryos vs HuR$^{fl/fl}$AcanA1-CreER^{T2}luc^{-} littermates injected with tamoxifen at E9.5 and harvested at E16.5. Alizarin red and alcian blue staining illustrates the altered ossification between HuR knockout (A & C HuR$^{fl/fl}$AcanA1-CreER^{T2}luc^{+}) and Cre^{-} (B & D HuR$^{fl/fl}$AcanA1-CreER^{T2}luc^{-}) littermates, particularly in the ribs, spine and craniofacial regions. (HuR$^{fl/fl}$AcanA1-CreER^{T2}luc^{+} n=2, HuR$^{fl/fl}$AcanA1-CreER^{T2}luc^{-} n=6).

3.2.1.3 Histological analysis of whole-mount stained embryo limbs reveals a shortening of the long bones in HuR knockout *embryos*

Previously, Sox2 Cre^{+} HuR knockout embryos presented with shorter long bones, with minimal ossification zones in the scapulae, femurs and tibia (Katsanou *et al.* 2009), but no detailed examination of skeletal cell morphology has been carried out in HuR knockout embryos. We therefore decided to histologically section the fore- and hind-limbs of alizarin red/alcian blue stained HuR knockout and Cre^{-} littermates (Figure 3.5). During tissue processing to prepare the samples for wax embedding, alcian blue staining was well retained in the tissue but alizarin red stain was lost. This loss of alizarin red appeared to be worse in the tissues from HuR knockout embryos (Figure 3.5 D-I). Nevertheless, the retained alcian blue staining allowed the cartilaginous and mineralised zones of the femur, tibia and fibula to be defined. The chondrocytes of the articular cartilage appear less organised in the HuR knockout embryos, with no distinction between hypertrophic, prehypertrophic and proliferative chondrocytes (Figure 3.5 F&I) when compared to the highly organised structure of the Cre^{-} embryos (Figure 3.5C). Hypertrophic chondrocytes in mutant embryos also appear morphologically different with a reduction in size (Figure 3.5 F&I).

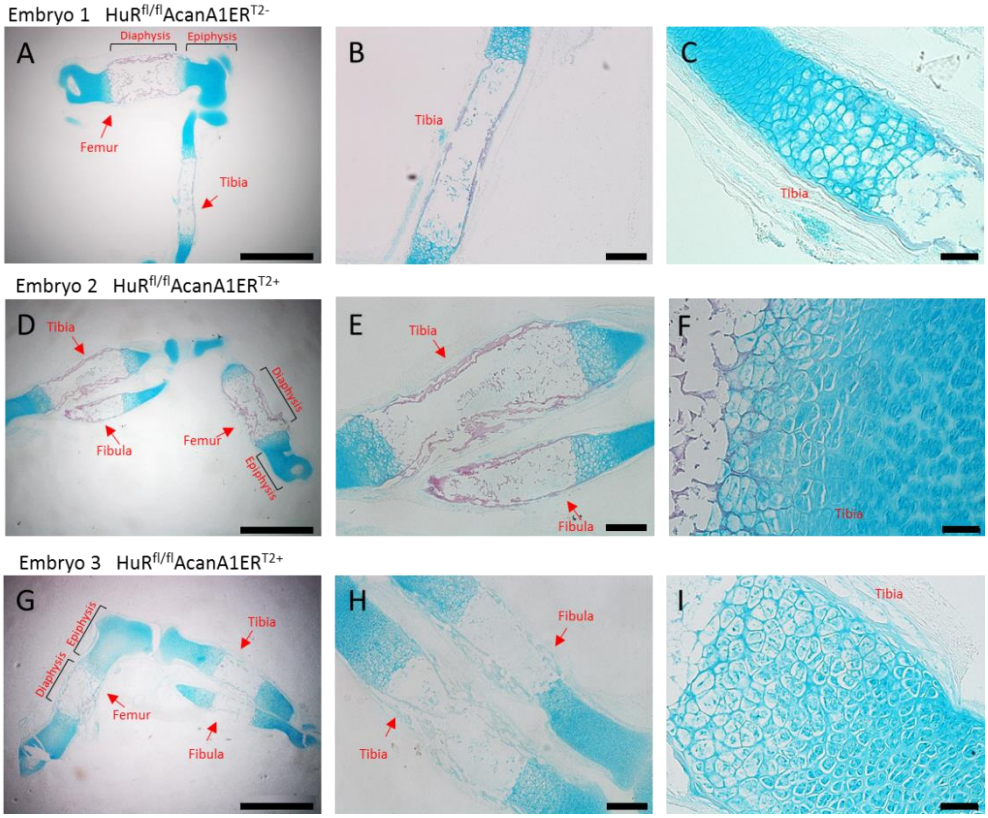

Figure 3.5. Representative histological sections of the hindlimbs from whole mount stained E16.5 HuR knockout and Cre^{-} embryos. Chondrocytes of the articular cartilage appear to be less organised in the epiphysis of HuR knockout embryos, with no distinction between hypertrophic, prehypertrophic and proliferative chondrocytes (F+I). Morphological differences due to a size reduction in hypertrophic chondrocytes also appears in HuR knockout embryos. The tibia, fibula, femur, epiphysis and diaphysis are shown. Scale bars A,D,G = 500µm; B,E,H = 100µm; C,F,I = 25µm. (HuR$^{fl/fl}$AcanA1-CreER^{T2}luc^{+} *n=2*; HuR$^{fl/fl}$AcanA1-CreER^{T2}luc^{-} *n=3*).

3.2.1.4 Micro CT analysis and bone volume

Low-resolution µCT scans of E16.5 HuR knockout embryos confirmed a delay in endochondral ossification of the ribs, IVD and craniofacial structures (Figure 3.6 B & C). Representative images of the scans depicts a lack of bone formation, particularly in the ribs (Figure 3.6 D) and altered ossification in the craniofacial structures (Figure 3.6 E), with the exception of the mandible which has mostly ossified in both knockout and Cre^{-} embryos. µCT analysis revealed however, no

statistically significant difference in bone volume between HuR knockout and Cre^- embryos ($p = \leq 0.0152$).

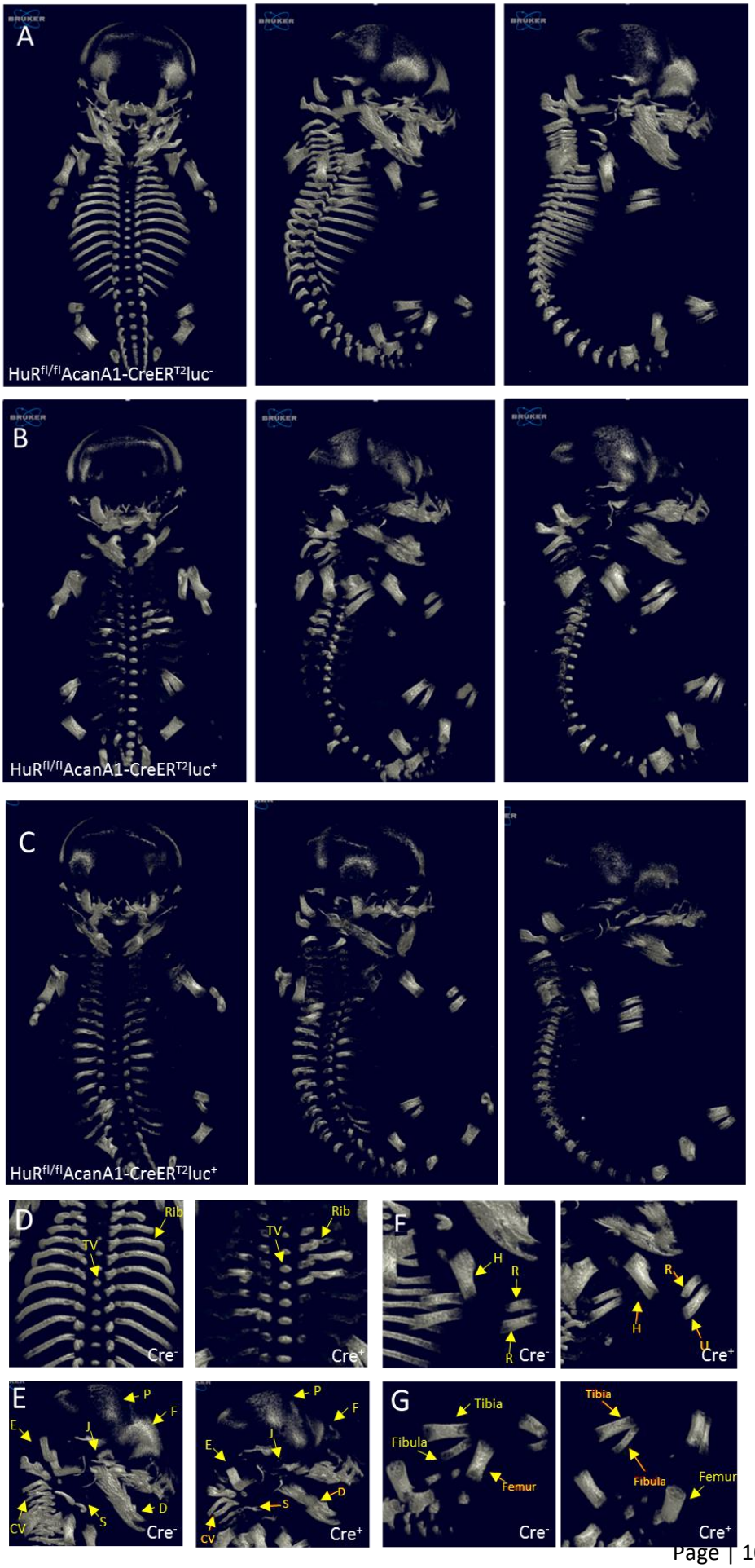
A
HuRfl/flAcanA1-CreERT2luc-
B
HuRfl/flAcanA1-CreERT2luc+
C
HuRfl/flAcanA1-CreERT2luc+
D
Rib
TV
Cre-
Rib
TV
Cre+
F
H
R
R Cre-
R
H
U
Cre+
E
P
F
E
J
D
S
CV
Cre-
P
F
E
J
S
D
CV
Cre+
G
Tibia
Fibula
Femur
Cre-
Tibia
Fibula
Femur
Cre+

Figure 3.6. Analysis of HuR$^{fl/fl}$AcanA1-CreER^{T2+} and HuR$^{fl/fl}$AcanA1-CreER^{T-+} embryos, injected with tamoxifen at E9.5 and harvested at E16.5. Micro CT analysis identified HuR knockout embryos exhibited impaired ossification (B&C) compared to Cre^{-} littermates (A). In particular, the ribs, spine (D) and craniofacial structures (E) exhibit the most severe changes in mineralisation in HuR knockout embryos. (F= frontal, J= jugal, P = parietal, E = exoccipital, TV = throatic vertebrae, Cv = cervical vertebrae, S= sternum, D= dentary, H= humerus, R= radius, U= Ulna). All mice are HuR$^{fl/fl}$, figures displayed as CreER^{T2}luc + or -.

3.2.2 *PRX1*-driven knockout of HuR results in altered long bone development

The use of aggrecan CreER^{T2}*luc* mice allowed knockout of HuR in cartilaginous tissues at specific time points during development. We also wanted to understand whether HuR was necessary for control of skeletal development before cartilage differentiation had taken place. We therefore crossed HuR$^{fl/fl}$ mice with non-inducible, transgenic Prx1-Cre mice were Cre recombinase is reported to be expressed in the early limb bud mesenchyme and developing craniofacial structures from E9.5 (Logan *et al.* 2002). Resulting progeny with the genotype HuR$^{fl/WT}$Prx1-Cre$^{+/-}$ were subsequently backcrossed to HuR$^{fl/fl}$ mice to produce litters were one in four embryos are of the phenotype HuR$^{fl/fl}$Prx1-Cre$^{+/-}$ (Figure 3.7A)

3.2.2.1 Genotyping and recombination assay

F2 progeny from HuR$^{fl/WT}$Prx1-Cre$^{+/-}$ and HuR$^{fl/fl}$ crosses were collected at E13.5 and E16.5. Embryos were genotyped via PCR for HuR status and for the presence of the Prx1 Cre recombinase gene. Gel electrophoresis revealed double transgenic embryos that contained both the floxed HuR alleles and Cre recombinase (Figure 3.7B).

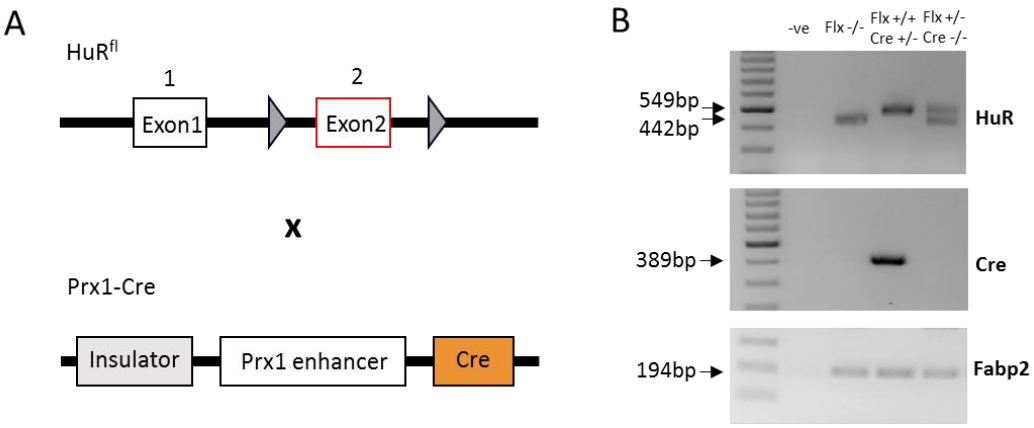

Figure 3.7. Schematic diagram showing the crossing of HuR$^{fl/fl}$ and Prx1-Cre mouse lines and resulting genotypes. **(A)** HuR$^{fl/fl}$ mice were crossed with *Prx1*-Cre$^{+/-}$ mice to yield a non-inducible transgenic line containing HuR$^{fl/fl}$ Prx1-Cre$^{+/-}$ that would result in HuR conditional knockout embryos. **(B)** Genotyping revealed HuR$^{fl/fl}$ Prx1-Cre$^{+/-}$ embryos.

3.2.2.2 Prx1-driven HuR knockout at gestation E13.5

3.2.2.2.1 Phenotype of Prx1-Cre driven HuR knockout embryos

During HuR *Prx1*-Cre embryo collection we noticed some were phenotypically different compared to their control littermates. Genotyping confirmed these phenotypically different embryos to be HuR$^{fl/fl}$Prx1-Cre^{+} embryos. Prx1-Cre mediated knockdown of HuR appeared to result in a severe shortening of both the hind- and fore- limbs in varying degrees of severity (Figure 3.8 B & C) when compared to Cre^{-} littermates (Figure 3.8A) at E13.5. The patterning of the digits was also affected with some HuR$^{fl/fl}$ Prx1-Cre^{+} embryos lacking any digit formation (Figure 3.8C). Craniofacial structures also appear to be affected by the tamoxifen recombination of HuR flox sites, with one embryo lacking a fully formed eye socket (Figure 3.8C). Another embryo also displayed a cleft palate (Figure 3.8D). All mutant embryos were also smaller in size than control littermates.

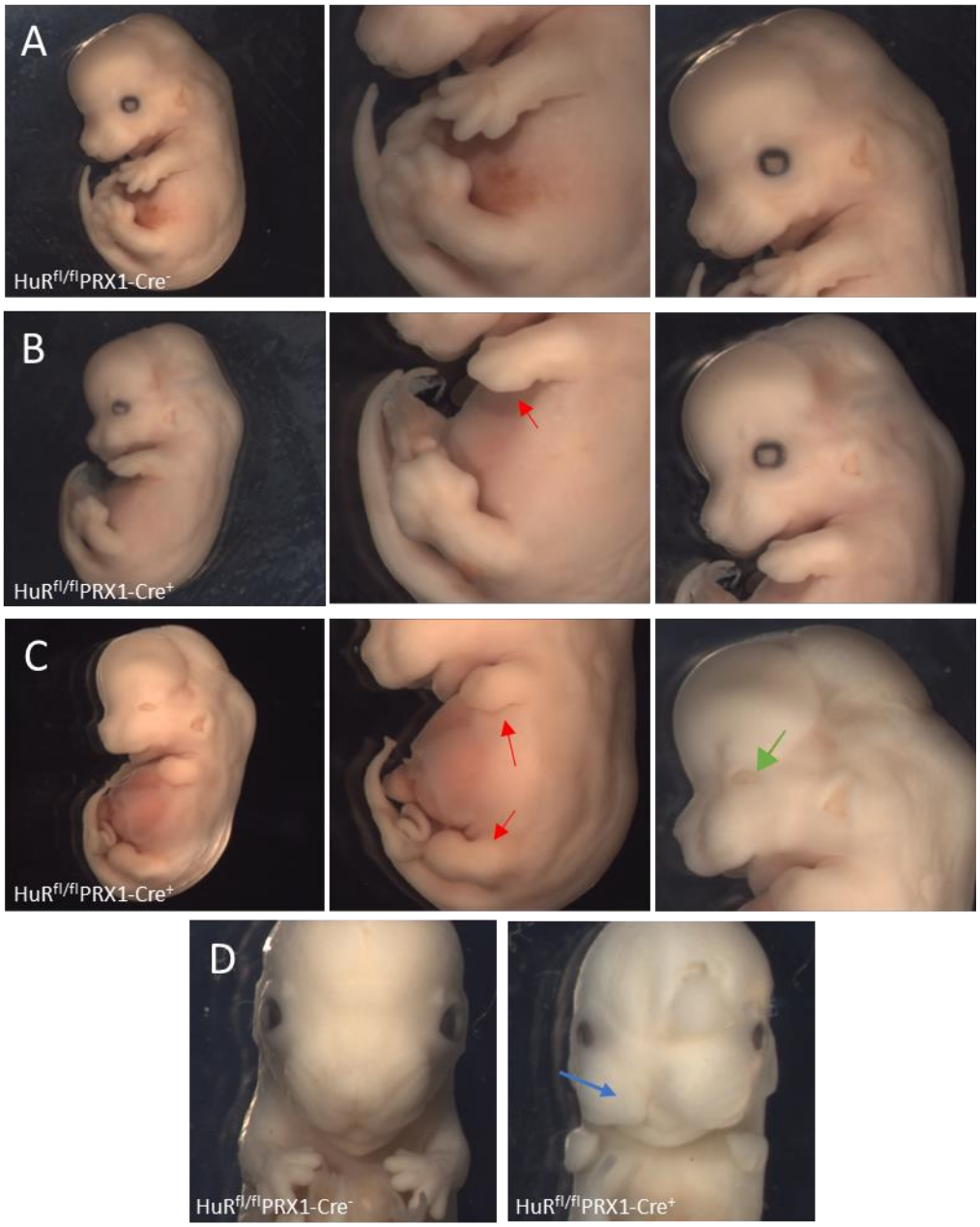

Figure 3.8. Representative photographs of HuR$^{fl/fl}$Prx1-Cre^{+} and HuR$^{fl/fl}$Prx1-Cre^{-} embryos at E13.5. *Prx1*-Cre mediated HuR knockdown leads to smaller embryos with stunted limb growth (red arrows), inadequate patterning of the digits and a flattened facial structure (B and C) when compared to Cre^{-} littermates (A). One embryo also displayed a cleft palate (blue arrow) (D), while another presented with a deformed eye socket (green arrow) (C). (HuR$^{fl/fl}$Prx1-Cre^{+} n= 10 HuR$^{fl/fl}$Prx1-Cre^{-} n=15)

3.2.2.2.2 Alizarin red and alcian blue whole-mount staining of HuR$^{fl/fl}$Prx1-Cre E13.5 embryos

E13.5 HuR$^{fl/fl}$AcanA1-CreER^{T2+} and control HuR$^{fl/fl}$AcanA1-CreER^{T2-} embryos were whole mount stained with alizarin red and alcian blue, again adapted from a previously described protocol (McLeod, 1980). As these embryos were younger than previously whole-mount stained embryos, they may have been damaged if placed directly into 1% KOH so they were instead cleared through the series of 20%, 50% and 80% glycerol: 1% KOH solutions straight after alizarin red and alcian blue staining. Examination of HuR$^{fl/fl}$Prx1-Cre^{+} embryos revealed a severe phenotype affecting cartilage development in the limbs as well craniofacial development (Figure 3.9 B-D). HuR$^{fl/fl}$ Prx1-Cre^{+} embryos present with severely stunted limb development and inappropriate patterning of the tibia/fibula, radius/ulna and paws indicating severely dysregulated chondrogenesis during limb bud development. Whole mount staining of Prx1-driven HuR$^{fl/fl}$Prx1-Cre^{+} embryos at E13.5 reveals that long bone cartilage formation has begun in embryo B, particularly in the hindlimb were tibia cartilage is present, however there is a distinct lack of autopod development. Embryo C also lacks autopod development but is also lacking in tibia development, while embryo D completely lacks development of bones that should be present after joint development, including the tibia/fibula and the radius/ulna. It appears that cartilage development of the ribs and spine is also altered in HuR$^{fl/fl}$Prx1-Cre^{+} embryos when compared to the complete structures of the Cre^{-} embryo. There is also some less severe differences in the cartilage formation of the craniofacial regions, most noticeably around the nose and eye socket and a shortened dentary in embryos C and D.

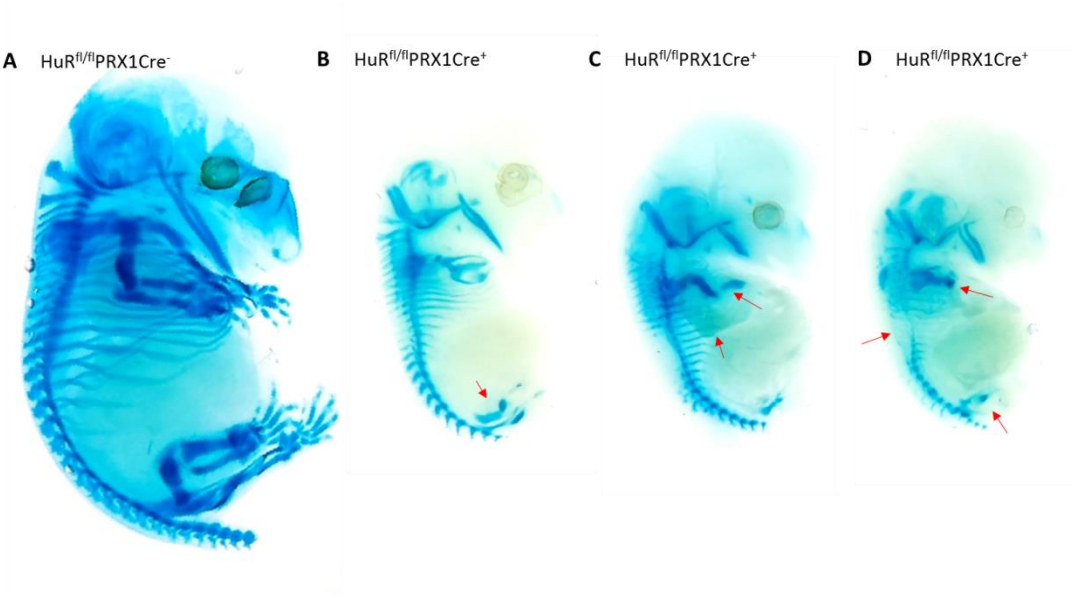

Figure 3.9. Representative whole mount skeletal staining of HuR$^{fl/fl}$Prx1-Cre^{+} embryos vs HuR$^{fl/fl}$Prx1-Cre^{-} littermate at E13.5. Embryos were stained with alcian blue and alizarin red to highlight cartilage and bone respectively, and cleared with KOH/glycerol as previously described. Endochondral bone formation has not yet begun in E13.5 embryos so alizarin red staining is absent from these embryos. Alcian blue staining shows a severe lack of cartilage development in varying degrees of severity in HuR$^{fl/fl}$Prx1-Cre^{+} embryos (B, C, D) compared to Cre^{-} (A). (HuR$^{fl/fl}$ Prx1-Cre^{+} n= 10, HuR$^{fl/fl}$Prx1-Cre^{-} n=15)

3.2.2.2.3 Histological analysis of E13.5 embryo limbs

To examine the phenotype of the cartilage in the affected long bones in more depth we histologically sectioned the entire fore- and hind- limbs of *Prx1*-Cre driven HuR knockout embryos and their Cre^{-} control counterparts. Limbs were sectioned at 5µM thickness and stained with toluidine blue and counterstained with fast green. Microscope analysis of stained sections confirmed disruption to the development of skeletal structures. In *Prx1*-mediated HuR knockout embryos there appeared to be no cartilage formation and a lack of definition of the developing forelimb (C) and hindlimb (L) autopods of embryo 3 when compared to patterning and cartilage development of the autopods in the forelimb (A) and hindlimb (J) of Cre^{-} embryo 1 (Figure 3.10). There was however, variability in the lack of cartilage development in HuR$^{fl/fl}$Prx1-Cre^{+} embryos as there is cartilage formation in both the forelimb (B) and hindlimb

(K) of embryo 2. HuR knockout driven by *Prx1*-Cre recombination also severely affected the forelimbs, were cartilage development of the long bones appears to be disrupted during chondrogenesis. The morphology of chondrocytes is also altered from rounded hypertrophic chondrocytes in the Cre^- embryos to a flattened and more compact state in HuR knockout embryo limbs (Figure 3.10 H & I).

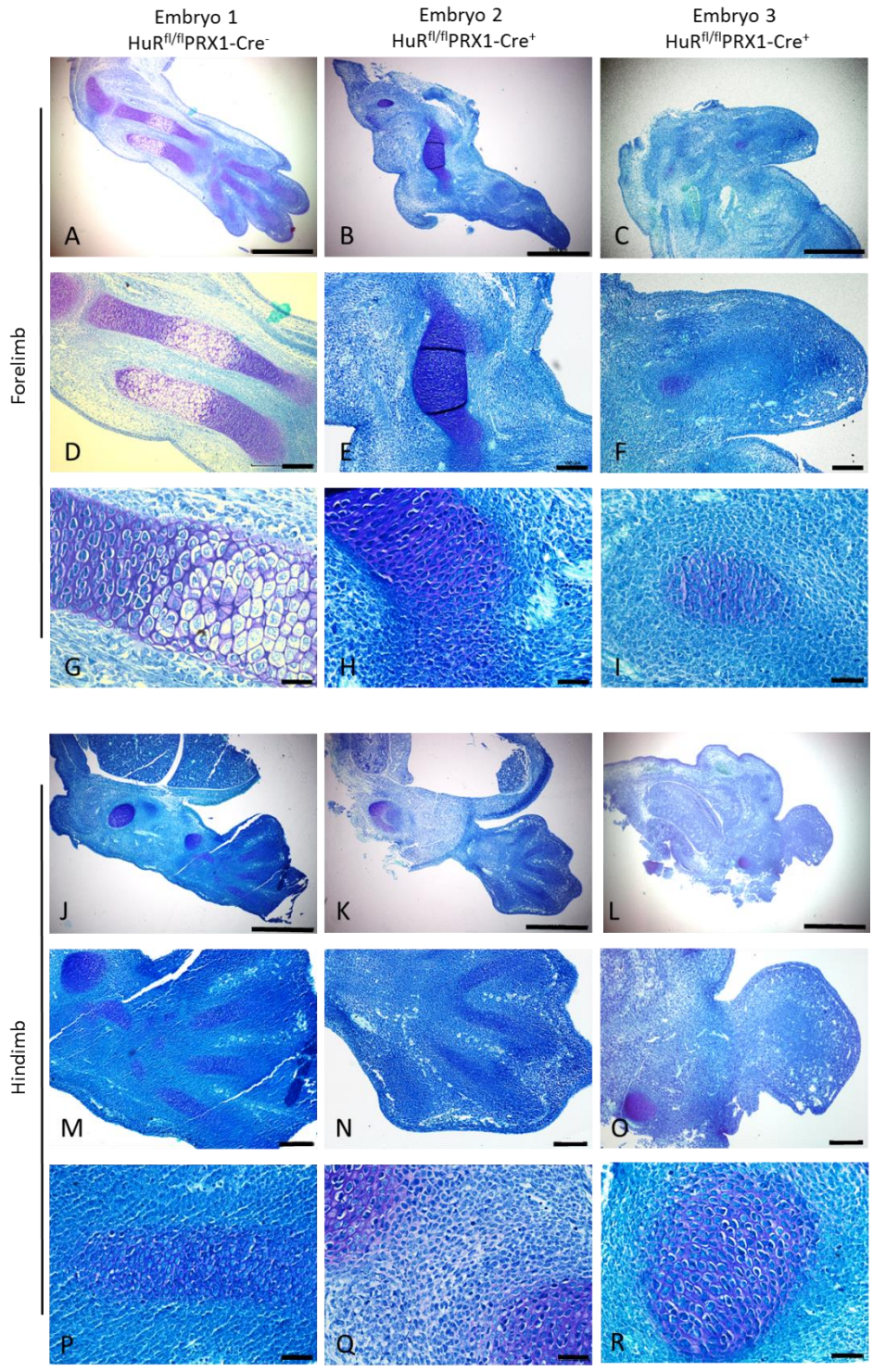

Figure 3.10. Representative histological sections of HuR$^{fl/fl}$Prx1-Cre^{+} and HuR$^{fl/fl}$Prx1-Cre^{-} E13.5 littermate embryo forelimbs and hindlimbs. Histological analysis confirmed a delay in the development of the long bones of the ulna and radius in HuR$^{fl/fl}$Prx1-Cre^{+} embryos 2 (B) and 3 (C) and in the hindlimb of embryo 3 (L), particularly during endochondral ossification. Chondrocyte morphology also appears to be altered in HuR$^{fl/fl}$Prx1-Cre^{+} embryos compared to HuR$^{fl/fl}$Prx1-Cre^{-}. Scale bars A,B,C,J,K,L = 500µm; D,E,F,M,N,O = 100µm; G,H,I,P,Q,R = 25µm. (HuR$^{fl/fl}$Prx1-Cre^{+} n= 6 HuR$^{fl/fl}$Prx1-Cre^{-} n=6)

3.2.2.3 Prx1-driven HuR knockout at gestation E16.5

3.2.2.3.1 Phenotype of Prx1-Cre driven HuR knockout embryos

In order to examine the role of HuR knockout during various time points of embryonic development, we next examined Prx1-Cre HuR knockout embryos at E16.5, after which point the skeleton is fully formed in wild type mice. Upon embryo collection, we again noticed differences between littermates, however differences were less severe than in E13.5 embryos. Genotyping confirmed these embryos to be of the genotype $HuR^{fl/fl}$Prx1-Cre^{+}. Prx1-mediated knockout of HuR resulted in substantially smaller embryos compared to Cre^{-} littermates (Figure 3.11), however, while limbs were overall smaller in size, they appeared to be normal in E16.5 embryos suggesting the severe effects observed in limb development at E13.5 had been rescued by E16.5.

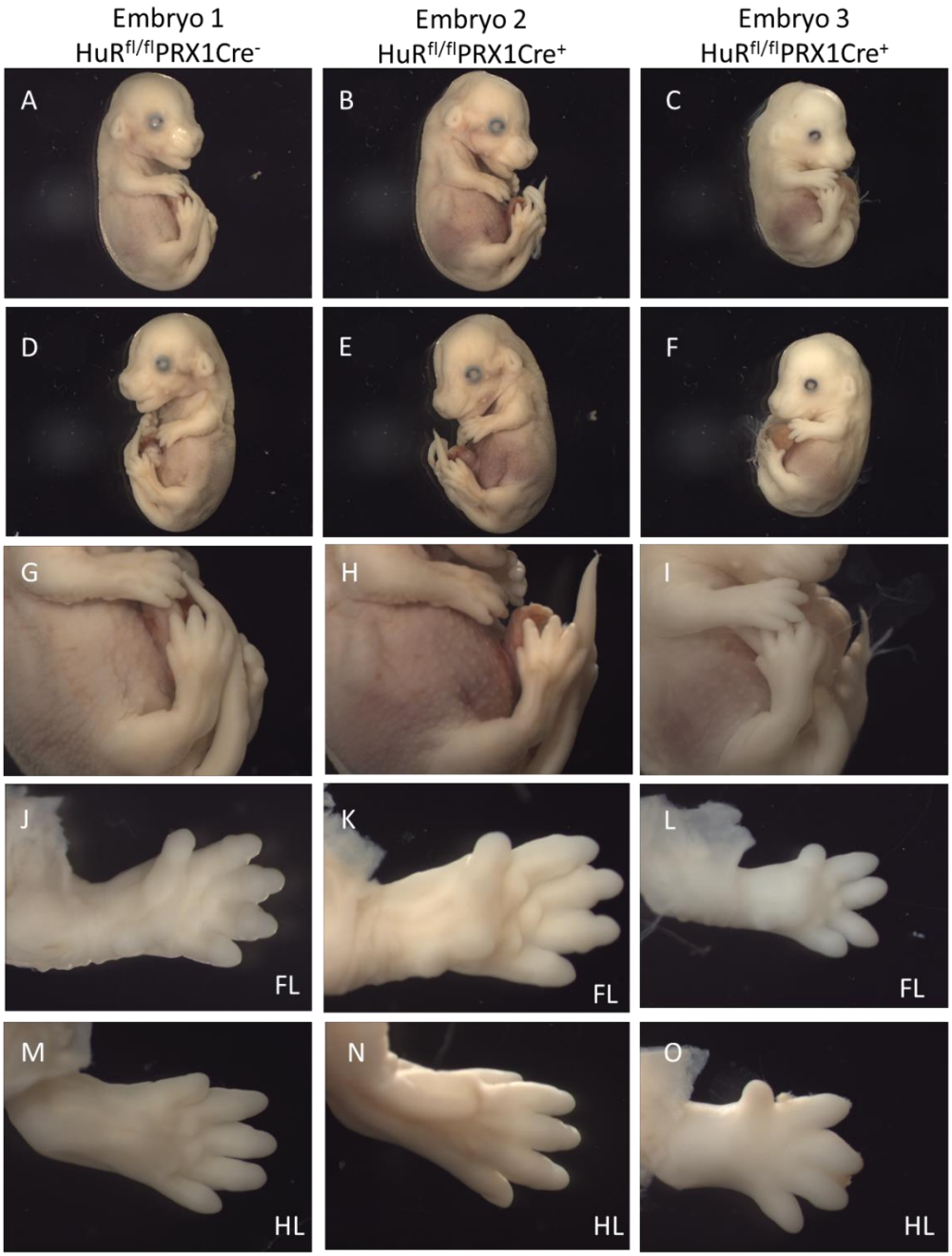

Figure 3.11. Representative photographs of HuR$^{fl/fl}$Prx1-Cre^{+} and HuR$^{fl/fl}$Prx1-Cre^{-} embryos at E16.5. *Prx1*-Cre mediated HuR knockdown leads to smaller embryos (Embryo 3) compared to Cre^{-} littermates (Embryo 1), however in varying degrees of severity (Embryo 2). It appears that Embryo 3 exhibits small delays in the development of the autopod of both the fore- and hind-limbs (L&O respectively) compared to Cre^{-} (J&M respectively). (FL = forelimb, HL = hindlimb). (HuR$^{fl/fl}$Prx1-Cre^{+} n= 4, HuR$^{fl/fl}$Prx1-Cre^{-} n=5)

3.2.2.3.2 Alizarin red and alcian blue whole-mount staining of HuR$^{fl/fl}$Prx1-Cre E16.5 embryos

In order to visualise the skeleton in E16.5 embryos, whole mount staining was again performed with alizarin red and alcian blue as previously described in *Methods section 2.2.1.1.1.* Examination of E16.5 embryos revealed differences in bone mineralisation of HuR$^{fl/fl}$Prx1-Cre^{+} embryos compared to their HuR$^{fl/fl}$Prx1-Cre^{-} counterparts (Figure 3.12). HuR$^{fl/fl}$Prx1-Cre^{+} embryos lacked any alizarin red staining and therefore any bone development (Figure 3.12 B & C). There was variation in the severity of HuR knockout embryos, with some more severely affected than others, with embryo C being smaller than embryo B. Differences were observed in the development of cartilage in knockout embryos, particularly in the craniofacial structure. While other structures, including the limbs that are severely affected at E13.5, did not seem to differ from their Cre^{-} littermates except for the overall size.

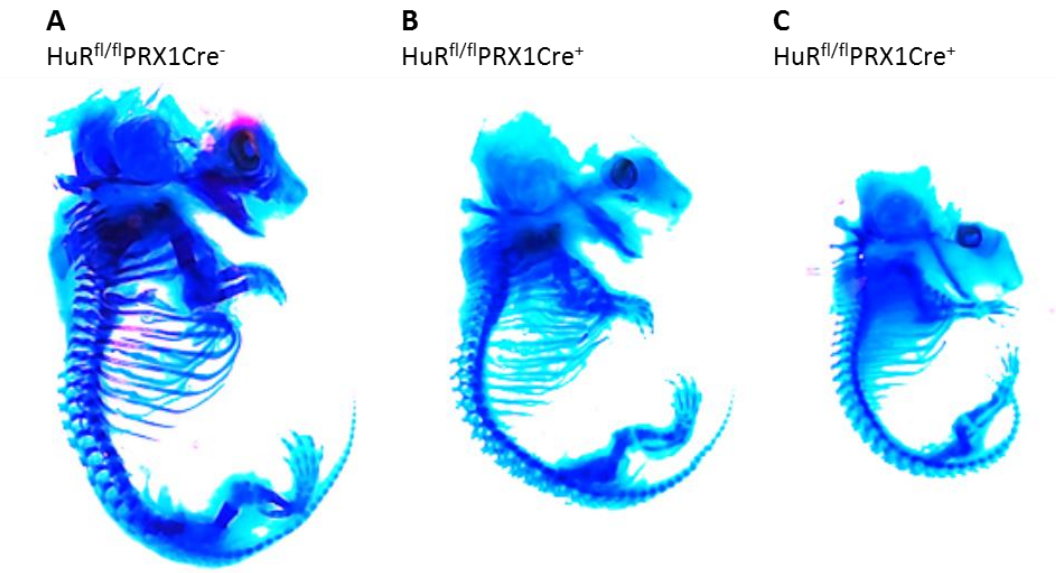

Figure 3.12. Representative whole mount skeletal staining of HuR$^{fl/fl}$Prx1-Cre^{+} embryos vs HuR$^{fl/fl}$ Prx1-Cre^{-} littermate at E16.5. To visualise bone and cartilage formation, embryos were stained with alizarin red and alcian blue, respectively and cleared with KOH/glycerol as previously described. HuR$^{fl/fl}$Prx1-Cre^{+} embryos are smaller (B&C) than their Cre^{-} littermates (A), to varying degrees. There is also a lack of alizarin red staining in HuR$^{fl/fl}$Prx1-Cre^{+} embryos suggesting bone mineralisation has not occurred (B&C). (HuR$^{fl/fl}$Prx1-Cre^{+} n= 4, HuR$^{fl/fl}$Prx1-Cre^{-} n=5)

3.2.2.3.3 Histological analysis of E16.5 embryo limbs

In order to further examine the rescued phenotype of the limb buds from Prx1-Cre driven E13.5 to E16.5 embryos, fore- and hind- limbs from E16.5 $HuR^{fl/fl}$Prx1-Cre^{+} embryos and their $HuR^{fl/fl}$Prx1-Cre^{-} littermates were histologically sectioned at 5µM thickness, stained with toluidine blue and counterstained with fast green. Analysis of the stained sections appeared to show a lack of mineralisation in the primary ossification center of the long bones including the ulna/radius and the tibia in embryo 3 (Figure 3.13 C, F, I & L) compared to Cre^{-} embryo 1 (A, D, G & J). The phenotype of embryo 2 seems to match that of the Cre^{-} phenotype (B, E, H & K). Cartilage formation of the digits of the forelimb in embryo 3 also appears delayed, which is similar to the delay in the development of the autopod in E13.5 embryos.

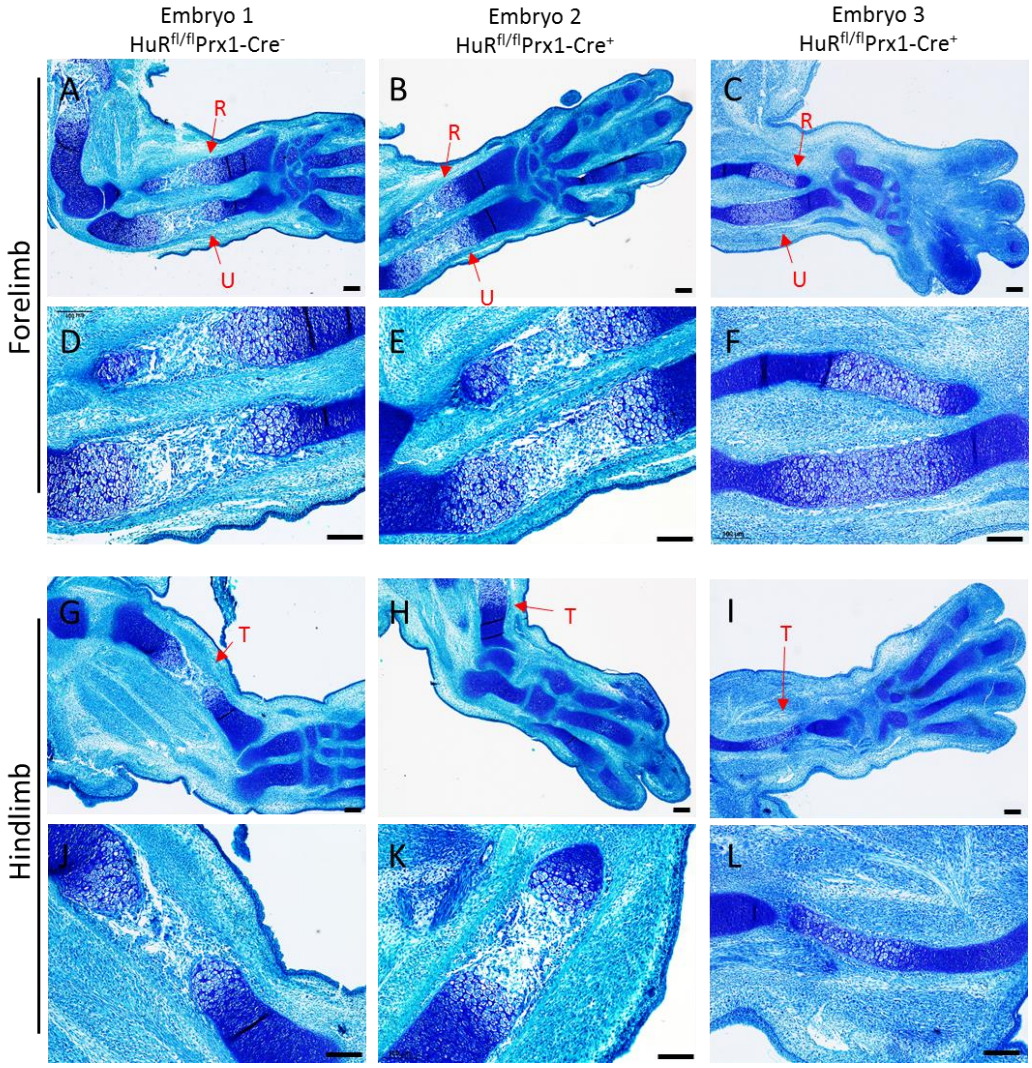

Figure 3.13. Representative histological sections of HuR$^{fl/fl}$Prx1-Cre^{+} and HuR$^{fl/fl}$ Prx1-Cre^{-} E16.5 littermate embryo forelimbs and hindlimbs. It would appear that HuR knockout in embryo 3 has resulted in a lack of bone formation in the center ossification region of the radius, ulna (F) and tibia (L) when compared to the rescued phenotype of embryo 2 (E&J) and the Cre^{-} embryo 1 (D&K). (U=ulna, R=radius, T=tibia). (Scales bars = 100µm) (HuR$^{fl/fl}$Prx1-Cre^{+} n= 4, HuR$^{fl/fl}$Prx1-Cre^{-} n=5).

3.2.2.3.4 Micro CT imaging of HuR$^{fl/fl}$ Prx1-Cre embryos at E16.5

E13.5 embryos have little to no bone formation yet and so µCT scanning at this stage was not an option for these embryos. We therefore µCT scanned HuR

floxed Prx1-Cre embryos at E16.5 in order to analysis the developing skeleton. In low-resolution µCT scans of E16.5 $HuR^{fl/fl}$Prx1-Cre^{+} embryos there appears to be a delay in the ossification of skeletal bone (Figure 3.14 B), including the ribs and intervertebral discs (IVD) (Figure 3.14 C) and craniofacial structures (Figure 3.14 D). In embryo 3 the fibula does not appear to have developed (Figure 3.13 I&L) and there is a shortening of the forelimbs (Figure 3.14 E), suggesting a lack of mineralisation of the long bones.

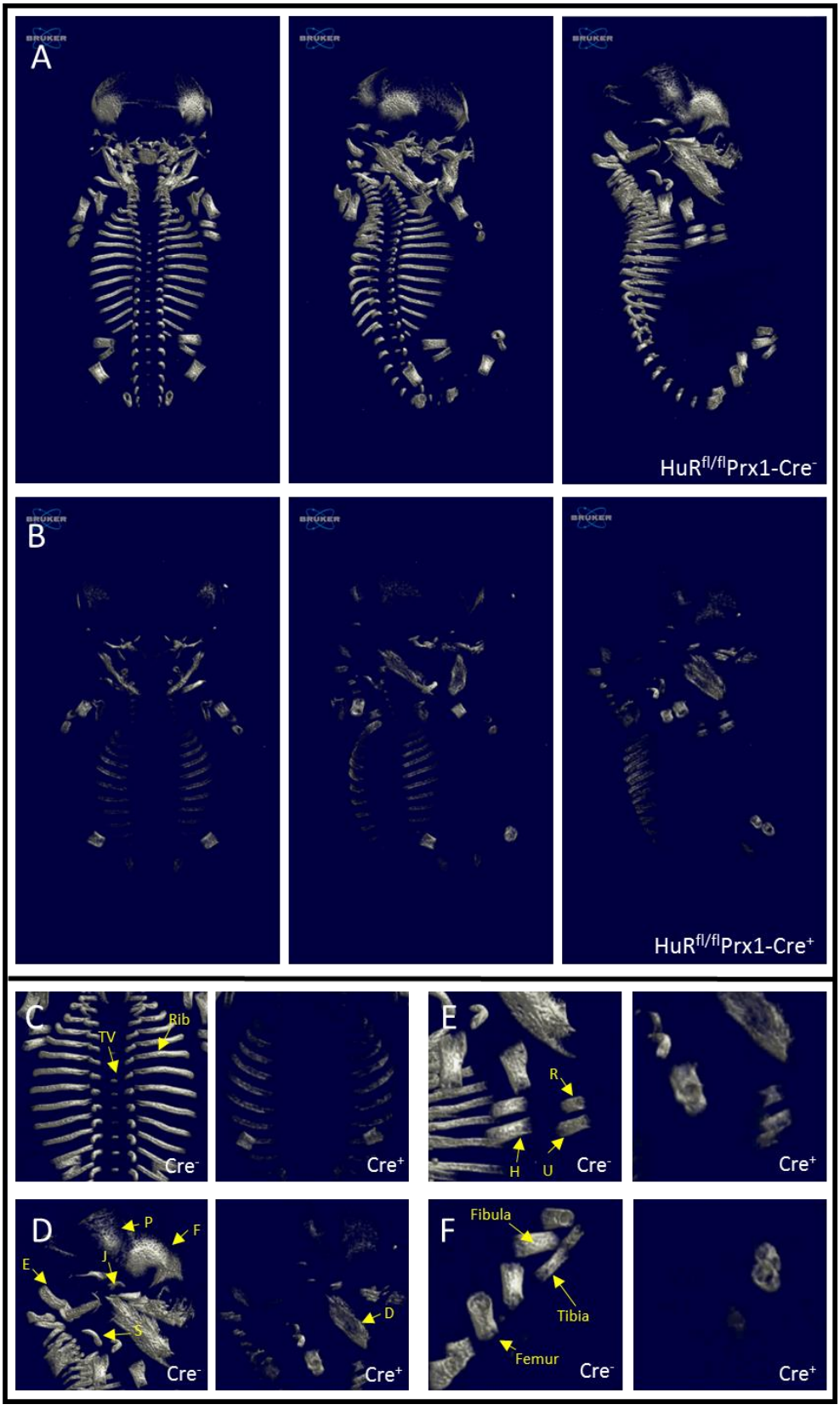
A
HuR^fl/fl Prx1-Cre^-
B
HuR^fl/fl Prx1-Cre^+
C
Rib
TV
Cre^-
Cre^+
E
R
H
U
Cre^-
Cre^+
D
P
F
E
J
S
Cre^-
D
Cre^+
F
Fibula
Tibia
Femur
Cre^-
Cre^+

Figure 3.14. Analysis of HuR$^{fl/fl}$Prx1-Cre^{+} and HuR$^{fl/fl}$Prx1-Cre^{-} embryos at E16.5. Micro CT analysis identified Prx1-driven HuR knockout embryos that exhibited impaired ossification (B) compared to Cre^{-} littermates (A). In particular, differences in bone mineralisation can be seen in the ribs, spine (C), craniofacial structures (D) and the long bones of the limbs (E and F). (F= frontal, J= jugal, P = parietal, E = exoccipital, TV = throatic vertebrae, Cv = cervical vertebrae, S= sternum, D= dentary, H= humerus, R= radius, U= Ulna). (HuR$^{fl/fl}$Prx1-Cre^{+} n= 4, HuR$^{fl/fl}$Prx1-Cre^{-} n=5)

3.3 Discussion

In this chapter, two murine lines were generated in order to knockout HuR *in vivo* in both a cartilage specific manner using CreER^{T2} under the control of the Aggrecan A1 enhancer, and a skeletal-specific manner were Cre recombinase was under the control of a *Prx1* regulatory element. Taken together, the data in this chapter suggests a role for HuR during skeletal development and demonstrates that HuR may be involved in the cellular processes affecting chondrogenesis and endochondral ossification.

Previously, skeletal defects were observed in embryos with a Sox2-Cre driven knockout of HuR that is induced early in embryonic development, phenotypes in particular included a shortening of the long bones and a delay in osteogenic ossification of the limbs, ribs and craniofacial structures of these mutants. Therefore the objectives of this chapter was to use AcanA1-CreER^{T2}*luc* and *Prx1*-Cre transgenic mice to drive the knockout of HuR in a chondrocyte-specific and limb bud mesenchyme-specific manner, targeting chondrocytes and the developing limb buds and craniofacial structures, respectively. In our Prx1-Cre^{+} HuR$^{fl/fl}$ E13.5 embryos we observed a similar but more severe skeletal phenotype resulting in the alteration of chondrogenesis and the mineralisation of the long bones which appears to have been delayed or stopped during development. One mutant embryo also had a cleft palate, which has previously been shown to affect Prx1$^{fl/fl}$Prx2$^{fl/fl}$ double mutants (ten Berge *et al.* 1998).

Vertebrate long bones form during the process of endochondral ossification in which chondrocytes proliferate, differentiate into hypertrophic chondrocytes

and are gradually replaced by bone matrix (Wuelling and Vortkamp 2010). The growth of a skeletal element depends on precise regulation of chondrocyte proliferation and hypertrophy, in particular proliferation of columnar chondrocytes and the expansion of the hypertrophic region (Karp *et al.* 2000). This process is coordinated and tightly regulated by secreted growth factors, which activate transcription factors specific to chondrocytes including Sox9 and Runx2, to ensure the continuous elongation of the epiphyseal growth plates (Wuelling and Vortkamp 2010).

The molecular mechanisms by which HuR affect chondrogenesis are still not clear. Interestingly, parathyroid hormone-related protein (PTHrP) is known to promote chondrogenesis and supress hypertrophy (Kim *et al.* 2008), while Hox genes are major regulators involved in the patterning of the vertebrate rib cage (McIntyre *et al.* 2007); both processes that are affected by cartilage- and skeletal- specific HuR knockout. Based on our current understanding of cartilage development and of HuR mRNA interactions, candidate processes of how HuR may affect chondrogenesis are described here.

3.3.1 Indian hedgehog and Parathyroid Hormone-related protein are key regulators of endochondral ossification

Indian hedgehog (Ihh), a member of the hedgehog family of secreted signalling molecules, is widely recognised as a critical regulator of long bone development and growth and regulates a number of processes. Ihh null mice exhibit long-bone defects and joint fusions, with severely abnormal long bone development as a result of reduced chondrocyte proliferation and delayed then abnormal chondrocyte maturation. These mice also completely lack any mature osteoblasts specifically in the endochondral skeleton, indicating that Ihh signalling plays multiple regulatory roles in endochondral bone formation (St-Jacques *et al.* 1999).

During embryonic cartilage development, Ihh is first detected at E11.5 in chondrocytes of the early cartilaginous condensation. Upon the initiation of hypertrophic differentiation production becomes restricted to prehypertrophic and hypertrophic chondrocytes that are adjacent to the proliferation zone. Ihh

participates in a negative feedback look were Ihh stimulates PTHrP production in the periarticular regions of the developing cartilage elements. PTHrP diffuses into the growth plate region and signals to the PTH/PTHrP receptor (Ppr1) to regulate chondrocyte differentiation by maintaining the cells in a proliferative state and prevents hypertrophic differentiation (Chau *et al.* 2011). As the epiphyseal growth plate continues to elongate, cells that become distant from the source of PTHrP differentiate into prehypertrophic and early hypertrophic chondrocytes which further express Ihh (Vortkamp *et al.* 1996, Chau *et al.* 2011). This negative feedback loop controls the distance between the hypertrophic zone and the articular surface of the joint (Salva and Merrill 2017). In the absence of Ihh, PTHrP expression is reduced which leads to accelerated hypertrophy of chondrocytes (Vortkamp *et al.* 1996), while targeted disruption of PTHrP or Ppr1 in mice results in a dwarfism phenotype as a result of a reduction in the proliferating zone of cells and an advanced onset of hypertrophic differentiation (Amizuka *et al.* 1994).

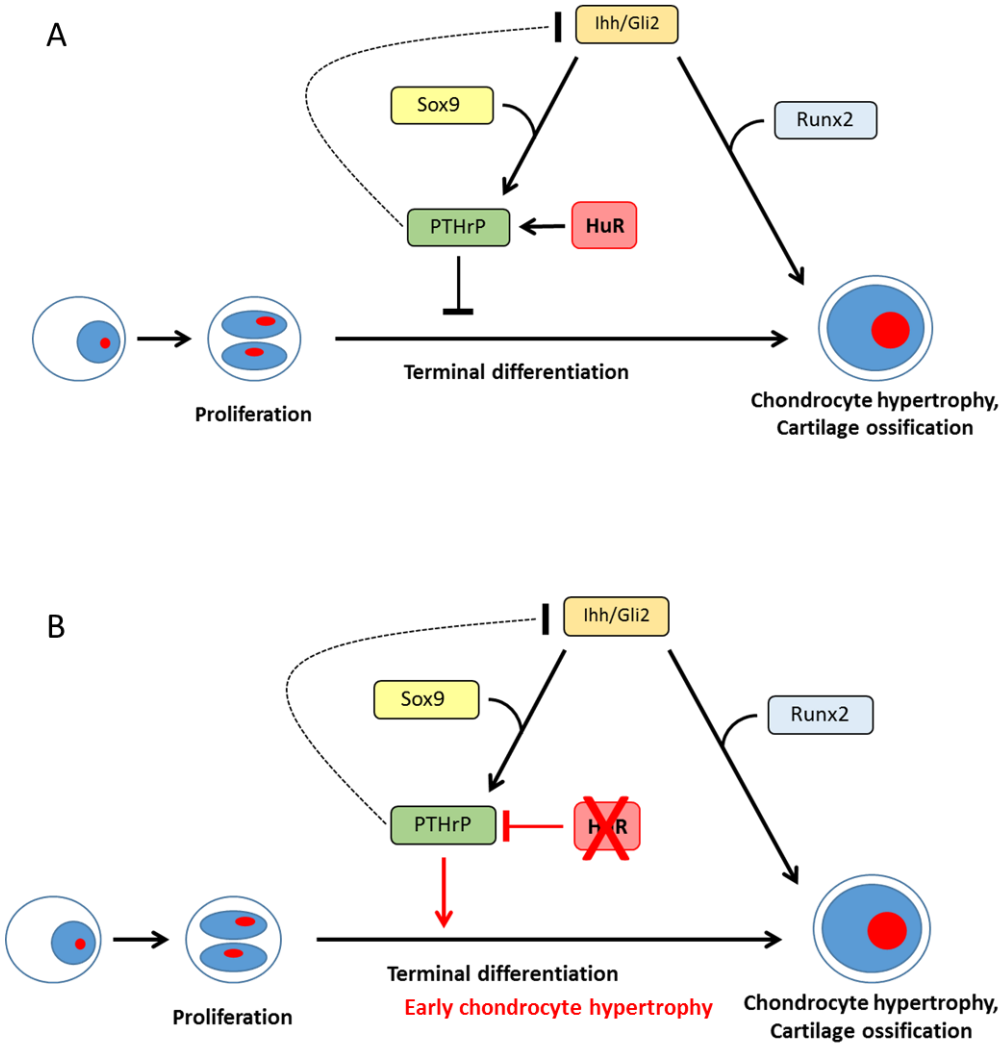

Figure 3.15. Schematic of the Ihh/PTHrP negative feedback loop during chondrogenesis. **(A)** PTHrP diffuses into the growth plate region maintains the cells in a proliferative state to prevent hypertrophic differentiation. Cells that become distant from the source of PTHrP differentiate into prehypertrophic and early hypertrophic chondrocytes which further express Ihh. In this normal model, HuR might directly stabilise PTHrP keeping chondrocytes in a proliferative state. **(B)** Working hypothesis of how HuR ablation might affect the Ihh/PTHrP negative feedback loop. HuR deletion potentially results in a lack of stability of PTHrP which may result in an inhibition of chondrocyte proliferation and early hypertrophy.

PTHrP is a peptide hormone whose mRNA is alternatively spliced to yield three isoforms (139, 141 and 173), which undergo extensive posttranslational processing to give rise to a family of mature secretary forms of the peptide. As previously described, PTHrP regulates cell growth and differentiation throughout embryonic development and in adult life. It is however, also a tumour survival factor for multiple cancers, including human renal cell carcinoma, and in this capacity its expression is regulated by mRNA stability. It has previously been found that PTHrP mRNA contains an AU-rich 3'UTR and is a target for HuR binding leading to upregulation of PTHrP by HuR through the increase of PTHrP mRNA stability (Danilin *et al.* 2009). HuR knockdown led to a decrease in PTHrP mRNA expression and a 70% reduction in the half-life of the main PTHrP mRNA isoform, 141, with papers reporting that HuR regulates PTHrP expression in human lung adenocarcinoma cells (Danilin *et al.* 2009, Lauriola *et al.* 2013).

Here, we describe how the ablation of HuR in both a chondrocyte- and skeletal-specific manner results in severely abnormal chondrogenesis and endochondral ossification, a process that is highly regulated by the Ihh-PTHrP negative feedback loop. PTHrP 34 is an isoform of PTHrP that has been shown to most significantly enhance chondrogenesis and suppress hypertrophy in MSCs (Lee and Im 2012). It is therefore possible that during normal chondrogenesis HuR binds to stabilise PTHrP mRNA, while in this study a lack of HuR has decreased PTHrP stability, which has disrupted the Ihh-PTHrP negative feedback process resulting in an inhibition of chondrocyte proliferation which may have an effect on skeletal development (Figure 3.15).

3.3.2 Hox genes

Previously, the identification of HuR target mRNAs revealed that the aberrant expression of genes that controlled axis specification and the patterning of skeletal segments, including *Hox* paralogous, correlated with embryonic defects in Sox2-mediated HuR knockout mice including poor outgrowth of the limb buds and fusions among the long and short limb elements (Katsanou *et al.* 2009). Interestingly, mRNA levels of *Hoxd13,* a regulator of limb patterning, is downregulated during ablation of HuR and is absent from E12.5 mouse

forelimbs *in vivo*, while *Hoxb9*, involved in the control of thoracic skeletal element specification, is upregulated (Katsanou *et al.* 2009)

It is also interesting to note that previously, HuR has been identified as a key regulator of RNA processing, expression and function of the Hox gene *Ubx* during neural development in *Drosophila*, through direct interaction (Rogulja-Ortmann *et al.* 2014). A previously described AU-rich element is present within the 3' UTR of *Ubx (Rogulja-Ortmann et al. 2014)* and, while *Ubx* is a Hox gene specific to insect species, it is possible that Hox genes involved in mouse skeletal patterning and limb outgrowth also contain AU-rich elements that may potentially interact directly or indirectly with HuR. *Hoxb6* has also been reported to contain AU-rich elements but has been shown to not interact with HuR (Katsanou *et al.* 2009).

3.3.3 Sox9 in limb bud development

Sox9 is expressed in mesenchymal cells before condensation in the developing skeleton and is continually expressed during chondrocyte differentiation (Jo *et al.* 2014). Sox9 null mice results in failed chondrogenesis as a result of a disruption to the PTHrP-Ihh regulatory loop due to its essential role in the expression of Ihh and PTHrP (Akiyama *et al.* 2002, Dy *et al.* 2012). Previously, our group has shown that SOX9 is controlled post-transcriptionally by mRNA turnover in response to cellular stress and that its half-life negatively correlates with the total SOX9 mRNA expression levels in both human articular chondrocytes (HAC) and bone marrow derived stem cells (BMSC) (Tew and Clegg 2011). SOX9 half-life has since been shown to not be significantly affected by siRNA-mediated knockdown of HuR in SW1353 cells (McDermott *et al.* 2016).

Previously, conditional Sox9 knockout utilising the same Prx1-Cre resulted in newborns with severely stunted limb growth (Akiyama *et al.* 2002). Skeletal staining with alizarin red and alcian blue indicated a complete absence of cartilage and bone with no discernible chondrogenic mesenchymal condensations that form the autopod digits. Little or no expression of Runx2, which is essential for osteoblast differentiation, was also detected in the limb

buds of the Sox9 knockout mice. There were no osteoblasts present in the mutants, suggesting Sox9 is crucial for the expression of Runx2 and the differentiation of osteoblasts. High levels of apoptosis was also observed in the mesenchymal cells of E13.5 Sox9 knockout embryos in areas were chondrogenic mesenchymal condensations differentiate to form cartilage. This also suggested that mesenchymal cells do not survive in the distal part of limb buds when Sox9 is not present.

Sox9 is critical in the processes of the chondrocyte differentiation pathway during endochondral bone formation and has been shown to associate with RNA-binding proteins (Girardot *et al.* 2018). As the phenotypes of $HuR^{fl/fl}$ Cre^{+} embryos observed in this chapter are similar to that observed in Prx1-Cre mediated Sox9 deficient embryos, there is possible that HuR may down-regulate Sox9 through an intermediate factor. This would disrupt chondrogenesis and perhaps play a role in the defects in endochondral ossification of the limbs and ribs we observe in Prx1- and Aggrecan–Cre $HuR^{fl/fl}$ embryos, respectively.

3.3.4 Regulation of bone cell differentiation

Skeletogenesis is formed by two developmental processes; 1) endochondral ossification which accounts for most skeletal elements including the long bones and 2) intramembranous ossification which is responsible for the formation of most of the craniofacial skeleton (Lefebvre and Bhattaram 2010). In intramembranous ossification, mesenchymal cells directly differentiation into osteoblasts to form bone (Shahi *et al.* 2017). During endochondral ossification however, aggregated mesenchymal cells are differentiated into chondrocytes, which are then progressively substituted by bone. The replacement of chondrocytes by bone cells is dependent on the mineralisation of the extracellular matrix in a highly regulated manner (Ortega *et al.* 2004).

BMPs and Runx2 are both able to stimulate osteoblast differentiation and bone formation (Phimphilai *et al.* 2006). BMPs activate signal transduction pathways, including SMAD proteins, in order to express target genes including Runx2.

Contrastingly, Runx2 directly binds to enhancer regions of target genes to induce osteoblast-specific gene expression (Phimphilai *et al.* 2006).

Bone morphogenetic proteins (BMPs), members of the TGF-β superfamily, regulate the maturation of mesenchymal osteochondroprogenitor cells to osteoblasts (Karamboulas *et al.* 2010). The BMP signalling pathway is essential for endochondral bone formation and disruption to this process can cause a vast range of skeletal anomalies (Beederman *et al.* 2013). For example, chondrocyte-specific knockout of Bmp2 resulted in chondrodysplasia with a severe disorganisation of chondrocytes in the growth plate that results in defects in chondrocyte proliferation, differentiation and apoptosis, ultimately leading to skeletal growth impairment (Shu *et al.* 2011).

Runx2 is essential for the commitment and differentiation of mineralising cell types during both endochondral ossification and intramembranous ossification. Global knockout of Runx2 results in a complete lack of ossification, owing to the mutational arrest of osteoblasts (Komori *et al.* 1997). Chondrocyte specific knockout of Runx2 resulted in lethality and failed endochondral ossification as a result of an absence of mature chondrocytes, vasculature and marrow in the limbs and the near absence of the proliferative zone in the growth plates (Haiyan Chen *et al.* 2014). Runx2 and BMPs cooperatively interact to stimulate osteoblast gene expression (Phimphilai *et al.* 2006). HuR may play a role in the post-transcriptional regulation and stabilisation of BMP and/or Runx2 *in vivo* and a by knocking out HuR in a chondrocyte- or skeletal- specific manner may alter their expression levels during endochondral ossification and have the potential to cause the severe skeletal defects we observed in this chapter.

These studies combined with our own suggest that HuR might post-transcriptionally regulate gene networks involved in limb patterning, outgrowth and axial and craniofacial skeletal development in a spatiotemporal manner through transcriptional and post transcriptional regulation. The mechanisms surrounding the severe skeletal phenotypes observed in this study, however, still remain unknown and currently unexplored. Previous work suggested HuR might interact indirectly with MMP13 (McDermott *et al.* 2016). As discussed, *Hox* genes, Sox9, BMPs and Runx2 are all involved in the regulation of skeletal

patterning, particularly in the regions that affect our *Aggrecan*- and *Prx1*- driven $HuR^{fl/fl}$ embryos. Therefore, in a similar pattern, one possibility here is that HuR may interact with a regulatory element that may promote activation or inactivate one or more of these genes and/or by a direct or indirect interaction with the Ihh/PTHrP negative feedback loop. More work is necessary to elucidate the mechanisms by which HuR acts on markers of chonrogenesis at the mRNA and protein level.

4 Analysing effect of inducible HuR knockout on osteoarthritis progression in young adult mice

4.1 Introduction

To determine the importance of HuR in skeletally mature animals, $HuR^{fl/fl}$AcanA1-$CreER^{T2+}$ mice were administered tamoxifen for flox site recombination in adult mouse cartilage and its effect on osteoarthritis progression was determined.

The biology of many post transcriptionally controlled genes has been investigated in relation to osteoarthritis and other degenerative joint diseases because of their roles in the regulation of ECM production and degradation in chondrocytes (Tew and Clegg 2011). The importance of post-transcriptional gene regulation in the development and progression of such diseases has been increasingly reported. To date, a number of studies have demonstrated that a wide variety of parameters including biomechanical stress, differentiation and cytokine signalling can regulate post transcriptional control in chondrocytes (Tew and Clegg 2011). These changing environments have been implicated in osteoarthritis by altering the control of cartilage homeostasis, which can contribute to altered rates of mRNA turnover.

Previously, it has been reported that a number of genes involved in the pathogenesis of osteoarthritis are differentially regulated at the post-transcriptional level (Tew *et al.* 2014). This study also reported that there is an increase in the number of rapidly turned over mRNAs in osteoarthritis chondrocytes, which suggests that osteoarthritis may affect the post-transcriptional regulatory mechanisms that control the expression of these genes. As RNA binding proteins are critical regulators of mRNA decay our lab has worked to investigate the influence of RNA binding proteins in articular cartilage. Previous work from our laboratory has identified RNA binding proteins as regulators of gene expression in chondrocytes (McDermott *et al.* 2016). In particular, TTP was demonstrated to be a modulator of Sox9 mRNA decay by acting as a suppressor of Sox9 expression leading to its instability. In parallel, a decrease in TTP levels also led to a stabilisation of Sox9 mRNA. Interestingly in the same study, it was also reported that siRNA-mediated knockdown of HuR significantly increased MMP13 expression in chondrogenic

cultures and also regulated the expression of a number of known transcriptional repressors of MMP13, including RUNX2 and SPI1 (McDermott *et al.* 2016). HuR is known to be ubiquitously expressed within mouse embryos (Ma *et al.* 1996), however, it was also found that protein levels of HuR were down-regulated in developing skeletal structures were levels of MMP13 are increased, particularly in hypertrophic chondrocytes (McDermott *et al.* 2016). MMP13 is expressed in hypertrophic chondrocytes during endochondral ossification and clinical investigation revealed patients with osteoarthritis have high MMP13 expression; its regulation by HuR is therefore particularly interesting and could point to a role for HuR in osteoarthritis development (Wang *et al.* 2013). Studies have shown that MMP13-overexpressing transgenic mice develop a spontaneous OA-like articular cartilage destruction phenotype (Neuhold *et al.* 2001). While mice deficient in MMP13 are resistant to osteoarthritic cartilage erosion, they are not resistant to chondrocyte hypertrophy or osteophyte development (Little *et al.* 2009).

The aims of this chapter were to analyse the role of HuR in mouse articular cartilage, examining both short term deletion as well as its role in the development and progression of osteoarthritis.

4.2 Results

4.2.1 Confirmation of loxP recombination and flox site recombination

HuR$^{fl/fl}$ AcanA1-CreER^{T2}*luc* mice were genotyped as previously described in *Methods Section 1.1.3* to identify Cre-positive and Cre-negative individuals who were homozygous for the HuR floxed alleles (Figure 4.1A). Cre expressing cells will also be expressing luciferase in these mice so, in order to confirm genotyping results, selected mice were injected with luciferin and then scanned using an IVIS machine to assess luciferase expression. A strong luminescent signal was observed in HuR$^{fl/fl}$AcanA*1*-CreERT2*luc*$^{+}$ mice but not HuR$^{fl/fl}$ CreER^{T2}*luc*$^{-}$ mice (Figure 4.1B).

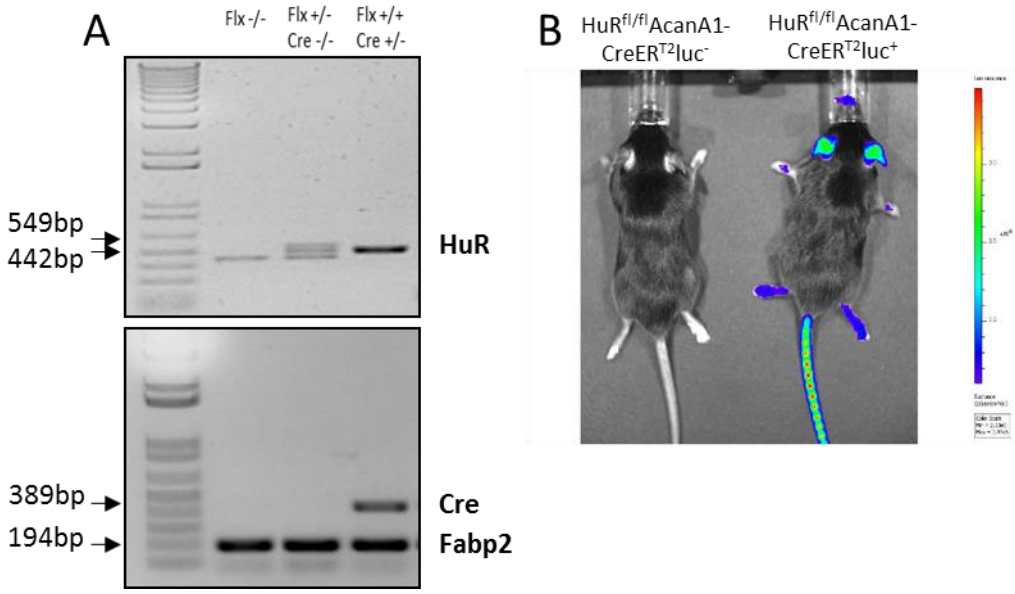

Figure 4.1. Genotyping and luciferase expression in HuR$^{fl/fl}$AcanA1-CreER^{T2}luc^{+} and HuR$^{fl/fl}$ AcanA1-CreER^{T2}lu-^{T} mice. **(A)** PCR and gel electrophoresis confirmed the genotypes of Aggrecan-driven Cre recombinase in mice that were hetero- or homozygous for HuR flox. **(B)** In these mice, luciferase is expressed bicistronically with the Cre. Cre expression in aggrecan-expressing tissues could therefore be confirmed using bioluminescence imaging of luciferase activity.

Next, to assess the efficiency of HuR knockout in the articular cartilage and other cartilaginous tissues of adult HuR$^{fl/fl}$AcanA1-CreER^{T2+} mice, we administered three evenly spaced doses over 1 week of 1mg/10g body weight tamoxifen to 6-week old HuR$^{fl/fl}$ AcanA1-CreER^{T2}*luc*$^{+}$ mice and their Cre^{-} littermates. We then sacrificed the mice after 2 weeks and collected tissue for recombination and western blot analysis. The DNA recombination assay was performed as described in in *Methods Section 1.2.2* using DNA isolated from the articular cartilage, tail, xiphoid and lumbar spine. PCR analysis and gel electrophoresis showed that the loxP sites flanking HuR had recombined and excised the HuR fragment in all tissues of HuR AcanA1-CreER^{T2}*luc* knockout mice compared to no recombination in Cre^{-} control mice (Figure 4.2A). To further confirm HuR knockdown at the protein level, western blot analysis was

conducted. Initially protein was extracted from the articular cartilage of both legs from one mouse but this did not yield enough protein to carry out a western blot. To overcome this, protein was extracted from the articular cartilage of both knees from three HuR$^{fl/fl}$AcanA1-CreER^{T2+} mice and pooled. The same process was conducted using three HuR$^{fl/fl}$AcanA1-CreER^{T2-} littermates. Consistent with the DNA recombination result, western blot analysis of these pooled samples demonstrated that HuR protein levels had decreased in the articular cartilage of HuR$^{fl/fl}$ AcanA1-CreER^{T2}*luc*$^{+}$ mice compared to Cre^{-} littermates two weeks after tamoxifen treatment (Figure 4.2B).

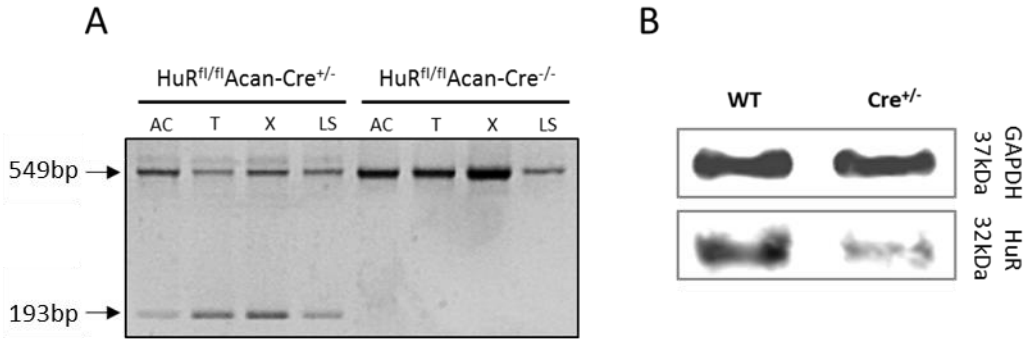

Figure 4.2. Recombination assay and western blot analysis suggesting protein reduction in HuR$^{fl/fl}$AcanA1-CreER^{T2}luc^{+} mice. (A) Recombination assay was performed on the isolated DNA from several cartilaginous tissues in both HuR$^{fl/fl}$ AcanA1CreER^{T2}*luc*$^{+}$ and HuR$^{fl/fl}$ AcanA1CreER^{T2}*luc*$^{-}$ mice. PCR followed by gel electrophoresis shows the higher molecular weight band which is the floxed allele, and the lower band is the same allele, which has been subject to Cre-mediate recombination **(B)** Western blot analysis was independently performed on the protein from the articular cartilage from three HuR$^{fl/fl}$AcanA1-CreER^{T2}*luc*$^{+}$ and three HuR$^{fl/fl}$AcanA1-Cre^{-} mice. Protein analysis revealed HuR protein levels are reduced in Cre-positive mice compared to Cre-negative littermates. (AC: articular cartilage, T: tail, X: xiphoid, LS: lumbar spine).

4.2.2 Tamoxifen delivery does not alter cartilage pathology in $HuR^{fl/fl}$AcanA1-$CreER^{T2+}$ mice after 5 weeks

Global HuR knockout results in embryonic lethality and knockout of HuR early in embryonic development results in severe skeletal defects (Katsanou *et al.,* 2009). In order to assess the initial severity of HuR recombination in the articular cartilage of young adult mice, $HuR^{fl/fl}$ AcanA1-$CreER^{T2}$*luc*$^{+}$ and their Cre^{-} counterparts were dosed three times in 1 week with 1mg/10g body weight in order to induce HuR knockout. Mice were sacrificed 5 weeks after the final injection and tissue collected. Mouse joints were fixed in 10% NBF for 48 hours followed by decalcification in 10% EDTA for 3 weeks. Joints were then processed for standard paraffin embedding for histological analysis.

4.2.2.1 Histological examination of $HuR^{fl/fl}$Acan-$CreER^{T2}luc^{+}$ and $HuR^{fl/fl}$Acan-$CreER^{T2}luc^{-}$ knee joints

To examine the articular cartilage, mice knee joints were sectioned coronally at 6µm across the entire joint. Sections were dewaxed, rehydrated and stained with toluidine blue and counter-stained with fast green. Histological analysis revealed no apparent phenotypic differences between $HuR^{fl/fl}$AcanA1$CreER^{T2+}$ and $HuR^{fl/fl}$AcanA1$CreER^{T2-}$ mice indicating that there is no acute change in the pathology of the articular cartilage or surrounding tissue in tamoxifen treated $HuR^{fl/fl}$AcanA1-Cre^{+} mice (Figure 4.3A) compared to control counterparts (Figure 4.3B) in either the medial and lateral compartments (Figure 4.3 C&D and E&F, respectively). A histopathology scoring system was used to quantify and assess articular cartilage lesion severity (Glasson *et al*. 2010).

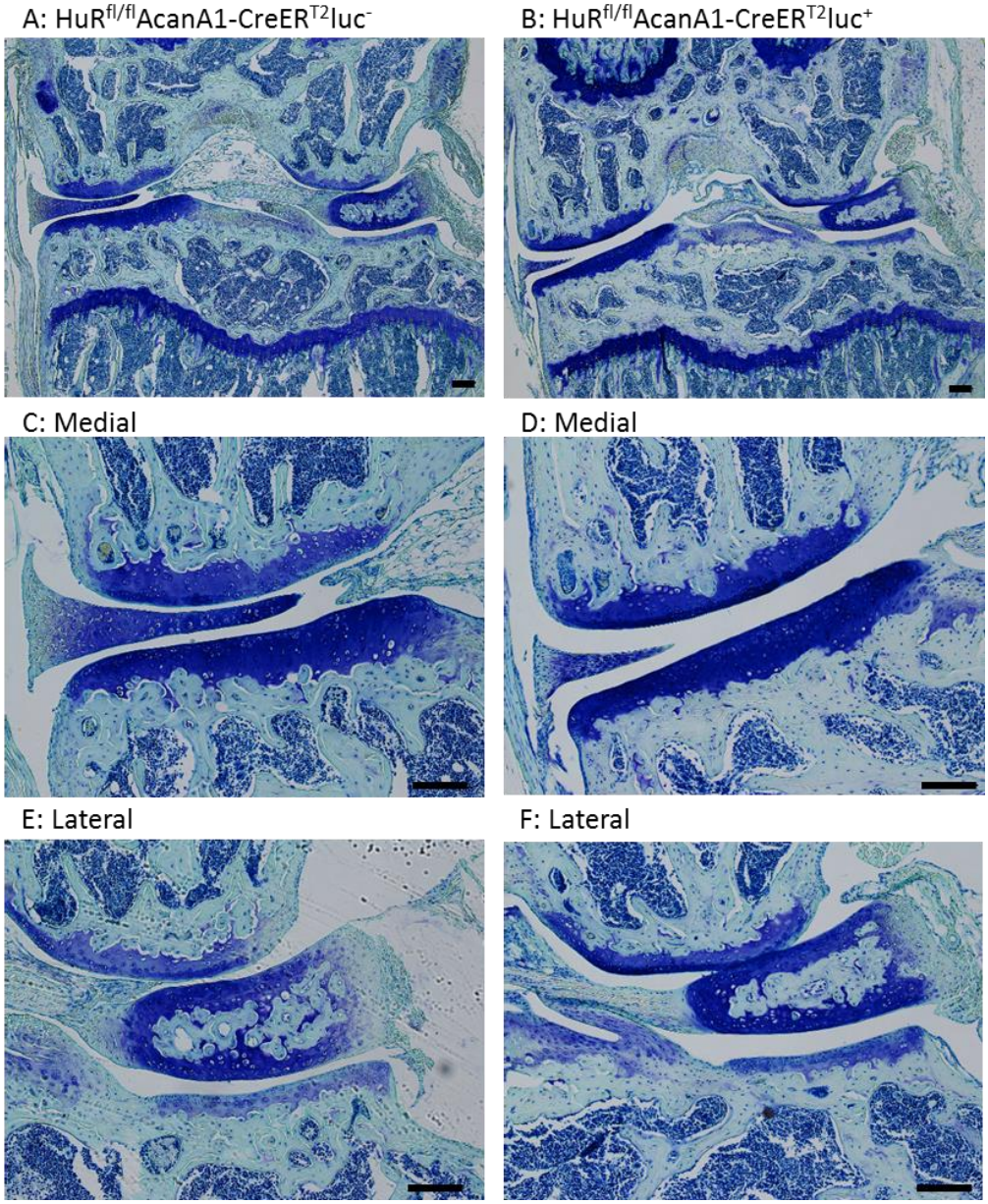

Figure 4.3. Representative histological images of toluidine blue stained HuR$^{fl/fl}$Acan-CreER^{T2}luc^{+} and HuR$^{fl/fl}$Acan-CreER^{T2}luc^{-} 6µm coronal sections. There is no apparent difference in the surface of the articular cartilage between Cre^{-} (A) and HuR$^{fl/fl}$ (B) sections. Medial (C&D) and lateral (E&F) compartments also do not contain any observable differences in the articular surface of Cre^{-} and HuR$^{fl/fl}$ mice. (HuR$^{fl/fl}$AcanA1-CreER^{T2}luc^{-} n=4; HuR$^{fl/fl}$AcanA1-CreER^{T2}luc^{+} n=4)

Lesion severity of the articular cartilage of these mice was scored using a modified form of the OARSI histopathology grading system for mouse osteoarthritis (Glasson *et al.* 2010), as described in *Methods section 1.4.4*. Four compartments (medial and lateral tibia and medial and lateral femur) from sections throughout the entire joint allowed for the most severe lesion to be determined as the maximum lesion score per joint and per compartment. Lesion severity was also graded in each compartment at 120µm intervals across the joint. This also allowed a mean grade per joint and per compartment to be obtained in order to measure any changes to the joint after tamoxifen induced recombination.

The lesion severity score of both $HuR^{fl/fl}$AcanA1-$CreER^{T2+}$ and control mice did not exceed grade 1 suggesting any damage to articular cartilage surface was minimal in the given time frame of 5 weeks following tamoxifen administration. Overall, there seems to be a slight increase in both the maximum and mean scores in $HuR^{fl/fl}$AcanA1-$CreER^{T2+}$ mice compared to control mice (Figure 4.4A), however there was no significant difference. There are also no significant differences in the maximum lesion severity score for each of the 4 compartments; however there appears to be an increase in the maximum severity of the lateral femur in $HuR^{fl/fl}$AcanA1-$CreER^{T2+}$ mice (Figure 4.4B). In keeping with this data, there are no significant differences in the mean lesion severity score of any compartment (Figure 4.4C).

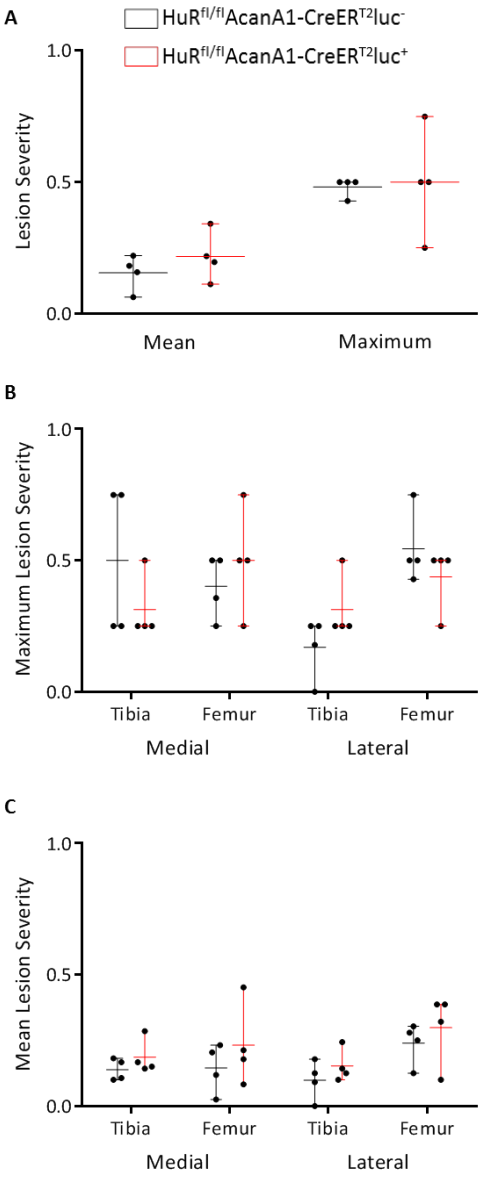

Figure 4.4. Lesion severity scores of HuR$^{fl/fl}$AcanA1-CreER^{T2+} knee joints 5 weeks after tamoxifen, compared to Cre^{-} counterparts. (A) The maximum and mean lesion severity scores were calculated across the whole joint for HuR$^{fl/fl}$ (red) and Cre^{-} mice. While there is a slight increase in the mean lesion severity score in HuR$^{fl/fl}$ mice, there is no significant difference (B) The maximum lesion severity score in the individual compartments of the joint. There is a small increase in the maximum score in both the medial femur and lateral tibia of HuR$^{fl/fl}$ mice compared to Cre^{-} mice but again there is no significance in the differences. (C) There is no statistically significant differences in the mean lesion severity score of the individual compartments. Data is presented as individual data points for each animal as well as the mean (horizontal line) and the standard deviation/error (error bars) for each group. (HuR$^{fl/fl}$AcanA1-CreER^{T2}luc^{-} n=4, HuR$^{fl/fl}$AcanA1-CreER^{T2}luc^{+} n=4)

4.2.2.2 Micro CT

Micro-CT (µCT) imaging is a valuable tool that can be used to investigate the morphometric changes in joints in animal models of osteoarthritis. µCT has successfully been used to study the changes in the subchondral bone architecture in the knee joints of collagenase-induced OA mice (Botter *et al.* 2008) and in surgical destabilisation models (Moodie *et al.* 2011). µCT has low sensitivity for soft tissue and therefore is a major challenge for imaging osteoarthritis models as the visualisation of the degenerative changes in

cartilage are compromised (Tremoleda *et al.* 2011). For analysis, the tibial epiphysis was therefore manually selected as representative of subchondral bone and osteoarthritis severity.

Prior to histological analysis, mice knee joints were scanned on a µCT scanner at 4.5µm voxel size with a rotation set of 0.3° (180° rotation) to assess bone density and volume. Projection images were acquired and computerised reconstruction of the 3D stack of images was performed using NRecon. Analysis was performed on the reconstructed 3D image stack which was rotated along all three major axes to align and position all samples the exact same way. The epiphysis of the tibia was manually selected with the volume of interest (VOI) tool using the easily identifiable growth plate as a reference point. The tibial epiphysis was further analysed for differences in bone volume, trabecular thickness and trabecular separation between $HuR^{fl/fl}$AcanA1-$CreER^{T2+}$ and $HuR^{fl/fl}$AcanA1-$CreER^{T2-}$ mice, which showed no significant differences in all parameters measured (Figure 4.5A, B&C, respectively).

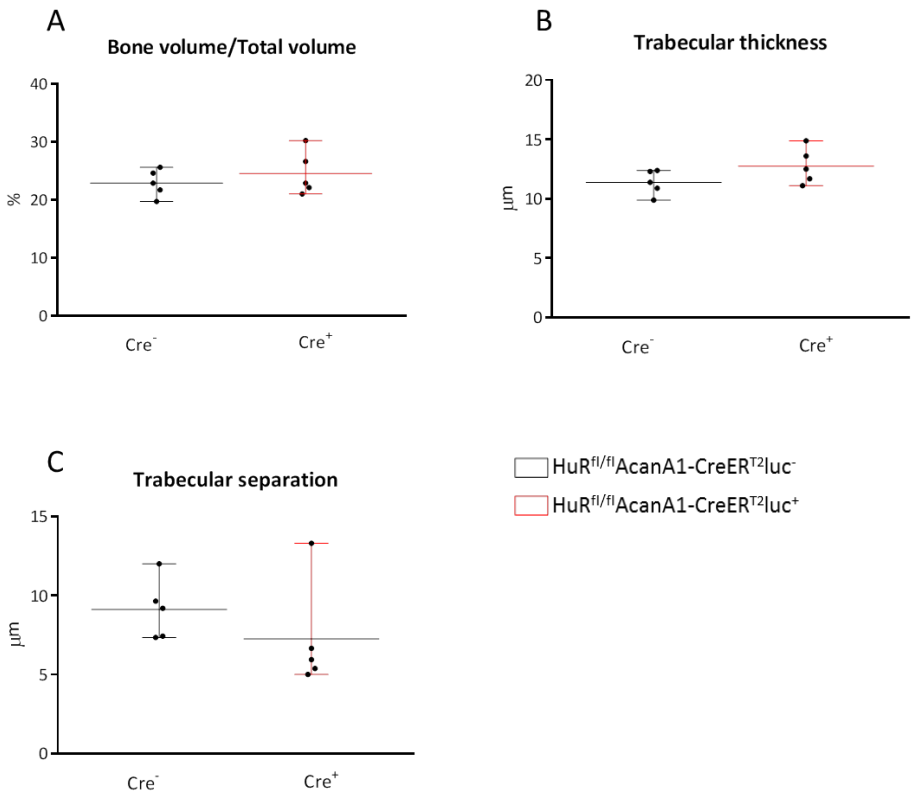

Figure 4.5. Micro-CT analysis of the tibial epiphysis in HuR$^{fl/fl}$AcanA1-CreER^{T2}luc^{+} mice and HuR$^{fl/fl}$AcanA1-CreER^{T2}luc^{-} counterparts 5 weeks after tamoxifen treatment. The tibial epiphysis was analysed for differences in bone volume (A), trabecular thickness (B) and trabecular separation (C) between HuR$^{fl/fl}$AcanA1-CreER^{T2+} mice and their Cre^{-} counterparts. No significant differences were observed. Data is presented as individual data points for each animal as well as the mean (horizontal line) and the standard deviation/error (error bars) for each group. (Bone volume p=<0.9212; Trabecular thickness p=<0.9072; Trabecular separation p=<0.3758). (HuR$^{fl/fl}$AcanA1-CreER^{T2}luc^{-} n=5; HuR$^{fl/fl}$AcanA1-CreER^{T2}luc^{+} n=5)

4.2.3 HuR knockout during the progression of DMM-induced osteoarthritis

4.2.3.1 DMM surgery

DMM is the most widely used model of post-traumatic osteoarthritis in mice due to its high reproducibility and its rapid onset and progression of disease. In order to preliminarily assess whether HuR knockout affects articular cartilage

during the progression of osteoarthritis, male HuR$^{fl/fl}$AcanA1-CreER^{T2}*luc*$^{+}$ and control Cre^{-} mice were dosed three times with 1mg/10g body weight tamoxifen at 6 weeks of age and DMM or SHAM surgery was performed at 10 weeks of age on the left leg, while the contralateral leg remained unoperated. The mice were sacrificed 5 weeks post-surgery and tissue collected and processed for µCT and histological examination.

4.2.3.2 Analysis and scoring of histological sections

The entire knee joint of both HuR$^{fl/fl}$AcanA1-CreER^{T2+} and HuR$^{fl/fl}$AcanA1-CreER^{T2-} mice that had either DMM or SHAM surgery were sectioned coronally and stained with toluidine blue and fast green. Histological analysis revealed that DMM surgery led to severe lesions in the articular cartilage of the DMM mice (Figure 4.6 A&B), while control SHAM surgery caused no damage (Figure 4.6 C&D).

The lesion severity scoring system was again applied to these mice in the same way as previously described by scoring the compartments of the medial and lateral tibia and femur and determining the maximal and mean lesion severity scores of the articular cartilage for each joint. First, the overall summed maximum score and the overall summed mean score was determined in HuR$^{fl/fl}$AcanA1-CreER^{T2+} DMM and SHAM mice and Cre^{-} DMM and SHAM mice (Figure 4.6 E&F, respectively). As expected there was a significant increase in the maximum and mean scores of DMM treated mice compared to SHAM mice, confirming DMM surgery was successful in inducing osteoarthritis. There was a small increase in the overall maximum (Figure 4.6E) and mean (Figure 4.6F) scores of HuR$^{fl/fl}$AcanA1-CreER^{T2+} mice compared to HuR$^{fl/fl}$AcanA1-CreER^{T2-} in both DMM and SHAM treated mice, however these observations were not statistically significant.

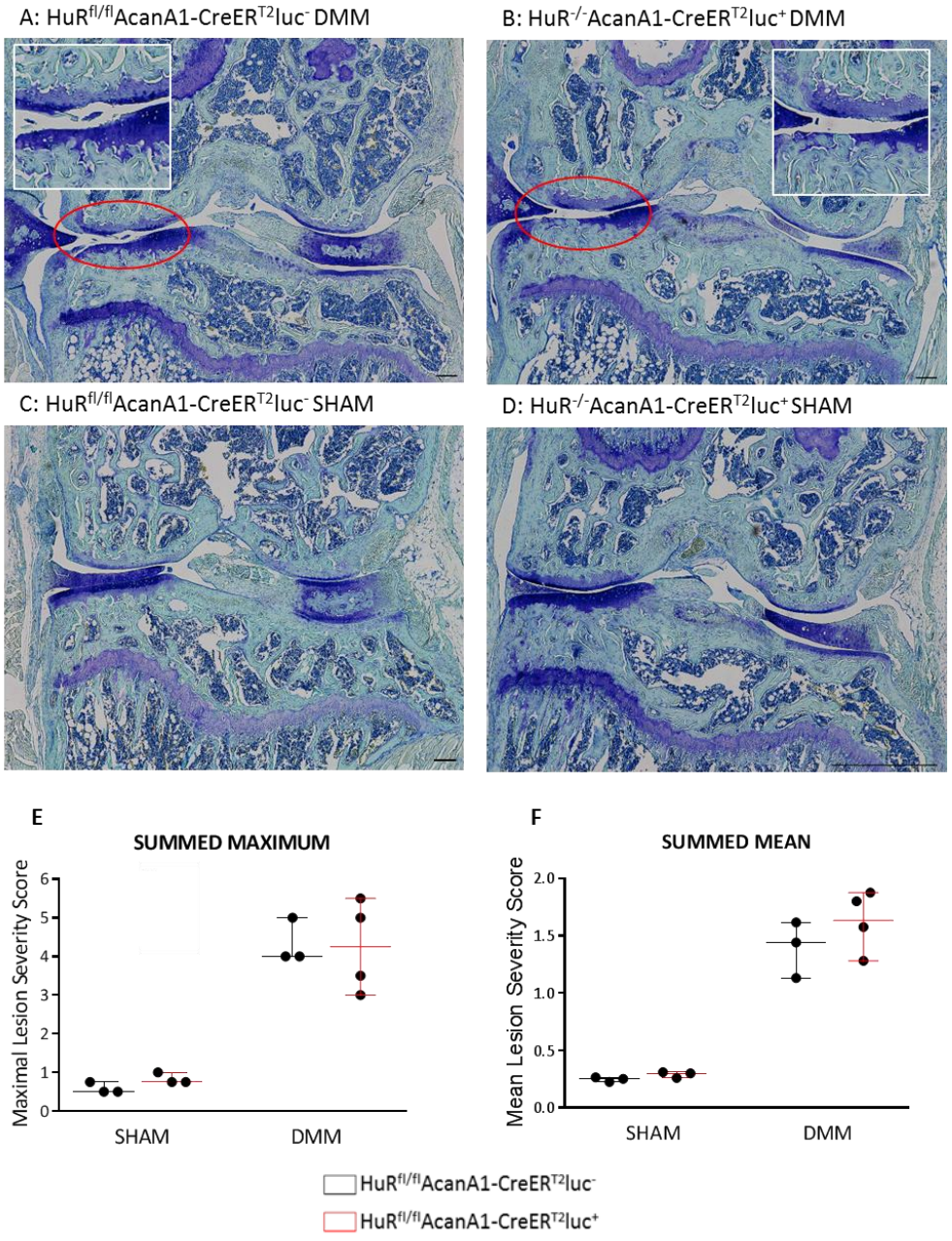

Figure 4.6. DMM surgery induces osteoarthritis progression in both HuR$^{fl/fl}$ and Cre^{-} mice. Toluidine blue stained sections of DMM performed on Cre^{-} (A) and HuR$^{fl/fl}$ (B) and control SHAM surgery performed on Cre^{-} (C) and HuR$^{fl/fl}$ (D). Maximum (E) and mean (F) grades of lesion in the entire knee joint are both slightly increased in DMM treated mice in response to tamoxifen. This difference however is minimal and is not significantly different. There is no difference in the lesion severity grade between HuR$^{fl/fl}$AcanA1-CreER^{T2+} and Cre^{-} mice upon SHAM surgery. Significant differences were observed between SHAM and DMM treated mice in both HuR$^{fl/fl}$AcanA1-CreER^{T2+} and Cre^{-} mice (p=<0.001). Red ring shows areas of high cartilage degradation. Data is presented as individual data points for each animal as well as the mean (horizontal line) and the standard deviation/error (error bars) for each group. (HuR$^{fl/fl}$AcanA1-CreER^{T2}luc^{-} SHAM n=3, DMM n=3; HuR$^{fl/fl}$AcanA1-CreER^{T2}luc^{+} SHAM n=3, DMM n=4)

Next, the lesion severity scores from the 4 compartments of the joint, the medial and lateral tibia and femur, were analysed. Images of toluidine blue stained sections of the medial compartments showed severe osteoarthritis lesions in the tibia and femur of DMM treated mice (Figure 4.7 A&B) compared to control SHAM animals (Figure 4.7 C&D). Lesion severity scores shows there is an increase in both the maximum and mean score of the DMM treated medial tibia compartment of $HuR^{fl/fl}$AcanA1-$CreER^{T2+}$ mice compared to their $HuR^{fl/fl}$AcanA1-$CreER^{T2-}$ counterparts (Figure 4.7 E&F). These differences, however, are not statistically significant. There was no difference in the severity score in the medial femur (Figure 4.7 G&H) and no differences in either the tibial and femoral surfaces of the lateral compartment (Figure 4.8).

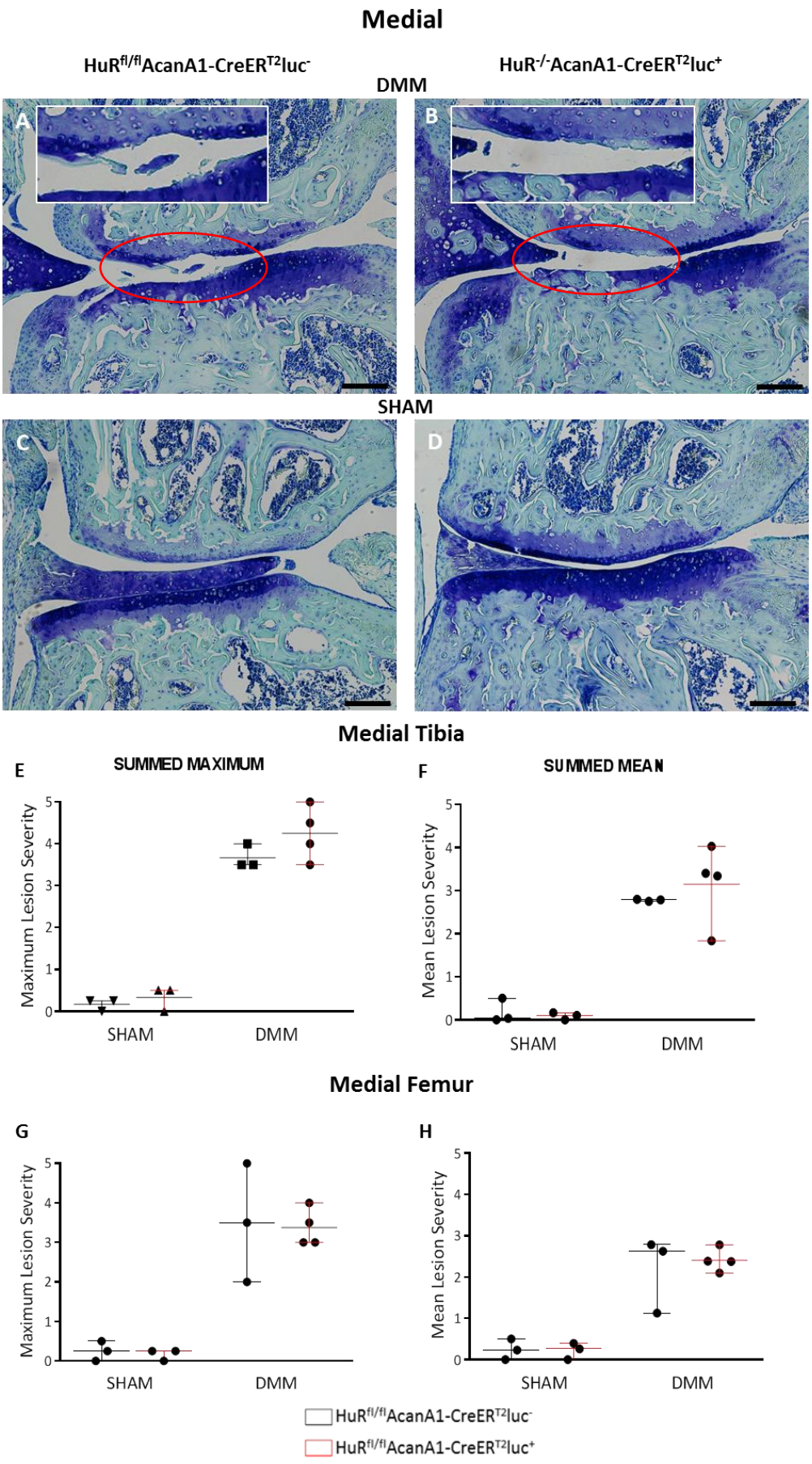
Medial
HuRfl/flAcanA1-CreERT2luc-
HuR-/-AcanA1-CreERT2luc+
DMM
A
B
SHAM
C
D
Medial Tibia
E
SUMMED MAXIMUM
Maximum Lesion Severity
SHAM
DMM
F
SUMMED MEAN
Mean Lesion Severity
SHAM
DMM
Medial Femur
G
Maximum Lesion Severity
SHAM
DMM
H
Mean Lesion Severity
SHAM
DMM
HuRfl/flAcanA1-CreERT2luc-
HuRfl/flAcanA1-CreERT2luc+

Figure 4.7. Histological and histopathology scoring analysis of the medial compartments of HuR$^{fl/fl}$AcanA1-CreER^{T2+} and HuR$^{fl/fl}$AcanA1-CreER^{T2-} knee joints treated with DMM and SHAM surgery. Histological analysis revealed similarities in articular structure in the medial compartments of Cre^{-} (A) and HuR$^{fl/fl}$AcanA1-CreER^{T2+} (B) mice that had undergone DMM surgery. This was confirmed via histopathology scoring were no significant difference was observed in either the tibial (E) or femoral (G) medial compartments when HuR was knocked out. Red ring shows areas of high cartilage degradation. Data is presented as individual data points for each animal as well as the mean (horizontal line) and the standard deviation/error (error bars) for each group. (Medial tibia DMM p=<0.09175, SHAM p= 0.21132; Medial femur DMM p=<0.1596, SHAM p=<0.5). (HuR$^{fl/fl}$AcanA1-CreER^{T2}luc^{-} SHAM n=3, DMM n=3; HuR$^{fl/fl}$AcanA1-CreER^{T2}luc^{+} SHAM n=3, DMM n=4)

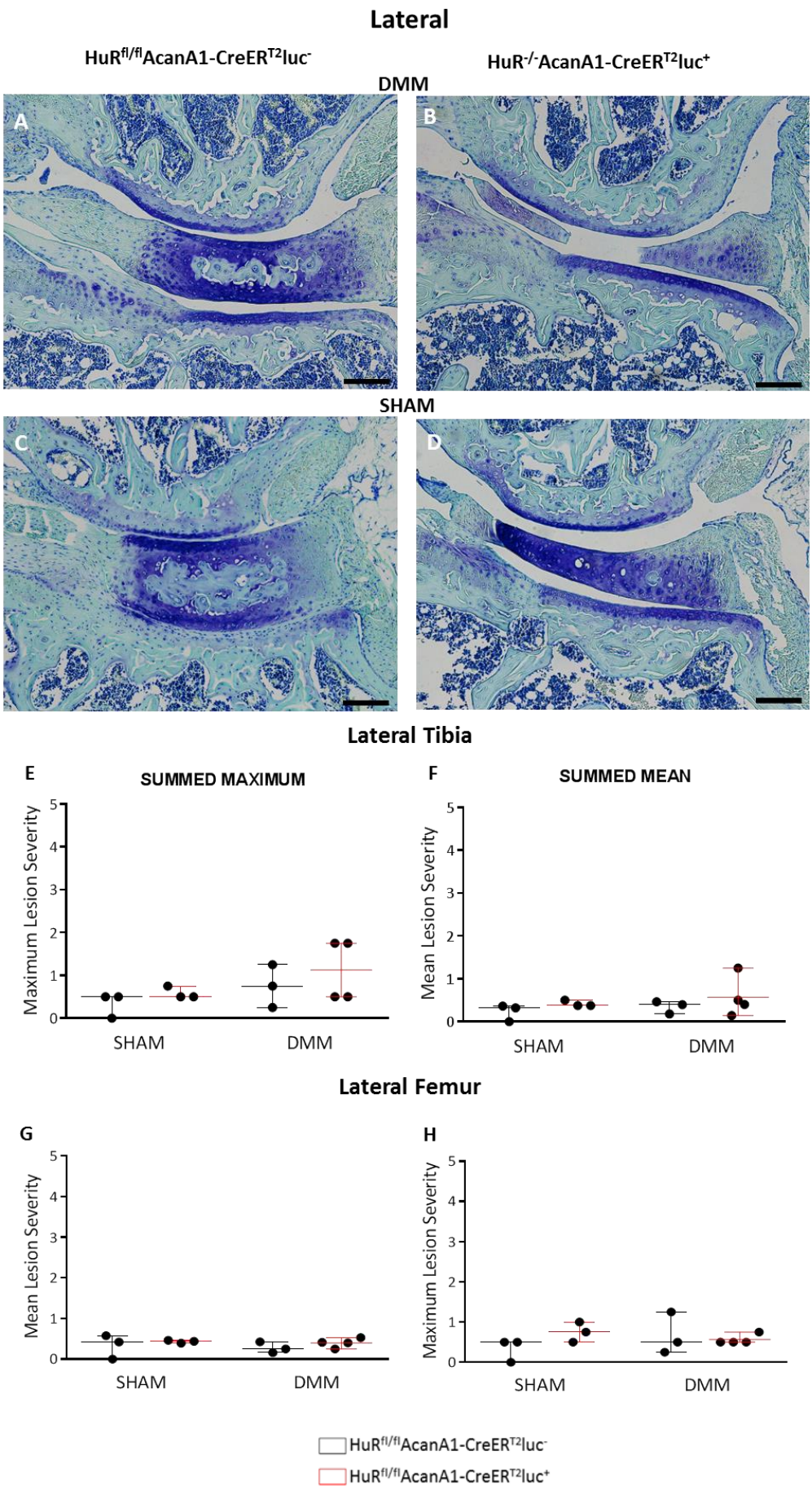
Lateral
HuRfl/flAcanA1-CreERT2luc-
HuR-/-AcanA1-CreERT2luc+
DMM
A
B
SHAM
C
D
Lateral Tibia
E
SUMMED MAXIMUM
Maximum Lesion Severity
SHAM
DMM
F
SUMMED MEAN
Mean Lesion Severity
Lateral Femur
G
Mean Lesion Severity
H
Maximum Lesion Severity
HuRfl/flAcanA1-CreERT2luc-
HuRfl/flAcanA1-CreERT2luc+

Figure 4.8. Histological and scoring analysis of the lateral compartments of HuR$^{fl/fl}$ and Cre^{-} knee joints treated with DMM and SHAM surgery. Histological analysis revealed no differences between the lateral compartments of Cre^{-} (A) and HuR$^{fl/fl}$AcanA1-CreER^{T2+} (B) mice that had undergone DMM surgery. This was also confirmed via histopathology scoring were no significant differences were observed in either the tibial (E) or femoral (G) medial compartments when HuR was knocked out. Data is presented as individual data points for each animal as well as the mean (horizontal line) and the standard deviation/error (error bars) for each group. (Lateral tibia DMM p=<0.18442, SHAM p=<0.21132; Lateral femur DMM p=<0.3709, SHAM 0.10394). (HuR$^{fl/fl}$AcanA1-CreER^{T2}luc^{-} SHAM n=3, DMM n=3; HuR$^{fl/fl}$AcanA1-CreER^{T2}luc^{+} SHAM n=3, DMM n=4)

4.2.3.3 Micro CT analysis

Knee joints from both DMM and SHAM HuR$^{fl/fl}$AcanA1-CreETR^{T2+} and HuR$^{fl/fl}$AcanA1-CreETR^{T2-} mice were scanned on a µCT scanner at 4.5µm voxel size with a rotation set of 0.3° (180° rotation) as previously described. Images were reconstructed and the 3D stack projection was orientated along all three major axes to position samples exactly the same for further analysis (Figure 4.9 C-F). The epiphysis of the tibia was manually selected with the VOI tool using the easily identifiable growth plate as a reference point (Figure 4.9 A&B). The medial meniscus has been destabilised in the DMM model compared SHAM mice (Figure 4.9 B&A, respectively). The BATman software was used for quantification of the selected tibial epiphysis. Bone volume, trabecular thickness and trabecular separation were analysed. No significant differences were observed between DMM and SHAM HuR$^{fl/fl}$AcanA1-CreER^{T2+} mice for any of these parameters (Figure 4.10 A-C), indicating that the progression of osteoarthritis in our DMM mice at 5 weeks did not significantly affect the subchondral bone and also that there was no influence of HuR knockdown at this time point.

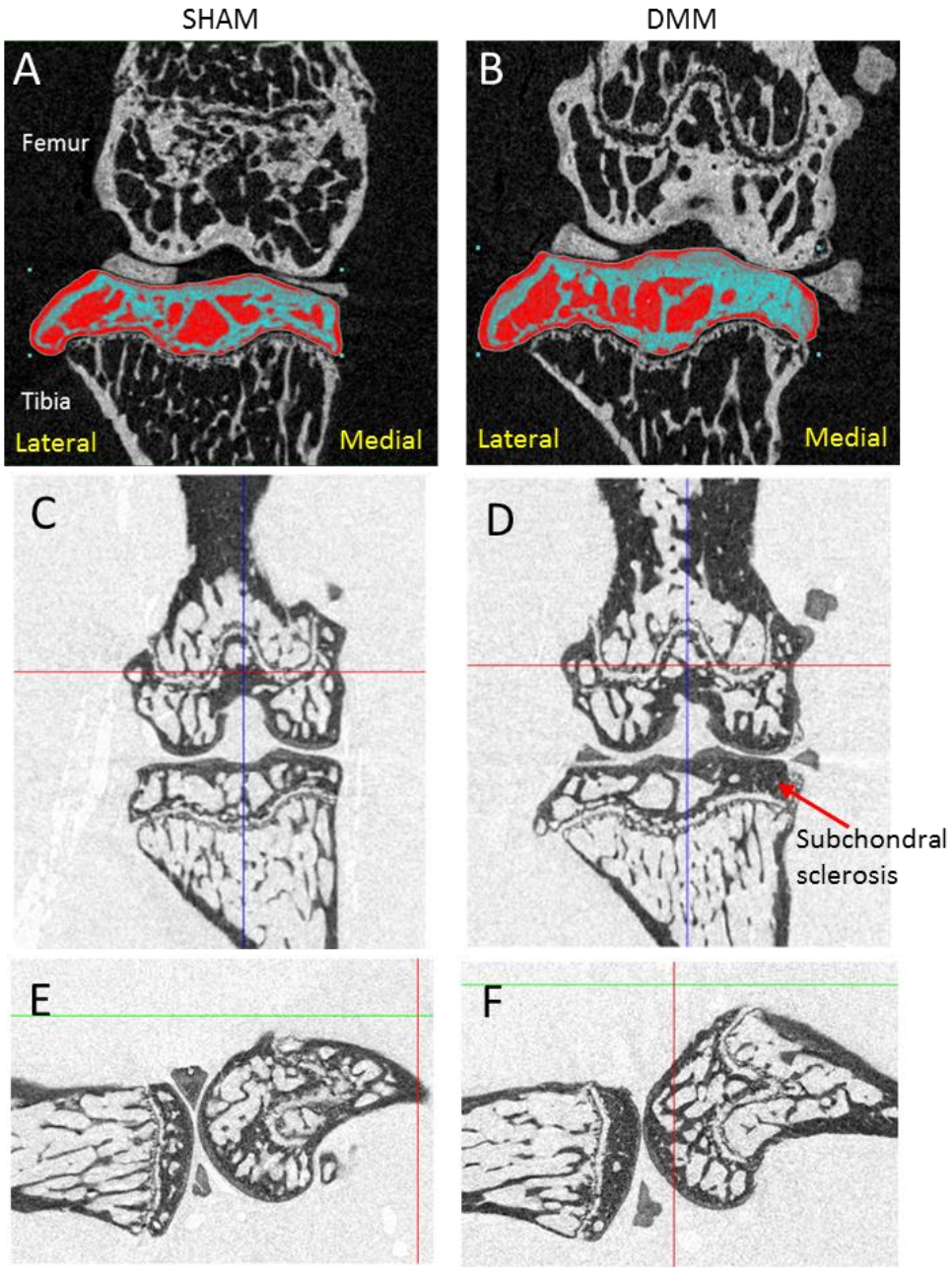

Figure 4.9. Micro CT analysis of SHAM and DMM HuR$^{fl/fl}$AcanA1-CreER^{T2+} mice knee joints. Knee joints were scanned and reconstructed using NRecon along the coronal plane (C&D) and the sagittal plane (E&F). The tibial epiphysis was manually selected as a representative of subchondral bone (A&B). The medial meniscus is destabilised in DMM surgery and a subchondral bone sclerosis is highlighted by the red arrow (D).

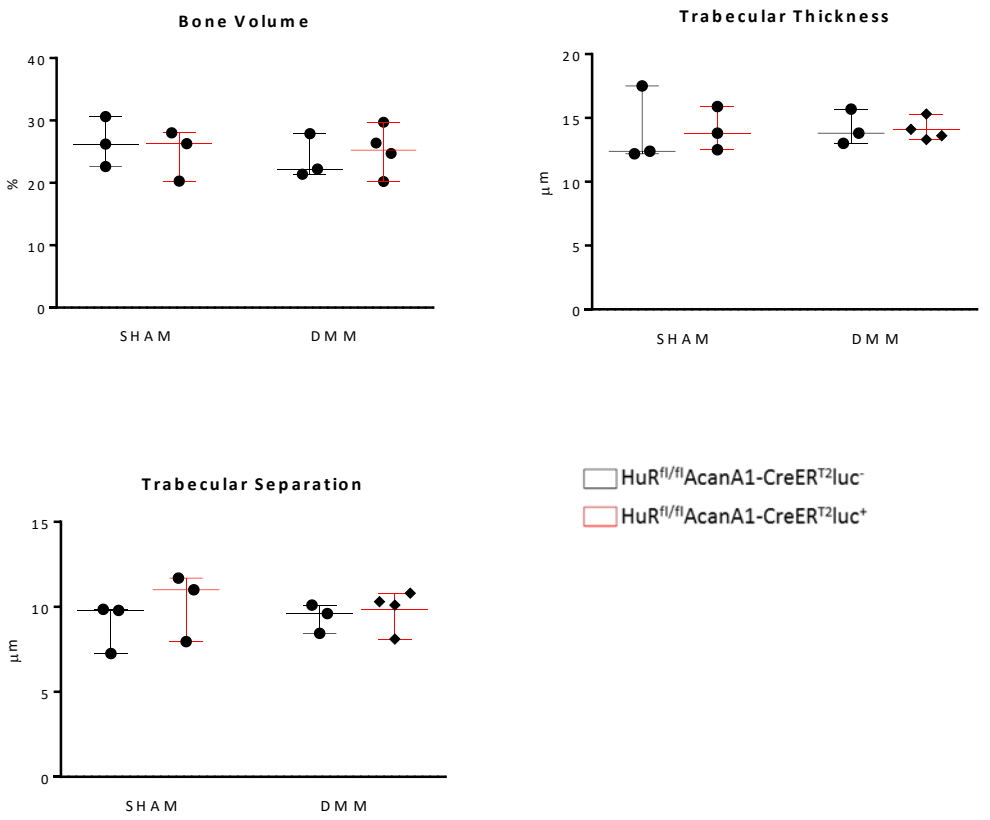

Figure 4.10. Micro-CT analysis of the tibial epiphysis in HuR$^{fl/fl}$AcanA1-CreER^{T2}luc^{+} mice that had undergone either DMM or SHAM surgery. There are no significant differences concerning the bone volume (A), trabecular thickness (B) or trabecular separation (C) in HuR$^{fl/fl}$AcanA1-CreER^{T2+} mice that had undergone DMM surgery compared to control SHAM mice. Data is presented as individual data points for each animal as well as the mean (horizontal line) and the standard deviation/error (error bars) for each group. (DMM bone volume p=<0.637; trabecular thickness p=<0.905; trabecular separation p=<0.606. SHAM bone volume p=<0.653; trabecular thickness p=<0.986; trabecular separation p=<0.429). (HuR$^{fl/fl}$AcanA1-CreER^{T2}luc^{-} SHAM n=3, DMM n=3; HuR$^{fl/fl}$AcanA1-CreER^{T2}luc^{+} SHAM n=3, DMM n=3)

4.3 Discussion

The regulation of articular cartilage mRNAs by post-transcriptional miRNAs and RNA binding proteins has emerged as a further tier of regulation in joint diseases such as osteoarthritis (Tew and Clegg, 2010). Recently, our group has found that HuR knockdown *in vitro* leads to an increase in the expression levels of the cartilage degrading enzyme MMP13 (McDermott *et al.,* 2016). This was the first time RNA binding proteins have been shown to post-transcriptionally

regulate genes in chondrocytes and implies a role for post-transcriptional regulation by HuR during chondrogenesis, and perhaps in osteoarthritis were MMP13 expression levels are elevated. The role of HuR has not previously been examined *in vivo* with respect to articular cartilage and osteoarthritis progression.

To date the RNA binding protein transgenic model that demonstrates the strongest phenotypic links toward a chondrogenic differentiation role has been the Sox2-Cre-driven model of HuR deficiency, which results in the severe skeletal phenotype described in *Chapter 1 section 1.5.2.1.3* (Katsanou *et al.,* 2009). In this chapter HuR was knocked down in a chondrocyte-specific manner in young adult HuR$^{fl/fl}$AcanA1-CreER^{T2}*luc*$^{+}$ mice after tamoxifen-mediated recombination of the loxP sites, determined by Cre-luciferase expression and western blot analysis. We had first evaluated the effect of HuR ablation on the pathology of the knee joint after 5weeks utilising histological and µCT analysis to determine whether any acute effects of HuR deficiency were visible. There was no significant difference in the pathology of the knee joint after this time, meaning for subsequent DMM experiments the response to joint instability is not clouded with an acute response to HuR loss. Adult systemic deletion of HuR results in total lethality of all mice within 10 days (Ghosh *et al.* 2009), we can therefore be confident that expression of the cre-recombinase in HuR$^{fl/fl}$AcanA1-CreER^{T2}*luc*$^{+}$ is restricted to cartilage, as induced HuR loss in this case does not lead to death or acute illness. In order to decipher whether HuR knockout affects articular cartilage a longitudinal study would need to be performed with a larger sample size. For example, a study examining the effect of interleukin-6 (IL-6) knockout in mice found that the gene knockout led to spontaneous osteoarthritis development only after 18 months of age whilst younger, 3-month old mice required collagenase injection into the joint to induce disease (de Hooge *et al.* 2005). Due to this potentially long time frame, we therefore decided to induce osteoarthritis in our cartilage-specific HuR$^{fl/fl}$AcanA1-CreER^{T2+} mice using the surgical DMM model.

4.3.1 Post-transcriptional regulation in osteoarthritis

Post-transcriptional regulation of genes has an important role in many biological processes and the disruption of this tier of regulation is often implicated in disease (Faour *et al.* 2003). The use of mouse models of osteoarthritis, including DMM surgery, have identified many of the cellular and molecular changes that occur in osteoarthritis (Shen *et al.* 2017), however post-transcriptional gene control in chondrocytes remains poorly understood. There is also evidence suggesting that genes important during chondrogenesis can be post-transcriptionally regulated in chondrocyte *in vitro* cultures. For instance, hyperosmotic stress has previously been shown to result in an increase in the mRNA levels of the essential cartilage transcription factor Sox9, associated with the regulation of SOX9 mRNA decay in human osteoarthritic chondrocytes via the p38 MAPK pathway (Tew *et al*., 2009). Furthermore, bone morphogenetic protein -2 (BMP-2), which is crucial to the development of the embryonic and post-natal skeleton can be regulated by TNFα in chondrocytes through alteration in its mRNA stability (Pizette and Niswander, 2000, Fukui *et al*., 2006). BMP-2 is particularly crucial in developing limb buds promoting the differentiation of prechondrogenic mesenchymal condensations into chondrocytes.

Here, we conducted a preliminary study examining the role of HuR knockdown 5 weeks after the induction of osteoarthritis via DMM surgery. As measured by osteoarthritis histopathology scoring, induction of specific HuR knockdown in articular cartilage did not significantly affect the severity of osteoarthritis disease progression. However, there was an increased variability in the HuR knockdown data with higher summed and maximal scores in the medial tibial compartment, which suggests that a larger, higher powered study is necessary. For non-preliminary studies a power analysis should be performed for all studies were groups are compared (Sexton *et al.,* 2008). The basic principle of a power calculation is to determine the number of individuals needed to detect a significant difference in treatment, as such in order to calculate sample size a general idea of the expected results in required (Noordzij *et al.,* 2010). As this is a preliminary study and we have very few sample subjects in each group of our

study, the results cannot be generalised to the wider population. It would therefore be necessary to complete this study with a larger sample size having completed a power calculation; this is performed and discussed in greater detail in the concluding chapter of this thesis.

4.3.2 HuR during osteoarthritis

While there is no significant difference in the articular cartilage of $HuR^{fl/fl}$AcanA1-$CreER^{T2+}$ mice compared to controls after DMM-induced joint instability, HuR may still play a role in the development of osteoarthritis. Genes known to influence osteoarthritis might be direct or indirect targets of HuR regulation, and there is evidence that this can occur. Runx2 is a crucial transcription factor involved in the regulation of chondrocyte hypertrophy, as well as an inducer of osteoblast differentiation, whose expression levels have been shown to be increased in human osteoarthritic cartilage (Zhong *et al.* 2016). An overexpression of Runx2 in transgenic mice results in an activation of MMP13 and ADAMTS5, both matrix degrading enzymes, in chondrocytes (Wang *et al.* 2012). Runx2 increases the transcription of MMP13 by binding to osteoblast-specific gene osteocalcin (OSE2), located in the proximal promotor of MMP13 (Hess *et al*, 2001). During chondrocyte differentiation, Runx2 also interacts with Osterix to cooperatively induce MMP13 expression (Nishimura *et al.* 2012). Runx2 undergoes multiple levels of regulation and miRNAs have been implicated in its post-transcriptional control during MSC lineage determination and in osteoarthritis (Huang *et al.* 2010, Martinez-Sanchez *et al.* 2012). A recent report identified Runx2 as a novel target of miR-105 and demonstrated that miR-105 expression is downregulated in osteoarthritis (Ji *et al.* 2016).

Recently, a study reported that, while control mice developed severe osteoarthritis-like defects including the degradation of articular cartilage and subchondral bone after DMM surgery, Aggrecan-$CreER^{T2}$*luc* driven knockout of Runx2 significantly ameliorated these defects. It was also shown that MMP13 levels were significantly reduced in Runx2 knockout mice. Taken together these findings suggest that osteoarthritis-like defects can be partially rescued after

Runx2 inhibition (Liao *et al.* 2017). Based on this and previous studies that demonstrate how Runx2 regulates MMP13 expression, and that it can be post-transcriptionally regulated by miRNAs, it is possible that RNA-binding proteins may also regulate Runx2 expression in chondrocytes and during osteoarthritis progression. Our group has previously reported that upon siRNA-mediated knockdown of HuR in chondrosarcoma cells and human articular chondrocytes the overall mRNA expression of Runx2 was decreased suggesting HuR may play a role in its regulation, however there was no change in Runx2 mRNA decay (McDermott *et al.* 2016). Because HuR works by increasing the stability of its target mRNAs, there would be the potential for a knockout of HuR to cause a downregulation of Runx2 expression through an intermediate factor and thus partially decelerate the rate of osteoarthritis progression. Further work, however, is required to confirm HuRs role in regulating genes involved in chondrogenesis and to conclude whether HuR plays an active role in the development of osteoarthritis. For example, a relatively simple initial experiment could be to use the wax embedded sections from the mice used in this DMM pilot study for immunohistochemical analysis. This would allow examination of the protein localisation of HuR, also confirming protein levels had been reduced *in vivo*, and the localisation and abundance of other genes of interest and potential targets of HuR. By examining the distribution and abundance of HuR and other markers of chondrogenesis we can identify genes differentially regulated by the knockdown of HuR during disease development *in vivo.*

In summary, this chapter reports that articular cartilage is not acutely affected by the loss of HuR in adult mice after 5 weeks. However, variability in the medial tibial compartment is interesting and would benefit from a higher powered study. It is possible that the effects of HuR deficiency in adults do not manifest until much later in adult life, however while we fully intended to explore this avenue Home Office project licence issues meant we had to halt this part of the project. This would, however, be a potential next step for the continuation of this work. It has previously been reported that inducing chondrocyte death by transgenic expression of toxins leads to a reduction in the

cell population but not does lead to cartilage damage (Zhang *et al.* 2016). This study also reported that after surgical induction of osteoarthritis in mice, cartilage damage was actually increased in mice with intact chondrocytes compared to animals were chondrocytes had been killed (Zhang *et al.* 2016). These findings suggest that chondrocyte death does not drive cartilage damage. Another study reported that HuR-deficiency in pancreatic ductal adenocarcinoma cells resulted in significantly elevated levels of cell death compared to control cells (Lal *et al.* 2017). While this study was performed on different cell types, it is possible that in our HuR transgenic mice, HuR knockdown might lead to chondrocyte cell death which may not alter the integrity of the articular surface. *In vitro* studies utilising chondrogenic cell lines and primary chondrocytes from HuR floxed mice would help to identify molecular changes that occur during HuR loss and provide a better insight into the post transcriptional functions of HuR in cartilage.

Although conditional inactivation or overexpression of genes via the Cre/loxP system is a common method to investigate the function of genes *in vivo*, one must keep in mind that this method has limitations. To achieve efficient gene recombination Cre/loxP relies on the potency of each transgenic promoter to drive the expression of the Cre recombinase, with transgene copy number usually proportional to expression strength (Elefteriou and Yang, 2012). Chromosomal position effect can cause this variability and can often relate to the insertion site of the transgene, which can insert into a transcriptionally more or less active chromosomal region. Tools are available to understand the relative intensity of Cre activity in different cells or tissues. The ROSA26-lacZ line has one copy of the bacterial gene lacZ inserted into chromosome 6 (Kisseberth *et al.,* 1999). The associated mouse promoter drives β-galactosidase expression in all adult tissues and, when generating a double transgenic line with inducible Cre recombinase, is a useful tool for visualising Cre recombinase expression after recombination (Guarente *et al.,* 1981). AcanA1-CreER^{T2}*luc* mice were used in this study to generate HuR knockout mice specifically in aggrecan expressing cells. AcanA1-CreER^{T2}*luc* mice were initially generated by Cascio in 2013 and were subsequently mated with the ROSA26-lacZ mice in order to

establish the areas of Cre recombinase expression *in vivo* (Cascio *et al*., 2013). This study reported that Cre recombinase under the aggrecan A1 reporter was activated by tamoxifen and was specifically expressed in cartilaginous structures and developing skeletal structures in embryos and cartilage tissues in adults. As this validation was confirmed prior to breeding with $HuR^{fl/fl}$ mice we can therefore be confident that Cre recombinase expression is restricted to chondrocytes in our double transgenic mice. However, while $CreER^{T2}$ is ~10 times more sensitive to 4OH-tamoxifen *in vivo* than the original CreERT, one major limitation of the $CreER^{T2}$ system is that it may be somewhat leaky, resulting in weak constitutive activation (Elefteriou and Yang, 2012).

One highly important parameter to consider when generating conditional knockout mice is the efficiency of flox recombination (Elefteriou and Yang, 2012). As discussed, Cre transgenic lines have varying levels of Cre recombinase expression, while floxed genes have differing chromosomal accessibility to be clipped by the Cre recombination, which combined leads to variable recombination efficiency (Elefteriou and Yang, 2012). It is therefore necessary to validate and confirm knockdown both at the mRNA and protein levels. This however proved a technically challenging aspect of the work presented in this chapter. For mRNA, we initially attempted to extract the RNA from the articular cartilage from individual mice, however the abundance of isolated RNA was very low and subsequent qRT-PCR was therefore unsuccessful. We next decided to pool the articular cartilage of several mice from the same genotype when extracting the RNA, this again resulted in low abundance RNA and qRT-PCR was unsuccessful. Extracting high-quality RNA in sufficient amounts from articular cartilage has previously been reported as challenging due to low cellularity and high proteoglycan content in the ECM (Bleu *et al.,* 2017; Ruettger *et al.,* 2010). After many attempts at optimising techniques for mRNA isolation and analysis proved unsuccessful we decided to examine the protein expression levels. However, isolating the protein from individual mice also resulted in low protein abundance that was undetected by western blot. We therefore also pooled the articular cartilage from 3 mice per experimental and control groups, the results of which are reported in figure 4.2B, this figure however is not great and the

amount of time already spent on this validation meant this was the best we could do. Further optimisation would enable more definitive levels of protein expression to be analysed. We are currently optimising immunohistochemical analysis for HuR on the histological sections taken from mice in this study in order to confirm HuR protein knockdown *in vivo.*

5 Analysis of HuR knockdown in chondrocytes *in vitro*

5.1 Introduction

As discussed in *Chapter 3*, HuR knockdown has a detrimental effect on the developing skeleton during embryonic development. Based on the results of *Chapter 4*, it would appear that HuR knockdown does not have an effect in the adult joint or during the progression of osteoarthritis. While phenotypic differences in the ribs, limbs and craniofacial structures of the developing embryo can be observed after HuR knockout, the molecular mechanisms affecting chondrocyte function remain unknown. This chapter will focus on the use of *in vitro* systems in order to determine the molecular mechanisms involved in the regulation of chondrocyte function by HuR.

5.1.1 Primary chondrocytes

Isolation and culture of primary chondrocytes is a commonly used method for studying the molecular mechanisms involved in the regulation of progression of chondrogenesis. Several culture models, including primary cultures of mouse, rabbit and rat chondrocytes, have proved useful tools for studying chondrogenesis. Especially since normal animal chondrocytes and chondrocytes/mesenchymal cells from developing or young tissue are more readily available than human chondrocytes, were generally only chondrocytes from old and/or osteoarthritic tissue can be obtained. Chondrocytes are generally isolated using enzymatic digestion of the tissue, typically with an initial digestion with trypsin or hyaluronidase to remove proteoglycan from the matrix, followed by collagenase to break down the collagen structure of the tissue. Collagenase D contains collagenase and other proteases that is ideal for gentle tissue dissociation of murine chondrocytes (Thirion and Berenbaum 2004). An important consideration when working with primary chondrocytes is that they quickly dedifferentiate in monolayer culture. This process is characterised by a loss of the cells' rounded morphology as they switch to a proliferative, fibroblastic phenotype. This change in phenotype is accompanied by reduced expression of chondrocyte marker genes such as Col2a1, aggrecan and Sox9, alongside a general reduction in ECM synthesis and an increase in expression fibroblastic genes such as Col1a1 (Hardingham *et al.* 2002).

5.1.2 Immortalised cell lines for studying chondrogenesis

When studying the molecular mechanisms of chondrogenesis *in vitro*, chondrogenic cell lines are frequently used as an alternative to primary chondrocytes (Phull *et al.,* 2016). There are several chondrogenic cell lines available, which range from transformed cells isolated from cartilage tumours to primary cells that have been immortalised in the laboratory (Phull *et al.,* 2016). Advantages of cell lines include their stable phenotype, relative ease of culture and their ability to generate large numbers of cells for large scale experiments (Maqsood *et al.,* 2013). However, their stable phenotype also represents a significant drawback to their use as it generally differs significantly from primary chondrocytes meaning that care has to be taken when interpreting results (Lorsch et al., 2014). Nevertheless, although immortalised cell lines cannot be substituted entirely for primary cultures, experiments using primary chondrocytes are limited by the number of cells that can be derived from tissue samples, the donor variability and the phenotypic instability of the cells when they are allowed to divide in adherent monolayer culture (Otero *et al.,* 2014). Overall, the ease of use and reproducibility of chondrocyte cells lines has led many scientists to use them for detailed molecular studies and for preliminary hypothesis generation studies, prior to validation of experimental conclusions in primary chondrocyte cultures (Otero *et al.,* 2014).

There are a number of cell lines that have been used for the study of chondrogenesis and osteogenesis including C3H10T1/2 (Lin *et al.* 2009), RCJ3 (Spagnoli *et al.* 2001) and CFK2 cells (Filion and Labelle 2004). When compared to all the chondrogenic cell lines, however, ATDC5 cells have been reported to exhibit a higher frequency of chondrogenic differentiation and are some of the most chondrocytic in their actions (Atsumi *et al.* 1990).

ATDC5 is a murine chondrogenic progenitor cell line derived from mouse embryo teratocarcinoma (AT805) cells that undergo cellular condensation and a sequential process of chondrocyte differentiation and eventually hypertrophy when insulin, transferrin and sodium selenite are added to the culture medium. Insulin is necessary as a growth factor, transferrin as an iron transporter and sodium selenite is a potent antioxidant (Atsumi *et al.* 1990). ATDC5 cells are

maintained in an undifferentiated state during their rapid proliferation, which allows large numbers of cells to be generated for use in *in vitro* culture systems to mimic cellular condensation during chondrogenesis. This cell line is therefore a useful *in vitro* model for exploring molecular mechanisms during chondrogenesis (Yao and Wang 2013).

Previous work examining the effect of RNA binding protein knockdown in primary human chondrocytes and in the human chondrosarcoma-derived cells SW1353 led to the observation that expression of HuR negatively regulates MMP13, as its knockdown via siRNA leads to significant and reproducible elevated levels of MMP13 expression with no notable difference in its rate of decay (McDermott *et al.* 2016). The distribution of HuR in mouse E13.5 and E16.5 embryos also led to regional differences in the expression of HuR being identified, with lower expression levels in hypertrophic chondrocytes and in those adjacent to regions involved in the regulation of mineralisation and long bone growth, including the perichondrium were MMP13 expression is elevated (McDermott *et al.* 2016). This finding is interesting because, as previously mentioned in *section 1.3.1.2.1*, MMP13 is considered a marker of terminal chondrocyte differentiation during endochondral ossification. In order to build upon these findings, experiments were performed to elucidate mechanistic details of HuR's role in chondrogenesis and osteoarthritis progression in the *in vitro* chondrocyte models: the ATDC5 cell line, and primary articular chondrocytes isolated from $HuR^{fl/fl}$ mice.

A high-throughput biochemical screen previously identified the low molecular weight compound, MS-444, as an inhibitor of HuR that was originally isolated from the culture broth of *Micromonospora* (Nakanishi *et al.* 1995). HuR homodimerises before binding to RNA, a process that is mediated by RRMs 1 and 2 (Kasashima *et al.* 2002, Meisner *et al.* 2007). MS-444 acts to interfere with the formation of HuR dimers and inhibits HuR's ability to bind to its target ARE-containing mRNAs and influences HuR's cytoplasmic location (Meisner *et al.* 2007). Primary chondrocytes from transgenic mice containing floxed sites and which conditionally express Cre recombinase are an ideal tool for studying the ablation of a specific gene *in vitro*. 4-hydroxytamoxifen has previously been

utilised to induce nuclear localisation of Cre recombinase in *in vitro* culture systems were cells contain both the floxed alleles and estrogen receptor-bound Cre recombinase under the control of a specific promoter (Yang *et al.* 2014). An alternative approach for the delivery of Cre recombinase is the use of viral vectors. Adenovirus vectors are a popular tool for foreign gene delivery to mammalian cells, in part due to their ability to infect many different cells types and tissues and because they don't require cell division for infection unlike retroviruses. Adenoviral vectors that express Cre recombinase have been utilised to mediate loxP recombination in *in vitro* systems (Badorf *et al.* 2002).

As previously discussed in *Chapter 3*, deletion of HuR in cartilage- and skeletal-specific manners during embryonic development leads to abnormalities in chondrogenesis and endochondral ossification. Exactly how loss of HuR causes a severely abnormal skeletal phenotype remains unknown. In this chapter, *in vitro* assays using both ATDC5 cells and murine primary chondrocytes are utilised to try to determine HuR's molecular impact during chondrocyte differentiation.

5.2 Results

5.2.1 Determining the optimum concentration of MS-444

The well-established chondrocytic cell line ATDC5 was used as a reproducible model of chondrogenic differentiation. (Kartsogiannis and Ng 2004). To determine optimum concentration for observing functional effects of HuR inhibition using MS-444, undifferentiated ATDC5 cells were plated at 6400 cells/cm^2 and treated with varying concentrations of MS-444 for 24 hours. RNA was extracted with TRIzol® and cDNA prepared for qRT-PCR quantification. Results were analysed using the comparative Ct method ($2^{-\Delta Ct}$) such that each genes mRNA was quantified relative to β-Actin. Were MS-444 was added to a treatment group, the same volume of DMSO was added to control groups.

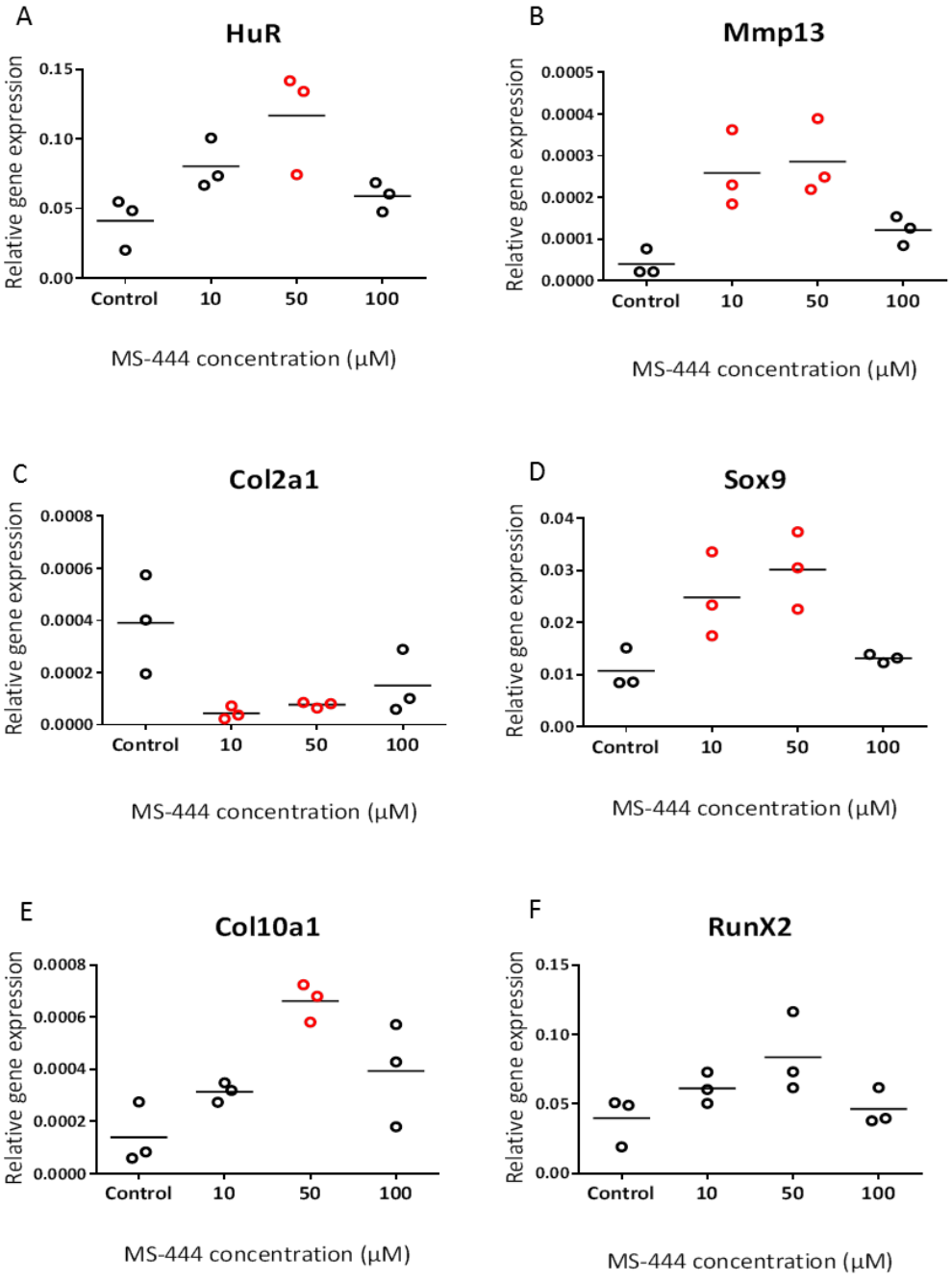

Figure 5.1. qRT-PCR analysis of mRNA expression levels of marker genes in ATDC5 cells treated with varying concentrations of the HuR inhibitor MS-444. ATDC5 cells were seeded at 6400 cells/cm^2 and treated with either 10µM, 50µM or 100µM of MS-444 for 24 hours. Red data points indicate statistically significant differences in the expression levels compared to that of control conditions without MS-444 ($p < 0.005$, one way ANOVA with Dunnett's post hoc testing). Horizontal lines represent the mean value of each data set. Each data point represents the result of an independent experimental replicate. (n=3)

Undifferentiated ATDC5 cells were treated with 10μM, 50μM and 100μM of MS-444. Analysis by qRT-PCR showed that gene expression levels of HuR were significantly increased when treated with 50μM of MS-444 for 24 hours (Figure 5.1A). MMP13 levels were significantly increased at both 10μM and 50μM (Figure 5.1B) but not at 100μM, suggesting saturation of MS-444 does not increase effectiveness of HuR inhibition. Col2a1 mRNA was detected at very low levels in the undifferentiated ATDC5 cells and was significantly reduced further by treatment with MS-444. (Figure 5.1C). Sox9 levels increased significantly at both 10 and 50μM (Figure 5.1D). Markers of terminal differentiation Col10a1 and Runx2 both observed an increase in gene expression (Figure 5.1E+F), with a significant increase of Col10a1 when treated with 50μM MS-444. Based on this data, we therefore decided to continue the rest of the experiments using 50μM MS-444.

5.2.2 HuR knockdown during chondrogenic differentiation

Differentiation of ATDC5 cells follows a well-defined and established endochondral program were the cells differentiate from chondroprogenitors to hypertrophic chondrocytes over 2 to 3 weeks following stimulation of confluent monolayers with insulin (Atsumi *et al.* 1990). Previously, the mRNA expression of Col2a1, Col10a1, Sox9 and RunX2 during chondrogenic differentiation of ATDC5 cells were analysed using qRT-PCR (Caron *et al.* 2016). It was shown that during differentiation of ATDC5 cells Col2a1 and Sox9 were increasingly expressed from day 7 onwards, which established chondrogenic differentiation and Col10a1 and Runx2 were also increased from day 7 and 10 marking chondrocyte hypertrophy (Caron *et al.* 2016). Interestingly Sox9 expression is also transiently increased in the first few hours of differentiation.

In order to measure the baseline mRNA levels of HuR and markers of chondrogenesis in ATDC5 cells during chondrogenic differentiation, cells were treated with differentiation media containing insulin for 21 days and RNA extracted at days 0, 4, 14 and 21. MMP13 was increasingly expressed from day

14 onwards to significantly different levels than that of days 0 and 4 (Figure 5.2B). To determine that chondrogenic differentiation had occurred, expression of the chondrocyte markers Col2a1 and Sox9 was measured alongside that of the markers of terminal differentiation Col10a1 and Runx2. Col2a1 and Col10a1 (Figure 5.2 C &E, respectively) had both increased expression by day 14 onwards, with a statistically significant increase of Col2a1 by day 21. Runx2 expression also increased over the course of chondrogenic differentiation, though not significantly, and plateaued by day 21 (Figure 5.2F). Sox9 expression significantly increased after day 4 to a steady state (Figure 5.2D). However, in this experiment any transient increase of Sox9 during the early stages of differentiation could not be detected.

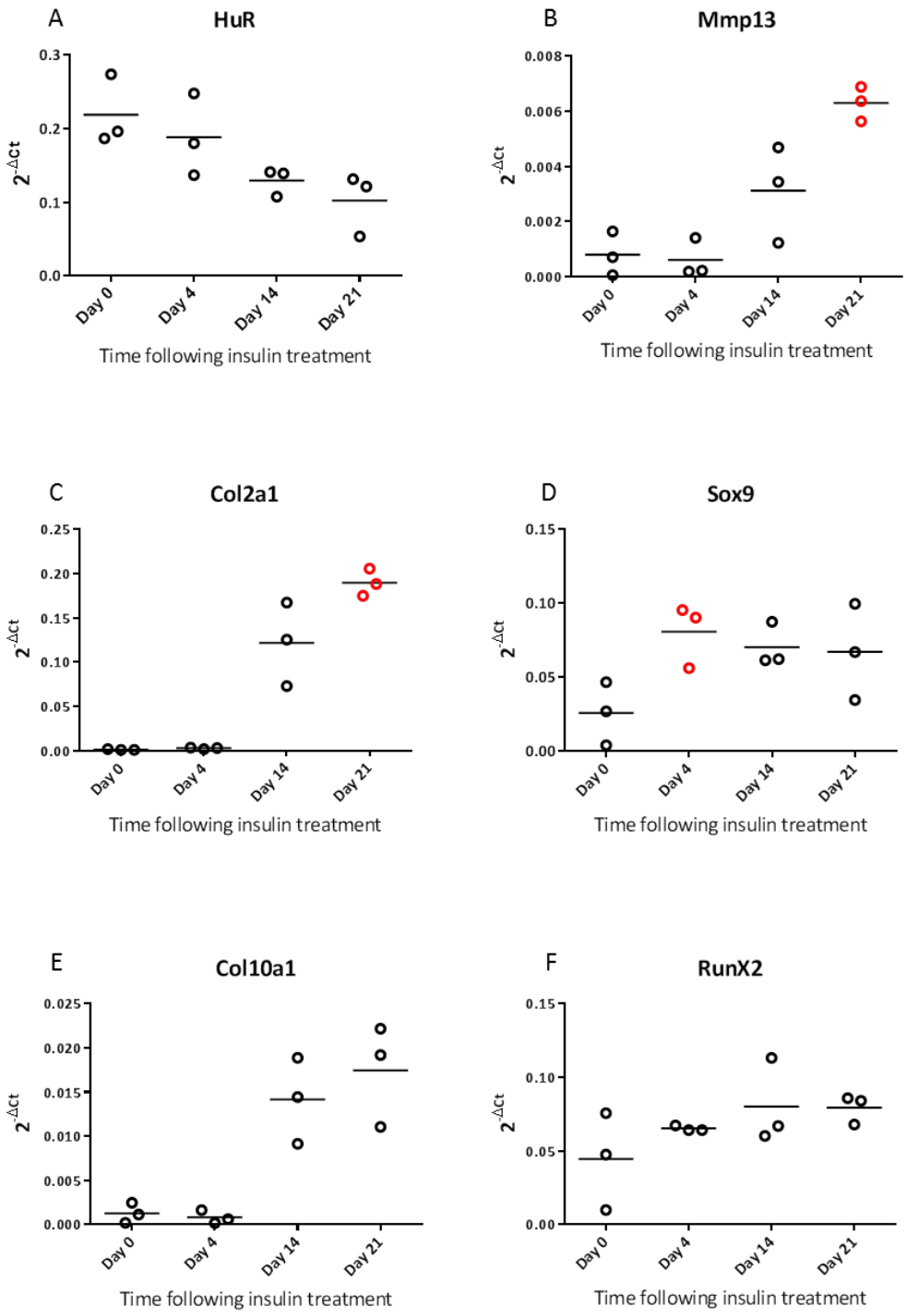

Figure 5.2. qRT-PCR analysis of mRNA expression levels of marker genes in ATDC5 cells that have undergone chondrogenic differentiation. ATDC5 cells were seeded at 6400 cells/cm^2. After 24 hours cells were differentiated in the chondrogenic lineage for 21 days with insulin treatment. Red data points indicate conditions were expression was significantly different to that of Day 0 conditions ($p < 0.05$, one-way ANOVA with Tukey's post hoc testing). Horizontal lines represent the mean value of each data set. Each data point represents the mean of an independent experimental replicate. (n=3)

To examine the effects of MS-444-mediated inhibition of HuR function during chondrocyte differentiation, ATDC5 cells were differentiated with insulin with or without the addition of 50μM MS-444 for the first 48 hours. RNA was extracted for qRT-PCR at 0, 1, 2, 4, 8, 24 and 48 hours and 4, 7, 10 and 14 days in order to ensure adequate representation of the mRNA levels over the course of the 14 days. Compared to cells without MS-444 treatment, HuR mRNA levels were only slightly decreased with the addition of MS-444 for the first 48 hours (Figure 5.3A). This is potentially because MS-444 was only added for the first 48 hours of chondrocyte differentiation and may have needed continuous treatment throughout the course of the experiment to observe significant changes compared to control conditions. MMP13 expression levels, however, were higher during the first hours of differentiation, when the MS-444 was present, but then appeared to be inhibited in the later stages of the process (Figure 5.3B). Col2a1, Aggrecan and Col10a1 mRNA levels steadily increased over the course of the experiment with no differences observed between the control and MS-444 treated cells (Figure 5.3 C, E + F respectively). Sox9 mRNA expression also increased over the course of the experiment with no difference between MS-444 treated cells and non-treated cells (Figure 5.3D). A reduction in Runx2 expression can be seen between 24 and 48hours in MS-444 treated cells compared to non-treated and a significant reduction in Runx2 expression is observed at day 14 (Figure 5.3G).

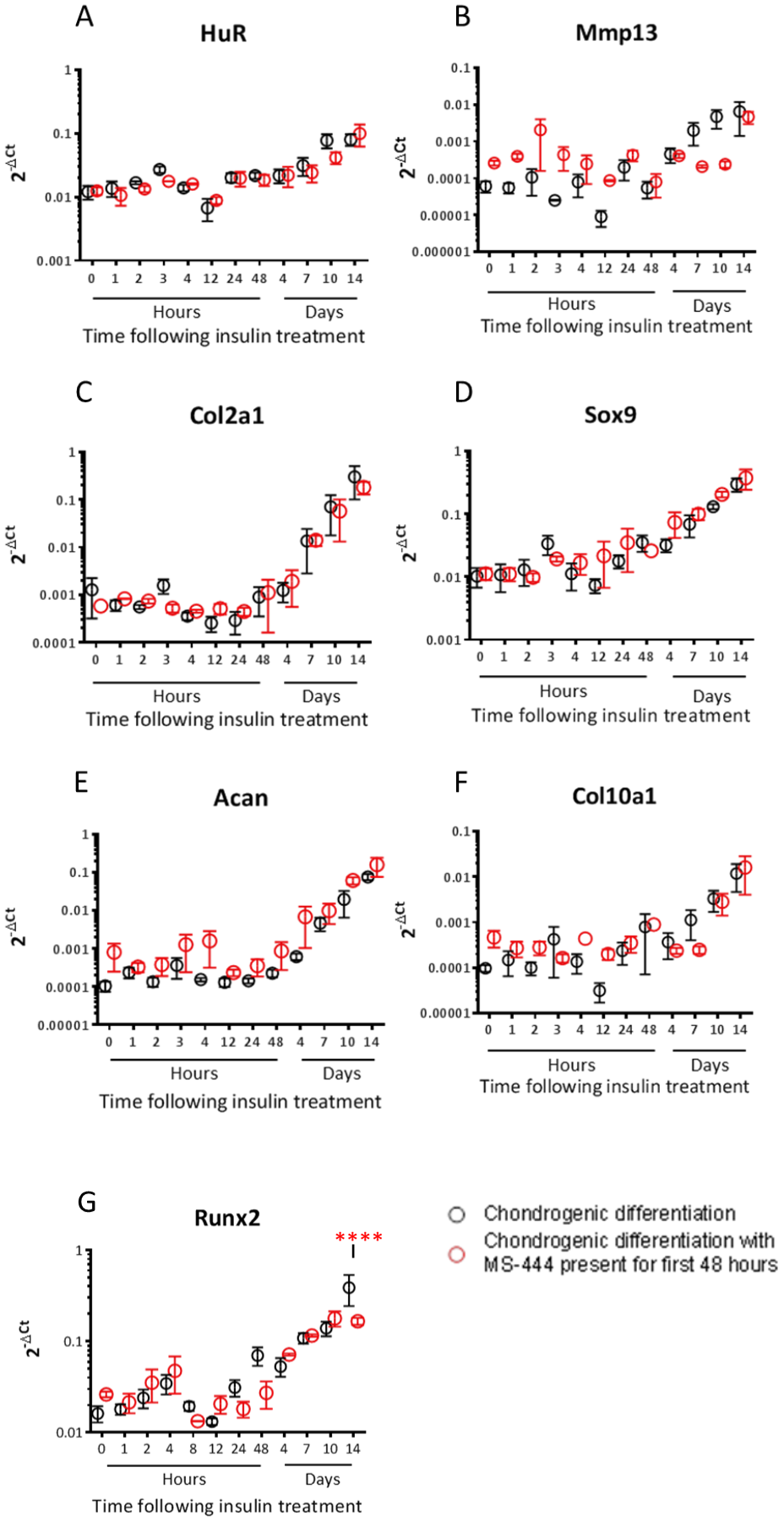
A
HuR
B
Mmp13
C
Col2a1
D
Sox9
E
Acan
F
Col10a1
G
Runx2
****
2-ΔCt
Hours
Days
Time following insulin treatment
Chondrogenic differentiation
Chondrogenic differentiation with
MS-444 present for first 48 hours

Figure 5.3. qRT-PCR analysis of mRNA expression levels of marker genes in ATDC5 cells undergoing chondrogenic differentiation for 14 days with or without 50μM MS-444 present during the first 48 hours of culturing. ATDC5 cells were seeded at 6400 cells/cm2 and treated with 50μM MS-444 for the first 48 hours of chondrogenic differentiation with the addition of insulin in differentiation media and time points taken at various intervals for 14 days. Note the X-axis is a categorical and not linear time scale. Each data point represents the mean of an independent experimental replicate. (**** = $p < 0.0001$) (n=3)

5.2.3 MS-444 treatment differentially regulates the mRNA levels of genes involved in chondrogenesis

Limited availability of MS-444 meant that continuous application over a 21-day time course was not possible. We instead decided to assess over a shorter time period of 7-days. ATDC5 cells were treated with 50μM MS-444 continuously for 7 days, a point at which many marker genes' expression is altered under chondrogenic conditions. Cells either remained undifferentiated or were differentiated with the addition of insulin in the culture medium. Here, induction of differentiation by insulin does not seem to alter HuR mRNA levels after 7 days (Figure 5.4A). However, after continuous treatment with MS-444 HuR levels in both differentiating and undifferentiated cells are significantly reduced, suggesting MS-444 does act to inhibit HuR but is not affected by the morphological state of the chondrocyte. MMP13 levels are significantly increased after MS-444 treatment compared to control and Day 0 (Figure 5.4B). MMP13 levels are increased in untreated differentiating ATDC5 cells (insulin treatment), however expression levels do not seem to increase again in differentiating cells with MS-444 treatment (M+I treatment). Col2a1 mRNA levels are decreased in all conditions when compared to day 0, however levels are increased when compared to control conditions after the 7 day time course (Figure 5.4C). Sox9 is significantly increased in differentiating cells due to an induction by insulin. Both undifferentiated and differentiating cells result in a significant repression of Sox9 expression after 7 days of continuous treatment with MS-444 (Figure 5.4D). As a marker for chondrocyte differentiation, it was no surprise that Col10a1 expression levels were increased during chondrocyte

differentiation in untreated cells due to insulin addition in cells without MS-444 (Figure 5.4E). However, mRNA levels of Col10a1 were inhibited to Day 0 levels by MS-444 treatment after 7 days of differentiation (M+I). Runx2 mRNA levels remained at similar levels to the control condition after 7 days of differentiation with insulin. MS-444 treatment however, significantly repressed the mRNA levels of Runx2 in both differentiating and undifferentiated cells (Figure 5.4F).

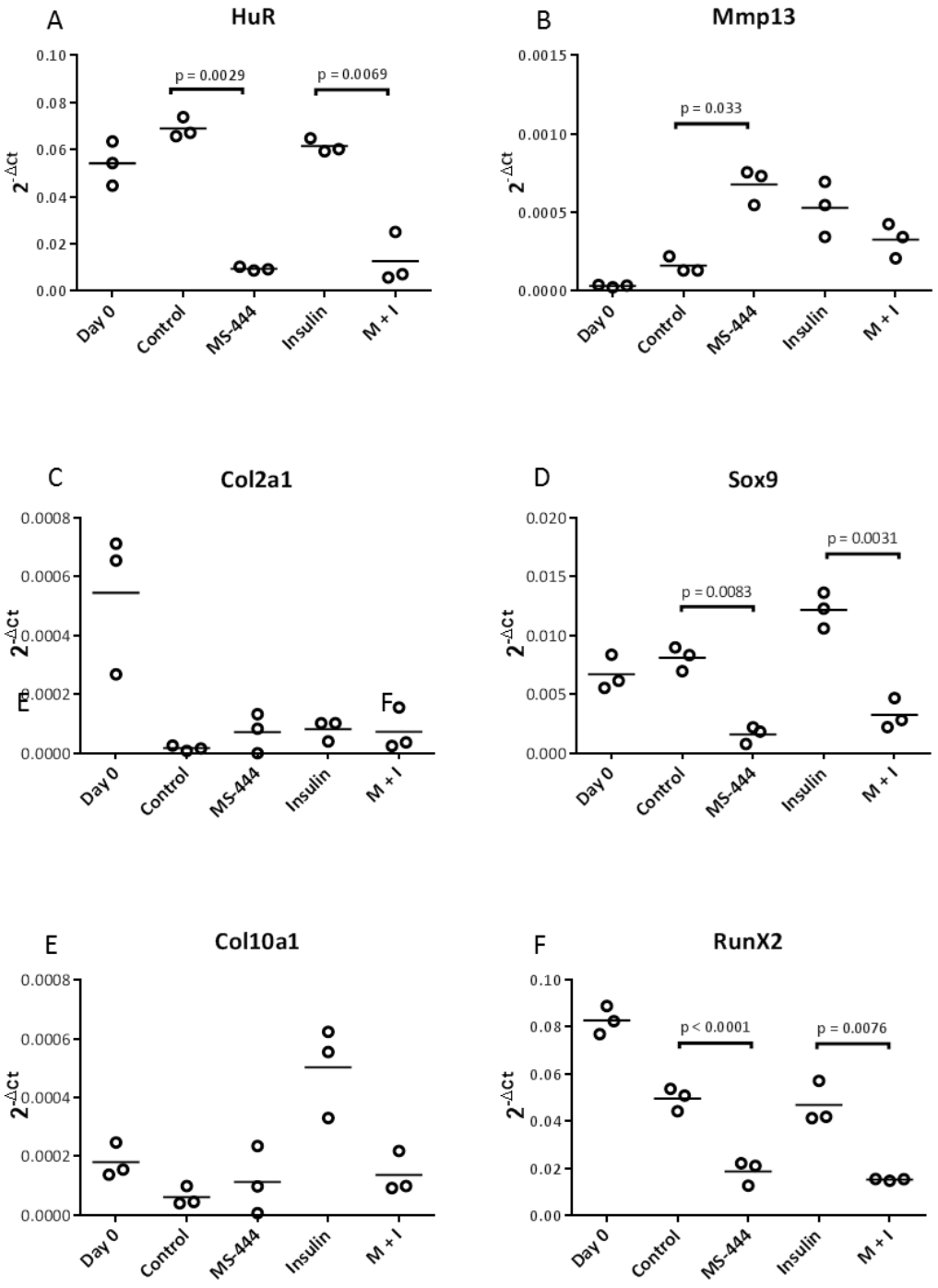

Figure 5.4. qRT-PCR analysis of mRNA expression levels of marker genes in ATDC5 cells treated with and without constant exposure to 50μM of the HuR inhibitor MS-444, in chondrogenically differentiated (insulin) and undifferentiated cells. ATDC5 cells were seeded at 6400 cells/cm^2. After 24 hours cells were switched to chondrogenic differentiation media for 7 days supplemented with 50μM MS-444 or equivalent volume of DMSO carrier as control. Data was analysed by two-way ANOVA with Tukey post hoc testing. p values for statistically significant differences between conditions are shown. Horizontal lines represent the mean value of each

data set. Each data point represents the mean of an independent experimental replicate. (M + I = 50µM MS-444 and Insulin) (n=3)

5.2.4 Knockdown of HuR in primary murine chondrocytes via tamoxifen

While chondrogenic cell lines are useful tools in the study of the molecular mechanisms involved in chondrogenesis, primary chondrocyte cultures remain one of the most powerful tools for the investigation of molecular events that are associated with chondrocyte differentiation. A process of dedifferentiation occurs to primary chondrocytes grown in monolayer, marked by a loss of collagen type II and aggrecan, and an induction of collagen type I expression (Kartsogiannis and Ng 2004). Dedifferentiation can be influenced by seeding density and is accelerated by growth in medium supplemented with serum and by passage number. We therefore only used primary chondrocytes up to and including passage three in experiments. The primary culture of immature murine articular chondrocytes (iMACs) and primary costal chondrocytes have previously been described (Lefebvre *et al.* 1994).

In order to observe the effect of HuR knockdown in murine primary chondrocytes, HuR$^{fl/fl}$AcanA1-CreER^{T2}*luc*$^{+}$ mice were crossed and resulting progeny used for chondrocyte isolation. Per biological replicate, one litter of neonates between 5 and 6 days old were sacrificed and both articular and costal chondrocytes were isolated via collagenase digestion as previously described in *Methods* section 2.6. Articular chondrocytes were seeded at a density of 8 x 10^3 cells/cm^2, while costal chondrocytes were seeded at 25 x 10^3 cells/cm^2 and allowed to proliferate for 7 days or until confluent prior to experiment. Both articular and costal chondrocytes exhibit a typical chondrocyte morphology, with a polygonal shape (Figure 5.5 A&B, respectively). There were, however, difficulties in the isolation of pure murine costal chondrocytes, in that removal of the muscle and other tissue from the rib cartilage was difficult and subsequently resulted in other cell populations being present in small amounts in culture (Figure 5.5B). The isolation of pure articular chondrocytes proved less difficult and resulted in cleaner populations of

chondrocytes. As a result iMACs were selected for future primary chondrocyte experiments.

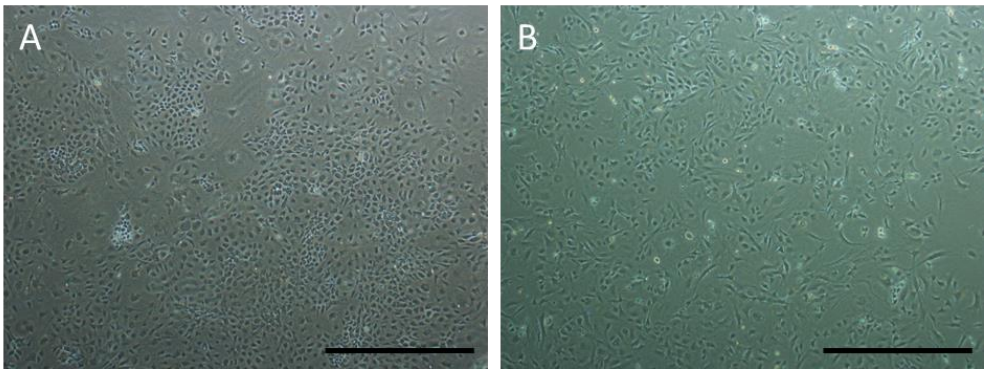

Figure 5.5. Primary articular chondrocytes 7 days after isolation from HuR$^{fl/fl}$ AcanA1-CreER^{T2}luc^{+} pups. Articular chondrocytes (A) and costal chondrocytes (B) were isolated from 5-6 day old HuR$^{fl/fl}$ AcanA1-CreER^{T2}*luc*$^{+}$ pups and proliferated for 7 days prior to experiment. Images were taken on a Nikon microscope 7 days after seeding onto 10cm cell culture dishes. (Scale bar = 100µm)

After murine articular chondrocyte isolation cells were left to reach confluence for 7 days, at which time cells were seeded into 6 well plates. 2 days after seeding, cells were treated for the first 24 hours with 100nM of 4-Hydroxytamoxifen, the active metabolite of tamoxifen which binds to the estrogen receptor of the CreER^{T2}*luc* complex to enable recombination of HuR flox sites. RNA was extracted from cells at 0, 24, 48 and 72 hours.

Compared to control conditions, 4-Hydroxytamoxifen treatment significantly reduces HuR mRNA expression levels by 48 hours suggesting recombination of the HuR floxed alleles has occurred, however the trend of HuR expression in tamoxifen treated cells still seems to increase over time in parallel to control cells (Figure 5.6A). Upon tamoxifen-mediated HuR knockdown in primary articular chondrocytes MMP13 expression levels reduce over the time course to

a significant difference by 72 hours (Figure 5.6B). This is opposite to what we see in MS-444-mediated HuR knock-down in ATDC5 cells were MMP13 levels increase upon tamoxifen treatment, but this may be due to mechanistic differences between cell lines and primary cells. There is no significant differences in the expression levels of both Col2a1 and Sox9 upon HuR knock-down (Figure 5.6 C&D, respectively). Expression levels of Acan are reduced by 48 hours though not significantly and return to control levels by 72 hours (Figure 5.6E), while Col10a1 expression is significantly increased 72hours after tamoxifen treatment (Figure 5.6F). Runx2 mRNA levels seem to be the most affected by tamoxifen-mediated HuR knock-down, with a significant reduction at 48 and 72 hours after tamoxifen treatment (Figure 5.6G). This is in keeping with a previous increase in Runx2 expression upon MS-444-mediated HuR knock-down in ATDC5 cells.

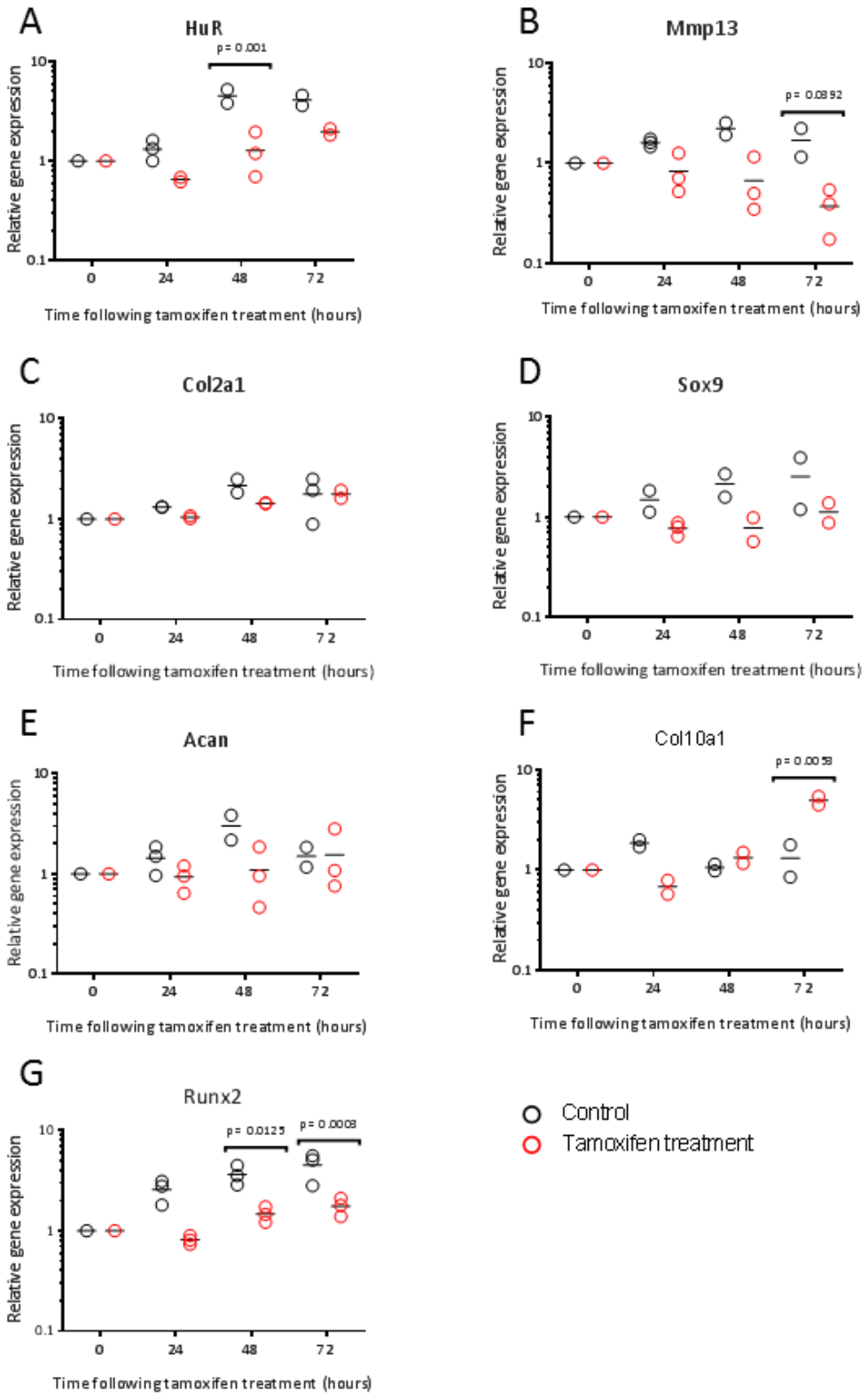
A
HuR
p = 0.001
B
Mmp13
p = 0.0892
C
Col2a1
D
Sox9
E
Acan
F
Col10a1
p = 0.0058
G
Runx2
p = 0.0125
p = 0.0008
Relative gene expression
10
1
0.1
0
24
48
72
Time following tamoxifen treatment (hours)
Control
Tamoxifen treatment

Figure 5.6. qRT-PCR analysis of mRNA expression levels of marker genes in HuR$^{fl/fl}$ AcanA1-CreER^{T2}luc^{+} primary articular chondrocytes treated with tamoxifen for the first 24 hours. After isolation of primary articular chondrocytes, cells were plated at 25 x 10^3 cells/cm^2 and treated with 100nM tamoxifen for the first 24 hours. RNA extraction was performed at 24, 28 and 72 hours following treatment. Absolute values are normalised to 0 hour. Data was analysed by two-way ANOVA with Tukey post hoc testing and p values for statistical significance between conditions are provided. Horizontal lines represent the mean value of each data set. Each data point represents the mean of an independent experimental replicate. (n=3)

5.2.5 Determining the optimum MOI for adenoviral infection

We next decided to utilise adenoviral infection of Cre adenovirus into isolated HuR$^{fl/fl}$ AcanA1-CreER^{T2}*luc*$^{-}$ articular chondrocytes for HuR knock-down. In order to minimise the amount of adenovirus used to reduce cell stress whilst still getting optimum infectivity, it is necessary to determine the optimum multiplicity of infection (MOI) in each cell type. MOI is the ratio between the number of virus particles in an infection and the number of host cells. In order to determine the optimum MOI in murine primary articular chondrocytes we used an adenovirus that expresses enhanced green fluorescent protein (eGFP) under the control of the ubiquitous cytomegalovirus (CMV) promoter. Since GFP is easily visualised under florescence microscopy, the eGFP adenovirus can be used to determine the transduction efficiency and to optimise the MOI in a specific cell type. After seeding onto 12-well culture plates, articular chondrocytes were treated for 24 hours with eGFP adenovirus at MOIs of 100, 125, 150, 175 and 200. After a further 24 hours cells were visualised under a microscope. eGFP expressed well in the cells under luminescent microscopy at MOI 200 (Figure 5.7B).

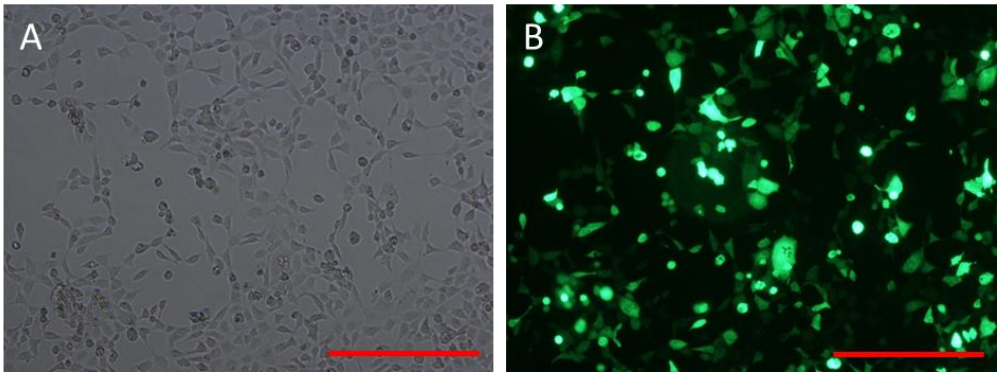

Figure 5.7. GFP fluorescence in HuR$^{fl/fl}$ AcanA1-CreER^{T2}luc^{-} primary articular chondrocytes at MOI of 200. Primary articular chondrocytes were seeded at 25 x 10^3 cells/cm^2 and treated with eGFP-adenovirus at MOI 200 after 24 hours. After a further 24 hours fluorescence was visualised using a Nikon Microscope. Scale bar = 100µm.

In order to quantify the number of cells infected, adenoviral-treated cultures were fixed in FACs medium and processed on a FACScan flow cytometer. Percentage uptake of eGFP into cells were as follows: MOI 100 - 73.7% (Figure 5.8B), MOI 125 - 79.9% (Figure 5.8C), MOI 150 - 82.4% (Figure 5.8D), MOI 175 - 77.5% (Figure 5.8E) and MOI 200 - 85% (Figure 5.8F). An optimum MOI of 200 was determined to gain 85% adenoviral uptake and was therefore used for subsequent Cre adenoviral transduction.

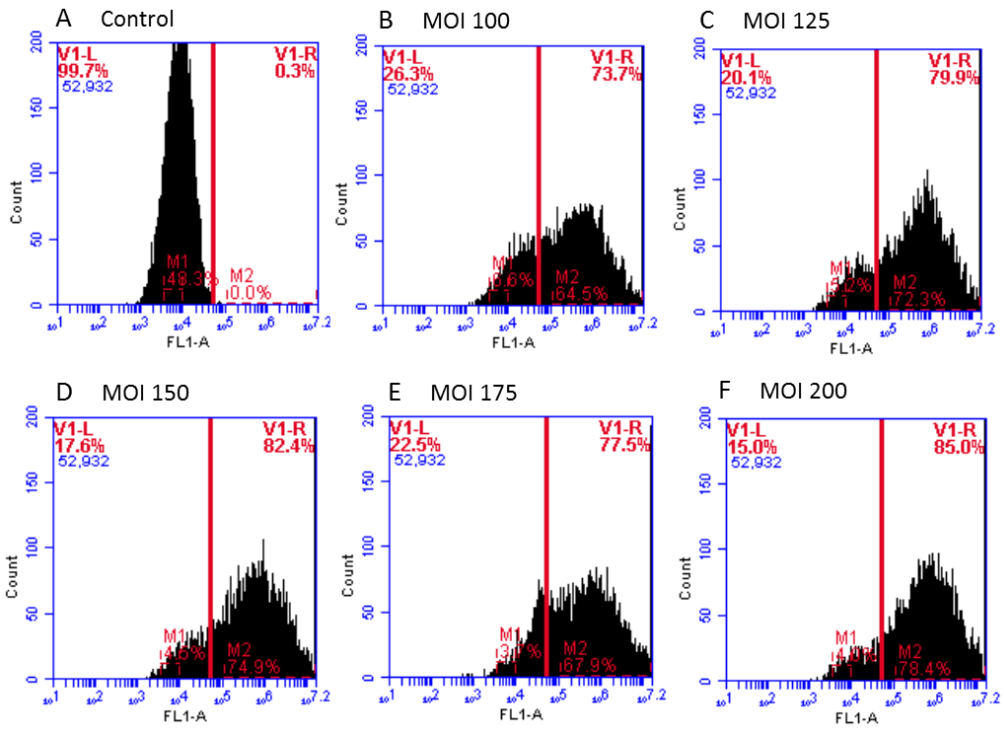

Figure 5.8. FACS analysis of eGFP expressing primary articular chondrocytes. Primary articular chondrocytes isolated from 4-day old HuR$^{fl/fl}$ AcanA1-CreER^{T2}*luc*$^{-}$ mice were incubated with eGFP adenovirus over a range of MOIs (100, 125, 150, 175 and 200) for 24 hours. After cell fixation cells were analysed on a FACScan flow cytometer machine and GFP expression quantified compared to control conditions. An optimum MOI of 200 was selected.

5.2.6 Knockdown of HuR in primary murine chondrocytes via Cre adenovirus

Having identified that high infection rates could be achieved in primary chondrocytes using the eGFP adenovirus we next used the same system to knockdown HuR in these cells. Cre recombinase was delivered to HuR$^{fl/fl}$ AcanA1-CreER^{T2}*luc*$^{-}$ murine articular chondrocytes via infection with a Cre-expressing adenovirus. Cells were seeded at a density of 25 x 10^3 cells/cm^2 and treated with a 200 MOI of Cre adenovirus for 24 hours, after which time adenovirus media was changed for normal proliferation media for a further 48 hours. RNA was collected at time points 0, 24, 48 and 72 hours (were 0 hours was immediately before adenoviral infection) in TRIzol® and qRT-PCR was used

to determine changes in gene expression for makers of chondrogenesis. Following adenoviral treatment of HuR$^{fl/fl}$ AcanA1-CreER^{T2}*luc*$^{-}$ primary chondrocytes, HuR expression levels were reduced over the 72-hour time course when compared to a control eGFP treatment of cells (Figure 5.9A). This was encouraging and suggested the knockdown of HuR via adenoviral transduction was successful. Other markers of chondrogenesis were not as clearly affected by Cre adenoviral treatment when compared to control conditions (Figure 5.9 B-F). There was, however, only one biological replicate performed for this experiment and to confirm the results and gain a better understanding of how HuR knockdown affects the molecular mechanisms associated with chondrogenesis in primary chondrocytes, more repetitions are necessary. For this data to be robust, a minimum of three biological repeats per experimental time point are needed. The use of biological replicates will diminish the amount of false positives that arise from the sampling process. As with the data presented here, technical replicates are also needed.

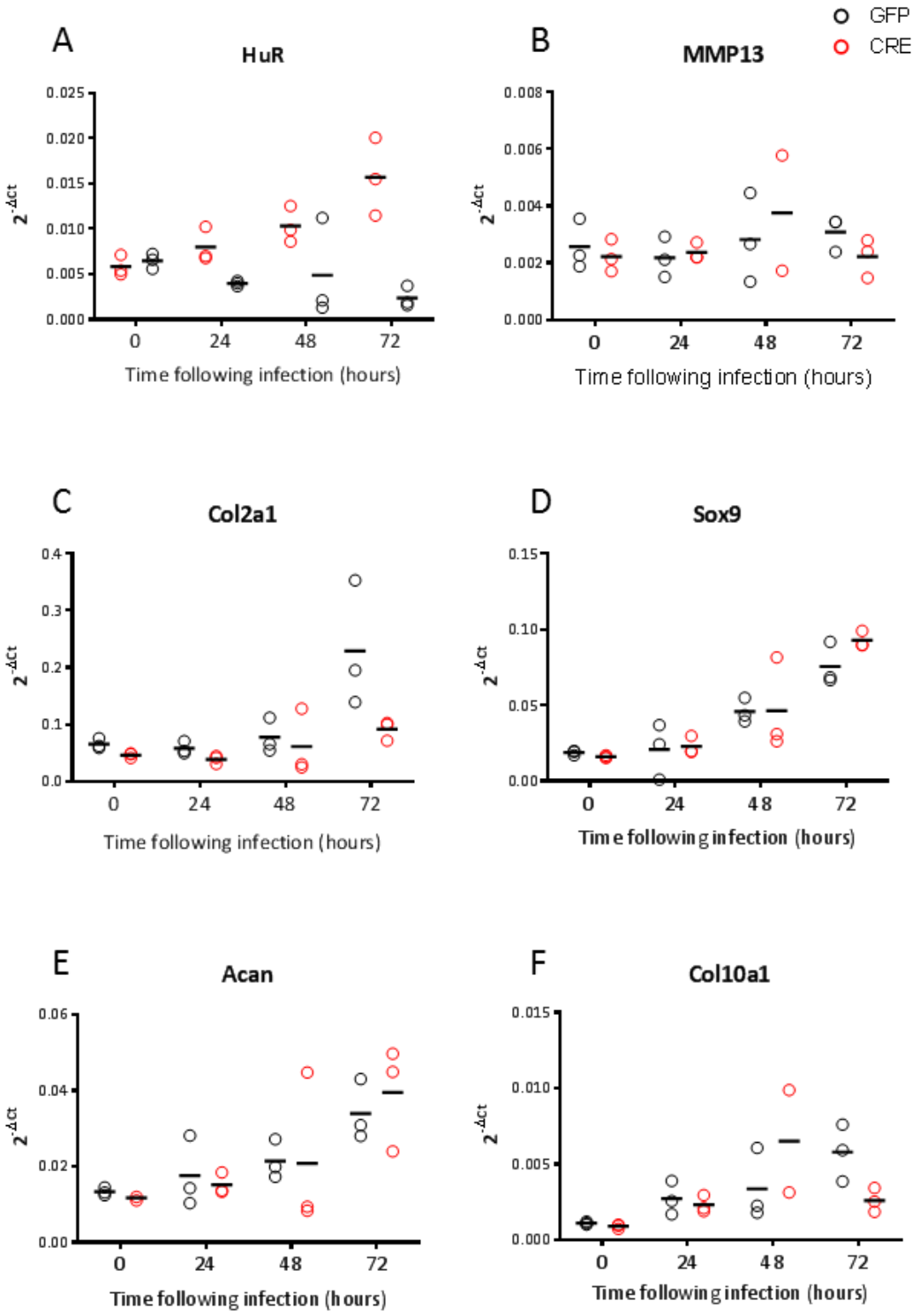

Figure 5.9. qRT-PCR analysis of marker genes in Cre and eGFP adenoviral treated primary murine articular chondrocytes. Articular chondrocytes were transfected with Cre adenovirus at an MOI of 200 for 24 hours followed by 48 hours in proliferation media. RNA was extracted at 0, 24, 48 and 72 hours after adenoviral infection for qRT-PCR analysis. Adenovirus eGFP was used as a control. (n=1. Technical replicates are shown).

5.3 Discussion

The objectives of this chapter were to use various methods of HuR knockdown in both the ATDC5 cell line and in primary murine articular chondrocytes to examine the effect of HuR knockdown during chondrogenesis and endochondral ossification. Few studies have highlighted the roles of HuR in regulating markers of chondrogenesis. Katsanou *et al* performed a microarray study on HuR knockout and WT mouse embryonic fibroblasts (MEFs) to determine HuR target mRNAs that are involved in embryonic development (Katsanou *et al.* 2009). While many genes involved in various biological processes were identified to be up (240) or down (155) regulated in HuR knockout MEFs, the aggrecanase ADAMTS5 was also found to be significantly upregulated in these cells. Other markers of chondrogenesis were not identified, however differences in cell types mean they may not be detected in any other cell types except those that they are specific to, for example aggrecan is a cartilage-specific protein and would not be present in MEF's.

Another study by Techasintana *et al* utilised RNA immunoprecipitation sequencing (RIP-Seq) and RNA-sequencing (RNA-Seq) to investigate the direct and indirect targets of HuR in HuR knockout $CD4^+$ T immune cells during activation and Th2 differentiation (Techasintana *et al.* 2015). Analysis revealed new HuR-associated targets that are crucial during T cell activation and immune mechanisms. To date, no study has investigated in detail target mRNAs of HuR during chondrogenesis and endochondral ossification.

We therefore decided to examine the molecular effects of HuR inhibition or knockdown in chondrogenic cultures to try to uncover potential mechanisms of action. ATDC5 cells are a well-established, *in vitro* model of chondrogenesis, so were used to explore HuRs role during chondrogenic differentiation. Critical genes involved in the regulation of mesenchymal progenitor cells to hypertrophic chondrocytes includes Sox9, Collagen type II and Aggrecan during chondrogenesis and Collagen type X, MMP13 and Runx2 during endochondral ossification (Li and Dong 2016). Based on this knowledge, this chapter examined

changes in the mRNA expression levels of various markers of chondrocyte differentiation when HuR is knocked down *in vitro.*

5.3.1 ATDC5 cells

qRT-PCR analysis of ATDC5 cells treated for 24 hours with various concentrations of the HuR inhibitor MS-444 did not provide any significant inhibition of HuR at any of the examined concentrations. However, while HuR levels did not detectably decrease in this experiment, MMP13 levels significantly increased. There was also a significant increase in Col10a1, another marker of chondrocyte differentiation, at 50µM MS-444 treatment. This is consistent with the proposed mechanism of action of MS-444, where MS-444 is reported to inhibit HuR homodimerisation and HuRs cytoplasmic translocation thereby preventing its function as a stabiliser of target mRNAs (Meisner *et al.,* 2007). This could suggest that HuR might play a role in maintaining chondrocytes in a proliferative state, while down-regulation of HuR allows chondrogenic differentiation. This theory parallels the previous working hypothesis in *Chapter 3,* that HuR might act upon the Ihh/PTHrP negative feedback loop and its deletion may lead to early chondrocyte hypertrophy and altered endochondral ossification, this is however speculative and more work will need to be complete to validate this theory. Due to the significant gene expression changes of all but Runx2 when treated with 50µM MS-444 treatment of ATDC5 cells, we decided to continue with this concentration for further treatment experiments.

ATDC5 cells were treated with MS-444 for the first 48 hours and subsequently differentiated down the chondrogenic lineage (Figure 5.3). Unexpectedly, Sox9 expression increased well into chondrocyte hypertrophy (day 10+) (Figure 5.3D). Runx2 expression was also significantly reduced by 14 days after MS-444 treatment compared to control conditions. After coming to the conclusion that continuous treatment of MS-444 was necessary for inhibition of HuR mRNA in ATDC5 cells, a 7-day time course of continuous treatment with MS-444 was performed and showed that MS-444 significantly down regulates HuR mRNA levels in both differentiated and proliferating ATDC5 cells. Interestingly, while MMP13 mRNA levels were significantly elevated after MS-444 treatment in

undifferentiated cells, upon induction of chondrogenesis MMP13 levels did not significantly change from control conditions. MS-444 treatment also resulted in a significant decrease in the mRNA expression levels of both Col10a1 and Runx2 during differentiation when compared with non-treated cells (Figure 5.4 E+F). This is contradictory to the mechanism by which MS-444 has been reported to inhibit HuRs ability to stabilise its target mRNAs, a inhibition of HuR should therefore result in an increase in its target mRNA levels. However, previous work has suggested that HuR may act through an indirect intermediate factor as HuR acts as a negative regulator of MMP13 but does not affect its rate of decay (McDermott et al., 2016). These observations are interesting as Runx2 is a marker of chondrocyte hypertrophy and has previously been shown to regulate MMP13 expression (Wang *et al.* 2004). Its ectopic expression has also been shown to result in the expression of hypertrophic markers including Col10a1 and MMP13 (Hess *et al.* 2001). Interestingly, in *Chapter 4* of this thesis there was no significant difference observed between chondrocyte-specific HuR knockout mice that had undergone DMM surgery and the control group that had undergone SHAM surgery. Runx2 expression levels are increased in human OA cartilage and the deletion of Runx2 in articular chondrocytes has been shown to decelerate the progression of DMM-induced osteoarthritis in adult mice (Wang *et al.* 2004, Liao *et al.* 2017). If MS-444 treatment does inhibit HuR that results in a direct or indirect reduction in Runx2 mRNA levels *in vitro*, it may be possible that a similar situation occurs *in vivo* in which HuR knockout in chondrocytes may result in a decrease in the progression of OA caused by or resulting in a direct or indirect reduction of the mRNA levels of Runx2. It is important to note, however, that these are not direct comparisons. The work in this chapter focuses on immortalised cell lines and primary chondrocytes isolated from neonates, which will still have a more developmental phenotype than those in the mice used for DMM who were 10-weeks old at the point of surgery. This theory also conflicts with findings of an increase in MMP13 mRNA levels upon knockdown of HuR in previous reports (McDermott *et al.* 2016), as increased MMP13 levels have been shown to have a direct impact on the progressive worsening of OA (Wang *et al.* 2013). Again, this comparison is between an immortalised cell line and primary chondrocytes undergoing

osteoarthritis chondrocyte responses and so could explain inconsistencies between the two sets of data. It has been reported that Sox9 can repress chondrocyte hypertrophy by blocking the activation of Runx2 (Zhou *et al.* 2006). Sox9 is a pivotal regulatory factor in chondrogenesis and is one of the earliest markers of chondrocyte differentiation in condensing mesenchyme (Lefebvre and Dvir-Ginzberg 2017). While the upregulation of Sox9 can promote chondrogenic differentiation in bone marrow-derived mesenchymal stem cells, it can also slow the process of chondrocyte hypertrophy; resulting in a reduction of Sox9 expression in hypertrophic chondrocytes (Akiyama *et al.* 2004, Yang *et al.* 2011).

These possible explanations of the changes in mRNA expression of markers of chondrogenesis also rely on MS-444 specifically inhibiting HuR. It is worth considering that MS-444 was initially discovered as an inhibitor of myosin light chain kinase, a regulatory enzyme in smooth muscle contraction (Nakanishi *et al*., 1995). While all MS-444 experiments in this project were carried out on the chondrogenic cell line ATDC5, it can still be possible that in the complex environment of the cell MS-444 could also affect other targets besides HuR. Further experiments would need to address this issue and look for off target effects of MS-444 treatment in cells. One such experiment that would address whether MS-444 is specific in its suggested mode of action at inhibiting HuR would be to treat cells that overexpress HuR with various concentrations of MS-444 and for varying amounts of time. Alternatively, Hoechst staining can be used to examine nucleus morphology. HuR plays a pivotal role in tumorigenesis, for example over-expression of HuR provides cancer cells with anti-apoptotic features (Abdelmohsen *et al.,* 2010), therefore cancer cells can be utilised and treated with MS-444 to examine effects on processes influenced by HuR expression including apoptosis. Previous studies have also examined whether MS-444-mediated COX2 mRNA dysregulation occurred through disruption of HuR/COX2 mRNA association via ribonucleoprotein immunoprecipitation (RNP-IP) (Blanco *et al.,* 2016). RNP-IP involves the immunoprecipitation of whole miR-silencing complexes that is capable of directly analysing miRNA and RNA binding protein function in a specific cellular context (Hassan *et al.,* 2010). This

level of analysis would be a useful next step in providing validation and insights into the specificity of MS-444-mediated HuR inhibition in ATDC5 cells.

5.3.2 Primary chondrocytes

While chondrocyte cell lines are extremely useful in the study of chondrocyte differentiation, they cannot be entirely substituted for primary chondrocyte cultures. Primary chondrocyte cultures have been developed to identify mechanisms involved in chondrocyte hypertrophic differentiation and cartilage matrix mineralisation and have become increasingly important since the generation of transgenic and floxed mouse models, providing a means to study gain- and loss-of-function approaches during chondrogenesis and endochondral ossification (Chen *et al.* 2007).

While we attempted to generate only pups that contained the Cre recombinase allele for experimental conditions, we were unable to distinguish between breeding mice that were homozygous or heterozygous for the Cre transgene via genotyping. It is therefore a limitation of this study that some pups used for the tamoxifen primary chondrocyte experimental conditions may not be positive for Cre, therefore generating a mixed population of Cre^+ and Cre^- cells between biological replicates.

In these experiments, HuR was knocked down in isolated primary murine chondrocytes using two approaches: either through activation of the endogenous $CreER^{T2}$*luc* expressed via the Acan promoter (tamoxifen treatment) or via delivery of active Cre via an adenovirus. Treatment of primary chondrocytes with tamoxifen caused HuR expression to decrease significantly by 48 hours (Figure 5.6A), while chondrocytes treated with Cre adenovirus also resulted in a knockdown of HuR but in a more stable and continuous manner than with tamoxifen (Figure 5.9A). This result was encouraging, however unfortunately only one biological replicate of Cre adenoviral treatment in primary articular chondrocytes could be performed due to available mice and time limitations. Further biological replicates are clearly necessary to validate and confirm this observation; as such no conclusions can be drawn from Cre adenoviral treated cell experiments. Additionally, in Figure 5.8, FACS analysis

showed the optimum MOI of eGFP in primary articular cartilage to be 200. This, however, can be lowered for subsequent experiments as the increase in the percent of cells expressing eGFP was not exponential. Virus toxicity is a concern with adenoviral vector delivery, therefore if a lower MOI gives a similar expression of viral expression it is worth considering the cost and benefit of a lower MOI to the cells. Future plans include increasing the n number of these experiments in order to assess the effect of HuR knock-down via Cre adenovirus on markers of chondrocytes.

Interestingly in the tamoxifen treated cells, we observe the same trend of a decrease in MMP13 and Runx2 expression levels as previously observed in MS-444 treated ATDC5 cells. Sox9 and Runx2 can interact in cells, with Sox9 inhibiting the activation of Runx2 by inducing a dose-dependent degradation of Runx2 via the promotion of Bapx1 (bagpipe homeobox protein homolog 1) and in turn slowing chondrocyte hypertrophy (Cheng and Genever 2010). In response, Runx2 can also inhibit Sox9 transactivity. MMP13 is also a downstream target of Runx2; with an increase in MMP13 expression as a result of an increase in Runx2 expression during osteoarthritis. MMP13 expression is also diminished in Runx2-deficient mice (Inada *et al.* 1999, Wang *et al.* 2004). This may potentially explain some of the results observed in *Chapter 3* in which HuR knockout during embryonic development lead to a delay in bone mineralisation. Runx2 is a transcription factor involved in the regulation of hypertrophic chondrocyte differentiation and is essential in bone formation (Kim *et al.* 1999). Skeletal analysis of heterozygous Runx2-deficient murine embryos revealed an absence of mineralised bone tissue resulting from a lack of endochondral ossification (Otto *et al.* 1997). If a downregulation of HuR *in vitro* results in a reduction of Runx2, also resulting in a reduction of MMP13, then this potentially may be occurring *in vivo* were ablation of HuR in chondrocyte- and skeletal- specific manners may result in a reduction of Runx2, which in turn may lead to a delay in chondrocyte hypertrophy and ultimately a delay in bone formation. This may also explain a lack of phenotypic differences between chondrocyte-specific $HuR^{fl/fl}$AcanA1-$CreER^{T2+}$ mice that have undergone DMM surgery and their $HuR^{fl/fl}$AcanA1-$CreER^{T2-}$ counterparts, as Runx2 is a critical gene in the progression of osteoarthritis. Bapx1 is also

regulated by Ihh, which we hypothesised in *Chapter 3* may be stabilised, along with PTHrP, by HuR in normal articular chondrocytes. As HuR acts to stabilise its target mRNAs in the cytoplasm, it would be expected that a knockdown of HuR would result in an increase in the turnover of affected mRNAs in chondrocytes. As such, we speculate that a downregulation of Runx2 is probably due to HuR acting on an intermediate factor which regulates Runx2 expression.

Transcriptome-wide studies, including microarray analysis and RNAseq examining the control of gene expression in both chondrocytes from healthy vs osteoarthritic cartilage and in chondrocytes that have undergone changes in their physiological conditions, have led to the identification of the processes and mechanisms involved in the control of chondrocyte gene expression (Aigner *et al.* 2004; Sato *et al.* 2006; Peffers *et al.* 2014). Further transcriptomic analysis would be necessary in order to strengthen the findings presented in this thesis. Currently, there have been no transcriptome-wide studies investigating the targets of HuR during chondrogenesis, endochondral ossification and osteoarthritis progression. Microarray and RNA-seq analysis performed on various other cell types during HuR knockdown have not identified any differentially expressed markers of chondrocytes. In particular we would like to carry out RNAseq on the RNA from Cre adenoviral treated primary articular chondrocytes. RNAseq sequences the entire transcriptome in a high-throughput and quantitative manner to provide precise measurements of the levels of transcripts, which in turn would identify genes targeted by HuR, and potential mechanisms of action.

A limitation of the *in vitro* studies in this project is the lack of validation that *in vitro* experiments have succeeded in reducing HuR protein levels, or cytoplasmic protein levels when using MS-444. This is something that needs to be further characterised. However, previous work in our laboratory carried out by Dr Simon Tew has provided evidence that a reduction in the mRNA of HuR also leads to a quick reduction in the protein levels of HuR in human mesenchymal stem cells (Figure 5.10).

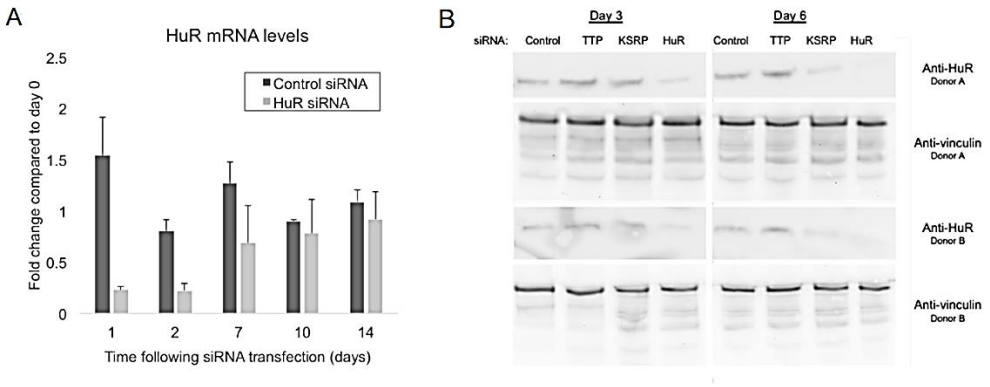

Figure 5.10. Both HuR mRNA and protein levels are knocked down after siRNA treatment in human mesenchymal stem cells. Human mesenchymal stem cells were treated with siRNAs targeting the expression of the RNA binding proteins TTP, KSRP and HuR. HuR siRNA was the only RNA binding protein whos mRNA (A) and protein (B) expression levels were reduced in a strong and rapid manner (A n=3 experimental replicates each in triplicate, B n=2 biological replicates). (Unpublished data).

When transfecting these cells with siRNAs targeting the expression of the RNA binding proteins TTP, KSRP and HuR, only the latter was able to consistently knockdown HuR protein levels after either 3 or 6 days (Figure 5.10B). The HuR siRNA significantly reduced HuR mRNA levels within 24 hours and this reduced level was maintained for several days (Figure 5.10A). This fast and efficient knock-down is indicative of a short-lived protein. In support of this, other studies have reported strong and rapid knock-down of HuR during *in vitro* via siRNA silencing experiments (Al-Ahmadi *et al*., 2013; Lebedeva *et al.,* 2011). Whilst these results suggest that HuR knock-down would also be efficient in the cell culture systems utilised in this project, it is worth noting that these experiments were performed on different cell types and in different species to those used in this project and also the difference in technologies between siRNA silencing, adenoviral gene delivery and tamoxifen-mediated recombination. In its current state, this study needs validation of HuR protein knock-down *in vitro* in order to validate the findings presented.

6 General Discussion

The regulation of gene expression and protein function occurs at multiple levels via multiple signalling pathways (Jonason *et al.* 2009). Post-transcriptional modification regulates mRNA translation and stability, a process controlled by miRNAs and RNA binding proteins interacting with the 3' AU-rich UTR of target mRNAs (Tew and Clegg 2010). The mechanistic details of the function of key regulators of post-transcriptional regulation, including RNA binding proteins and miRNAs, are still poorly understood and limited studies have examined post-transcriptional regulation in relation to cartilage biology.

Our group has been interested in the post-transcriptional control of chondrocyte genes and have recently reported that a number of mRNAs exhibit altered decay rates in chondrocytes from osteoarthritis patients compared to those from healthy individuals (Tew *et al.* 2014). It has also been reported that siRNA-mediated knockdown of RNA binding proteins also led to alterations in mRNA decay rates and changes in chondrocyte gene expression levels (McDermott *et al.* 2016). The distribution of HuR was also examined in murine embryos, were it was observed that levels of HuR were reduced in hypertrophic chondrocytes and in those adjacent to the perichondrium, regions implicated in long bone growth and mineralisation. The condensing mesenchyme of the future digits of developing E13.5 embryos also displayed a 'checkerboard' appearance of HuR distribution (McDermott *et al.* 2016).

HuR-null embryos exhibit embryonic lethality as a result of defects in the placenta (Katsanou *et al.* 2009). It was also reported that conditional knockout of HuR driven by Sox2-Cre overcomes this lethality but results in a developmental phenotype that includes a severe skeletal dysplasia. Long bones were shortened and showed minimal ossification zones in the scapulae, femurs and tibia. Mutant embryos also displayed syndactyly in both forelimbs and hindlimbs and fusion in the digits. Craniofacial ossification was also delayed in mutant embryos (Katsanou *et al.* 2009). Taken together, these studies suggested a role for HuR in the post-transcriptional regulation of skeletal development.

This project set out to investigate the role of HuR in the skeleton of developing and adult mice. Two HuR knockout mouse models were developed to gain

insights about the physiological role of the HuR protein during skeletal development. In *Chapter 3* cartilage-specific and skeletal-specific HuR knockout mice were generated for the first time, and used to demonstrate a role for HuR in endochondral ossification and limb patterning during embryonic development. After observing cartilage and bone development via whole-mount staining and μCT analysis, it was found that HuR knockout during embryonic development resulted in a phenotype that affects cartilage development in the limbs, ribs and craniofacial structures as a result of severely dysregulated chondrogenesis and a delay in mineralisation. Histological analysis also revealed that the morphology and organisation of chondrocytes was also altered and, taken together, this data suggests HuR plays an important role in skeletal development, particularly during endochondral ossification. There are limitations to any project, particularly those that include *in vivo* work.

One limitation to this study is the type of controls used to compare against experimental conditions. Many new mouse alleles are generated when a neomycin-resistance selection cassette (neo cassette) is included in the construction of a floxed allele for Cre-loxP conditional knockout experiments. Retention of the neo cassette often reduces gene expression, sometimes causing hypomorphic phenotypes or increasing the expression of the transgene (Dorà *et al*., 2016). HuR floxed mice were generated using a neo cassette in the generation of the floxed allele. In this project, $HuR^{fl/fl}$ Cre^{-} mice were used as controls. In hindsight, this is not a full control as does not take into account any effects, if any, caused by the floxed alleles. It has previously been found that some floxed alleles that retain the neo cassette are not equivalent to wild-type alleles. For example, Pax6 is an important developmental gene with important roles in the development of the eye. A previous study reported that homozygous $Pax6^{fl/fl}$ and heterozygous $Pax6^{fl/+}$ mice were viable, fertile and phenotypically indistinguishable from wild-type mice, however detailed investigation of the eye had not been carried out (Simpson *et al.,* 2009). A subsequent analysis reported that while homozygous $Pax6^{fl/fl}$ and heterozygous $Pax6^{fl/+}$ mice had no overt qualitative eye abnormalities, morphometric analysis identified $Pax6^{fl/fl}$ mice to have thicker corneas that are also smaller in diameter

(Dorà *et al.,* 2016). This study also revealed that eye phenotypes in $Pax6^{fl/-}$ compound heterozygotes had displayed more severe eye abnormalities than those in $Pa6^{+/-}$ heterozygous, suggesting that the $Pax6^{fl}$ allele is not equivalent to the wild-type $Pax6^{+}$ allele (Dorà *et al.,* 2016). In order to be draw conclusions on the negative effects of HuR knockout on skeletal development, controls such as $HuR^{WT}Cre^{+}$ would be needed to elucidate any phenotypic effects that might arise as a result of the floxed alleles.

Another potential problem with using the Cre/loxP system is the potential toxicity of Cre expression to cells. Several reports indicate that Cre recombinase might lead to toxic effects as a consequence of Cre targeting sites in genomic DNA that share limited homology with the loxP sequence, thereby inducing mis-recombination, DNA damage and an alteration in the normal proliferation rate (Forni *et al.,* 2006). Most strains in which Cre is expressed seem to develop normally and do not show any overt signs of Cre toxicity, however *in vitro* studies on cells lacking exogenous loxP sites have shown that Cre recombinase can cause decreased growth, chromosomal aberrations and cytopathic effects (Loonstra *et al*., 2001; Pfeifer *et al.,* 2001). It has been suggested that Cre toxicity results from long-term expression of high levels of the enzyme and therefore, in this study, additional controls of Aggrecan-$CreER^{T2}$ and Prx1-Cre mice with no other transgenic alterations (*ie.* no flox sites) should have been included as controls.

There were also many issues that arose during this project in relation to the use of mouse models. In particular, a Home Office project licence issue arose half way through this project which resulted in a legal requirement to cull all experimental mice and drastically reduce the numbers of our colonies. This occurred at a crucial time when $HuR^{fl/fl}$AcanA1-$CreER^{T2}luc^{+}$ mice had been staggered into an aging study. As a result a large part of the study, where tamoxifen treated $HuR^{fl/fl}$AcanA1-$CreER^{T2}luc^{+}$ and control mice were being aged to identify any long term effects of HuR knockout on the pathology of the knee joints, had to be cut short. As a result of the staggered breeding, mice were also not of the same age at the time of culling. Due to having to reduce the number of mice in the colonies we also lost valuable time when we were eventually able

to re-breed our mice as the process to increase our numbers took approximately 6 months. On top of this the embryonic development aspect of this project required many timed matings to be set up, with more than 60% of these resulting in no pregnancy or a dramatically reduced litter size. A consideration that is often overlooked when using *in vivo* models is the effect of human interaction on the mice. While many environmental conditions within our animal facility are tightly regulated, noise is not a factor that is controlled, yet has been shown to increase physiological distress in mice (Lauer *et al.,* 2009). During the total length of this project the animal unit has had two large construction sites within close proximity that has caused noticeable vibrations and sound pressures into the facility. It has also been shown that excessive noise by construction equipment leads to an in increase in still births and a reduction in litter sizes in mice, which may provide an explanation for the small litter sizes and the high number of unsuccessful pregnancies observed during this project (Rasmussen *et al.,* 2009; Reynolds *et al.,* 2010).

Previous studies have investigated the role of post-transcriptional regulation in osteoarthritis (Tew *et al.* 2014). RNA binding proteins play a crucial role in post-transcriptional regulation and our laboratory has recently identified gene regulation following knockdown of the RNA binding proteins HuR and TTP in human chondrocytes (McDermott *et al.* 2016). Genes regulated included those coding for the matrix degrading extracellular proteinases MMP13 and ADAMTS5. It was therefore decided to explore the role of HuR during osteoarthritis disease progression. Data from *Chapter 4*, in which osteoarthritis was induced via DMM surgery in $HuR^{fl/fl}$AcanA1-$CreER^{T2}$ mice generated in *Chapter 3*, suggested there is no statistically significant change between Cre^{+} and Cre^{-} mice but there was an increased mean osteoarthritis score with increased variability. It is worth noting that the surgical work carried out in this project was a pilot study with the aim of carrying out a fully powered study at a later date. A biologically relevant response to DMM in knockout mice vs. controls would be an increase in the average score of 1. Based on the preliminary findings in this project (SD = 0.81) and assuming a power of 0.8 and a type I error of 0.05 then 11 animals would be needed for each sample group.

The work presented here has provided the basis for a larger study which is now currently being carried out in our lab with a larger sample size.

In order to investigate the molecular mechanisms underpinning the defects in skeletal development that were found in the limb and cartilage specific HuR knockout embryos, *in vitro* assays utilising both the murine chondrogenic cell line ATDC5 and primary murine chondrocytes were developed in *Chapter 5*. This *in vitro* data suggests that HuR expression might be required for the appropriate regulation of a number of known chondrocyte marker genes including the master transcription factor Sox9, Runx2 and Mmp13, of which the latter two are known to be critically involved in the regulation of chondrocyte hypertrophy and endochondral ossification. This data is complemented by the severe skeletal dysplasia we see in HuR knockout embryos, were a delay in endochondral ossification and mineralisation is observed, alongside a disorganised structure to chondrocyte morphology. However, it is worth noting the limitations that exist with the *in vitro* work carried out in this project.

MS-444 is a small molecular weight inhibitor of HuR; however it was initially discovered as an inhibitor of myosin light chain kinase activity (Nakanishi *et al.,* 1995). This paper reported that 10µM of MS-444 was enough to inhibit the enzyme activity by 50% (IC_{50}) and worked by inhibiting Ca2+ and calmodulin-dependent activity of smooth muscle myosin light chain kinase (Nakanishi *et al.,* 1995). MS-444 was then reported as a small molecular weight inhibitor of HuR and was shown to interfere with HuR binding to its target mRNAs and influence cytoplasmic localisation of HuR (Meisner *et al.* 2007). Prior to this, MS-444 was described as an anticancer agent (Tatsuta *et al.,* 1997) and Meisner therefore proposed that the anti-tumorigenic, anti-angiogenic and the anti-inflammatory effects of MS-444 were due (in part) to its strong role as a HuR inhibitor (Miesner *et al.* 2007). It can therefore be a possibility that in the complex environment of the cell, MS-444 also affects other targets besides HuR. An important outstanding question is whether MS-444s effect on the regulation of known markers of chondrogenesis including Mmp13, Sox9 and RunX2 is directly due to the inhibition of HuR.

Another limitation, as previously discussed in chapter 5, is that we cannot be certain that all primary chondrocytes used for tamoxifen knockdown of HuR express Cre recombinase (Fig 5.6). Due to the nature of transgenics when utilising Cre recombinase, it is not possible to identify mice that are homozygous for Cre using standard genotyping techniques. The standard procedure to produce mice that are homozygous for Cre recombinase is to track the genotype of breeding for progenies that are all subsequently Cre positive. This is a long process and, for this study, was not attainable due to the majority of other experiments requiring mice heterozygous for Cre recombinase. In order to overcome this limitation in future work, transgenic mice would need to be lineage tracked and only mice resulting from confirmed Cre homozygotes be used for experiments requiring Cre recombinase in all cells.

By utilising transgenic technology, we have been able to develop novel chondrocyte- and skeletal- specific HuR knockout mice and use these for temporal and spatial *in vivo* examination of the roles HuR plays in both embryonic development and in adult mice during osteoarthritis. We have also utilised tissue culture techniques in order to assess the mechanisms on which HuR is acting at the molecular level. In this project, we have identified potential molecular mechanisms by which HuR affects chondrogenesis and skeletal development. It was, however, not in the scope of this study to identify all of the genes that HuR may regulate in chondrocytes and this still requires further investigation. In order to shed more light on the complex role of HuR in chondrogenesis, it would be useful to perform analysis such as RNAseq as this would identify changes in the transcriptome.

This work has provided strong evidence that HuR plays a vital role in the regulation of chondrogenesis and has opened the door for further investigation of HuR, particularly in the regulation of endochondral ossification and skeletal bone development. In particular, our group is currently working on CRISPR/Cas9 (Clustered Regularly Interspaced Short Palindromic Repeats/associated protein-9 nuclease) genomic editing of HuR *in vitro*. CRISPR/Cas9 is a simple yet highly efficient and versatile system and allows precise gene editing. By generating

HuR deleted chondrocytic cell lines the specific mechanisms HuR influences in chondrocytes can be determined using transcriptomic analysis. Further work into HuR's role in embryonic development and in the progression of osteoarthritis presented in Chapters 3 and 4, respectively, is also currently ongoing to improve the numbers generated from this project.

Polyadenylation, as previously described in Chapter 1, is the addition of the poly(A) tail to the 3' end of newly synthesised mRNA and is essential for gene expression (Millevoi and Vagner, 2010). Transcriptome-wide studies have reported that most genes contain multiple poly(A) signals and are subject to alternative polyadenylation, an important post-transcriptional process that has been implicated in a variety of developmental and disease processes (Elkon *et al.,* 2013; Shi, 2012; Tian *et al.,* 2005). For example, E2F transcription factors has been shown to contribute to global 3' UTR shortening during proliferation, which can activate oncogenes in mammalian cells thereby contributing to tumorigenesis (Elkon *et al.,* 2012; Mayr and Bartel, 2009). Interestingly HuR has been reported to influence alternative polyadenylation (Zhu *et al*., 2007; Al-Ahmadi *et al.,* 2009), specifically in Drosophila where HuR inhibits RNA processing at proximal polyadenylation sites resulting in extra-long 3'UTRs as a result of recruitment by paused polymerase II (Oktaba *et al.,* 2015). It would therefore be an interesting next step to examine how HuRs role in influencing alternative polyadenylation might affect chondrocyte gene expression, since the presence of ARE alternative forms allows differentiation regulation of mRNA decay.

Improving our understanding of cartilage biology is the basis on which treatments are developed for people suffering with degenerative joint disease. Such treatments would vastly improve their quality of life and lower the economic burden associated with age-related joint disease.

7 References

Abdelmohsen K., Lal, A., Kim, H., Gorospe, M. (2007) 'Posttranscriptional orchestration of an anti-apoptotic program by HuR', *Cell cycle*, 1;6(11),1288-92.

Abdelmohsen K, Pullmann R Jr, Lal A, Kim HH, Galban S, Yang X, Blethrow JD, Walker M, Shubert J, Gillespie DA, Furneaux H and Gorospe M (2007) 'Phosphorylation of HuR by Chk2 regulates SIRT1 expression', *Mol Cell,* 25(4), 543-57.

Abdelmohsen K and Gorospe M. (2010) 'Posttranscriptional regulation of cancer traits by HuR', RNA, 1, 214-229.

Aigner, T., A. Zien, A. Gehrsitz, P. Gebhard and L. McKenna. (2001) 'Anabolic and catabolic gene expression pattern analysis in normal versus osteoarthritic cartilage using complementary DNA–array technology.' *Arthritis & Rheumatism*, 44(12), 2777-2789.

Aigner, T., Saas, J., Zien, A., Zimmer, R., Gebhard, P. M. and Knorr, T. (2004) 'Analysis of differential gene expression in healthy and osteoarthritic cartilage and isolated chondrocytes by microarray analysis', *Cartilage and Osteoarthritis*, 100, 109-127.

Akaike, Y., Masuda, K., Kuwano, Y., Nishida, K., Kajita, K., Kurokawa, K., Satake, Y., Shoda, K., Imoto, I. and Rokutan, K. (2014) 'HuR regulates alternative splicing of the TRA2 gene in human colon cancer cells under oxidative stress', *Molecular and cellular biology*, 34(15), 2857-2873.

Akiyama, H., Chaboissier, M.-C. C., Martin, J. F., Schedl, A. and de Crombrugghe, B. (2002) 'The transcription factor Sox9 has essential roles in successive steps of the chondrocyte differentiation pathway and is required for expression of Sox5 and Sox6', *Genes and development*, 16(21), 2813-2828.

Akiyama, H., Lyons, J. P., Mori-Akiyama, Y., Yang, X., Zhang, R., Zhang, Z., Deng, J. M., Taketo, M. M., Nakamura, T., Behringer, R. R., McCrea, P. D. and de

Crombrugghe, B. (2004) 'Interactions between Sox9 and beta-catenin control chondrocyte differentiation', *Genes and development*, 18(9), 1072-1087.

Akkiraju, H. and Nohe, A. (2015) 'Role of Chondrocytes in Cartilage Formation, Progression of Osteoarthritis and Cartilage Regeneration', *Journal of developmental* biology, 3(4), 177-192.

Al-Ahmadi, W., Al-Ghamdi, M., Al-Haj, Al-Saif, M and Khabar, K (2009) 'Alternative polyadenylation variants of the RNA binding protein, HuR: abundance, role of AU-rich elements and auto-Regulation' Nucleic acids research, 37(11), 3612-3624.

Al-Ahmadi, W., Al-Ghamdj, M., Al-Souhibanj, N and Khabar, S (2013) 'miR-29a inhibition normalizes HuR over-expression and aberrant AU-rich mRNA stability in invasive cancer', *The Journal of Pathology*, 230(1)

Amano, K., Hata, K., Sugita, A., Takigawa, Y., Ono, K., Wakabayashi, M., Kogo, M., Nishimura, R., and Yoneda, T (2009) 'Sox9 family members negatively regulate maturation and calcification of chondrocytes through up-regulation of parathyroid hormone-related protein', *Mol. Biol. Cell* 20, 4541–4551

Ambesajir, A., Kaushik, A., Kaushik, J and Petros S (2012) 'RNA interference: A futuristic tool and its therapeutic applications' *Saudi journal of biological sciences,* 19, 395-403.

Amizuka, N., Warshawsky, H., Henderson, J. E., Goltzman, D. and Karaplis, A. C. (1994) 'Parathyroid hormone-related peptide-depleted mice show abnormal epiphyseal cartilage development and altered endochondral bone formation', *The Journal of cell biology*, 126(6), 1611-1623.

Archer CW and Francis-West P (2003) 'The chondrocyte', *Int. J. Biochem. Cell Bio*l, 35, 401–404.

arcOGEN, C. (2012) 'Identification of new susceptibility loci for osteoarthritis (arcOGEN): a genome-wide association study', *The Lancet*, 380(9844), 815-823.

Astakhova, A and Chistyakov (2018) 'Regulation of the ARE-binding proteins, TTP (tristetraprolin) and HuR (human antigen R), in inflammatory response in astrocytes' *Neurochemistry International,* 118, 82-90

Atsumi, T., Miwa, Y., Kimata, K. and Ikawa, Y. (1990) 'A chondrogenic cell line derived from a differentiating culture of AT805 teratocarcinoma cells', *Cell differentiation and development : the official journal of the International Society of Developmental Biologists*, 30(2), 109-116.

Badorf, M., Edenhofer, F., Dries, V. and genesis, K.-S. (2002) 'Efficient in vitro and in vivo excision of floxed sequences with a high-capacity adenoviral vector expressing CRE recombinase', *Genesis*, 33(3), 119-24.

Barreau, C., Paillard, L., Osborne, HB (2005) 'AU-rich elements and associated factors: are there unifying principles?', *Nucleic acids research*, 33:7138-7150.

Barve, R. A., Minnerly, J. C., Weiss, D. J., Meyer, D. M., Aguiar, D. J., Sullivan, P. M., Weinrich, S. L. and Head, R. D. (2007) 'Transcriptional profiling and pathway analysis of monosodium iodoacetate-induced experimental osteoarthritis in rats: relevance to human disease', *Osteoarthritis and cartilage*, 15(10), 1190-1198.

Beederman, M., Lamplot, J. D., Nan, G., Wang, J., Liu, X., Yin, L., Li, R., Shui, W., Zhang, H., Kim, S. H., Zhang, W., Zhang, J., Kong, Y., Denduluri, S., Rogers, M. R., Pratt, A., Haydon, R. C., Luu, H. H., Angeles, J., Shi, L. L. and He, T.-C. C. (2013) 'BMP signaling in mesenchymal stem cell differentiation and bone formation', *Journal of biomedical science and engineering*, 6(8A), 32-52.

Bhattacharyya, SN and Habermacher, R (2006) 'Relief of microRNA-mediated translational repression in human cells subjected to stress', Cell, 125(6), 1111-24

Bi, W., Deng, JM., Zhang, Z., Behringer, R (1999) 'Sox9 is required for cartilage formation', *Nature Genetics,* 22, 85-89

Birk D and Bruckner P (2005) 'Collagen suprastructures', *Collagen*, 185-205.

Blanco, FF., Preet, R., Aguado, A., Vishwakarma, V., Stevens, LE., Vyas, A., Padhye, S., Xu, L., Weir, SJ., Anant, S (2016) 'Impact of HuR inhibition by the small molecule MS-444 on colorectal cancer cell tumorigenesis', Oncotarget, 7, 74043.

Blalock, D., Miller, A., Tilley, M., Wang, J (2015) 'Joint instability and osteoarthritis. Clinical medicine insights', *Arthritis and musculoskeletal disorders*, 8, 15-23.

Bobick B and Kulyk W (2008) 'Regulation of cartilage formation and maturation by mitogen-activated protein kinase signaling', *Birth Defects Res C Embryo Today*, 84(2):131-54.

Böhm BB, Aigner T, Roy B, Brodie TA, Blobel CP, Burkhardt H (2005) 'Homeostatic effects of the metalloproteinase disintegrin ADAM15 in degenerative cartilage remodeling', *Arthritis Rheum*, 52(4):1100-9.

Botter, S. M., van Osch, G. J., Waarsing, J. H., van der Linden, J. C., Verhaar, J. A., Pols, H. A., van Leeuwen, J. P. and Weinans, H. (2008) 'Cartilage damage pattern in relation to subchondral plate thickness in a collagenase-induced model of osteoarthritis', *Osteoarthritis and cartilage*, 16(4), 506-514.

Bouabe, H and Okkenhaug, K (2013) 'Gene targeting in mice: a review', *Methods in molecular biology*, 1064, 315-336.

Brennan, CM, and Cmls, S-JA (2001) 'HuR and mRNA stability', *Cellular and Molecular Life Sciences CMLS,* 58(2), 266-277

Brew, K, and Nagase, H (2010) 'The tissue inhibitors of metalloproteinases (TIMPs): an ancient family with structural and functional diversity', *Biochimica et biophysica acta*, 1803(1), 55-71

Brooks, S. A., Connolly, J. E. and Rigby, W. F. C. (2004) 'The role of mRNA turnover in the regulation of tristetraprolin expression: evidence for an extracellular signal-regulated kinase-specific, AU-rich element-dependent, auto-regulatory pathway', *The Journal of Immunology*, 172(12), 7263-7271.

Buckwalter JA, Saltzman C, Brown T (2004) 'The impact of osteoarthritis: implications for research', *Clin Orthop Relat Res,* (427):S6-15.

Burleigh, A., Chanalaris, A, Gardiner, M., Driscoll, C., Boruc, O., Saklatvala, J and Vincent, T (2012) 'Joint immobilization prevents murine osteoarthritis and reveals the highly mechanosensitive nature of protease expression in vivo', *Arthritis & Rheumatism*, 64(7), 2278-2288.

Burrage, PS and Mix, KS., (2006) 'Matrix metalloproteinases: role in arthritis', *Front Bioscience*, 11(1), 529

Carapuço, M., Nóvoa, A., Bobola, N. and Mallo, M (2005) 'Hox genes specify vertebral types in the presomitic mesoderm', *Genes and development*, 19(18), 2116-2121.

Carballo, E. and Blackshear, P. J. (2001) 'Roles of tumor necrosis factor-alpha receptor subtypes in the pathogenesis of the tristetraprolin-deficiency syndrome', *Blood*, 98(8), 2389-2395.

Carballo, E., Lai, W and Blackshear, P (1998) 'Feedback inhibition of macrophage tumor necrosis factor-alpha production by tristetraprolin', *Science,* 281(5379), 1001-1005.

Caron, M. M., Emans, P. J., Sanen, K., Surtel, D. A., Cremers, A., Ophelders, D., van Rhijn, L. W. and Welting, T. J. (2016) 'The Role of Prostaglandins and COX-Enzymes in Chondrogenic Differentiation of ATDC5 Progenitor Cells', *PloS one*, 11(4), e0153162.

Cascio, L., Liu, K., Nakamura, H., Chu, G., Lim, N. H., Chanalaris, A., Saklatvala, J., Nagase, H. and Bou-Gharios, G. (2014) 'Generation of a mouse line harboring a Bi-transgene expressing luciferase and tamoxifen-activatable creER(T2) recombinase in cartilage', *Genesis*, 52(2), 110-119.

Cawston, T. E. and Young, D. A. (2010) 'Proteinases involved in matrix turnover during cartilage and bone breakdown', *Cell and tissue research*, 339(1), 221-235.

Chau, M., Forcinito, P., Andrade, A. C., Hegde, A., Ahn, S., Lui, J. C., Baron, J. and Nilsson, O. (2011) 'Organization of the Indian hedgehog--parathyroid hormone-related protein system in the postnatal growth plate', *Journal of molecular endocrinology*, 47(1), 99-107.

Cheah, K., Lau, E., Au, P and Tam, P (1991) 'Expression of the mouse alpha 1 (II) collagen gene is not restricted to cartilage during development' *Development*, 111(4), 945-53

Chen, H., Ghori-Javed, F., Rashid, H., Adhami, M., Serra, R., Gutierrez, S and Javed, A (2014) 'Runx2 regulates endochondral ossification through control of chondrocyte proliferation and differentiation', *Journal of bone and mineral research : the official journal of the American Society for Bone and Mineral Research*, 29(12), 2653-2665.

Chen, J., Huang, F., Du, X. and Tong, J. (2014) 'Expression and significance of MMP3 in synovium of knee joint at different stage in osteoarthritis patients', *Asian Pacific Journal of Tropical Medicine*, 7(4), 297-300.

Chen, M., Lichtler, A. C., Sheu, T. J., Xie, C., Zhang, X., O'Keefe, R. J. and Chen, D. (2007) 'Generation of a transgenic mouse model with chondrocyte-specific and tamoxifen-inducible expression of Cre recombinase', *Genesis*, 45(1), 44-50.

Chen, D., J., Shen, W., Zhao, T., Wang, L and Hamilton, J (2017) 'Osteoarthritis: toward a comprehensive understanding of pathological mechanism' *Bone research*, 5, 16044

Chenette, D. M., Cadwallader, A. B., Antwine, T. L., Larkin, L. C., Wang, J., Olwin, B. B. and Schneider, R. J. (2016) 'Targeted mRNA Decay by RNA Binding Protein AUF1 Regulates Adult Muscle Stem Cell Fate, Promoting Skeletal Muscle Integrity', *Cell reports*, 16(5), 1379-1390.

Cheng, A. and Genever, P. G. (2010) 'SOX9 determines RUNX2 transactivity by directing intracellular degradation', *Journal of bone and mineral research : the official journal of the American Society for Bone and Mineral Research*, 25(12), 2680-2689.

Christiansen, B., Guilak,, K., Lockwood, A., Olson, S., Pitsillides, A, Sandell, L, Silva, M., van der Meulen, M and Haudenschild, D (2015) 'Non-invasive mouse models of post-traumatic osteoarthritis' *Osteoarthritis and cartilage* 23(10), 1627-1638.

Clark, A. (2000) 'Post-transcriptional regulation of pro-inflammatory gene expression', *Arthritis research*, 2(3), 172-174.

Clouet, J., Vinatier, C., Merceron, C., Pot-vauce, M., Maugars, P., Weiss, G., Grimandi and Guicheux, J (2009) 'From osteoarthritis treatments to future regenerative therapies for cartilage', *Drug discovery today,* 14(19-20), 913-925.

Cho, S.-J., Jung, Y-S., Zang and Chen, X (2012), 'The RNA-binding protein RNPC1 stabilizes the mRNA encoding the RNA-binding protein HuR and cooperates with HuR to suppress cell proliferation', The Journal of biological chemistry, 287(18), 14535-14544.

Cléry, A. (2013) 'From Structure to function of RNA binding domains', *Madame Curie Bioscience Database*. Landes Bioscience, 2000-2013

Coolidge, C. J. and Patton, J. G. (2000) 'A new double-stranded RNA-binding protein that interacts with PKR', *Nucleic acids research*, 28(6), 1407-1417.

Cortes M, Baria A and Schwartz N (2009) 'Sulfation of chondroitin sulfate proteoglycans is necessary for proper Indian hedgehog signaling in the developing growth plate' *Development,* 136(10): 1697–1706.

Couly, G., Creuzet, S., Bennaceur, S. and Le Douarin, N. (2002) 'Interactions between Hox-negative cephalic neural crest cells and the foregut endoderm in patterning the facial skeleton in the vertebrate head', *Development*, 129(4), 1061-1073

Creuzet, S., Couly, G. and Le Douarin, N. M. (2005) 'Patterning the neural crest derivatives during development of the vertebrate head: insights from avian studies', *Journal of anatomy*, 207(5), 447-459.

Cserjesi, P., Lilly, B., Bryson, L and Wang Y (1992) 'MHox: a mesodermally restricted homeodomain protein that binds an essential site in the muscle creatine kinase enhancer', Development, 115, 1087-1101.

Culley, KL., Dragomir, CL., Chang, J., Wondimu, EB., Coico, J., Plumb, DA., Otero, M and Goldring, MB (2015) 'Mouse models of osteoarthritis: surgical model of posttraumatic osteoarthritis induced by destabilization of the medial meniscus', *Methods in molecular biology,* 1226, 143-173.

Dai, W., Zhang, G. and Makeyev, E. (2011) 'RNA-binding protein HuR autoregulates its expression by promoting alternative polyadenylation site usage', *Nucleic acids research*, 40(2), 787-800.

Danilin, S., Sourbier, C., Thomas, L., Rothhut, S., Lindner, V., Helwig, J.-J. J., Jacqmin, D., Lang, H. and Massfelder, T. (2009) 'von Hippel-Lindau tumor suppressor gene-dependent mRNA stabilization of the survival factor parathyroid hormone-related protein in human renal cell carcinoma by the RNA-binding protein HuR', *Carcinogenesis*, 30(3), 387-396.

Davidson, B., van de Loo, FA., van den Berg, WB., van der Kraan, PM (2014) 'How to build an inducible cartilage-specific transgenic mouse', *Arthritis research & therapy*, 16, 210.

Davis, A. P., Witte, D. P., Hsieh-Li, H. M., Potter, S. S. and Capecchi, M. R. (1995) 'Absence of radius and ulna in mice lacking hoxa-11 and hoxd-11', *Nature*, 375(6534), 791-795.

de Crombrugghe, B., Lefebvre, V. and Nakashima, K. (2001) 'Regulatory mechanisms in the pathways of cartilage and bone formation', *Current opinion in cell biology*, 13(6), 721-727.

de Crombrugghe, B., Lefebvre, V and Behringer, RR (2000) 'Transcriptional mechanisms of chondrocyte differentiation', Matrix Biology, 19(5), 389-394.

de Hooge, A., van de Loo, F., Bennink, M. B., Arntz, O. J., de Hooge, P. and van den Berg, W. B. (2005) 'Male IL-6 gene knock out mice developed more advanced osteoarthritis upon aging', *Osteoarthritis and cartilage*, 13(1), 66-73.

de Silanes, I. L., Zhan, M., Lal, A. and Yang, X. (2004) 'Identification of a target RNA motif for RNA-binding protein HuR', *PNAS*, 101(9), 2987-2992.

De Souza RL, Matsuura M, Eckstein F, Rawlinson SC, Lanyon LE, Pitsillides AA (2005) 'Non-invasive axial loading of mouse tibiae increases cortical bone formation and modifies trabecular organization: a new model to study cortical and cancellous compartments in a single loaded element', *Bone,* 37(6):810-8.

Dean, J., Wit, R., Mahtani, K., Sully, G., Clark, A and Saklatvala, J (2001) 'The 3' untranslated region of tumor necrosis factor alpha mRNA is a target of the mRNA-stabilizing factor HuR', *Mol Cell Biol,* 21(3), 721-730.

Dijkgraaf, L., de Bont, G., Boering, G and Liem, R (1995) 'The structure, biochemistry, and metabolism of osteoarthritic cartilage: a review of the literature', *Journal of oral and maxillofacial surgery : official journal of the American Association of Oral and Maxillofacial Surgeons,* 53(10), 1182-1192.

Dixon DA, Kaplan CD, McIntyre TM, Zimmerman GA and Prescott SM (2000) 'Post-transcriptional control of cyclooxygenase-2 gene expression. The role of the 3'-untranslated region', *J Biol Chem*, 275(16):11750-7

Dixon DA, Tolley ND, King PH, Nabors LB, McIntyre TM, Zimmerman GA and Prescott SM (2001) 'Altered expression of the mRNA stability factor HuR promotes cyclooxygenase-2 expression in colon cancer cells', *J Clin Invest,* 108(11):1657-65.

Dora, NJ., Crookshanks, AJF and Leung KKY (2016) 'Analysis of compound heterozygotes reveals that the mouse floxed Pax6tm1Ued allele produces abnormal eye phenotypes' Transgenic Research, 25(5), 679-692.

Doller, A.; Pfeilschifter, J and Eberhardt, W (2008) 'Signalling pathways regulating nucleo-cytoplasmic shuttling of the mRNA-binding protein HuR', *Cell Signal,* 20, 2165–2173

Dy, P., Wang, W., Bhattaram, P., Wang, Q., Wang, L., Ballock, R. T. and Lefebvre, V. (2012) 'Sox9 directs hypertrophic maturation and blocks osteoblast differentiation of growth plate chondrocytes', *Developmental cell*, 22(3), 597-609.

Echtermeyer, F., Bertrand, J., Dreier, R., Meinecke, I., Neugebauer, K., Fuerst, M., Lee, Y., Song, Y., Herzog, C., Theilmeier, G. and Pap, T. (2009) 'Syndecan-4 regulates ADAMTS-5 activation and cartilage breakdown in osteoarthritis', *Nature Medicine*, 15(9), 1072-1076.

Elefteriou, F and Yang, X (2011) 'Genetic mouse models for bone studies-strengths and limitations', *Bone*, 49, 1242-1254.

Elkon, R and Ugalde, AP (2013) 'Alternative cleavage and polyadenylation: extent, regulation and function', Nature Reviews Genetics, 14, 496-506.

Elkon, R., Drost, J., van Haaften, G., Jenal, M., Schrier, M., Oude Vrielink, JA and Agami, R (2012) 'E2F mediates enhanced alternative polyadenylation in proliferation' Genome biology, 13(7), R59

Embade, N., Fernández-Ramos, M., Varela-Rey, N., Beraza, M., Sini, V., Gutiérrez de Juan, A., Woodhoo, N., Martínez-López, B., Rodríguez-Iruretagoyena, F., Bustamante, A., de la Hoz, A. Carracedo, D., Xirodimas, M., Rodríguez, S., Lu, J., Mato, M and Martínez-Chantar, M (2012) 'Murine double minute 2 regulates Hu antigen R stability in human liver and colon cancer through NEDDylation.', *Hepatology,* 55(4), 1237-1248.

Eyre, DR, Pietka, T and Weis, M (2004) 'Covalent cross-linking of the NC1 domain of collagen type IX to collagen type II in cartilage', Journal of Biological Chemistry, 279, 2568-2574.

Eyre, D (2002) 'Collagen of articular cartilage', *Arthritis research*, 4, 30-35.

Fan, X. C and Steitz, J.A (1998) 'Overexpression of HuR, a nuclear-cytoplasmic shuttling protein, increases the in vivo stability of ARE-containing mRNAs', *The EMBO journal*, 17(12), 3448-3460.

Fang H and Beier F (2014) 'Mouse models of osteoarthritis: modelling risk factors and assessing outcomes', *Nat Rev Rheumatol,* 10(7):413-21

Faour, W. H., Mancini, A., He, Q. W and A., D. J (2003) 'T-cell-derived Interleukin-17 Regulates the Level and Stability of Cyclooxygenase-2 (COX-2) mRNA through Restricted Activation of the p38 Mitogen-activated Protein', *Journal of Biological Chemistry*, 278(29), 26897-26907.

Feil, R., Wagner, J., Metzger, D and Chambon, P. (1997) 'Regulation of Cre recombinase activity by mutated estrogen receptor ligand-binding domains', *Biochemical and Biophysical Research Communications*, 28; 237(3), 752-757.

Felson DT, Anderson JJ, Naimark A (1988) 'Obesity and knee osteoarthritis. The Framingham Study', *Ann Intern Med,* 109: 18–24.

Fernández-Tajes J, of the … S-H-A. 2014. Genome-wide DNA methylation analysis of articular chondrocytes reveals a cluster of osteoarthritic patients. Annals of the Rheumatic Diseases, 73, 668-677.

Filion, C. and Labelle, Y. (2004) 'The oncogenic fusion protein EWS/NOR-1 induces transformation of CFK2 chondrogenic cells', *Experimental cell research*, 297(2), 585-592.

Forni, PE., Scuoppo, C and Imayoshi, I (2006) 'High levels of Cre expression in neuronal progenitors cause defects in brain development leading to microencephaly and hydrocephaly', Journal of Neuroscience, 26(37), 9593-9602.

Fosang, A. J., Rogerson, F. M. and East, C. J. (2008) 'ADAMTS-5: the story so far', *European cells and materials*, 5(15), 11-26.

Foster JW, Dominguez-Steglich MA, Guioli S, Kwok C, Weller PA, Stevanović M, Weissenbach J, Mansour S, Young ID and Goodfellow PN (1994) 'Campomelic dysplasia and autosomal sex reversal caused by mutations in an SRY-related gene', *Nature,* 372(6506):525-30.

Fox, S., Bedi, A. and Rodeo, S. A. (2009) 'The basic science of articular cartilage: structure, composition, and function', *Sports health*, 1(6), 461-468.

Foster, JW., Dominguez-Steglich, MA and Guioli S (1994) 'Campomelic dysplasia and autosomal sex reversal caused by mutations in an SRY-related gene', *Nature*, 372, 525-530.

Freida, L (1996) 'Histotechnology: a Self-Instructional Text', 2nd edition, *Carson*, 154-156

Fromental-Ramain, C., Warot, X., Lakkaraju, S., Favier, B., Haack, H., Birling, C., Dierich, A., Doll e, P. and Chambon, P. (1996) 'Specific and redundant functions of the paralogous Hoxa-9 and Hoxd-9 genes in forelimb and axial skeleton patterning', *Development (Cambridge, England)*, 122(2), 461-472.

Gabai, V. L., L. Meng, G. Kim, T. A. Mills, I. J. Benjamin and M. Y. Sherman (2012) 'Heat shock transcription factor Hsf1 is involved in tumor progression via regulation of hypoxia-inducible factor 1 and RNA-binding protein HuR', *Molecular and cellular biology,* 32(5), 929-940.

García-Carvajal, Z. Y (2013) 'Cartilage tissue engineering: the role of extracellular matrix (ECM) and novel strategies', *Regenerative medicine and tissue engineering,* Chapter 15, DOI 10.5772/55917.

García-Mauriño SMM, Rivero-Rodríguez F, Velázquez-Cruz A, Hernández-Vellisca M, Díaz-Quintana A, De la Rosa MA, Díaz-Moreno I (2017) 'RNA Binding Protein Regulation and Cross-Talk in the Control of AU-rich mRNA Fate', Frontiers in molecular biosciences, 4, 71.

Gardiner, M. D., T. L. Vincent, C. Driscoll, A. Burleigh, G. Bou-Gharios, J. Saklatvala, H. Nagase and A. Chanalaris (2014) 'Transcriptional analysis of micro-dissected articular cartilage in post-traumatic murine osteoarthritis', *Osteoarthritis and cartilage*, 23(4), 616-628.

Gendron-Maguire, M., Mallo, M., Zhang, M. and Gridley, T. (1993) 'Hoxa-2 mutant mice exhibit homeotic transformation of skeletal elements derived from cranial neural crest', *Cell*, 75(7), 1317-1331.

Gerstberger S, Hafner M and Tuschi T (2014) 'A census of human RNA-binding Proteins, *Nature review genetics,* doi:10.1038/nrg3813

Geyer, M., S. Grässel, R. H. Straub and G. Schett (2009) 'Differential transcriptome analysis of intraarticular lesional vs intact cartilage reveals new candidate genes in osteoarthritis pathophysiology', Osteoarthritis and cartilage, 17(3), 328-335.

Ghosh, M., Aguila, H. L., Michaud, J., Ai, Y., Wu, M.-T. T., Hemmes, A., Ristimaki, A., Guo, C., Furneaux, H. and Hla, T. (2009) 'Essential role of the RNA-binding protein HuR in progenitor cell survival in mice', *The Journal of clinical investigation*, 119(12), 3530-3543.

Girardot, M., Bayet, E., Maurin, J., Fort, P., Roux, P. and Raynaud, P. (2018) 'SOX9 has distinct regulatory roles in alternative splicing and transcription', *Nucleic acids research*.

Glasson, S. S., Askew, R., Sheppard, B. and Carito, B. (2005) 'Deletion of active ADAMTS5 prevents cartilage degradation in a murine model of osteoarthritis', *Nature*, 434(7033), 644-648.

Glasson SS, Blanchet TJ, Morris EA (2007) 'The surgical destabilization of the medial meniscus (DMM) model of osteoarthritis in the 129/SvEv mouse', *Osteoarthritis and cartilage*, 15, 1061-1069.

Glasson, S. S., Chambers, M. G., Van Den Berg, W. B. and Little, C. B. (2010) 'The OARSI histopathology initiative - recommendations for histological assessments of osteoarthritis in the mouse', *Osteoarthritis and cartilage*, 18, 17-23.

Glasson SS, Askew R, Sheppard B, Carito B, Blanchet T, Hak-Ling M, Flannery C, Kanki K, Wang E, Peluso D, Yang Z, Majumdar M and Morris E (2004) 'Characterization of and osteoarthritis susceptibility in ADAMTS-4–knockout mice', *Arthritis and rheumatology,* 50(8), 2547-58.

Glisovic, T., J. L. Bachorik, J. Yong and G. Dreyfuss (2008) 'RNA-binding proteins and post-transcriptional gene regulation', *FEBS letters,* 582(14),1977-1986.

Goldring MB (2006) 'The control of chondrogenesis', Journal of cellular biochemistry, 97(1).

Goldring MB and Marcu KB (2012) 'Epigenomic and microRNA-mediated regulation in cartilage development, homeostasis, and osteoarthritis', *Trends in molecular medicine*, 18(2), 109-118.

Gosset, M., Berenbaum, F., Thirion, S. and Jacques, C. (2008) 'Primary culture and phenotyping of murine chondrocytes', *Nature Protocols*, 3(8), 1253-1260.

Govindaraju, S. and B. S. Lee (2013) 'Adaptive and maladaptive expression of the mRNA regulatory protein HuR', *World journal of biological chemistry*, 4(4), 111-118.

Graham, A., Papalopulu, N. and Krumlauf, R. (1989) 'The murine and Drosophila homeobox gene complexes have common features of organization and expression', *Cell*, 57(3), 367-378.

Gratacós, F. M. and Brewer, G. (2010) 'The role of AUF1 in regulated mRNA decay', *Wiley Interdisciplinary Reviews: RNA*, 1(3), 457-473.

Greene G, Banquy X, Lee D, Lowrey D, Yu J and Irealachvili J (2011) 'Adaptive mechanically controlled lubrication mechanism found in articular joints', *PNAS*, 108(13), 5255-5259.

Grogan, S. P., Duffy, S. F., Pauli, C. and Koziol, J. A. (2013) 'Zone-specific gene expression patterns in articular cartilage', *Arthritis & Rheumatology*, 65(2), 418-428.

Guarente L, Ptashne M (1981) 'Fusion of Escherichia coli lacZ to the cytochrome c gene of Saccharomyces cerevisiae', *Proc Natl Acad Sci,* 78, 2199-2203.

Guilak, F., W. R. Jones, H. P. Ting-Beall and G. M. Lee (1999) 'The deformation behavior and mechanical properties of chondrocytes in articular cartilage', *Osteoarthritis and cartilage*, 7(1), 59-70.

Güttinger S, Mühlhäusser P, Koller-Eichhorn R, Brennecke J and Kutay U (2004) 'Transportin2 functions as importin and mediates nuclear import of HuR', *Proceedings of the National Academy of Sciences of the United States of America,* 101, 2918-2923.

Guzman RE, Evans MG, Bove S, Morenko B, Kilgore K (2003) 'Mono-iodoacetate-induced histologic changes in subchondral bone and articular cartilage of rat femorotibial joints: an animal model of osteoarthritis', *Toxicol Pathol*, 31(6):619-24.

Hamilton DL and Abremski K (1984) 'Site-specific recombination by the bacteriophage P1 lox-Cre system. Cre-mediated synapsis of two lox sites', *J Mol Biol,* 178(2):481-6.

Han, J., Lee, Y., Yeom, K.-H. H., Nam, J.-W. W., Heo, I., Rhee, J.-K. K., Sohn, S. Y., Cho, Y., Zhang, B.-T. T. and Kim, V. N. (2006) 'Molecular basis for the recognition of primary microRNAs by the Drosha-DGCR8 complex', *Cell*, 125(5), 887-901.

Han, J., Lee, Y., Yeom, K. H., Kim, Y. K. and Jin, H. (2004) 'The Drosha-DGCR8 complex in primary microRNA processing', *Genes & Development*, 18(24), 3016-3027.

Han, Y. and Lefebvre, V. (2008) 'L-Sox5 and Sox6 drive expression of the aggrecan gene in cartilage by securing binding of Sox9 to a far-upstream enhancer', *Molecular and cellular biology*, 28(16), 4999-5013.

Hardingham, T., Tew, S. and Murdoch, A. (2002) 'Tissue engineering: chondrocytes and cartilage', *Arthritis research*, 4(3), S63-68.

Hassan MQ, Gordon JA, Lian JB, van Wijnen AJ, Stein JL and Stein GS (2010) 'Ribonucleoprotein immunoprecipitation (RNP-IP): a direct in vivo analysis of microRNA-targets', *Journal of cellular biochemistry*, 110, 817-822.

Henry SP, Liang S, Akdemir KC and de Crombrugghe B (2012) 'The postnatal role of Sox9 in cartilage', J Bone Miner Res, 27(12), 2511-2525.

Herjan, T., Yao, P., Qian, W., Li, X., Liu, C., Bulek, K., Sun, D., Yang, W.-P. P., Zhu, J., He, A., Carman, J. A., Erzurum, S. C., Lipshitz, H. D., Fox, P. L., Hamilton, T. A. and Li, X. (2013) 'HuR is required for IL-17-induced Act1-mediated CXCL1 and CXCL5 mRNA stabilization', *Journal of immunology*, 191(2), 640-649.

Hess, J., Porte, D., Munz, C. and Angel, P. (2001) 'AP-1 and Cbfa/runt physically interact and regulate parathyroid hormone-dependent MMP13 expression in osteoblasts through a new osteoblast-specific element 2/AP-1 composite element', *The Journal of biological chemistry*, 276(23), 20029-20038.

Huang, J., Zhao, L., Xing, L. and cells, C.-D. (2010) 'MicroRNA-204 regulates Runx2 protein expression and mesenchymal progenitor cell differentiation', *Stem cells*, 28(2), 357-364.

Hunziker EB (2002) 'Articular cartilage repair: basic science and clinical progress', A review of the current status and prospects, Osteoarthritis and cartilage, 10(6), 432-463.

Hutvágner, G., McLachlan, J. and Pasquinelli, A. E. (2001) 'A cellular function for the RNA-interference enzyme Dicer in the maturation of the let-7 small temporal RNA', *Science*, 3;293(5531), 834-838.

Inada, M., Yasui, T., Nomura, S. and Miyake, S. (1999) 'Maturational disturbance of chondrocytes in Cbfa1-deficient mice', *Developmental Dynamics*, 214(4), 279-290.

Indra, AK., Warot, X., Brocard, J., Bornert, JM., Xiao, JH., Chambon, P and Metzger, D. (1999) 'Temporally-controlled site-specific mutagenesis in the basal layer of the epidermis: comparison of the recombinase activity of the tamoxifen-inducible Cre-ER(T) and Cre-ER(T2) recombinases', *Nucleic acids research*, 15;27(22), 4324-4327.

Iozzo, R. V. and Schaefer, L. (2015) 'Proteoglycan form and function: A comprehensive nomenclature of proteoglycans', *Matrix biology : journal of the International Society for Matrix Biology*, 42, 11-55.

Jaisser, F (2000) 'Inducible gene expression and gene modification in transgenic mice'*, J Am Soc Nephrol*, PMID: 11065338.

Ji, Q., Xu, X., Xu, Y., Fan, Z., Kang, L., Li, L., Liang, Y., Guo, J., Hong, T. and Li, Z. (2016) 'miR-105/Runx2 axis mediates FGF2-induced ADAMTS expression in osteoarthritis cartilage', *Journal of Molecular Medicine*, 94(6), 681-694.

Jiang P, Coller H (2012) 'Functional interactions between microRNAs and RNA binding proteins', *MicroRNA,* 1(1):70-9.

Jo, A., Denduluri, S., Zhang, B., Wang, Z., Yin, L., Yan, Z., Kang, R., Shi, L. L., Mok, J., Lee, M. J. and Haydon, R. C. (2014) 'The versatile functions of Sox9 in development, stem cells, and human diseases', *Genes & Diseases*, 1(2), 149-161.

Jonason, J. H., Xiao, G., Zhang, M., Xing, L. and Chen, D. (2009) 'Post-translational Regulation of Runx2 in Bone and Cartilage', *Journal of dental research*, 88(8), 693-703.

Kang, M.-J., Ryu, M.-G. Lee, J. Han, J.-H. Lee, T.-K. Ha, D.-S. Byun, K.-S. Chae, B.-H. Lee, H. Chun, K. Lee, H.-J. Kim and Chi, S (2008) 'NF-kappaB activates

transcription of the RNA-binding factor HuR, via PI3K-AKT signaling, to promote gastric tumorigenesis', *Gastroenterology,* 135(6), 2030.

Karamboulas, K., Dranse, H. J. and Underhill, M. T. (2010) 'Regulation of BMP-dependent chondrogenesis in early limb mesenchyme by TGFβ signals', *Journal of Cell Science*, 123(12), 2068-2076.

Karp, S. J., Schipani, E., St-Jacques, B., Hunzelman, J., Kronenberg, H. and McMahon, A. P. (2000) 'Indian hedgehog coordinates endochondral bone growth and morphogenesis via parathyroid hormone related-protein-dependent and -independent pathways', *Development*, 127(3), 543-548.

Karsdal, M. A. and Madsen, S. H. (2008) 'Cartilage degradation is fully reversible in the presence of aggrecanase but not matrix metalloproteinase activity', *Arthritis Research Therapy*, 10(3), R63.

Kartsogiannis, V. and Ng, K. W. (2004) 'Cell lines and primary cell cultures in the study of bone cell biology', *Molecular and cellular endocrinology*, 228(1-2), 79-102.

Kasashima, K., Sakashita, E., Saito, K. and Sakamoto, H. (2002) 'Complex formation of the neuron-specific ELAV-like Hu RNA-binding proteins', *Nucleic acids research*, 30(20), 4519-4526.

Katsanou, V., Milatos, S. and Yiakouvaki, A. (2009) 'The RNA-binding protein Elavl1/HuR is essential for placental branching morphogenesis and embryonic development', *Molecular and cellular biology*, 29(10), 2762-2776.

Katsanou V, Papadaki O and Milatos S (2005) 'HuR as a negative posttranscriptional modulator in inflammation', Molecular cell, 19(6), 777-789.

Kawanami, A., Matsushita, T., Chan, Y. Y. and Murakami, S. (2009) 'Mice expressing GFP and CreER in osteochondro progenitor cells in the periosteum', *Biochemical and biophysical research communications*, 386(3), 477-482.

Kelwick, R., Desanlis, I., Wheeler, G. N. and Edwards, D. R. (2015) 'The ADAMTS (A Disintegrin and Metalloproteinase with Thrombospondin motifs) family', *Genome biology*, 16(1), 113.

Kiani C, Chen L, Wu YJ, Yee AJ and Yang BB (2002), 'Structure and function of aggrecan', *Cell res*, 12(1), 19-32.

Kim, I. S., Otto, F., Zabel, B. and Mundlos, S. (1999) 'Regulation of chondrocyte differentiation by Cbfa1', *Mechanisms of development*, 80(2), 159-170.

Kim, Y.-J. J., Kim, H.-J. J. and Im, G.-I. I. (2008) 'PTHrP promotes chondrogenesis and suppresses hypertrophy from both bone marrow-derived and adipose tissue-derived MSCs', *Biochemical and biophysical research communications*, 373(1), 104-108.

Kim, Y., Murao, H., Yamamoto, K., Deng, J. M., Behringer, R. R., Nakamura, T. and Akiyama, H. (2011) 'Generation of transgenic mice for conditional overexpression of Sox9', *Journal of bone and mineral metabolism*, 29(1), 123-129.

Kisseberth WC, Brettingen NT, Lohse JK, Sandgren EP (1999) 'Ubiquitous expression of marker transgenes in mice and rats', *Dev Biol,* 214, 128-138.

Kmita, M., Tarchini, B., Zàkàny, J., Logan, M., Tabin, C. J. and Duboule, D. (2005) 'Early developmental arrest of mammalian limbs lacking HoxA/HoxD gene function', *Nature*, 435(7045), 1113-1116.

Komori, T., Yagi, H., Nomura, S., Yamaguchi, A., Sasaki, K., Deguchi, K., Shimizu, Y., Bronson, R. T., Gao, Y. H., Inada, M., Sato, M., Okamoto, R., Kitamura, Y., Yoshiki, S. and Kishimoto, T. (1997) 'Targeted Disruption of Cbfa1 Results in a Complete Lack of Bone Formation owing to Maturational Arrest of Osteoblasts', *Cell*, 89(5), 755-764.

Komori, T (2010) 'Regulation of bone development and extracellular matrix protein genes by RUNX2', *Cell Tissue Res*, 339, 189–195

Kopec J, Sayre E, Schwartz T and Jordan J (2014) 'Occurrence of Radiographic Osteoarthritis of the Knee and Hip Among African Americans and Whites: A Population-Based Prospective Cohort Study', *Arthritis Care Res,* 65(6): 928–935.

Krishnamurthy P, Rajasingh J, Lambers E, Qin G, Losordo DW, Kishore R (2009) 'IL-10 inhibits inflammation and attenuates left ventricular remodeling after myocardial infarction via activation of STAT3 and suppression of HuR', *Circulation research,* 104,18.

Kuratani S, Martin JF, Wawersik S, Lilly B, Eichele G and Olson E (1994) 'The expression pattern of the chick homeobox gene gMHox suggests a role in patterning of the limbs and face and in compartmentalization of somites', *Developmental biology,* 161(2), 357-369.

Kuyinu, E. L., Narayanan G., Nair LS and Laurencin CT (2016) 'Animal models of osteoarthritis: classification, update, and measurement of outcomes', *J Orthop Surg Res,* 11, 19.

Lal, S., Cheung, E. C., Zarei, M., Preet, R., Chand, S. N., Mambelli-Lisboa, N. C., Romeo, C., Stout, M. C., Londin, E., Goetz, A., Lowder, C. Y., Nevler, A., Yeo, C. J., Campbell, P. M., Winter, J. M., Dixon, D. A. and Brody, J. R. (2017) 'CRISPR Knockout of the HuR Gene Causes a Xenograft Lethal Phenotype', *Molecular Cancer Research*, 15(6), 696-707.

Lakso M., Sauer B., Mosinger B, Lee, E., Manning, R, Yu, S., Mulder, K and Westphal, H (1992) 'Targeted oncogene activation by site-specific recombination in transgenic mice. *Proc Natl Acad*, 89(14, 6232.

Lal A, Kawai T, Yang X, Mazan-Mamczarz K and Gorospe M (2005) 'Antiapoptotic function of RNA-binding protein HuR effected through prothymosin α', *EMBO J,* 24(10), 1852-1862.

Lampropoulou-Adamidou, K. and Lelovas, P. (2014) 'Useful animal models for the research of osteoarthritis', *European Journal of Orthopaedic Surgery & Traumatology*, 24(3), 263-271.

Lauer AM, May B, Hao Z and Watson J (2009) 'Sound levels in modern rodent housing rooms are an uncontrolled environmental variable with fluctuations mainly due to human activities', Lab Anim, 38(5), 154-160.

Lauing K, Cortes M, Domowicz M, Henry J, Baria A and Schwartz N (2015) 'Aggrecan is required for growth plate cytoarchitecture and differentiation', *Dev Biol,* doi: 10.1016/j.ydbio.2014.10.005

Lauriola, L., Serini, S., Granone, P., Lanza, P., Martini, M., Calviello, G. and Ranelletti, F. O. (2013) 'Hu/elav RNA-binding protein HuR regulates parathyroid hormone related peptide expression in human lung adenocarcinoma cells', *Histology and histopathology*, 28(9), 1205-1216.

Le Bleu HK, Kamal FA, Kelly M, Ketz JP, Zuscik MJ, Elbarbary RA (2017) 'Extraction of high-quality RNA from human articular cartilage', *Analytical biochemistry,* 518:, 34-138.

Lebedeva, S., Jens, M., Theil, K., Schwanhäusser, B., Selbach, M., Landthaler, M. and Rajewsky, N. (2011) 'Transcriptome-wide analysis of regulatory interactions of the RNA-binding protein HuR', *Molecular cell*, 43(3), 340-352.

Leco KJ, Waterhouse P, Sanchez OH, Gowing KL, Poole AR, Wakeham A, Mak TW and Khokha R (2001) 'Spontaneous air space enlargement in the lungs of mice lacking tissue inhibitor of metalloproteinases-3 (TIMP-3)', The Journal of clinical investigation, 108, 817-829.

Lee, J.-M. M. and Im, G.-I. I. (2012) 'PTHrP isoforms have differing effect on chondrogenic differentiation and hypertrophy of mesenchymal stem cells', *Biochemical and biophysical research communications*, 421(4), 819-824.

Lee, Y., Kim, M., Han, J., Yeom, K. H. and Lee, S. (2004) 'MicroRNA genes are transcribed by RNA polymerase II', *The EMBO Journal*, 23(20), 4051-4060.

Lefebvre, V. and Bhattaram, P. (2010) 'Vertebrate skeletogenesis', *Current topics in developmental biology*, 90, 291-317.

Lefebvre, V. and Dvir-Ginzberg, M. (2017) 'SOX9 and the many facets of its regulation in the chondrocyte lineage', *Connective tissue research*, 58(1), 2-14.

Lefebvre V, Huang W, Harley V, Goodfellow P and de Crombrugghe (1997) 'SOX9 is a potent activator of the chondrocyte-specific enhancer of the pro alpha1 (II) collagen gene' Mol Cell Biol, 17(4), 2336-2346.

Lefebvre, V., Garofalo, S., Zhou, G., Metsäranta, M., Vuorio, E. and De Crombrugghe, B. (1994) 'Characterization of primary cultures of chondrocytes from type II collagen/beta-galactosidase transgenic mice', *Matrix biology : journal of the International Society for Matrix Biology*, 14(4), 329-335.

Levadoux-Martin M, Gouble A, Jegou B, Vallet-Erdtmann V, Jacques A, Mercier P and Morello D (2003) 'Impaired gametogenesis in mice that overexpress the RNA-binding protein HuR', EMBO Rep, 4(4), 394-399.

Li, J and Dong, S. (2016) 'The Signaling Pathways Involved in Chondrocyte Differentiation and Hypertrophic Differentiation', *Stem cells international*, 2016, 2470351.

Li S, Chen L, Peng X, Wang C, Qin B, Tan D, Han C, Yang H, Ren X, Liu F, Xu C and Zhou X (2018) 'Overview of the reporter genes and reported mouse models', Animal models and experimental medicine, 1(1).

Li, X., Kazan, H. and Lipshitz, H. D. (2014) 'Finding the target sites of RNA-binding proteins', *Wiley Interdisciplinary Reviews: RNA*, 5(1), 111-130.

Li H, Park S, Kilburn B, Jelinek MA, Henschen-Edman A, Aswad DW, Stallcup MR and Laird-Offringa IA (2002), 'Lipopolysaccharide-induced methylation of HuR, an mRNA-stabilizing protein, by CARM1. Coactivator-associated arginine methyltransferase'*, J Biol Chem*, 277(47):44623-30

Li ZC, Xiao J, Peng JL (2014) 'Functional annotation of rheumatoid arthritis and osteoarthritis associated genes by integrative genomewide gene expression profiling analysis'*, PLoS One*, 9: e85784.

Liao, L., Zhang, S., Gu, J., Takarada, T., Yoneda, Y., Huang, J., Zhao, L., Oh, C.-d. D., Li, J., Wang, B., Wang, M. and Chen, D. (2017) 'Deletion of Runx2 in Articular Chondrocytes Decelerates the Progression of DMM-Induced Osteoarthritis in Adult Mice', *Scientific reports*, 7(1), 2371.

Lieberthal J, Sambamurthy N, Scanzello CR (2015) 'Inflammation in joint injury and post-traumatic osteoarthritis', *Osteoarthritis Cartilage,* 23: 1825–1834.

Lin, E. A., Kong, L., Bai, X.-H. H., Luan, Y. and Liu, C.-J. J. (2009) 'miR-199a, a bone morphogenic protein 2-responsive MicroRNA, regulates chondrogenesis via direct targeting to Smad1', *The Journal of biological chemistry*, 284(17), 11326-11335.

Lin S and Gregory RI (2015) 'MicroRNA biogenesis pathways in cancer', *Nature reviews. Cancer, 15*, 321-333.

Little, C. B., Barai, A., Burkhardt, D., Smith, Fosang, A. J., Werb, Z., Shah, M. and Thompson, E. W. (2009) 'Matrix metalloproteinase 13-deficient mice are resistant to osteoarthritic cartilage erosion but not chondrocyte hypertrophy or osteophyte development', *Arthritis and rheumatism*, 60(12), 3723-3733.

Little CB and Zaki S (2012) 'What constitutes an "animal model of osteoarthritis"–the need for consensus?', Osteoarthritis and cartilage, 20(4), 261-267.

Livak, K. J. and Schmittgen, T. D. (2001) 'Analysis of relative gene expression data using real-time quantitative PCR and the 2- CT method', *methods*, 25(4), 402-408.

Liu B, Qu L and Yan S (2015) 'Cyclooxygenase-2 promotes tumor growth and suppresses tumor immunity', *Cancer cell intel*, 15:106. doi: 10.1186/s12935-015-0260-7

Loeser RF, Olex AL, McNulty MA, Carlson CS, Callahan M, Ferguson C, Chou J, Leng X and Fetrow J (2012) 'Microarray analysis reveals age-related differences in gene expression during the development of osteoarthritis in mice', Arthritis & Rheumatology, 64(3), 705-717.

Logan, M., Martin, J. F., Nagy, A., Lobe, C., Olson, E. N. and Tabin, C. J. (2002) 'Expression of Cre Recombinase in the developing mouse limb bud driven by a Prxl enhancer', *Genesis*, 33(2), 77-80.

Long F and Ornitz D (2013) 'Development of the endochondral skeleton', *Cold Spring Harb Perspect Biol,* 5(1):a008334

Loonstra A, Vooijs M, Beverloo B, Al Allak B, van Drunen E, Kanaar R, Berns and Jonkers J (2001) 'Growth inhibition and DNA damage induced by Cre recombinase in mammalian cells' Proc Natl Acad Sci, 98(16), 9209.

Lorsch, J; Collins, F and Lippincott-Schwartz, J (2014) 'Fixing problems with cell lines. Technologies and policies can improve authentication', *Science,* 346(6216): 1452–1453.

Loughlin, J. (2015) 'Genetic contribution to osteoarthritis development: current state of evidence', *Current opinion in rheumatology*, 27(3), 284-288.

Lu, J. Y., Sadri, N. and Schneider, R. J. (2006) 'Endotoxic shock in AUF1 knockout mice mediated by failure to degrade proinflammatory cytokine mRNAs', *Genes & Development*, 20(22), 3174-3184.

Lunde, B. M., Moore, C. and Varani, G. (2007) 'RNA-binding proteins: modular design for efficient function', *Nature reviews: Molecular Cell Biology*, 8(6), 479-490.

Luo, Y., D. Sinkeviciute, Y. He, M. Karsdal, Y. Henrotin, A. Mobasheri, P. Önnerfjord and A. Bay-Jensen (2017) 'The minor collagens in articular cartilage', *Protein & cell,* 8(8), 560-572.

Ma, W. J., Cheng, S., Campbell, C., Wright, A. and Furneaux, H. (1996) 'Cloning and characterization of HuR, a ubiquitously expressed Elav-like protein', *The Journal of biological chemistry*, 271(14), 8144-8151.

Ma HLL, Blanchet TJ, Peluso D, Hopkins B, Morris EA and Glasson SS (2007) 'Osteoarthritis severity is sex dependent in a surgical mouse model', *Osteoarthritis and cartilage*, 15, 695-700.

Mak, M. C., K. M. Lam, P. K. Chan, Y. B. Lau, W. H. Tang, P. K. K. Yeung, B. C. Ko, S. M. Chung and S. K. Chung (2011) 'Embryonic lethality in mice lacking the nuclear factor of activated T cells 5 protein due to impaired cardiac development and function', *PloS one,* 6(7).

Mayr C and Bartel DP (2009) 'Widespread shortening of 3'UTRs by alternative cleavage and polyadenylation activates oncogenes in cancer cells', *Cell,* 138, 673-684.

Malfait, A.-M. M., Liu, R.-Q. Q., Ijiri, K., Komiya, S. and Tortorella, M. D. (2002) 'Inhibition of ADAM-TS4 and ADAM-TS5 prevents aggrecan degradation in osteoarthritic cartilage', *The Journal of biological chemistry*, 277(25), 22201-22208.

Mallo, M. and Alonso, C. R. (2013) 'The regulation of Hox gene expression during animal development', *Development*, 140(19), 3951-3963.

Mallo, M., Wellik, D. M. and Deschamps, J. (2010) 'Hox genes and regional patterning of the vertebrate body plan', *Developmental biology*, 344(1), 7-15.

Maris, C., Dominguez, C. and Allain, F. H. T. (2005) 'The RNA recognition motif, a plastic RNA-binding platform to regulate post-transcriptional gene expression', *The FEBS journal*, 272(2), 2118-2131.

Martel-Pelletier J, Barr AJ, Cicuttini FM, Conaghan PG, Cooper C, Goldring MB, Goldring SR, Jones G, Teichtahl AJ and Pelletier J-P (2016) 'Osteoarthritis', *Nature Reviews Disease Primers*, 2, 16072.

Martin, J. F. and Olson, E. N. (2000) 'Identification of a prx1 limb enhancer', *Genesis*, 26(4), 225-229.

Martin, J. F., A. Bradley and E. N. Olson (1995) 'The paired-like homeo box gene MHox is required for early events of skeletogenesis in multiple lineages', *Genes & development*, 9(10), 1237-1249.

Martinez-Sanchez, A., Dudek, K. A. and L., M.-C. (2012) 'Regulation of human chondrocyte function through direct inhibition of cartilage master regulator SOX9 by microRNA-145 (miRNA-145)', *Journal of Biological Chemistry*, 287(2), 916-924.

Maqsood M, Matin M, Bahrami A and Ghasroldasht M (2013) 'Immortality of cell lines: challenges and advantages of establishment', *Cell Biology,* 37(10).

Mason RM, Chambers MG, Flannelly J, Gaffen JD, Dudhia J and Bayliss MT (2001) 'The STR/ort mouse and its use as a model of osteoarthritis', Osteoarthritis and Cartilage, 9(2), 85-91.

Mason RM, Chambers MG, Flannelly J, Gaffen JD, Dudhia J, Bayliss MT (2001), *Osteoarthritis Cartilage*, 9(2):85-91.

Matoulkova E, Michalova E, Vojtesek B and Hrstka R (2012) 'The role of the 3'untranslated region in post-transcriptional regulation of protein expression in mammalian cells', RNA biology, 9(5), 563-76.

McCoy, A., M (2015) 'Animal models of osteoarthritis: comparisons and key considerations', *Veterinary pathology*, 52(5), 803-818.

McDermott, B. T., Ellis, S., Bou-Gharios, G., Clegg, P. D. and Tew, S. R. (2016) 'RNA binding proteins regulate anabolic and catabolic gene expression in chondrocytes', *Osteoarthritis and cartilage*, 24(7), 1263-1273.

McIntyre, D. C., Rakshit, S., Yallowitz, A. R., Loken, L., Jeannotte, L., Capecchi, M. R. and Wellik, D. M. (2007) 'Hox patterning of the vertebrate rib cage', *Development*, 134(16), 2981-2989.

McLeod, J. M. (1980) 'Differential staining of cartilage and bone in whole mouse fetuses by alcian blue and alizarin red S', *Teratology*, 22(3), 299-301.

Meisner, N.-C. C., Hintersteiner, M., Mueller, K., Bauer, R., Seifert, J.-M. M., Naegeli, H.-U. U., Ottl, J., Oberer, L., Guenat, C., Moss, S., Harrer, N., Woisetschlaeger, M., Buehler, C., Uhl, V. and Auer, M. (2007)

'Identification and mechanistic characterization of low-molecular-weight inhibitors for HuR', *Nature chemical biology*, 3(8), 508-515.

Millevoi S and Vagner S (2010) 'Molecular mechanisms of eukaryotic pre-mRNA 3' end processing regulation', *Nucleic acids research*, 38, 2757-2774.

Miyaki S, Nakasa T, Otsuki S, Grogan S, Higashiyama R, Inoue A, Kato Y, Sata T, Lotz M and Asahara H (2009) 'MicroRNA-140 is expressed in differentiated human articular chondrocytes and modulates interleukin-1 responses', Arthritis & Rheumatism, 60(9).

Moodie, J. P., Stok, K. S., Müller, R., Vincent, T. L. and Shefelbine, S. J. (2011) 'Multimodal imaging demonstrates concomitant changes in bone and cartilage after destabilisation of the medial meniscus and increased joint laxity', *Osteoarthritis and cartilage*, 19(2), 163-170.

Mobasheri, A., G. Kalamegam, G. Musumeci and M. E. Batt (2014) 'Chondrocyte and mesenchymal stem cell-based therapies for cartilage repair in osteoarthritis and related orthopaedic conditions', *Maturitas,* 78(3), 188-198.

Muir H (1978) 'Proteoglycans of cartilage'*, J Clin Pathol Suppl*, 12: 67–81.

G Murphy (2011) 'Tissue inhibitors of metalloproteinases', *Genome biology,* 12(11), 233.

Nagy A (2000) 'Cre recombinase: the universal reagent for genome tailoring', *Genesis,* 26(2), 99-109.

Nakanishi, K. (2016) 'Anatomy of RISC: how do small RNAs and chaperones activate Argonaute proteins?', *Wiley Interdisciplinary Reviews: RNA*, 7(5), 637-660.

Nakanishi, S., Chiba, S., Yano, H., Kawamoto, I. and Matsuda, Y. (1995) 'MS-444, a new inhibitor of myosin light chain kinase from Micromonospora sp. KY7123', *The Journal of antibiotics*, 48(9), 948-951.

Neuhold, L. A., Killar, L., Zhao, W., Sung, M. L., Warner, L., Kulik, J., Turner, J., Wu, W., Billinghurst, C., Meijers, T., Poole, A. R., Babij, P. and DeGennaro, L. J. (2001) 'Postnatal expression in hyaline cartilage of constitutively active human collagenase-3 (MMP-13) induces osteoarthritis in mice', *The Journal of clinical investigation*, 107(1), 35-44.

Newman, B. and Wallis, G. A. (2003) 'Skeletal dysplasias caused by a disruption of skeletal patterning and endochondral ossification', *Clinical genetics*, 63(4), 241-251.

Newton, P. T., Staines, K. A. and Spevak, L. (2012) 'Chondrogenic ATDC5 cells: An optimised model for rapid and physiological matrix mineralisation', *International Journal of Molecular Medicine*, 30(5), 1187-1190.

Nishimura, R., Hata, K., Ikeda, F. and Ichida, F. (2008) 'Signal transduction and transcriptional regulation during mesenchymal cell differentiation', *Journal of bone and mineral metabolism*, 26(3), 203-212.

Nishimura, R., Wakabayashi, M., Hata, K., Matsubara, T., Honma, S., Wakisaka, S., Kiyonari, H., Shioi, G., Yamaguchi, A., Tsumaki, N., Akiyama, H. and Yoneda, T. (2012) 'Osterix regulates calcification and degradation of chondrogenic matrices through matrix metalloproteinase 13 (MMP13) expression in association with transcription factor Runx2 during endochondral ossification', *The Journal of biological chemistry*, 287(40), 33179-33190.

Nohno T, Koyama E, Myokai F, Taniguchi S, Ohuchi H, Saito T and Noji S (1993) ‘A chicken homeobox gene related to Drosophila paired is predominantly expressed in the developing limb’, Developmental Biology, 158(1), 254-264.

Noordzij, M., Tripepi, G. and Dekker, F. W. (2010) 'Sample size calculations: basic principles and common pitfalls', *Nephrology Dialysis Transplantation*, 25(5), 1388-1393.

Oktaba K, Zhang W, Lotz TS, Jun DJ, Lemke SB, Ng SP, Esposito E, Levine M and Hilgers V (2015) ‘ELAV links paused Pol II to alternative polyadenylation in the Drosophila nervous system’, Molecular cell, 57, 341-348.

Ortega, N., Behonick, D. J. and Werb, Z. (2004) 'Matrix remodeling during endochondral ossification', *Trends in cell biology*, 14(2), 86-93.

Otto, F., Thornell, A. P., Crompton, T., Denzel, A., Gilmour, K. C., Rosewell, I. R., Stamp, G. W., Beddington, R. S., Mundlos, S., Olsen, B. R., Selby, P. B. and Owen, M. J. (1997) 'Cbfa1, a candidate gene for cleidocranial dysplasia syndrome, is essential for osteoblast differentiation and bone development', *Cell*, 89(5), 765-771.

Panda, A. C., Abdelmohsen, K. and Yoon, J. H. (2014) 'RNA-binding protein AUF1 promotes myogenesis by regulating MEF2C expression levels', *Molecular Cellular Biology*, 34(16), 3106-3119.

Pasold J, Osterberg A, Peters K, Taipaleenmäki H, Säämänen AM, Vollmar B, Müller-Hilke B (2013) 'Reduced expression of Sfrp1 during chondrogenesis and in articular chondrocytes correlates with osteoarthritis in STR/ort mice', *Exp Cell Res*, 10;319(5):649-59

Peffers, M. J., Liu, X. and Clegg, P. D. (2014) 'Transcriptomic profiling of cartilage ageing', *Genomics data*, 2, 27-28.

Phimphilai, M., Zhao, Z., Boules, H., Roca, H. and Franceschi, R. T. (2006) 'BMP signaling is required for RUNX2-dependent induction of the osteoblast phenotype', *Journal of bone and mineral research : the official journal of the American Society for Bone and Mineral Research*, 21(4), 637-646.

Pineault, K. M. and Wellik, D. M. (2014) 'Hox genes and limb musculoskeletal development', *Current osteoporosis reports*, 12(4), 420-427.

Phull A, Eo S, Abbas Q, Ahmed M and Kim S (2016) 'Applications of Chondrocyte-Based Cartilage Engineering: An Overview', *Biomed Res Int*, doi: 10.1155/2016/1879837

Poole, C. A (1997) 'Articular cartilage chondrons: form, function and failure', *Journal of anatomy,* 191(1), 1-13.

Poulet, B., Hamilton, R. W. and Shefelbine, S. (2011) 'Characterizing a novel and adjustable noninvasive murine joint loading model', *Arthritis & Rheumatology*, 63(1), 137-147.

Poulet, B (2017) 'Models to define the stages of articular cartilage degradation in osteoarthritis development', *International journal of experimental pathology*, 98(3).

Rahmati M, Nalesso G, Mobasheri A, Mozafari M (2017) 'Aging and osteoarthritis: Central role of the extracellular matrix', *Ageing Res Rev,* 40:20-30

Rasmussen S, Glickman G, Norinsky R, Quimby FW and Tolwani RJ (2009) 'Construction noise decreases reproductive efficiency in mice', *Journal of the American Association for Laboratory Animal Science,* 48, 363-370.

Ruettger A, Neumann S, Wiederanders B and Huber R (2010) 'Comparison of different methods for preparation and characterization of total RNA from cartilage samples to uncover osteoarthritis in vivo', *BMC research notes*, 3, 7.

Rhee, D.K., Marcelino, J., Baker, M., Gong, Y., Smits, P., Lefebvre, V., Jay, G.D., Stewart, M., Wang, H., Warman, M.L. and Carpten, J.D. (2005) 'The secreted glycoprotein lubricin protects cartilage surfaces and inhibits synovial cell overgrowth', *The journal of clinical investigation*, 115(3), 622-631.

Ricci, E. P., Kucukural, A., Cenik, C. and Mercier, B. C. (2014) 'Staufen1 senses overall transcript secondary structure to regulate translation', *Nature Structural and Molecular Biology*, 21(1), 26-35.

Rigueur, D. and Lyons, K. M. (2014) 'Methods in Molecular Biology', *Methods in Molecular Biology*, 1130, 113-121.

Rodova M, Lu Q, Woodbury B, Crist J, Gardner B, Yost J, Zhong X, Anderson C and Wang J (2011) 'Nfat1 Regulates Adult Articular Chondrocyte Function Through Its Age-Dependent Expression Mediated by Epigenetic Histone Methylation', *JBMR,* 26(8), 1974-1986.

Rogulja-Ortmann, A., Picao-Osorio, J., Villava, C., Patraquim, P., Lafuente, E., Aspden, J., Thomsen, S., Technau, G. M. and Alonso, C. R. (2014) 'The RNA-binding protein ELAV regulates Hox RNA processing, expression and function within the Drosophila nervous system', *Development*, 141(10), 2046-2056.

Roos EM (2005) 'Joint injury causes knee osteoarthritis in young adults', *Curr Opin, Rheumatol*, 17: 195–200.

Ross, M. H, & Pawlina, W. (2011) 'Histology : a text and atlas : with correlated cell and molecular biology', *6th ed.* Philadelphia: Wolters Kluwer/Lippincott Williams & Wilkins Health.

Roughley, P. J. and Mort, J.S (2014) 'The role of aggrecan in normal and osteoarthritic cartilage', *Journal of experimental orthopaedics*¸ 1(1), 8.

Roughley PJ, Lee ER (1994) 'Cartilage proteoglycans: Structure and potential functions', Microsc Res. Tech, 28:385–397.

Salva, J. E. and Merrill, A. E (2017) 'Signaling networks in joint development', *Developmental Dynamics*, 246(4), 262-274.

Sanduja S, Blanco F, Young L, Kaza V and Dixon D (2012) 'The role of tristetraprolin in cancer and inflammation', *Front Biosci,* 17, 174-188.

Sekiya I, Tsuji K, Koopman P, Watanabe H, Yamada Y, Shinomiya, Nifuji A and Noda M (2000) 'SOX9 enhances aggrecan gene promoter/enhancer activity and is up-regulated by retinoic acid in a cartilage-derived cell line, TC6', Journal of Biological Chemistry, 275, 10738-10744.

Sato, T., Konomi, K., Yamasaki, S. and Aratani, S. (2006) 'Comparative analysis of gene expression profiles in intact and damaged regions of human osteoarthritic cartilage', *Arthritis & Rheumatology*, 54(3), 808-817.

Scanzello CR (2017) 'Role of low-grade inflammation in osteoarthritis', *Current opinion in rheumatology,* 29, 79-85.

Sexton, S. A., Ferguson, N. and Pearce, C. (2008) 'The misuse of 'no significant difference'in British orthopaedic literature', *The Annals of The Royal College of Surgeons of England*, 90(1), 58-61.

Shahi, M., Peymani, A. and Sahmani, M. (2017) 'Regulation of Bone Metabolism', *Reports of biochemistry & molecular biology*, 5(2), 73-82.

Shen Z and Malter J (2015) 'Regulation of AU-Rich Element RNA Binding Proteins by Phosphorylation and the Prolyl Isomerase Pin1', *Biomolecules,* 5(2): 412–434

Shen, J., Abu-Amer, Y., O'Keefe, R. J. and McAlinden, A. (2017) 'Inflammation and epigenetic regulation in osteoarthritis', *Connective tissue research*, 58(1), 49-63.

Shi Y (2012) 'Alternative polyadenylation: new insights from global analyses', *RNA,* 18, 2105-2117.

Schmitz N, Laverty S, Kraus VB and Aigner T (2010) 'Basic methods in histopathology of joint tissues', Osteoarthritis and cartilage, 18, 3-6.

Shu, B., Zhang, M., Xie, R., Wang, M., Jin, H., Hou, W., Tang, D., Harris, S. E., Mishina, Y., O'Keefe, R. J., Hilton, M. J., Wang, Y. and Chen, D. (2011) 'BMP2, but not BMP4, is crucial for chondrocyte proliferation and

maturation during endochondral bone development', *Journal of Cell Science*, 124(20), 3428-3440.

Shukunami, C., Ishizeki, K., Atsumi, T., Ohta, Y., Suzuki, F. and Hiraki, Y. (1997) 'Cellular Hypertrophy and Calcification of Embryonal Carcinoma Derived Chondrogenic Cell Line ATDC5 In Vitro', *Journal of Bone and Mineral Research*, 12(8), 1174-1188.

Simpson TI, Pratt T, Mason JO and Price DJ (2009) 'Normal ventral telencephalic expression of Pax6 is required for normal development of thalamocortical axons in embryonic mice', *Neural development,* 4, 19.

Sokolowski M, Furneaux H and Schwartz S (1999) 'The inhibitory activity of the AU-rich RNA element in the human papillomavirus type 1 late 3' untranslated region correlates with its affinity for the elav-like HuR protein', *Journal of virology,* 73, 1080-1091.

Spagnoli, A., Hwa, V., Horton, W. A., Lunstrum, G. P., Roberts, C. T., Chiarelli, F., Torello, M. and Rosenfeld, R. G. (2001) 'Antiproliferative effects of insulin-like growth factor-binding protein-3 in mesenchymal chondrogenic cell line RCJ3.1C5.18. relationship to differentiation stage', *The Journal of biological chemistry*, 276(8), 5533-5540.

Spellman, R., Llorian, M. and Smith, C. (2007) 'Crossregulation and Functional Redundancy between the Splicing Regulator PTB and Its Paralogs nPTB and ROD1', *Molecular cell*, 27(3), 420-434.

Srikantan S and Gorospe M (2012) 'HuR function in disease', *Frontiers in bioscience,* 17, 189-205.

St-Jacques, B., Hammerschmidt, M. and McMahon, A. P. (1999) 'Indian hedgehog signaling regulates proliferation and differentiation of chondrocytes and is essential for bone formation', *Genes & Development*, 13(16), 2072-2086.

Staines KA, Poulet B, and Wentworth AN and Pitsillides AA (2017) 'The STR/ort mouse model of spontaneous osteoarthritis–an update' *Osteoarthritis and Cartilage*, 25(6), 802-808.

Stanton, H., Melrose, J., Little, C. B. and Fosang, A. J. (2011) 'Proteoglycan degradation by the ADAMTS family of proteinases', *Biochimica et biophysica acta*, 1812(12), 1616-1629.

Stanton, H., Rogerson, F. M., East, C. J., Golub, S. B., Lawlor, K. E., Meeker, C. T., Little, C. B., Last, K., Farmer, P. J., Campbell, I. K., Fourie, A. M. and Fosang, A. J. (2005) 'ADAMTS5 is the major aggrecanase in mouse cartilage in vivo and in vitro', *Nature*, 434(7033), 648-652.

Strong LC (1944) 'Genetic Nature of the Constitutional States of Cancer Susceptibility and Resistance in Mice and Men', *The Yale journal of biology and medicine,* 17, 289-299.

Sulzbacher, I. (2013) 'Osteoarthritis: histology and pathogenesis', *Wiener Medizinische Wochenschrift*, 163(9-10), 212-219.

Takaishi H, Kimura T, Dalal S, Okada Y and D'Armiento J (2008) 'Joint diseases and matrix metalloproteinases: a role for MMP-13', *Current pharmaceutical biotechnology,* 9, 47-54.

Talwar, S., J. Jin, B. Carroll, A. Liu, M. B. Gillespie and V. Palanisamy (2011) 'Caspase-mediated cleavage of RNA-binding protein HuR regulates c-Myc protein expression after hypoxic stress', *The Journal of biological chemistry*, 286(37), 32333-32343.

Takaishi H, Kimura T, Dalal S, Okada Y, D'Armiento J (2008) 'Joint diseases and matrix metalloproteinases: a role for MMP-13', *Curr Pharm Biotechnol*, 9(1):47-54.

Tatsuta, K., Nakanishi, S., Takahashi, I. Preparation of MS-444 derivatives as immunosuppressive and anti-itching agents; (Kyowa Hakko Kogyo Co., Ltd., Japan). Application:WO 9832750, A1 19980730, CAN 129:148903, AN 1998: 527326, 1998.

Taylor, G. A., Carballo, E., Lee, D. M., Lai, W. S., Thompson, M. J., Patel, D. D., Schenkman, D. I., Gilkeson, G. S., Broxmeyer, H. E., Haynes, B. F. and Blackshear, P. J. (1996) 'A Pathogenetic Role for TNFα in the Syndrome of Cachexia, Arthritis, and Autoimmunity Resulting from Tristetraprolin (TTP) Deficiency', *Immunity*, 4(5), 445-454.

Techasintana, P., Davis, J. W., Gubin, M. M., Magee, J. D. and Atasoy, U. (2015) 'Transcriptomic-Wide Discovery of Direct and Indirect HuR RNA Targets in Activated CD4+ T Cells', *PloS one*, 10(7), e0129321.

ten Berge, D., Brouwer, A., Korving, J., Martin, J. F. and Meijlink, F. (1998) 'Prx1 and Prx2 in skeletogenesis: roles in the craniofacial region, inner ear and limbs', *Development*, 125(19), 3831-3842.

Tetsunaga, T., Nishida, K., Furumatsu, T., Naruse, K., Hirohata, S., Yoshida, A., Saito, T. and Ozaki, T. (2011) 'Regulation of mechanical stress-induced MMP-13 and ADAMTS-5 expression by RUNX-2 transcriptional factor in SW1353 chondrocyte-like cells', *Osteoarthritis and cartilage*, 19(2), 222-232.

Tew, S. R. and Clegg, P. D. (2010) 'Post-transcriptional gene regulation in chondrocytes', *Biochemical Society transactions*, 38(6), 1627-1631.

Tew, S. R. and Clegg, P. D. (2011) 'Analysis of post transcriptional regulation of SOX9 mRNA during in vitro chondrogenesis', *Tissue engineering. Part A*, 17(13-14), 1801-1807.

Tew, S. R. and Hardingham, T. E. (2006) 'Regulation of SOX9 mRNA in human articular chondrocytes involving p38 MAPK activation and mRNA stabilization', *The Journal of biological chemistry*, 281(51), 39471-39479.

Tew, S. R., Li, Y., Pothacharoen, P., Tweats, L. M., Hawkins, R. E. and Hardingham, T. E. (2005) 'Retroviral transduction with SOX9 enhances re-expression of the chondrocyte phenotype in passaged osteoarthritic human articular chondrocytes', *Osteoarthritis and cartilage*, 13(1), 80-89.

Tew, S. R., McDermott, B. T., Fentem, R. B., Peffers, M. J. and Clegg, P. D. (2014) 'Transcriptome-wide analysis of messenger RNA decay in normal and osteoarthritic human articular chondrocytes', *Arthritis & Rheumatology*, 66(11), 3052-3061.

Thirion, S. and Berenbaum, F. (2004) 'Culture and phenotyping of chondrocytes in primary culture', *Methods in molecular medicine*, 100, 1-14.

Tian B, Hu J, Zhang H and Lutz CS (2005) ‘A large-scale analysis of mRNA polyadenylation of human and mouse genes’, *Nucleic acids research,* 33, 201-212.

Trabucchi, M., Briata, P., Garcia-Mayoral, M., Haase, A. D., Filipowicz, W., Ramos, A., Gherzi, R. and Rosenfeld, M. G. (2009) 'The RNA-binding protein KSRP promotes the biogenesis of a subset of microRNAs', *Nature*, 459(7249), 1010.

Tremoleda, J. L., Khalil, M., Gompels, L. L., Wylezinska-Arridge, M., Vincent, T. and Gsell, W. (2011) 'Imaging technologies for preclinical models of bone and joint disorders', *EJNMMI research*, 1(1), 11.

Troeberg, L. and Nagase, H. (2012) 'Proteases involved in cartilage matrix degradation in osteoarthritis', *Biochimica et biophysica acta*, 1824(1), 133-145.

Tsang, K., Wa Tsang, S., Chan, D. and Cheah, K. S. (2014) 'The chondrocytic journey in endochondral bone growth and skeletal dysplasia', *Birth defects research. Part C, Embryo today : reviews*, 102(1), 52-73.

Tsang K, Chan D and Cheah K (2015) 'Fate of growth plate hypertrophic chondrocytes: Death or lineage extension?', Development, *Growth and Differentiation*, 57(2).

Tuddenham L, Wheeler G, Ntounia-Fousara S, Water J, Hajihosseini MK, Clark I, Dalmay T (2006) 'The cartilage specific microRNA-140 targets histone deacetylase 4 in mouse cells', FEBS Letters, 580(17), 4214-4217.

Tuerk and, Gold L (1990) 'Systematic evolution of ligands by exponential enrichment: RNA ligands to bacteriophage T4 DNA polymerase', *Science,* 249, 505-510.

Uren PJ, Burns SC, Ruan J, Singh KK, Smith AD and Penalva LO (2011) 'Genomic analyses of the RNA-binding protein Hu antigen R (HuR) identify a complex network of target genes and novel characteristics of its binding sites', *The Journal of biological chemistry,* 286, 37063-37066.

van der Kraan, P. M., P. Buma, T. van Kuppevelt and W. B. van den Berg (2002) 'Interaction of chondrocytes, extracellular matrix and growth factors: relevance for articular cartilage tissue engineering', Osteoarthritis and cartilage, 10(8), 631-637.

van Osch GJ, van der Kraan PM, Vitters EL, Blankevoort L and van den Berg WB (1993) 'Induction of osteoarthritis by intra-articular injection of collagenase in mice. Strain and sex related differences', *Osteoarthritis and cartilage,* 1, 171-177.

Vandesompele, J., De Preter, K., Pattyn, F., Poppe, B., Van Roy, N., De Paepe, A. and Speleman, F. (2002) 'Accurate normalization of real-time quantitative RT-PCR data by geometric averaging of multiple internal control genes', *Genome biology*, 3(7).

Vega RB, Matsuda K, Oh J, Richardson JA, Karsenty G and Olson E (2004) 'Histone Deacetylase 4 Controls Chondrocyte Hypertrophy during Skeletogenesis', *Cell*, 119, 555-566.

Verma, P. and Dalal, K. (2011) 'ADAMTS 4 and ADAMTS 5: Key enzymes in osteoarthritis', *Journal of Cellular Biochemistry*, 112(12), 3507-3514.

Vessey, J. P., Macchi, P., Stein, J. M. and Mikl, M. (2008) 'A loss of function allele for murine Staufen1 leads to impairment of dendritic Staufen1-RNP delivery and dendritic spine morphogenesis', *PNAS*, 105(42), 16374-16379.

Vincent TL and Watt FE (2018) Osteoarthritis, *Medicine,* 46, 187-195.

Vortkamp, A., Lee, K., Lanske, B. and Segre, G. V. (1996) 'Regulation of rate of cartilage differentiation by Indian hedgehog and PTH-related protein', *Science*, 273(5275), 613.

Wahl MC, Will CL, Lührmann R (2009) 'The spliceosome: design principles of a dynamic RNP machine'*, Cell,* 136(4), 701-18.

Wagner T, et al. 1994. Autosomal sex reversal and campomelic dysplasia are caused by mutations in and around the SRY-related gene SOX9. Cell 79:1111-1120.

Wang, G., Zhang, Y., Zhao, X., Meng, C. and Ma, L. (2015) 'MicroRNA-411 inhibited matrix metalloproteinase 13 expression in human chondrocytes', *American Journal of Translational Research*, 7(10), 2000-2006.

Wang, M., Sampson, E. R., Jin, H., Li, J., Ke, Q. H., Im, H.-J. and Chen, D. (2013) 'MMP13 is a critical target gene during the progression of osteoarthritis', *Arthritis research & therapy*, 15(1), 1-11.

Wang J, Guo Y, Chu H and Guan Y (2013) 'Multiple functions of the RNA-binding protein HuR in cancer progression, treatment responses and prognosis'*, Int J Mol Sci*, 14(5), 10015-10041.

Wang, M., Tang, D., Shu, B., Wang, B., Jin, H., Hao, S., Dresser, K. A., Shen, J., Im, H.-J. J., Sampson, E. R., Rubery, P. T., Zuscik, M. J., Schwarz, E. M., O'Keefe, R. J., Wang, Y. and Chen, D. (2012) 'Conditional activation of β-catenin signaling in mice leads to severe defects in intervertebral disc tissue', *Arthritis and rheumatism*, 64(8), 2611-2623.

Wang, X., Manner, P. A., Horner, A., Shum, L., Tuan, R. S. and Nuckolls, G. H. (2004) 'Regulation of MMP-13 expression by RUNX2 and FGF2 in osteoarthritic cartilage', *Osteoarthritis and cartilage*, 12(12), 963-973.

Wang, Y., Liu, J., Huang, B. O., Xu, Y. M. and Li, J. (2015) 'Mechanism of alternative splicing and its regulation', *Biomedical Reports*, 3(2), 152-158.

Wang J, Gardner BM, Lu Q, Rodova M, Woodbury BG, Yost JG, Roby KF, Pinson DM, Tawfik O and Anderson HC (2009) 'Transcription factor Nfat1 deficiency causes osteoarthritis through dysfunction of adult articular chondrocytes', *J Pathol,* 219(2):163-72.

Wellik, D. M. and Capecchi, M. R. (2003) 'Hox10 and Hox11 genes are required to globally pattern the mammalian skeleton', *Science*, 301(5631), 363-367.

Wienholds E, Kloosterman WP, Miska E, Alvarez-Saavedra E, Berezikov E, de Bruijn, Horvitz HR, Kauppinen S and Plasterk RH (2005) 'MicroRNA expression in zebrafish embryonic development' S*cience*, 309(5732), 310-1.

Wilhelmi G and Faust R (1976) 'Suitability of the C57 black mouse as an experimental animal for the study of skeletal changes due to ageing, with special reference to osteo-arthrosis and its response to tribenoside', *Pharmacology,* 14(4):289-96.

Wijdan Al-Ahmadi, Maha Al-Ghamdi, Latifa Al-Haj, Maher Al-Saif, and Khalid S. A (2009) 'Alternative polyadenylation variants of the RNA binding protein, HuR: abundance, role of AU-rich elements and auto-Regulation', *Nucleic Acids Res*, 37(11): 3612–3624.

Winzen, R.; Kracht, M.; Ritter, B.; Wilhelm, A.; Chen, C.Y.; Shyu, A.B.; Müller, M.; Gaestel, M.; Resch, K and Holtmann, H (1999) 'The p38 MAP kinase pathway signals for cytokine-induced mRNA stabilization via MAP kinase-activated protein kinase 2 and an AU-rich region-targeted mechanism', *EMBO J,* 18, 4969–4980.

Wuelling, M. and Vortkamp, A. (2010) 'Transcriptional networks controlling chondrocyte proliferation and differentiation during endochondral ossification', *Pediatric nephrology*, 25(4), 625-631.

Wurth L (2012) 'Versatility of RNA-Binding Proteins in Cancer', *Comp Funct Genomics*, 178525

Yang, B., Guo, H., Zhang, Y., Chen, L., Ying, D. and Dong, S. (2011) 'MicroRNA-145 regulates chondrogenic differentiation of mesenchymal stem cells by targeting Sox9', *PloS one*, 6(7).

Yang, W., Lee, Y. H., Jones, A. E. and Woolnough, J. L. (2014) 'The histone H2A deubiquitinase Usp16 regulates embryonic stem cell gene expression and lineage commitment', *Nature Communications*, 5, 3818.

Yao, Y. and Wang, Y. (2013) 'ATDC5: An excellent in vitro model cell line for skeletal development', *Journal of Cellular Biochemistry*, 114(6), 1223-1229.

Young LE, Sanduja S, Bemis-Standoli K, Pena EA, Price RL and Dixon DA (2009) 'The mRNA binding proteins HuR and tristetraprolin regulate cyclooxygenase 2 expression during colon carcinogenesis', *Gastroenterology*, 136, 1669-1679.

Yoshida, C. A., Yamamoto, H., Fujita, T., Furuichi, T., Ito, K., Inoue, K., Yamana, K., Zanma, A., Takada, K., Ito, Y., and Komori, T (2004) 'Runx2 and Runx3 are essential for chondrocyte maturation, and Runx2 regulates limb growth through induction of Indian hedgehog', *Genes Dev*, 18, 952–963

Yoshihara Y, Nakamura H, Obata K, Yamada H, Hayakawa T, Fujikawa K, Okada Y (2000) 'Matrix metalloproteinases and tissue inhibitors of metalloproteinases in synovial fluids from patients with rheumatoid arthritis or osteoarthritis', *Ann Rheum Dis*, 59(6):455-61

Yu J and Urban JP (2010) 'The elastic network of articular cartilage: an immunohistochemical study of elastin fibres and microfibrils', *J Anat,* 216(4):533-41

Yucesoy B, Charles LE, Baker B and Burchfiel CM (2015) 'Occupational and genetic risk factors for osteoarthritis: a review', *Work,* 50(2), 261-273.

Zeng, Y. and Cullen, B. R. (2003) 'Sequence requirements for micro RNA processing and function in human cells', *Rna*, 9(1), 112-123.

Zhang, M., Mani, S. B., He, Y., Hall, A. M., Xu, L., Li, Y., Zurakowski, D., Jay, G. D. and Warman, M. L. (2016) 'Induced superficial chondrocyte death reduces catabolic cartilage damage in murine posttraumatic osteoarthritis', *The Journal of clinical investigation*, 126(8), 2893-2902.

Zhang J, Zhao J, Jiang W, Shan X, Yang X and Gao J (2012) 'Conditional gene manipulation: Cre-ating a new biological era', *J Zhejiang Univ Sci B*, 13(7), 511-524.

Zhang M, Egan B and Wang J (2016) 'Epigenetic mechanisms underlying the aberrant catabolic and anabolic activities of osteoarthritic chondrocytes', *Int J Biochem Cell Biol,* doi: 10.1016/j.biocel.2015.04.019

Zhong, L., Huang, X., Karperien, M. and Post, J. N. (2016) 'Correlation between gene expression and osteoarthritis progression in human', *International Journal of Molecular Science*, 17(7), 1126.

Zhou, G., Zheng, Q., Engin, F., Munivez, E., Chen, Y., Sebald, E., Krakow, D. and Lee, B. (2006) 'Dominance of SOX9 function over RUNX2 during skeletogenesis', *Proceedings of the National Academy of Sciences of the United States of America*, 103(50), 19004-19009.

Zhu M, Chen M, Lichtler AC, O'Keefe RJ and Chen D (2008) 'Tamoxifen-inducible Cre-recombination in articular chondrocytes of adult Col2a1-CreER(T2) transgenic mice', *Osteoarthritis and cartilage*, 16, 129-130.

Zhu H, Zhou H-LL, Hasman RA and Lou H (2007) 'Hu proteins regulate polyadenylation by blocking sites containing U-rich sequences', *The Journal of biological chemistry*, 282, 2203-2210.

8 Appendix

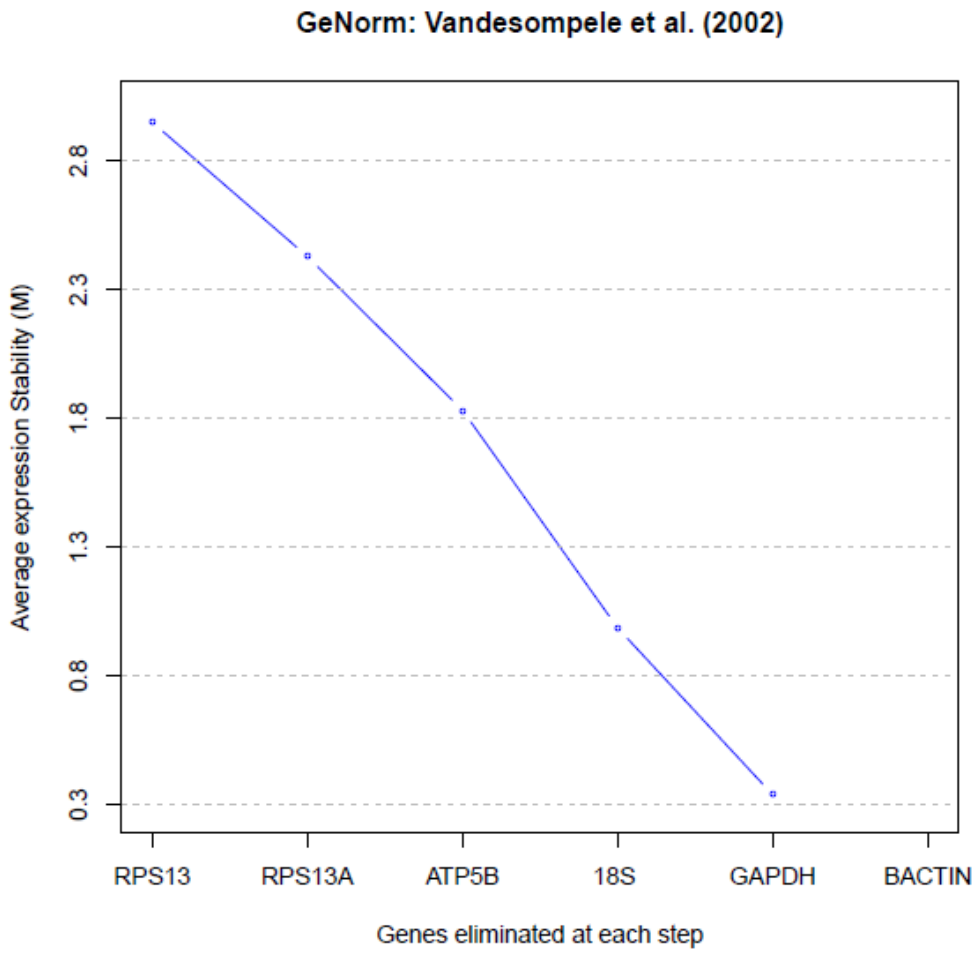

Supplementary Figure 1. PCR housekeeping gene primer validation. GeNorm output depicting β-Actin as the best housekeeping gene for qRT-PCR in ATDC5 cells.